

Stony Brook University



OFFICIAL COPY

The official electronic file of this thesis or dissertation is maintained by the University Libraries on behalf of The Graduate School at Stony Brook University.

© All Rights Reserved by Author.

Mechanistic evaluation of NSD3
in the pathogenesis of acute myeloid leukemia

A Dissertation Presented
by

Chen Shen

to
The Graduate School

in Partial Fulfillment of the
Requirements
for the Degree of
Doctor of Philosophy
in
Molecular and Cellular Biology

Stony Brook University
May 2016

Stony Brook University

The Graduate School

Chen Shen

We, the dissertation committee for the above candidate for the

Doctor of Philosophy degree, hereby recommend

acceptance of this dissertation.

Dr. Christopher R. Vakoc– Dissertation Advisor

Associate Professor, Cold Spring Harbor Laboratory

Dr. Alea A. Mills - Chairperson of Defense

Professor, Cold Spring Harbor Laboratory

Dr. Adrian R. Krainer

Professor, Cold Spring Harbor Laboratory

Dr. Lloyd C. Trotman

Associate Professor, Cold Spring Harbor Laboratory

Dr. Ed Luk

Assistant Professor, Department of Biochemistry and Cell Biology,
Stony Brook University

Dr. Christopher M. Hammell

Assistant Professor, Cold Spring Harbor Laboratory

This dissertation is accepted by the Graduate School

Charles Taber

Dean of the Graduate School

Abstract of the Dissertation

Mechanistic evaluation of NSD3 in the pathogenesis of acute myeloid leukemia

by

Chen Shen

Doctor of Philosophy

in

Molecular and Cellular Biology

Stony Brook University

2016

The bromodomain and extra-terminal (BET) protein BRD4 is a validated drug target in hematological malignancies, owing to its essential role in sustaining oncogenic transcriptional programs. To gain insight into the cancer-relevant mechanistic function of BRD4, I have investigated its mechanism of transcriptional activation in the MLL-fusion subtype of acute myeloid leukemia (AML) with experimental approaches including small hairpin RNA (shRNA) knockdown, clustered regularly-interspaced short palindromic repeats (CRISPR)-Cas9 knockout, biochemistry, RNA sequencing (RNA-Seq) and chromatin immunoprecipitation sequencing (ChIP-Seq). In this study, I demonstrate that the AML maintenance function of BRD4 requires its interaction with NSD3, which belongs to a subfamily of H3K36 methyltransferases. Unexpectedly, AML cells were found to only require a short isoform of NSD3 that lacks the methyltransferase domain. I show that NSD3-short is an adaptor protein that sustains leukemia by linking BRD4 to the CHD8 chromatin remodeler, by utilizing a Pro-Trp-Trp-Pro (PWWP) module, and by employing an acidic transactivation domain. Phenotypic and transcriptional effects of genetic targeting of NSD3 or CHD8 mimic the effects of BRD4 inhibition. Furthermore, BRD4, NSD3, and CHD8 colocalize across the AML genome and are each released from super-enhancer regions upon chemical inhibition of BET bromodomains. These findings suggest that BET inhibitors exert therapeutic effects in leukemia by evicting BRD4-NSD3-CHD8 complexes from chromatin to suppress transcription.

Dedication Page

I sincerely dedicate this thesis to my beloved family, dear teachers and friends.

Table of Contents

List of Figures	viii
List of Tables	x
List of Abbreviations	xi
Acknowledgments.....	xiii
Chapter 1: Introduction.....	1
1.1 Acute myeloid leukemia	1
1.1.1 Epidemiology and symptoms of acute myeloid leukemia	1
1.1.2 Genetics of AML	2
1.1.3 Classifications and diagnosis of AML.....	2
1.1.4 Current therapies for AML patients.....	3
1.2 BRD4 and BET inhibitors.....	6
1.2.1 Basic mechanism of BRD4 functions.....	6
1.2.2 Direct BRD4 interaction with transcription factors.....	8
1.2.3 BET inhibitors.....	11
1.2.4 Therapeutic targeting of BRD4 with small molecules.....	12
1.3 A uncharacterized NSD family protein NSD3.....	21
Chapter 2: A Short Isoform of NSD3 Lacking Catalytic Function Is Essential in Acute Myeloid Leukemia.....	24
2.1 NSD3 is required for AML cell proliferation	26
2.2 NSD3 is required for maintaining the undifferentiated state of AML cells	30
2.3 <i>c-Myc</i> is an essential target gene of NSD3 in AML maintenance	30
2.4 NSD3 regulates a similar global gene profile with BRD4 in AML.....	33
2.5 A short isoform of NSD3 is essential in AML	35
Chapter 3: NSD3-short Binds Directly to the BRD4 ET Domain.....	39
3.1 NSD3 is an ET-domain associated protein	39
3.2 NSD3-short 100-263 is a BRD4 interacting domain	41
3.3 NSD3-short 100-263 Binds BRD4 ET-domain directly.....	44
3.4 Dissociation of NSD3 from BRD4 impairs ET domain functions	46

Chapter 4: NSD3-short Is an Adaptor Protein that Links BRD4 to the CHD8 Chromatin Remodeling Enzyme	50
4.1 CHD8 is required for AML cell proliferation.....	50
4.2 CHD8 is required for maintaining the undifferentiated state of AML cells	56
4.3 CHD8 regulates a similar global gene profile with NSD3 and BRD4 in AML	58
4.4 NSD3-short bridges BRD4 to the CHD8 chromatin remodeler	60
Chapter 5: BRD4 Recruits NSD3 and CHD8 to Super-Enhancer Regions at Oncogene Loci.....	62
5.1 BRD4, NSD3, and CHD8 colocalize at active promoters and enhancers across the AML genome	62
5.2 BRD4 recruits NSD3 and CHD8 to the <i>Myc</i> +1.7 Mb super-enhancer region.....	66
Chapter 6: NSD3-short Uses Four Distinct Interaction Surfaces to Sustain AML Cell Proliferation	71
6.1 NSD3-short uses a PWWP reader module to sustain AML cell proliferation.....	71
6.2 NSD3-short possesses an acidic transactivation domain	76
6.3 CRISPR-Cas9 scanning of exons encoding NSD3-short in AML.....	78
Chapter 7: Conclusions and Perspectives	82
7.1 Summary	82
7.2 Discussions	84
7.2.1 BRD4 in AML maintenance	84
7.2.2 Functions of the PWWP domain in NSD3-short	86
7.2.3 Functions of NSD3-long	87
7.2.4 Interactions between NSD3 and BET family proteins other than BRD4	87
7.3 Perspectives and future directions	88
Chapter 8: Extended Materials and Methods.....	91
8.1 Cell culture.....	91
8.2 Cell lines and plasmids	91
8.3 Competition assay to measure cell proliferation.....	93
8.4 RT-qPCR.....	95
8.5 Protein lysate preparation for Western blotting	97
8.6 May-Grünwald-Giemsa Cytospin staining	97
8.7 c-Kit/Mac-1 staining and flow cytometry.....	97

8.8 Immunoprecipitation.....	98
8.9 FLAG-NSD3-short IP-mass spectrometry.....	98
8.10 FLAG-NSD3-short IP iTRAQ mass spectrometry.....	100
8.11 Peptide pull-down assay	102
8.12 GAL4 luciferase reporter assay	103
8.13 Expression and purification of recombinant GST-NSD3 fragments from bacteria.....	103
8.14 Cloning, expression, and purification of recombinant proteins from Sf9 cells	104
8.15 Surface plasmon resonance.....	105
8.16 Molecular Graphics.....	106
8.17 CRISPR-Cas9 targeting of <i>Chd8</i> and <i>Nsd3</i>	106
8.18 Chromatin immunoprecipitation.....	109
8.19 RNA-Seq and ChIP-Seq library construction.....	111
8.20 RNA-Seq analysis.....	111
8.21 ChIP-Seq analysis.....	112
8.22 Accession numbers	113
8.23 Animal studies	113
8.24 Antibodies.....	113
Bibliography	115
Appendix.....	134
A. IP-MS results.....	134
B. iTRAQ results	146
C. sgRNAs sequences used in pool screening	156
D. Gene sets	176

List of Figures

Figure 1.1 A diagram of the alternative transcript isoforms of the gene <i>WHSC1L1</i>	23
Figure 2.1 Domain architectures of human BRD4 and NSD3.....	25
Figure 2.2 Workflow of GFP depletion assay to evaluate sensitivity of cells to shRNA-based targeting of specific proteins. A decrease of GFP signal indicates that the introduced shRNA suppresses gene expression essential for cell proliferation.....	25
Figure 2.3 NSD3 is required for AML maintenance.	28
Figure 2.4 NSD3 does not have a broad impact on cell proliferation.....	29
Figure 2.5 NSD3 is required for maintaining the undifferentiated state of AML cell.....	31
Figure 2.6 <i>c-Myc</i> is an essential target gene of NSD3 in AML.....	32
Figure 2.7 NSD3 regulates a similar global gene profile with BRD4 in AML.	34
Figure 2.8 A short isoform of NSD3 is essential in AML.	37
Figure 2.9 NSD3-short is essential for transcriptional activation.....	38
Figure 3.1 NSD3-short is an ET-domain associated protein.	40
Figure 3.2 NSD3-short 100-263 is BRD4 interacting domain.	43
Figure 3.3 NSD3-short 100-263 binds BRD4 ET-domain directly.....	45
Figure 3.4 Dissociation of NSD3 from BRD4 impairs ET domain functions.....	49
Figure 4.1 CHD8 is required for AML cell proliferation.	54
Figure 4.2 CRISPR-scanning of exons encoding <i>Chd8</i> in AML.....	55
Figure 4.3 CHD8 is required for maintaining the undifferentiated state of AML cell.	57
Figure 4.4 CHD8 regulates a similar global gene profile with NSD3 and BRD4 in AML.	59
Figure 4.5 NSD3-short bridges BRD4 to the CHD8 chromatin remodeler.....	61
Figure 5.1 Genomewide colocalization of BRD4, NSD3, and CHD8 at active promoters and enhancers across the AML genome.	64
Figure 5.2 Colocalization of BRD4, NSD3, and CHD8 at oncogene loci.....	65
Figure 5.3 Recruitment of NSD3-short is solely dependent on BRD4 interacting region.	68
Figure 5.4 BRD4 recruits NSD3 and CHD8 to the <i>Myc</i> +1.7 Mb super-enhancer region in AML.	69
Figure 5.5 BRD4 recruits NSD3 and CHD8 to the super-enhancer regions at oncogene loci.	70
Figure 6.1 NSD3-short uses four distinct regions to sustain AML cell proliferation.....	73

Figure 6.2 Functions of the PWWP domain within NSD3-short.....	75
Figure 6.3 NSD3-short possesses an acidic transactivation domain.....	77
Figure 6.4 CRISPR-Cas9 scanning of exons encoding <i>Nsd3-short</i> in AML.....	80
Figure 6.5 Dissociation of BRD4 with point mutation impacts NSD3-short function in AML...	81
Figure 7.1 Model for NSD3-short functions in AML maintenance.....	83

List of Tables

Table 1.1 Summary of commonly mutated genes in AML encoding chromatin regulators.....	5
Table 1.2 Summary of commonly used BET inhibitors.	15
Table 1.3 Summary of therapeutic studies evaluating BET inhibitors.	16
Table 8.1 List of shRNAs sequence.....	94
Table 8.2 Primers used for RT-qPCR for mouse genes.....	96
Table 8.3 List of sgRNAs sequences.	107
Table 8.4 Primers used for CHIP-qPCR.....	110

List of Abbreviations

ADPKD	autosomal dominant polycystic kidney disease
AML	acute myeloid leukemia
Ara C	cytosine arabinoside
AWS	Associated with SET domain region
B-ALL	B-cell acute lymphoblastic leukemia
BDI	bromodomain I
BDII	bromodomain II
BET	bromodomain and extra-terminal
BLBC	basal-like breast cancer
CARD	activation and recruitment domain
CDK9	cyclin-dependent kinase 9
ChIP	chromatin immunoprecipitation
ChIP-Seq	ChIP sequencing
CRISPR	clustered regularly-interspaced short palindromic repeats
CTD	C terminal domain
DLBCL	diffuse large B-cell lymphoma
DNR	daunorubicin
Dox	doxycycline
ELN	European Leukemia Net
EMT	epithelia-mesenchymal transition
ES	Ewing sarcomas
ET	extraterminal domain
FAB	French-American-British
FBS	fetal bovine serum
FDR	false discovery rate
GBM	Glioblastoma Multiforme
GFP	green fluorescent protein
GSEA	Gene Set Enrichment Analysis
GVHD	graft-versus-host disease
H3K36	histone H3 lysine 36
HCC	human hepatocellular carcinoma
IP	immunoprecipitation
IPA	Ingenuity Pathway Analysis
LSC	leukemia stem cell
MACS	Model based analysis of ChIP-Seq
MCC	Merkel cell carcinoma
MCL	Mantle cell lymphoma
MEF	mouse embryonic fibroblast
MLL	mixed lineage leukemia
MOI	multiplicity of infection
MPNST	malignant peripheral nerve sheath tumor

MSCV	murine stem cell virus
NES	normalized enrichment score
NMC	NUT midline carcinoma
P-TEFb	positive transcription elongation factor b
PAH	pulmonary arterial hypertension
PAM	protospacer adjacent motif
PDAC	pancreatic ductal adenocarcinoma
PEL	primary effusion lymphoma
PHD	plant homeodomain finger
PWWP	Pro-Trp-Trp-Pro chromatin reader module
RNA-Seq	RNA sequencing
RPKM	reads per kilobase per million
RT-qPCR	reverse transcription-quantitative polymerase chain reaction
SET	Su(var)3-9, enhancer-of-zeste and trithorax
shRNA	small hairpin RNA
sgRNA	single guide RNA
SPR	surface plasmon resonance
T-ALL	T-cell acute lymphoblastic leukemia
TAD	transcription activation domain
Tam-R	Tamoxifen-resistant
TF	transcription factor
WHO	World Health Organization

Acknowledgments

In the past five years, I have experienced an amazing adventure in my life. I owe my gratitude to many people who have made this dissertation possible and my PhD study one of the most memorable times.

Firstly, I would like to express the deepest thanks to my thesis advisor Dr. Chris Vakoc. I am very lucky to conduct my PhD researches under the guidance of Chris. He has set up an excellent model for me to become a passionate and successful scientist. I appreciate his generous contributions of time, ideas, and funding during my entire PhD study. The great training and support obtained from Chris not only makes me a better scientist but also provides me with a good start for future career.

Moreover, Dr. Junwei Shi has become a great teacher for me since my rotation in Vakoc lab. His kind instructions helped me overcome a lot of difficulties during my research and graduate study. Our lab manager, Joe Milazzo has been offering me so much support over the past five years. I am very thankful to all the Vakoc lab members present and past for sharing the techniques, ideas and many important moments with me.

I would also like to thank my amazing collaborators for helping me accomplish my research projects, particularly, Dr. Jonathan Ipsaro, Dr. Leemor Joshua-Tor, Dr. Darryl Pappin, Dr. Olga Anczuków, Dr. Camila Dos Santos and Dr. Ming-Ming Zhou. All the facilities in Cold Spring Harbor Laboratory have been a great help for me to work and study here.

I am also thankful to my thesis committee: Dr. Alea Mills, Dr. Adrian Krainer, Dr. Lloyd Trotman, Dr. Chris Hammell and Dr. Ed Luk for numerous discussions, suggestions and continuous supports during my pursuit of PhD.

I am also lucky to obtain a great deal of joys and motivations from my dear friends nearby and far away. Most importantly, my family has always been the strongest support during my ups and downs. They are my endless source of love, happiness and energy; they are my forever beliefs.

Chapter 1: Introduction

Chromatin regulators control the transition between transcriptionally active and silent chromatin states by catalyzing and binding histone modifications (Jenuwein and Allis 2001; Ram et al. 2011). Systematic cancer genomic studies have indicated that somatic mutations in genes encoding chromatin regulators are a common mechanism to drive tumorigenesis (Garraway and Lander 2013). Therefore, chromatin regulators are thought to be potential therapeutic targets for cancer treatment. Over the past decade, the FDA has approved a number of small-molecule inhibitors against chromatin regulatory pathways (Zuber et al. 2011b; Dawson and Kouzarides 2012). However, the therapeutic potential of most of the chromatin regulators as targets for cancer treatment and underlying mechanisms largely remain unexplored.

1.1 Acute myeloid leukemia

1.1.1 Epidemiology and symptoms of acute myeloid leukemia

AML is an aggressive hematopoietic malignancy. It is a relatively rare disease that accounts for 1.2% of estimated new cancer cases and 1.8% of estimated cancer deaths in the USA (Siegel et al. 2015). In this disease, myeloid cells are blocked at an early stage of hematopoiesis and gain aberrant self-renewal abilities. These immature leukemia cells rapidly accumulate in bone marrow and in the peripheral blood system, thereby interfering with normal blood cell production. Since the normal hematopoietic functions are disrupted, leukemia patients usually display a series of symptoms, such as anemia, bleeding and infections.

1.1.2 Genetics of AML

Due to recent advances in genomic techniques, especially next-generation sequencing, the genomic landscape of AML is well understood (Dohner et al. 2015). Whole genome and exon sequencing of 200 AML patient samples has revealed only an average of 13 mutations per sample, which is much fewer than the number of mutations in other adult cancers (Cancer Genome Atlas Research 2013). Chromatin regulators are one of the gene classes that are frequently mutated in AML, suggestive of their important roles in the disease maintenance and progression. Table 1.1 summarizes the commonly mutated genes encoding chromatin regulators identified in these 200 AML patient samples (Cancer Genome Atlas Research 2013).

Deregulation of chromatin regulators caused by chromosomal translocations and somatic mutations can contribute significantly to leukemogenesis (Redner et al. 1999; Krivtsov and Armstrong 2007; Chen et al. 2010). One example is the H3K4 methyltransferase mixed lineage leukemia (MLL), which can form fusion proteins with a diverse array of partner proteins (Krivtsov and Armstrong 2007). The resulting MLL-fusion protein has lost its H3K4 methyltransferase activity and instead recruits alternative effector complexes, such as the H3K79 methyltransferase DOT1L. DOT1L is required for the maintenance of the MLL translocation-associated oncogenic transcriptional program, such as HOXA9 and MEIS1A (Bernt et al. 2011). Chemical inhibition of DOT1L is a promising therapeutic approach in MLL-fusion leukemia now under investigation in clinical trials (NCT02141828) (Neff and Armstrong 2013).

1.1.3 Classifications and diagnosis of AML

Diagnosis of AML requires initial examination of a peripheral blood smear to detect immature leukemia blasts, followed by bone marrow biopsy as a definitive diagnosis. Besides

light microscopy and flow cytometry methods, cytogenetic and genetic studies may also be performed for further disease classification and prognosis.

Based on the type and maturity of leukemia cells, AML can be divided into 8 subtypes from M0 to M7 according to the French-American-British (FAB) classification system (Bennett et al. 1976). More recently however, the World Health Organization (WHO) has combined morphology, immunophenotype, genetic and clinical features to form a new classification system, which contains more descriptive and meaningful information for prognosis (Harris et al. 1999; Falini et al. 2010). Compared with the FAB system, the WHO system is more widely used and employs less stringent criteria to define AML, which only requires more than 20% of leukemic myeloblasts to be present in the blood or bone marrow for the diagnosis, while the FAB system uses 30% of blasts as the cutoff (Harris et al. 1999; Amin et al. 2005).

1.1.4 Current therapies for AML patients

The first-line therapeutic strategy for AML treatment is chemotherapy comprised of induction therapy and consolidation therapy, which has remained almost unchanged for more than 30 years (Dohner et al. 2015). The aim of induction therapy is to achieve a complete remission, the definition of which is often debated (de Greef et al. 2005). The so-called "7+3" (or "3+7") induction regimen constitutes seven days of continuous intravenous infusion of cytosine arabinoside (Ara C) and three days of intravenous push of daunorubicin (DNR) (Yates et al. 1973). Complete remission rates can reach 60-85% in adults not older than 60 years, in comparison to only 40-60% in patients older than 60 years (Dohner et al. 2015).

After induction therapy, almost all the patients will relapse without further intervention (Cassileth et al. 1988). The following consolidation therapy aims to eliminate any non-detectable

leukemia cells and cure the disease. For patients that are 60 years old or younger and with favorable European Leukemia Net (ELN) genetic risk profile, 2-4 cycles of intermediate-dose of cytarabine will achieve a 60-70% cure rate, while for patients older than 60 the cure rate remains poor (Dohner et al. 2015). Allogeneic hematopoietic-cell transplantation is another option for patients with high risk of relapse or who had unsuccessful primary induction therapy (Dohner et al. 2015).

Moreover, with an increasing amount of knowledge of the genomic and epigenomic mutation landscapes of AML, targeted therapies are starting to emerge as potential new therapeutic options. The therapeutic efficacies of these new agents are now under intense clinical evaluation, including the small molecule inhibitors targeting cell signaling regulators (eg: FLT3, KIT), cell-cycle regulators (eg: MDM2, PLK, CDK, PI3K, mTOR), epigenetic factors (IDH1/2, BET, LSD1, HDACs), and factors involved in nuclear export (XPO1) processes (Dohner et al. 2015).

Table 1.1 Summary of commonly mutated genes in AML encoding chromatin regulators.

	Mutations	Frequencies
Chromatin Modifiers	MLL-fusion	5.5%
	NUP98-NSD1	1.5%
	ASXL1	2%
	EZH2	1.5%
DNA Methylation	DNMT3A	26%
	DNMT3B	1%
	DNMT1	0.5%
	TET1	1%
	TET2	8%
	IDH1/IDH2	20%

1.2 BRD4 and BET inhibitors

The Bromodomain and Extra-Terminal (BET) family protein BRD4 is a general chromatin regulator that recognizes the acetyl-lysine residues and regulates transcription (Wu and Chiang 2007; Shi and Vakoc 2014). Pharmacologic targeting of BET proteins presents therapeutic effects in various cancers and inflammatory diseases via inhibition of BRD4 functions, which has made BRD4 an exciting new drug targets in oncology.

1.2.1 Basic mechanism of BRD4 functions

The mammalian BET family consists of mammalian BRD2, BRD3, BRD4 and BRDT proteins. In this family, proteins contain two conserved bromodomains (BDI and BDII), an extraterminal domain (ET) as well as a C terminal domain (CTD), that is only present in BRD4 and BRDT (Wu and Chiang 2007).

The bromodomains of BRD4 were shown to bind acetyl-lysine on histone H3 and H4, by which means BRD4 is docked on specific genomic loci (Dhalluin et al. 1999; Dey et al. 2003). Moreover, several recent studies showed that BET proteins, particularly BRD4, could also recognize the acetylated lysine residues on several transcription factors which occurs in a cell type-specific manner (Lamonica et al. 2006; Huang et al. 2009; Brown et al. 2014; Shi et al. 2014; Roe et al. 2015).

As a general transcriptional coactivator, BRD4 is present in an active form of the positive transcription elongation factor b (P-TEFb) complex. The core P-TEFb complex is comprised of a catalytic subunit cyclin-dependent kinase 9 (CDK9) and its regulatory subunit Cyclin T1/T2/K (Zhou et al. 2012). When not bound by the inhibitory subunit 7SK/HEXIM, CDK9 can phosphorylate the negative factors DSIF and NELF, thereby releasing the promoter-poised Pol II

to initiate transcription elongation (Zhou et al. 2012). Meanwhile, phosphorylation of serine 2 by CDK9 at the Pol II CTD is coupled with transcription elongation and further provides a binding platform for other processing factors (Hsin and Manley 2012; Zhou et al. 2012). BRD4 can also positively regulate P-TEFb functions without altering its catalytic activity (Yang et al. 2005). When bound to BRD4, P-TEFb is prevented from being sequestered by 7SK/HEXIM and this active form of the P-TEFb complex is recruited to promoter-proximal regions (Jang et al. 2005; Yang et al. 2005). Provocatively, even though BRD4 lacks a classic kinase domain, it has been reported to regulate Pol II elongation by directly phosphorylating serine 2 at its CTD in an in vitro kinase assay (Devaiah et al. 2012). However, this atypical kinase function of BRD4 needs to be further validated by more biochemical evidence. BRD4 can directly bind P-TEFb with two binding surfaces: one is 1209–1362aa within the CTD domain of BRD4 that interacts with both Cyclin T1 and CDK9 and the other is the bromodomain II (BDII) domain that binds to acetylated Cyclin T1 (Jang et al. 2005; Bisgrove et al. 2007; Schroder et al. 2012).

Besides proteins interacting with the BRD4 CTD domain, proteomic screens have revealed additional factors that associate with the BRD4 ET domain, including NSD3, JMJD6, and GLTSCR1, although the functional relevance of these interactions is largely uncertain (Rahman et al. 2011; Liu et al. 2013). Through its interaction with BRD4, JMJD6 was reported to erase repressive histone marks and release the inhibitory regulation of P-TEFb by demethylating 7SK (Liu et al. 2013)

By mass spectrometry, BRD4 was also identified to be physically associated with mammalian Mediator complex (Jiang et al. 1998). The Mediator complex, comprised of 20 protein subunits, interacts with Pol II as well as general transcription factors and stimulates transcriptional activation (Kim et al. 1994). The interaction between BRD4 and Mediator was

later supported by their genomic co-localization and functional overlap in AML (Donner et al. 2010; Loven et al. 2013; Bhagwat et al. 2016).

1.2.2 Direct BRD4 interaction with transcription factors

Transcription factors (TFs) are proteins that bind to specific DNA sequences to control the transcription of both nearby genes or far away genes that can be looped back by long-range enhancer-promoter interactions (Latchman 1997; Lee and Young 2013). BRD4 could occupy various cell-type specific cis-elements, although it lacks a DNA sequence specific binding domain. Together this suggests that the recruitment of BRD4 to these cell type specific genomic loci could be mediated by TFs. Indeed, BRD4 can be recruited to promoter and enhancer regions by acetylated histone tails, which are established by the recruitment of acetyltransferases by TFs (Shi and Vakoc 2014). Meanwhile, TFs can recruit BRD4 by direct interactions either in acetylation-dependent or -independent way (Shi and Vakoc 2014).

An earlier study performed a biochemical screen with purified proteins for individual incubation with recombinant FLAG-tagged human BRD4 protein and identified a group of BRD4-interacting TFs including p53, YY1, c-Jun, AP2, Myc/Max heterodimer, C/EBP α and C/EBP β (Wu et al. 2013a). Since these TFs are purified from *E. coli*, BRD4 presumably directly binds them in an acetylation-independent manner. Specifically, the authors identified two distinct regions that bind to the p53 C terminal regulatory region, one of which requires a CK2 dependent phosphorylation-PDID region (Wu et al. 2013a). In the absence of phosphorylation, p53 binds to the BID region, a basic residue-enriched interaction domain conserved in BET proteins, to form an unfavorable complex to associate with DNA (Wu et al. 2013a). At the same time, the N-terminal cluster of phosphorylation sites (NPC) within the PDID region blocks the

interaction between BDII and chromatin. Upon phosphorylation, p53 binds to the PDID region while BID interacts with NPC competitively to release auto-inhibition of BDII (Wu et al. 2013a). This active form of the complex is also able to interact with DNA (Wu et al. 2013a). This study suggests that BRD4 is targeted to sequence-specific DNA regions by direct association with TFs in an acetylation independent manner. Moreover, this interaction could be under the regulation of signal transduction cascades.

Besides histone tails, the bromodomains of BRD4 could also recognize specific histone-like acetylated regions of TFs. For example, hematopoietic TF GATA-1 contains a histone-like sequence motif K^{ac}GKK^{ac} which is diacetylated by CBP and presents a binding site for BDI of BRD3 (Gamsjaeger et al. 2011; Lamonica et al. 2011). Further study also showed that GATA-1 recruits other BET proteins, namely BRD2 and BRD4, to chromatin besides BRD3 (Stonestrom et al. 2015). BET proteins in turn can promote GATA-1 chromatin occupancy and activate transcription of erythroid genes (Lamonica et al. 2011; Stonestrom et al. 2015). Similarly, the hematopoietic TF ERG has also been shown to co-occupy with BRD4 across the genome in a cell line derived from a mouse model MLL-AF9/Nras^{G12D} AML (Roe et al. 2015). Lysine 96 and 99 of ERG, separated by two glycine residues, can be acetylated by p300. This K^{ac}GGK^{ac} motif highly resembles the histone H4K5/K8 di-acetylation site. Either the treatment with the BRD4 inhibitor JQ1 or K96R/K99R mutation disrupted the interaction between ERG and BRD4, indicating that BRD4 binds ERG in a manner dependent on acetyl-lysine residues (Roe et al. 2015). BET inhibitors, which interrupted the association between ERG/GATA-1 with BET proteins, impair the induction of specific hematopoietic genes in these settings (Lamonica et al. 2011; Roe et al. 2015; Stonestrom et al. 2015).

TWIST is a key helix-loop-helix transcription factor which is associated with normal mesoderm development and epithelial-mesenchymal transition (EMT) during cancer progression (Shi et al. 2015a). TWIST contains a motif that resembles the histone H4 sequence. When diacetylated by TIP60, the GK^{ac}GGK^{ac} motif of TWIST presents a docking site specifically for BDII of BRD4 and recruits BRD4/P-TEFb/RNA-PolIII complex (Shi et al. 2014). This study suggests a model in which BRD4 binds to chromatin in a cooperative manner, in which BDI and BDII bind to the histone tail and TWIST respectively. Pharmacological inhibition of the TWIST-BRD4 interaction with BET inhibitors or through genetic knockdown of the TWIST target gene *Wnt5a* led to suppression of basal-like breast cancer (BLBC) development and progression both *in vitro* and *in vivo* (Shi et al. 2014).

Another example is Aire, an essential transcriptional regulator in immunologic tolerance (Peterson et al. 2008; Mathis and Benoist 2009). A series of acetylated lysine residues within Aire's caspase activation and recruitment domain (CARD) are required for the interaction between Aire and BRD4 (Yoshida et al. 2015). The phosphorylation of T69 within CARD is likely responsible for binding CBP and enabling the acetylation events to recruit BRD4 (Yoshida et al. 2015). Through binding the BDI of BRD4, Aire can be bridged to the P-TEFb complex to regulate downstream gene expression (Yoshida et al. 2015). This model is supported by data showing that disruption of the Aire:BRD4 interaction impaired the association of Aire with P-TEFb and Aire-induced gene transcription (Yoshida et al. 2015). Furthermore, BET inhibitors compromise thymic negative selection of self-reactive specificity in mice (Yoshida et al. 2015). These data may provide an explanation for the point mutations of Aire observed in autoimmune disease patients (Yoshida et al. 2015).

NF- κ B is an inducible TF that translocates from the cytosol into the nucleus and activates gene transcription involved in the immune system and tumorigenesis (Hayden and Ghosh 2012). The association between BRD4 and NF- κ B pathway was established by the interaction of RelA/p65 subunit of NF- κ B with BRD4 (Huang et al. 2009; Wu et al. 2013b; Zou et al. 2014). Via a P300-dependent acetylation, both bromodomains of BRD4 can bind acetylated RelA at lysine 310 (Huang et al. 2009; Wu et al. 2013b; Zou et al. 2014). BRD4 coactivates NF- κ B and protects RelA from ubiquitination and degradation (Huang et al. 2009; Wu et al. 2013b; Zou et al. 2014). Although acetylation of K310 does not resemble the classic acetylated histone motif, the K310R mutation suppressed the recruitment of BRD4 and P-TEFb and the activation of NF- κ B target genes (Huang et al. 2009; Wu et al. 2013b). Treatment with BET inhibitor in different disease settings indicated a global downregulation of NF- κ B target genes and suppression of inflammatory responses and tumorigenesis (Anand et al. 2013; Brown et al. 2014; Zou et al. 2014). Beyond these observations, a study in endothelial cells showed that TNF α stimulation led to a large variability in BRD4 recruitment to RelA bound sites (Brown et al. 2014). Compared with the genes located near typical enhancers, genes near super-enhancers exhibited greater induction upon TNF α stimulation (Brown et al. 2014). This work raises the question as to whether TFs, instead of histone modifications, could be the major driving force of BRD4 recruitment to enhancer regions since the dynamic changes of BRD4 occupancy were not consistent with histone acetylation (Brown et al. 2014; Xu and Vakoc 2014).

1.2.3 BET inhibitors

BET inhibitors are a class of small molecules that reversibly bind the bromodomains of BET proteins. Although these inhibitors are able to target two bromodomains (BDI and BDII) of

BET proteins with selectivity (Picaud et al. 2013), it has not been reported that inhibitors could discriminate among BET proteins (BRD2, BRD3, BRD4 and BRDT) (Filippakopoulos and Knapp 2014).

BET inhibitors were first developed in the early 1990s as potential anti-inflammatory and anti-tumor agents (patent JP H0228181, JP 2008156311, EP 2239264). However, BET inhibitors did not receive widespread attention until the therapeutic activities of JQ1 and I-BET762 (GSK525762) were discovered in NUT midline carcinoma (NMC) and sepsis (Filippakopoulos et al. 2010; Nicodeme et al. 2010). Both of these inhibitors have notably higher affinity for bromodomains of the BET family over other subfamilies and release BET proteins from chromatin by competing with acetylated peptides (Prinjha et al. 2012). Later studies identified a large number of BET inhibitors with different chemical scaffolds. Table 1.2 summarizes specific BET inhibitors widely used in basic research and clinical trials.

1.2.4 Therapeutic targeting of BRD4 with small molecules

In the past few years, pre-clinical studies have revealed significant therapeutic activities of BET inhibitors in a series of malignancies, inflammatory and cardiovascular diseases (Table 1.3). These effects are mainly due to the suppression of a BRD4-dependent transcriptional program linked to oncogenesis, inflammatory response, cardiomyocyte hypertrophy as well as lipid metabolism (Filippakopoulos and Knapp 2014; Shi and Vakoc 2014).

BRD4-NUT fusion protein occurs in a rare form of squamous cell carcinoma NMC and retain the chromatin reader bromodomains of BRD4 (French 2012). This fusion protein, dependent on acetyl-lysine binding ability of BRD4, causes differentiation block of squamous cells, maintains tumor cell growth and likely drives “megadomains” with the length of up to 2

Mb (French et al. 2008; French et al. 2014; Grayson et al. 2014; Alekseyenko et al. 2015).

Chemical inhibition of the BRD4 bromodomains represents a promising therapeutic approach in this disease and for the first time exhibits therapeutic activity for a BET inhibitor in a pre-clinical NMC model (Filippakopoulos et al. 2010). Currently, two patients have responded to the BET inhibitor OTX015 with tumor regression and symptomatic relief but no intolerable side effects (Stathis et al. 2016).

Nevertheless, a variety of experiments indicate that the primary target of BET inhibitors is the wild type form of BRD4. Pre-clinical studies identified BRD4 as a drug target in blood malignancies lacking *BRD4* rearrangements including AML, multiple myeloma and lymphoma (Dawson et al. 2011; Delmore et al. 2011; Mertz et al. 2011; Zuber et al. 2011b; Chapuy et al. 2013). AML cells are hypersensitive to BRD4 knockdown and to pharmacological BET inhibition (Dawson et al. 2011; Mertz et al. 2011; Zuber et al. 2011b), an observation that has motivated several ongoing clinical trials of BET inhibitors in human AML patients (Clinicaltrials.gov Identifiers: NCT02158858, NCT02308761, and NCT01943851). The therapeutic potential of targeting BRD4 in AML stems from its role in maintaining the expression of several key oncogenes, including *MYC*, *BCL2*, and *CDK6* (Dawson et al. 2011; Mertz et al. 2011; Zuber et al. 2011b). In leukemia cells, each of these loci possesses large clusters of BRD4-occupied enhancers, termed super-enhancers, which are assembled through the coordinated action of hematopoietic transcription factors and the lysine acetyltransferase activity of p300 (Loven et al. 2013; Shi et al. 2013b; Dawson et al. 2014; Roe et al. 2015). While molecular mechanisms that target BRD4 to specific genomic sites in AML have been identified (Roe et al. 2015), the effector proteins required for BRD4-dependent transcriptional activation in this disease remain largely unknown.

Moreover, the efficacy of BET inhibitors has also been observed in various solid tumors without genetic alterations of BRD4, such as breast cancer and lung cancer (Table 1.3). These pre-clinical studies encouraged the development of drug-like BET inhibitors and several have entered phase I clinical trials to evaluate the drug safety and efficacy in cancer patients (Clinicaltrials.gov Identifiers: NCT01587703; NCT01943851; NCT02259114; NCT01713582; NCT01949883; NCT02158858; NCT01987362).

Table 1.2 Summary of commonly used BET inhibitors.

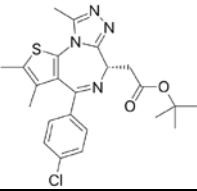
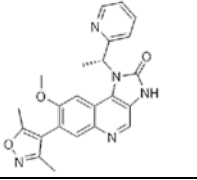
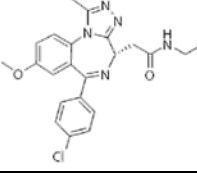
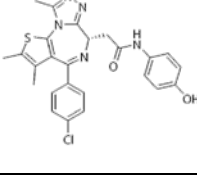
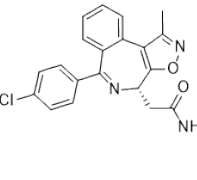
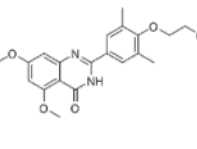
Name	Source	Chemical Structure	Type	Application	Ref
JQ1	Dana Farber Cancer institute		Thienodiazepines	Widely used in research studies	(Filippakopoulos et al. 2010; Bamborough et al. 2012)
I-BET 151	GSK		Isoxazoles	Widely used in research studies	(Bamborough et al. 2012)
I-BET 762	GSK		Benzo-diazepines	In phase I clinical trials in patients with NUT midline carcinoma, solid tumors and hematologic malignancies (NCT01587703; NCT01943851)	(Nicodeme et al. 2010)
OTX-015	OncoEthix		Thienodiazepine	In phase I clinical trials in patients with NUT midline carcinoma, solid tumors and hematologic malignancies (NCT02259114; NCT01713582)	(Miyoshi 2010; Gautschi 2014)
CPI-0610	Consellation		Thienodiazepine	In phase I clinical trials in patients with lymphoma, multiple myeloma and other hematologic malignancies (NCT01949883; NCT02158858)	(Albrecht et al. 2016)
TEN-010	Tensha	N/A	Thienodiazepine	In phase I clinical trials in patients with NUT midline carcinoma (NCT01987362)	(Filippakopoulos and Knapp 2014)
RVX-208	Resverlogix		Quinazolone	In phase II clinical trials in patients with atherosclerosis and Type II diabetes (NCT 01058018; NCT01728467)	(Bailey et al. 2010; Nicholls et al. 2012; Khmelnsky et al. 2013)

Table 1.3 Summary of therapeutic studies evaluating BET inhibitors.

BET inhibitor	Relevant BET protein target	Disease type	Disease subtype	Mouse model	Ref
dBET1	BRD4	Cancer	Acute myeloid leukemia (AML)	Human leukemia xenograft	(Winter et al. 2015)
JQ1	BRD4	Cancer	AML	Human cell line xenograft	(Devaraj et al. 2015)
JQ1	Not demonstrated	Cancer	AML	Mice transplanted with Myc-overexpressing AMLs	(Bronfield et al. 2015)
I-BET 151	BRD4	Cancer	AML	Mice transplanted with NPM1c AMLs	(Dawson et al. 2014)
JQ1	BRD4	Cancer	AML	Mice transplanted with shMll3; shNf1;p53-/-;MLL-AF9 AML	(Chen et al. 2014)
JQ1	BRD4	Cancer	AML	Genetically engineered mouse (GEM) model with MLL-AF9 oncogene	(Zuber et al. 2011b)
I-BET 151	Not demonstrated	Cancer	AML	Human cell line xenograft	(Dawson et al. 2011)
JQ1	BRD4	Cancer	AML	IDH2 R172K GEM model	(Chen et al. 2013)
I-BET 151	BRD4	Cancer	AML	NPM1c GEM model	(Dawson et al. 2014)
JQ1	BRD4	Cancer	AML	Human cell line xenograft	(Fiskus et al. 2014)
JQ1	Not demonstrated	Cancer	B-cell acute lymphoblastic leukemia (B-ALL)	Patient sample xenograft	(Ott et al. 2012)
JQ1	Not demonstrated	Cancer	B-ALL	Human cell line xenograft	(Da Costa et al. 2013)
JQ1	BRD4	Cancer	T cell acute lymphoblastic leukemia (T-ALL)	Human cell line xenograft	(Knoechel et al. 2014)
JQ1	Not demonstrated	Cancer	T-ALL	Tal1/Lmo2 GEM model	(Roderick et al. 2014)
JQ1	Not demonstrated	Cancer	T-ALL	Human cell line xenograft	(Loosveld et al. 2014)
JQ1	BRD4	Cancer	T-cell leukemia	Rat-1-Tax GEM model	(Wu et al. 2013b)
OTX-015	BRD4	Cancer	B-cell lymphoma	Human cell line xenograft	(Boi et al. 2015)
MS417	BRD4	Cancer	Breast cancer	PI3K; Myc tumor cell allografts	(Stratikopoulos et al. 2015)
JQ1/MS417	BRD4	Cancer	Breast cancer	Human cell line xenograft	(Shi et al. 2014)
I-BET 151	BRD4	Cancer	Breast cancer	Murine cell line xenograft	(Alsarraj et al. 2013)

JQ1	BRD4	Cancer	Burkitt's lymphoma and AML	Human cell line xenograft	(Mertz et al. 2011)
MS417	BRD4	Cancer	Colorectal Cancer	Human cell line xenograft	(Hu et al. 2015)
CPI-203	BRD2/4	Cancer	Diffuse large B-cell lymphoma (DLBCL)	Human cell line xenograft	(Ceribelli et al. 2014)
JQ1	BRD4	Cancer	DLBCL	Human cell line xenograft	(Chapuy et al. 2013)
JQ1	Not demonstrated	Cancer	DLBCL	Human cell line xenograft	(Trabucco et al. 2015)
JQ1	BRD4	Cancer	Effusion lymphoma	Human cell line xenograft	(Tolani et al. 2014)
JQ1	BRD4	Cancer	ER+ breast cancers	Human cell line xenograft	(Bihani et al. 2015)
JQ1	BRD3/4	Cancer	Ewing sarcomas (ES)	Human cell line xenograft	(Hensel et al. 2015)
JQ1	BRD2/3/4	Cancer	Glioblastoma	Patient sample xenograft	(Cheng et al. 2013)
I-BET 151	BRD4	Cancer	Glioblastoma	Human cell line xenograft	(Pastori et al. 2014)
JQ1	Not demonstrated	Cancer	Glioblastoma Multiforme (GBM)	Rat cell line allografts	(Rajagopalan et al. 2014)
JQ1	BRD4	Cancer	Human hepatocellular carcinoma (HCC)	Human cell line xenograft	(Li et al. 2015)
JQ1	Not demonstrated	Cancer	Lung adenocarcinoma	DDR2L63V TP53L/L GEM model	(Xu et al. 2015)
JQ1	BRD4	Cancer	Lung adenocarcinoma	Human cell line xenograft	(Langdon et al. 2015)
JQ1	BRD4	Cancer	Lung cancer	Human cell line xenograft	(Zou et al. 2014)
JQ1	BRD4	Cancer	Lymphoma	Human cell line xenograft	(Tolani et al. 2014)
RVX-2135	Not demonstrated	Cancer	Lymphoma	Mouse cell line allografts	(Bhadury et al. 2014)
JQ1	BRD4	Cancer	Lymphoma	Human cell line xenograft	(Gopalakrishnan et al. 2015)
JQ1	BRD4	Cancer	Malignant peripheral nerve sheath tumor (MPNST)	Nf1 null and p53 null GEM model	(Patel et al. 2014)
JQ1	BRD4	Cancer	MPNST	Nf1/p53/Suz12 mutant GEM model	(De Raedt et al. 2014)
JQ1	Not demonstrated	Cancer	Mantle cell lymphoma (MCL)	Human cell line xenograft	(Sun et al. 2015a)
CPI-203	Not demonstrated	Cancer	MCL	Human cell line xenograft	(Moros et al. 2014)

JQ1	BRD4	Cancer	Medulloblastoma	Human cell line xenograft	(Venkataraman et al. 2014)
JQ1	BRD4	Cancer	Medulloblastoma	Hh-driven tumor allografts	(Tang et al. 2014)
I-BET 151	BRD4	Cancer	Medulloblastoma	Medulloblastomas allografts from Ptch1+/- GEM	(Long et al. 2014)
JQ1	BRD4	Cancer	Medulloblastoma	Human cell line xenograft	(Bandopadhyay et al. 2014)
JQ1	BRD4	Cancer	Medulloblastoma	Primary sample xenograft	(Bandopadhyay et al. 2014)
JQ1	BRD4	Cancer	Medulloblastoma	Human cell line xenograft	(Henssen et al. 2013)
I-BET 151	Not demonstrated	Cancer	Melanoma	Human cell line xenograft	(Heinemann et al. 2015)
I-BET 151	BRD2/3/4	Cancer	Melanoma	Human cell line xenograft	(Gallagher et al. 2014)
MS417	BRD4	Cancer	Melanoma	Human cell line xenograft	(Segura et al. 2013)
JQ1	Not demonstrated	Cancer	Merkel cell carcinoma (MCC)	Human cell line xenograft	(Shao et al. 2014)
JQ1	BRD4	Cancer	MCC	Human cell line xenograft	(Sengupta et al. 2015)
JQ1	Not demonstrated	Cancer	MCC	Human cell line xenograft	(Kannan et al. 2015)
JQ1	BRD4-NUT	Cancer	Midline carcinoma	Patient sample xenograft	(Filippakopoulos et al. 2010)
I-BET 151 /I-BET 762	BRD4	Cancer	Multiple myeloma	Human cell line xenograft	(Chaidos et al. 2014)
JQ1	BRD4	Cancer	Multiple myeloma	Human cell line xenograft	(Delmore et al. 2011)
JQ1	Not demonstrated	Cancer	Neuroblastoma	Human cell line xenograft	(Lee et al. 2015b)
OTX-015	BRD4	Cancer	Neuroblastoma	Human cell line xenograft	(Henssen et al. 2015)
JQ1	BRD4	Cancer	Neuroblastoma	Transplanted tumors from LSL-MYCN;Dbh-iCre mice	(Althoff et al. 2015)
JQ1	BRD3/BRD4	Cancer	Neuroblastoma	Human cell line xenograft	(Shahbazi et al. 2016)
JQ1	BRD4	Cancer	Neuroblastoma	Human cell line/primary sample xenograft and MYCN-amplified GEM model	(Puissant et al. 2013)
I-BET 762	BRD4	Cancer	Neuroblastoma	Human cell line xenograft	(Wyce et al. 2013b)

JQ1	Not demonstrated	Cancer	Osteosarcoma	Mouse cell line allografts	(Baker et al. 2015)
JQ1	BRD4	Cancer	Osteosarcoma	Human cell line xenograft	(Lee et al. 2015a)
JQ1	Not demonstrated	Cancer	Ovarian cancer	Orthotopic xenografts of ovarian cancer cells from T121+ p53f/f Brca1f/f serous ovarian cancer mouse model	(Qiu et al. 2015)
JQ1	BRD4	Cancer	Ovarian cancer	Human cell line xenograft	(Baratta et al. 2015)
JQ1	BRD4	Cancer	Pancreatic ductal adenocarcinoma (PDAC)	Intraductal papillary mucinous neoplasm (IPMN) derived PDA tumor cell allografts	(Roy et al. 2015)
JQ1	Not demonstrated	Cancer	PDAC	Kras; p53 mutant GEM model	(Mazur et al. 2015)
JQ1	Not demonstrated	Cancer	PDAC	Human cell line xenograft	(Garcia et al. 2015)
CPI-203	Not demonstrated	Cancer	Pancreatic neuroendocrine tumors	Human cell line xenograft	(Wong et al. 2014)
JQ1	BRD4	Cancer	Prostate Cancer	Pten loxP/loxP ;Trp53 loxP/loxP GEM	(Cho et al. 2014)
JQ1	BRD4	Cancer	Prostate cancer	Human cell line xenograft	(Lochrin et al. 2014)
JQ1/ I-BET 762	BRD4	Cancer	Prostate cancer	Human cell line xenograft	(Asangani et al. 2014)
JQ1	BRD2/3/4	Cancer	Prostate cancer	Human cell line xenograft	(Chan et al. 2015)
JQ1	Not demonstrated	Cancer	Prostate cancer	Pten deficient and p53 null GEM model	(Cho et al. 2014)
I-BET 762	Not demonstrated	Cancer	Prostate cancer	Human cell line xenograft	(Wyce et al. 2013a)
JQ1	Brd3/4	Cancer	Tamoxifen-resistant (Tam-R) breast cancer	Human cell line xenograft	(Feng et al. 2014)
JQ1	BRD4	Cancer	Triple-negative breast cancer	Human cell line xenograft	(Shu et al. 2016)
JQ1	BRD4	Cancer	Uveal melanoma	Human cell line xenograft	(Ambrosini et al. 2015)
I-BET 151	BRD4	Inflammation/ Immune	Acute graft-versus-host disease (GVHD)	MHC-disparate BALB/c→B6 BMT model	(Sun et al. 2015b)
RVX-208	Not demonstrated	Inflammation/ Immune	Atherosclerosis	Hyperlipidemic ApoE deficient mice	(Jahagirdar et al. 2014)
JQ1	BRD4	Inflammation/ Immune	Atherosclerosis	Low-density lipoprotein (LDL) receptor-deficient (Ldlr ^{-/-}) hypercholesterole mouse model	(Brown et al. 2014)
JQ1	BRD4	Inflammation/ Immune	Autoimmunity	MRL-lpr lupus mice	(Wei et al. 2015)

I-BET 762	Not demonstrated	Inflammation/ Immune	Autoimmunity	Adoptive transfer T cells in EAE disease model	(Bandukwala et al. 2012)
JQ1	BRD2/4	Inflammation/ Immune	Autoimmunity	CIA/EAE disease models of T cell autoimmune	(Mele et al. 2013)
MS417	BRD4	Inflammation/ Immune	Chronic kidney inflammation	HIV -1 transgenic mice (Tg26)	(Zhang et al. 2012)
MS417	Not demonstrated	Inflammation/ Immune	Diabetic nephropathy	Diabetic db/db mice	(Liu et al. 2014)
I-BET 151	BRD4	Inflammation/ Immune	Encephalomyelitis	Autoimmune encephalomyelitis mouse model of multiple sclerosis	(Barrett et al. 2014)
JQ1	BRD2/3/4	Inflammation/ Immune	Endotoxic shock	LPS stimulation	(Belkina et al. 2013)
I-BET 762	BRD2/3/4	Inflammation/ Immune	Endotoxic shock and sepsis	LPS-, heat-killed bacteria- or caecal ligation puncture stimulations	(Nicodeme et al. 2010)
JQ1	BRD4	Inflammation/ Immune	Periodontitis	Murine periodontitis model	(Meng et al. 2014)
JQ1	Not demonstrated	Inflammation/ Immune	Psoriasis	Mouse model of psoriasis-like inflammation	(Nadeem et al. 2015)
JQ1	BRD4	Inflammation/ Immune	Rheumatoid arthritis	Collagen-induced arthritis (CIA) mice	(Zhang et al. 2015)
JQ1	Not demonstrated	Inflammation/ Immune	Rheumatoid arthritis	Collagen-induced arthritis mice	(Xiao et al. 2015)
I-BET151	Not demonstrated	Inflammation/ Immune	Rheumatoid arthritis	K/BxN serum-induced arthritis mice	(Tough et al. 2015)
I-BET 726	Not demonstrated	Inflammation/ Immune	Sepsis	Septic shock mouse model	(Gosmini et al. 2014)
JQ1	BRD4	Kidney disease	Autosomal dominant polycystic kidney disease (ADPKD)	Pkd1 knockout GEM model	(Zhou et al. 2015)
JQ1	BRD4	Addiction	Cocaine-Induced Plasticity	Repeated cocaine injections and self-administration mice/rats	(Sartor et al. 2015)
JQ1	BRD4	Cardiovascular	Heart Failure	TAC/PE infusion mimic condition of heart failure	(Anand et al. 2013)
JQ1	BRD4	Cardiovascular	Heart Failure	TAC mimic condition of heart failure	(Spiltoir et al. 2013)
JQ1	BRD4	Cardiovascular	Pulmonary arterial hypertension (PAH)	Sugen/hypoxia rat model	(Meloche et al. 2015)
JQ1	BRD4	Fibrosis	Liver fibrosis	Carbon tetrachloride-induced fibrosis in mouse models	(Ding et al. 2015)
JQ1	BRD4	Fibrosis	Lung fibrosis	Bleomycin-induced lung fibrosis	(Tang et al. 2013a)
JQ1	BRD2/4	Fibrosis	Lung fibrosis	Bleomycin-induced lung fibrosis	(Tang et al. 2013b)

1.3 An uncharacterized NSD family protein NSD3

NSD3 (encoded by *WHSC1L1*) is a member of the NSD family of histone H3 lysine 36 (H3K36) methyltransferases, which function as oncoproteins in a variety of different cancer contexts (Li et al. 2009; Lucio-Eterovic and Carpenter 2011). The mammalian NSD family is composed of three members: NSD1, NSD2 and NSD3. All of them contain a Su(var)3-9, enhancer-of-zeste and trithorax (SET) domain, which displays H3K36 dimethyltransferase activity with nucleosomes as substrates. NSD2 is the only clearly identified H3K36 dimethyltransferase both in vivo and in vitro (Li et al. 2009). NSD family proteins possess multiple potential chromatin-binding motifs such as PHD and PWWP domains.

NSD3 exists as three different isoforms (long, short, and whistle) (Figure 1.1), with the long isoform possessing a H3K36 methyltransferase SET domain and seven chromatin reader modules (five PHD fingers and two PWWP domains) (Angrand et al. 2001; Kim et al. 2006). It has been reported that the fifth PHD domain of NSD3-long recognizes unmodified H3K4 and trimethylated H3K9 (He et al. 2013) while the PWWP domain is a weak reader of H3K36me_{2/3} (Vermeulen et al. 2010; Wu et al. 2011; Sankaran et al. 2016). NSD3-whistle is a testes-specific isoform that includes the catalytic SET domain and a C-terminal PWWP domain (Kim et al. 2006). NSD3-short is less than half the size of NSD3-long and lacks the catalytic SET domain and six of the chromatin reader modules, but retains a single N-terminal PWWP domain that binds to histone H3 when it is methylated at lysine 36 (Vermeulen et al. 2010; Wu et al. 2011; Sankaran et al. 2016).

While functions of the different NSD3 isoforms have been largely unexplored, one study suggests that NSD3-long can promote neural crest specification and migration through its H3K36 methyltransferase activity (Jacques-Fricke and Gammill 2014). A rare subset of AML

patients have been found to harbor a translocation involving *NUP98* and *WHSC1L1*, which generate fusions of NUP98 with NSD3-long and NSD3-short (Rosati et al. 2002). In midline carcinoma, rare chromosomal translocations lead to the formation of NSD3-NUT fusion oncoproteins, which also contain a region common to NSD3-short and NSD3-long (French et al. 2014). *WHSC1L1* also resides in a region on chromosome 8p11-12 that is commonly amplified in human breast and lung cancers, which has implicated NSD3 as an oncoprotein in these diseases (Tonon et al. 2005; Yang et al. 2010).

Despite the substantial evidence linking NSD3 to the pathogenesis of cancer, molecular mechanisms underlying its oncogenic function are unknown. Prior studies have shown that NSD3 can associate with BRD4 in nuclear lysates, although the nature of this interaction and its functional relevance remain unclear (Rahman et al. 2011; French et al. 2014).

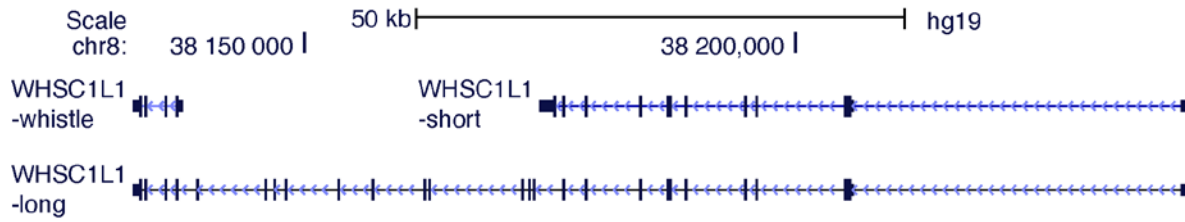


Figure 1.1 A diagram of the alternative transcript isoforms of the gene *WHSC1L1*. Wide boxes represent coding regions, lines represent introns and arrows show the direction of transcription.

Chapter 2: A Short Isoform of NSD3 Lacking Catalytic Function Is Essential in Acute Myeloid Leukemia

Because of successes in pre-clinical studies (Table 1.3) and phase I clinical trials in patients with acute myeloid leukemia (Berthon et al. 2016) and lymphoma (Amorim et al. 2016), components that operate in a “BRD4 pathway” may present additional therapeutic opportunities. Therefore, the mechanistic evaluation of this pathway is of high value.

With CRISPR-Cas9 scanning of *Brd4*, our lab previously identified the BRD4 CTD and ET domains (Figure 2.1) as requirements for the proliferation of RN2 cells, which is a cell line derived from a mouse model of MLL-AF9/*Nras*^{G12D} AML (Zuber et al. 2011a; Shi et al. 2015b). As mentioned earlier, BRD4 CTD has been linked to P-TEFb complex, thus promotes transcriptional elongation. However, the mechanism in which ET domain of BRD4 maintains AML is largely unknown. Therefore, it is interesting to investigate how ET-interacting proteins promote BRD4 function in leukemia maintenance.

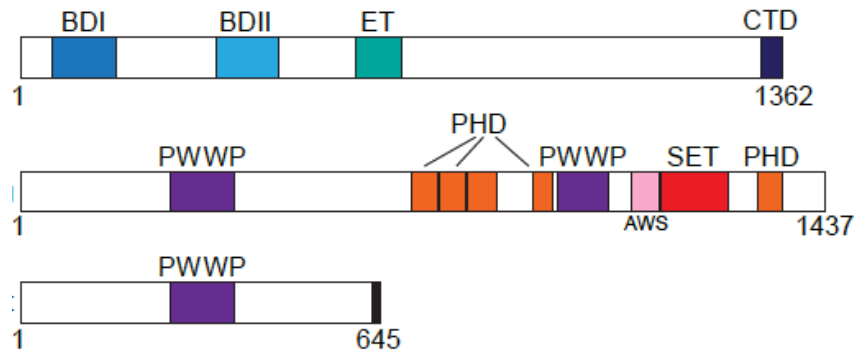


Figure 2.1 Domain architectures of human BRD4 and NSD3. BDI: bromodomain I, BDII: bromodomain II, ET: extraterminal domain, CTD: C-terminal domain. PWWP: Pro-Trp-Trp-Pro chromatin reader module. PHD: plant homeodomain finger. AWS: Associated with SET domain region, SET: Su(var)3-9, enhancer-of-zeste and trithorax domain which catalyzes H3K36 methylation. A region unique to NSD3-short is represented by a black rectangle.

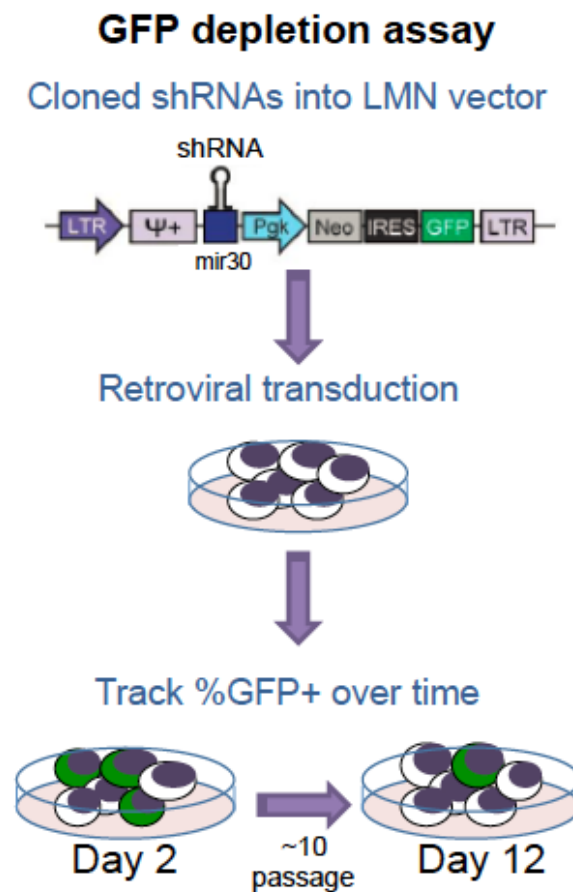


Figure 2.2 Workflow of GFP depletion assay to evaluate sensitivity of cells to shRNA-based targeting of specific proteins. A decrease of GFP signal indicates that the introduced shRNA suppresses gene expression essential for cell proliferation.

2.1 NSD3 is required for AML cell proliferation

To examine the molecular function of the BRD4 ET domain in AML, we measured the sensitivity of RN2 cells to small hairpin RNA (shRNA)-based targeting of known ET-associated proteins GLTSCR1, JMJD6, and NSD3 (Rahman et al. 2011; Liu et al. 2013) with a green fluorescent protein (GFP) depletion assay (Figure 2.2). In this assay, RN2 cells were retrovirally transduced with the individual LMN shRNA vectors, which express the shRNA and GFP from constitutive promoters. shRNA-induced proliferation arrest was monitored by GFP-negative cells outcompeting GFP-positive cells, which is represented as fold depletion. Among these candidates, only NSD3 shRNAs (which target exons common to both long and short isoforms) reduced the proliferation of RN2 cells *in vitro* (Figure 2.3A). The requirement of NSD3 in RN2 cells was repeatedly investigated and the knockdown efficiency of NSD3 shRNAs was evaluated with both reverse transcription-quantitative polymerase chain reaction (RT-qPCR) and Western blotting (Figure 2.6C and D). We generated a polyclonal antibody that recognizes the long and short NSD3 isoforms because commercial antibodies gave inconsistent results. I tested the antibody by western blotting, immunoprecipitation (IP) and chromatin immunoprecipitation (ChIP), and used it throughout my thesis.

Moreover, to exclude tissue culture artifacts, I also confirmed the requirement of NSD3 in human AML cell lines HL-60, MOLM-13, and NOMO-1 (Figure 2.3B-E) as well as *in vivo* mouse experiments, which showed less disease burden and a survival benefit in NSD3 deficient mice (Figure 2.3F-G).

In order to rule out the possibility that NSD3 has a broad impact for cell proliferation, sensitivity to NSD3 knockdown in immortalized mouse embryonic fibroblasts (MEFs) and a variety of mouse cancer cell lines were measured over 10 days. A heatmap was generated

according to the fold depletion (Figure 2.4A) and suggests a preferential sensitivity to NSD3 knockdown in AML and B cell-acute lymphocytic leukemia (B-ALL) cell lines. Since cell proliferation rate could be a factor that impacts on the sensitivity to NSD3 knockdown, GFP depletion assays were also performed for longer time periods in MEFs and prostate cancer (MycCap) and cholangiocarcinoma (CHC1) cancer cell lines (Figure 2.4B-D) to confirm that NSD3 is not required for cell proliferation in those cell lines.

These results collectively prompted our investigation of NSD3 as a candidate effector of BRD4 that supports AML maintenance.

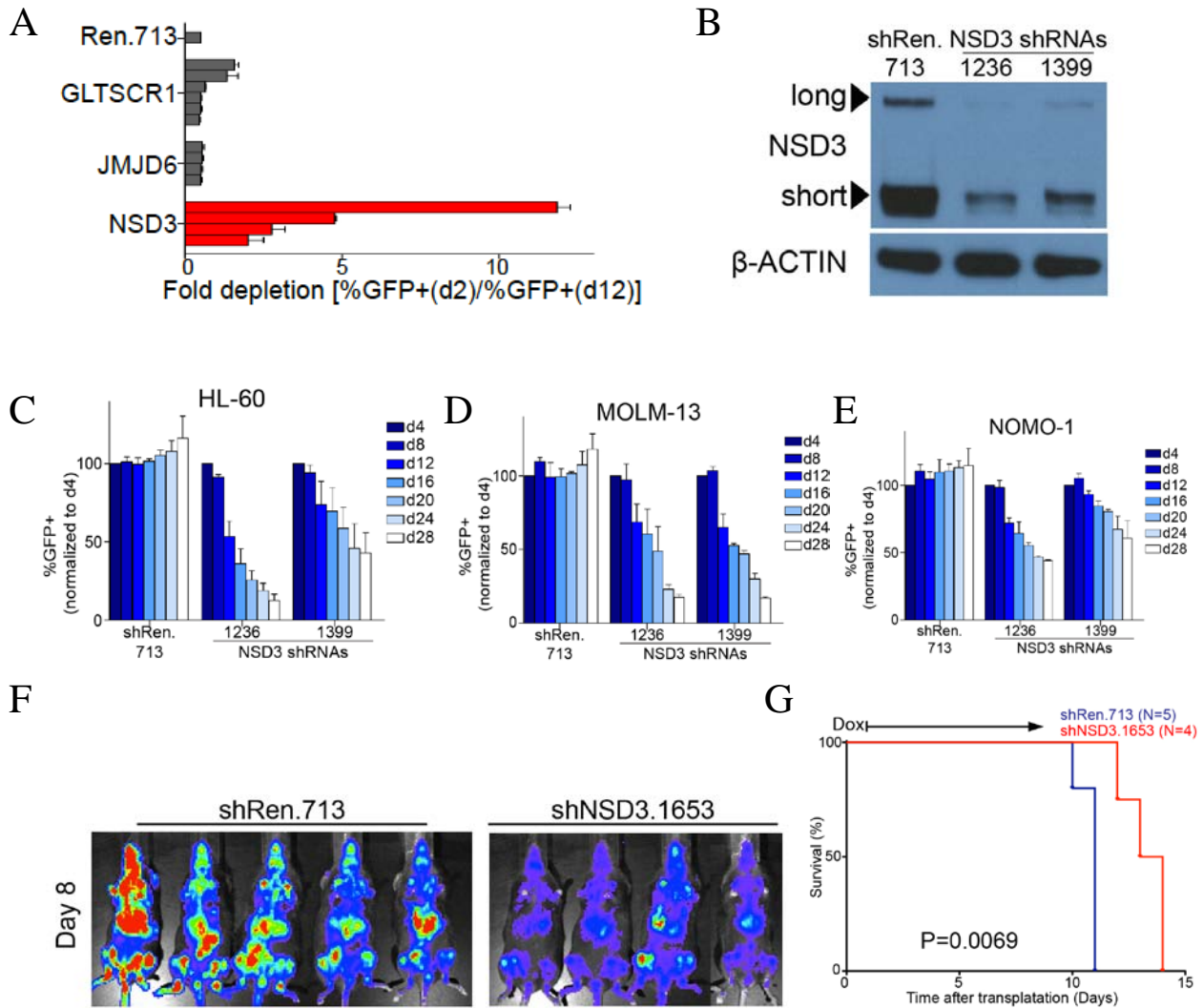


Figure 2.3 NSD3 is required for AML maintenance.

(A) Competition-based assay in RN2 cells evaluating effects of the indicated LMN shRNAs (which express GFP) on cell proliferation. Each horizontal bar represents the average fold-decrease in GFP percentage for an independent shRNA over 10 days in culture. (B) Western blotting of whole cell lysates in human OPM-1 cells transduced with the indicated MLS-shRNA constructs. A representative experiment of three biological replicates is shown. (C-E) Competition-based assay in human AML cell lines evaluating effects of the indicated MLS shRNAs (which express a GFP) on cell proliferation. GFP percentages were normalized to day 4 (d4) measurements. (F) Bioluminescent imaging of mice transplanted with RN2 cells harboring the indicated TRMPV-Neo-shRNAs. Dox was administered 1 day after transplant. (G) Kaplan-Meier survival curves of recipient mice transplanted with the indicated TRMPV-Neo-shRNA leukemia lines. The interval of dox treatment is indicated by the arrow. Statistical significance compared to shRen.713 was calculated using a log-rank test. All error bars represent SEM for n=3.

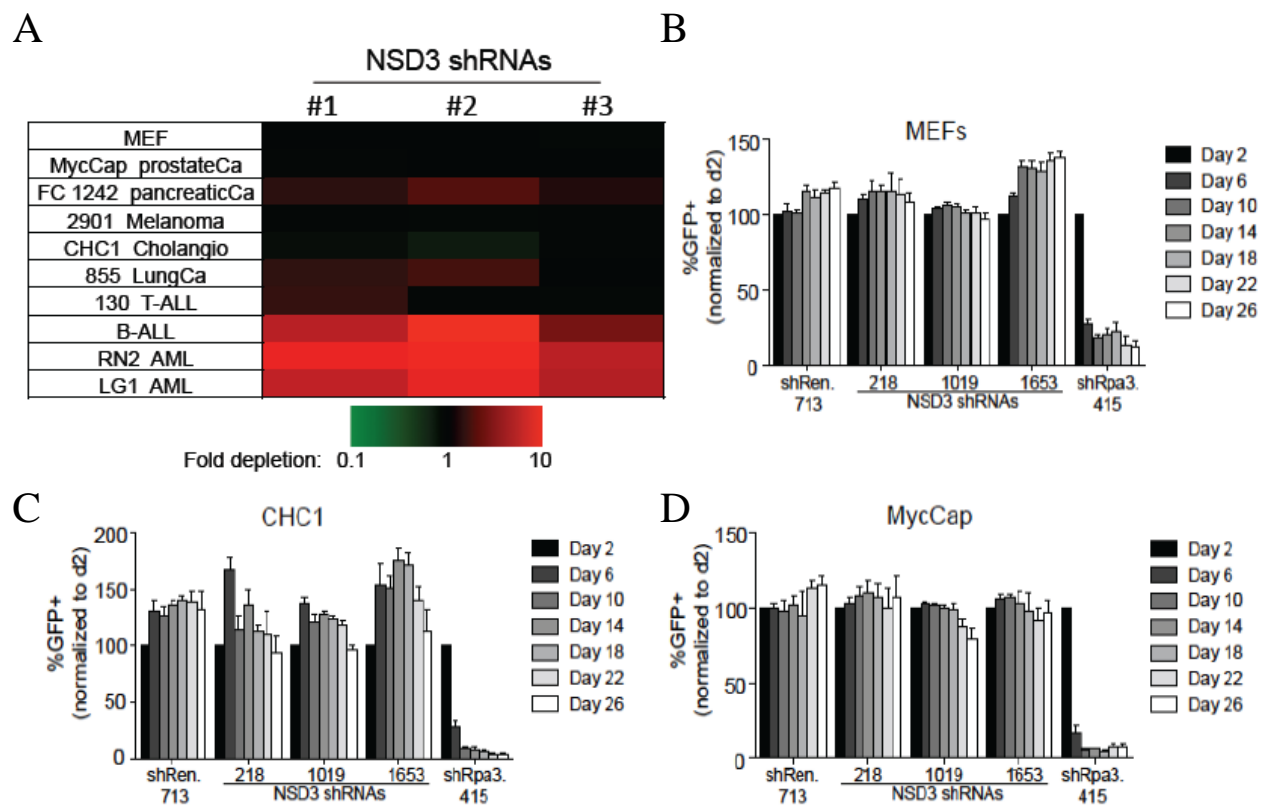


Figure 2.4 NSD3 does not have a broad impact on cell proliferation. (A) Fold depletion in GFP percentage for independent shRNAs over 10 days shown by heatmap (B-D) Competition-based assay in indicated cells evaluating effects of the indicated LMN shRNAs (which express GFP) on cell proliferation. GFP percentages were normalized to day 2 (d2) measurements. All error bars represent SEM for n=3.

2.2 NSD3 is required for maintaining the undifferentiated state of AML cells

To further examine whether targeting NSD3 leads to similar phenotypic effects caused by BRD4 suppression in AML cells either by shRNA knockdown or JQ1 treatment, the differentiation state of AML cells was evaluated after NSD3 knockdown by shRNAs. RN2 cells were retrovirally introduced with TRMPV-Neo shRNA and followed by doxycycline (dox) treatment for 96 hours to induce the expression of shRNAs. Using flow cytometry, a decrease in the expression of c-Kit and an increase in Mac-1 on the cell surface was observed upon NSD3 knockdown, which is a myeloid differentiation immunophenotype that has previously been associated with BRD4 inhibition (Figure 2.5A) (Zuber et al. 2011b). Moreover, targeting of NSD3 caused RN2 cells to undergo morphological changes associated with terminal myeloid differentiation (Figure 2.5B). This differentiation phenotype was prevented if c-Myc was expressed ectopically from a retroviral promoter (Figure 2.5B).

2.3 *c-Myc* is an essential target gene of NSD3 in AML maintenance

The proliferation arrest of RN2 cells caused by knockdown of endogenous NSD3-long and -short was rescued by ectopically expressing c-Myc (Figure 2.6A and B). Analogous to prior analyses of BRD4 inhibition in RN2 cells, knockdown of NSD3 resulted in a decrease in the expression of c-Myc both at the mRNA and protein level (Figure 2.6C and D). These data suggest that c-Myc is an essential downstream of NSD3 in AML.

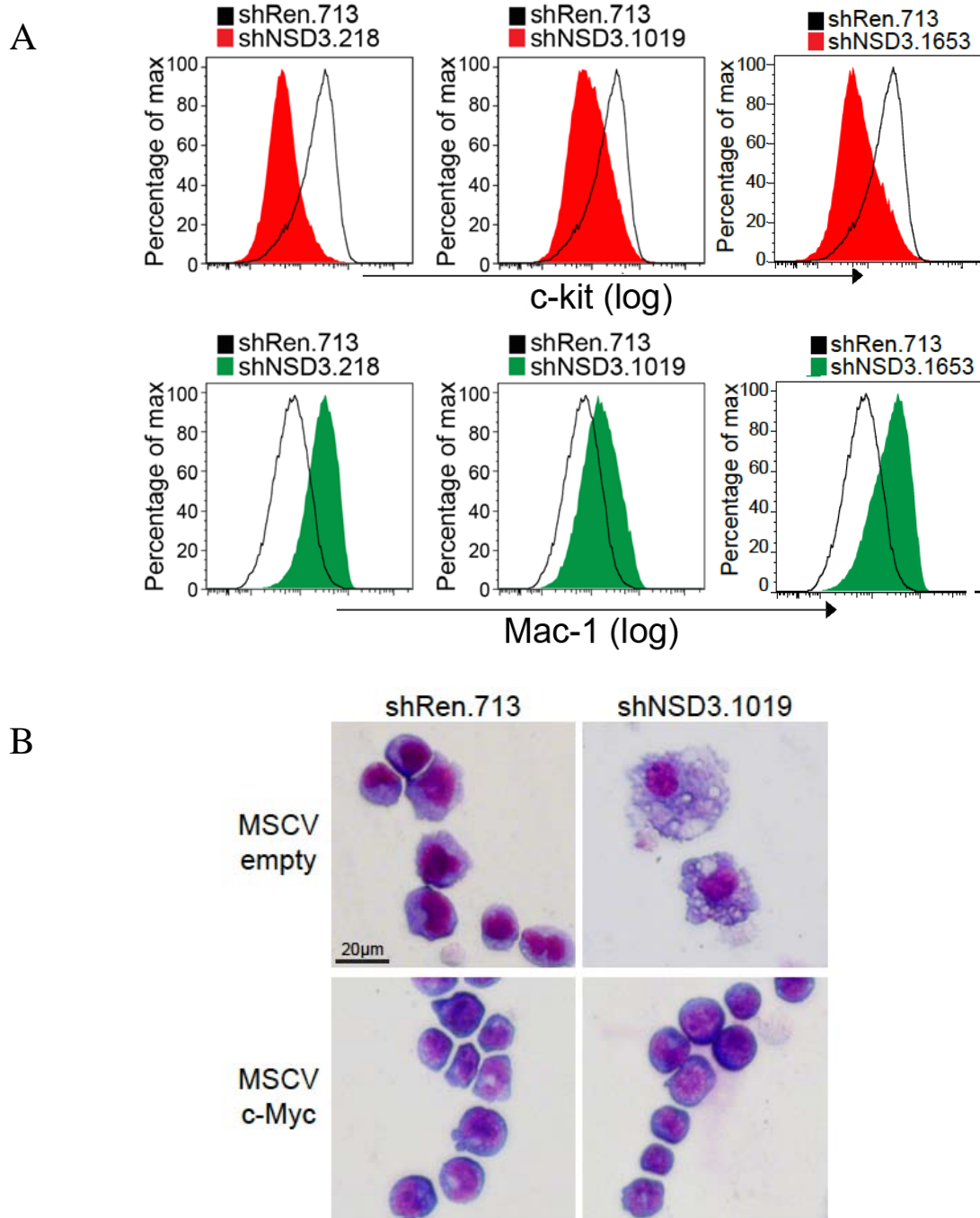


Figure 2.5 NSD3 is required for maintaining the undifferentiated state of AML cell. (A) Flow cytometry analysis of c-Kit and Mac-1 stained RN2 cells following TRMPV-Neo shRNA induction with dox for 96 hours. Gating was performed on dsRed+/shRNA+ cells. A representative experiment of three biological replicates is shown. (B) Light microscopy of May-Grünwald/Giemsa-stained RN2 cells expressing the indicated NSD3 shRNAs in the presence or absence of ectopic c-Myc expression. shRNA expression was induced using the TRMPV-Neo vector treated with dox for 4 days. Imaging was performed with a 40x objective. A representative image of three independent biological replicates is shown.

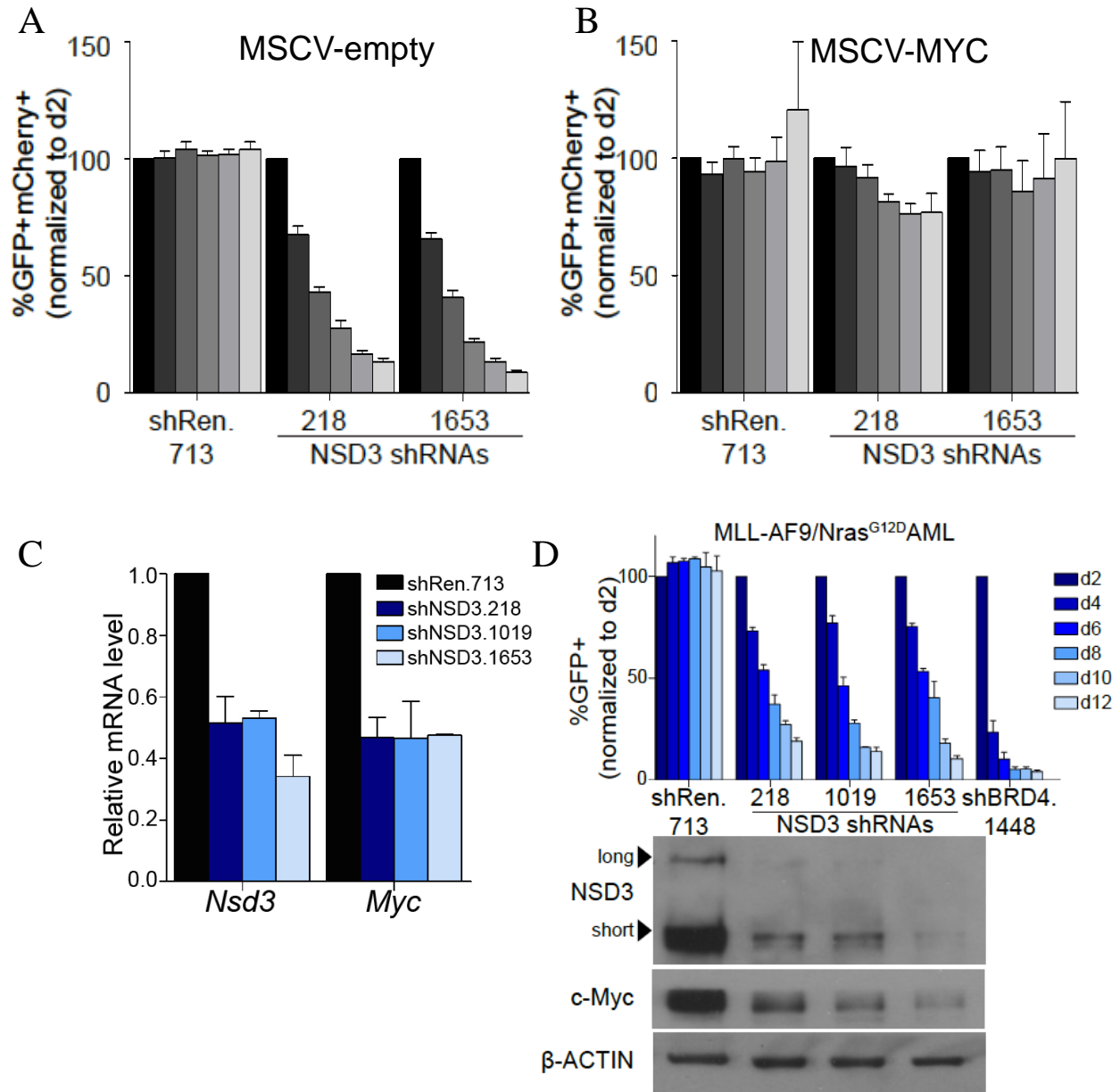


Figure 2.6 *c-Myc* is an essential target gene of NSD3 in AML. (A and B) Competition-based assay evaluating the effect of the *c-Myc* cDNA on the proliferation arrest induced by NSD3 shRNAs. Results were normalized to the d2 percentage of GFP+mCherry+ cells. (C) RT-qPCR analysis performed for RN2 cells expressing the indicated TRMPV-Neo shRNAs following 48 hours of dox treatment. Results are normalized to *Gapdh*. (D) (top) Competition-based assays to evaluate the effect of NSD3 LMN shRNAs on RN2 cell proliferation. GFP percentages are normalized to d2 measurements. (bottom) Western blotting analysis of whole cell lysates prepared from RN2 cells transduced with the indicated TRMPV-Neo constructs following 48 hours of dox treatment. A representative experiment of three biological replicates is shown. All error bars represent the SEM for n=3.

2.4 NSD3 regulates a similar global gene profile with BRD4 in AML

Finally, to compare the global gene regulatory profile between BRD4 and NSD3, RNA-Seq analysis was performed in RN2 cells after NSD3 knockdown. Gene expression in RN2 cells expressing two independent NSD3 shRNAs was compared to that expressing a Ren.713 shRNA. Log₂ fold changes in gene expression were ranked and ran into Gene Set Enrichment Analysis (GSEA), which is a computational method to determine whether a defined set of genes presents statistically significant differences in expression patterns between two groups (Subramanian et al. 2005).

GSEA confirmed that targeting of NSD3 led to significant changes in gene expression signatures previously associated with BRD4 function in leukemia cells (Figure 2.7A-D) (Zuber et al. 2011b). GSEA revealed a significant upregulation of a macrophage signature and a downregulation of a leukemia stem cell (LSC) signature (Somerville et al. 2009) upon NSD3 knockdown (Figure 2.7A and B), suggesting a role for NSD3 in maintaining an undifferentiated state of AML cells. A similar profile of gene expression changes after BRD4 knockdown (Zuber et al. 2011b) was also observed, as well as Myc target genes (Schuhmacher et al. 2001) (Figure 2.7C and D). Collectively, these results indicate that BRD4 and NSD3 regulate an overlapping gene profile in AML.

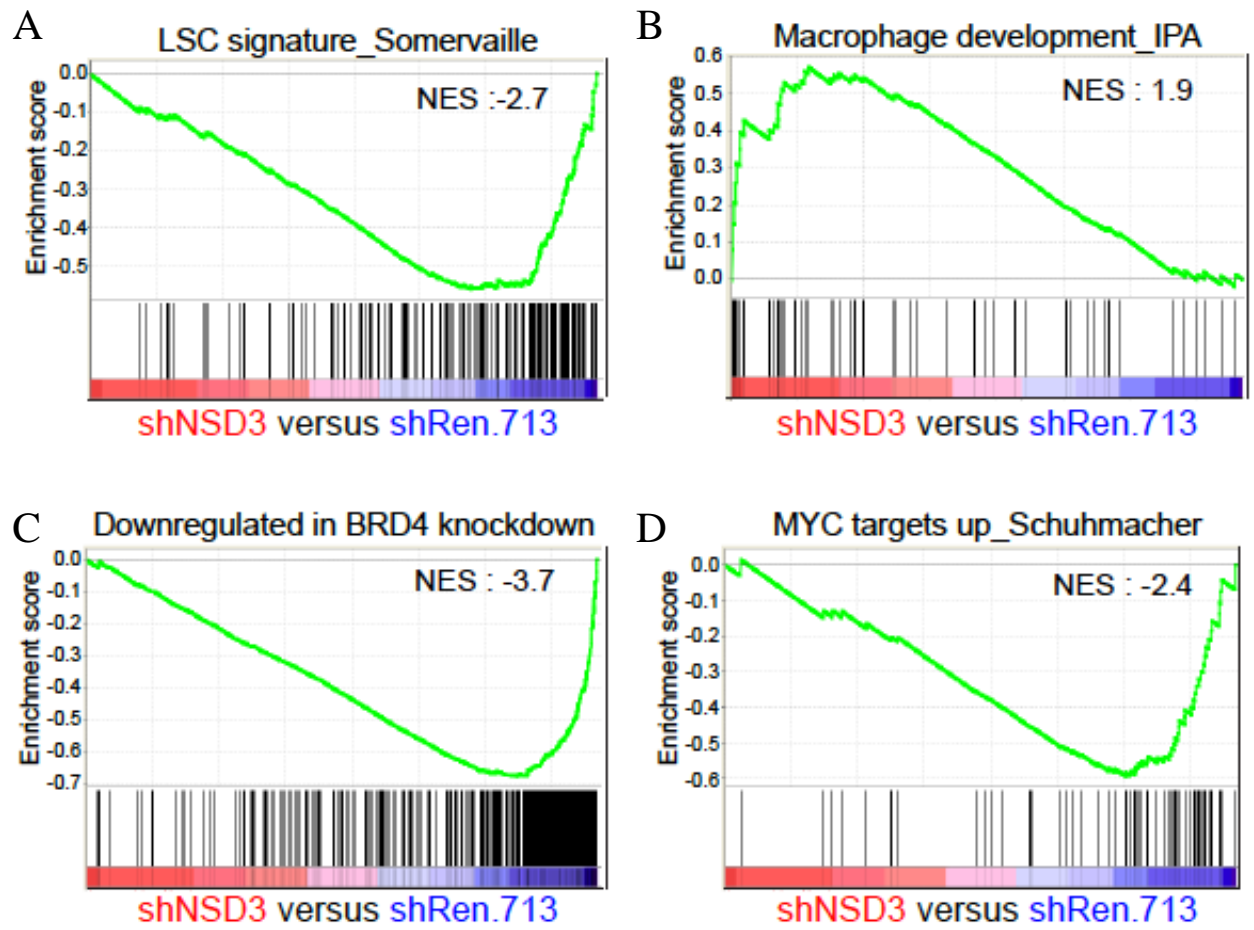


Figure 2.7 NSD3 regulates a similar global gene profile with BRD4 in AML. (A-D) GSEA of RNA-Seq data obtained from RN2 cells expressing NSD3 TRMPV-Neo shRNAs (induced with dox for 48 hours). Two independent NSD3 shRNAs were compared to a Ren.713 shRNA in this analysis. NES: normalized enrichment score. For each of the indicated gene sets shown, the false discovery rate (FDR) and nominal p-value were <0.01.

2.5 A short isoform of NSD3 is essential in AML

While NSD3 contains two major isoforms, the NSD3-short was consistently expressed at higher levels than NSD3-long in all the cell lines tested in this study (Figure 2.3B, Figure 2.6D, Figure 3.1A and B). This prompted me to investigate whether the enzymatic function of NSD3-long could contribute to BRD4 function in AML. To first investigate which isoform is required in AML, I knocked down NSD3-long alone to evaluate the impact on RN2 cell proliferation. Compared to those shRNAs targeting exons shared by NSD3-long and NSD3-short which suppressed RN2 proliferation (Figure 2.6D), shRNAs that selectively suppressed NSD3-long resulted in no significant effects either on cell proliferation or c-Myc expression (Figure 2.8A).

Because it is hard to design shRNAs that only target NSD3-short, I performed an shRNAs/cDNA rescue assay to evaluate the function of NSD3-short to support AML cell proliferation. I generated RN2 cells that ectopically express human NSD3-short. The proliferation arrest caused by knockdown of endogenous NSD3-long and -short was rescued by expressing an shRNA-resistant NSD3-short cDNA (Figure 2.8B and C). The same results were observed in the human AML cell line HL60 (Figure 2.8D and E). Silent substitutions were introduced in human NSD3-short cDNA for overexpression in HL60 cells (Figure 2.8D-F).

Furthermore, I confirmed that NSD3-short is essential for transcriptional activation as well. In RN2 cells upon NSD3 knockdown, shRNA-resistant NSD3-short maintains the expression of c-Myc and other NSD3 regulatory genes identified by RNA-Seq (Figure 2.9A). Moreover, GAL4-luciferase reporter assays also revealed that NSD3-short activates transcriptional activation to a much greater extent than NSD3-long (Figure 2.9B).

These unexpected results indicated that the seemingly unimportant protein, lacking the enzymatic functions, is the essential isoform for AML maintenance. This finding suggests that to

achieve the anti-tumor activity, pharmacological inhibition of NSD3 should target the short isoform instead of the enzymatic SET domain.

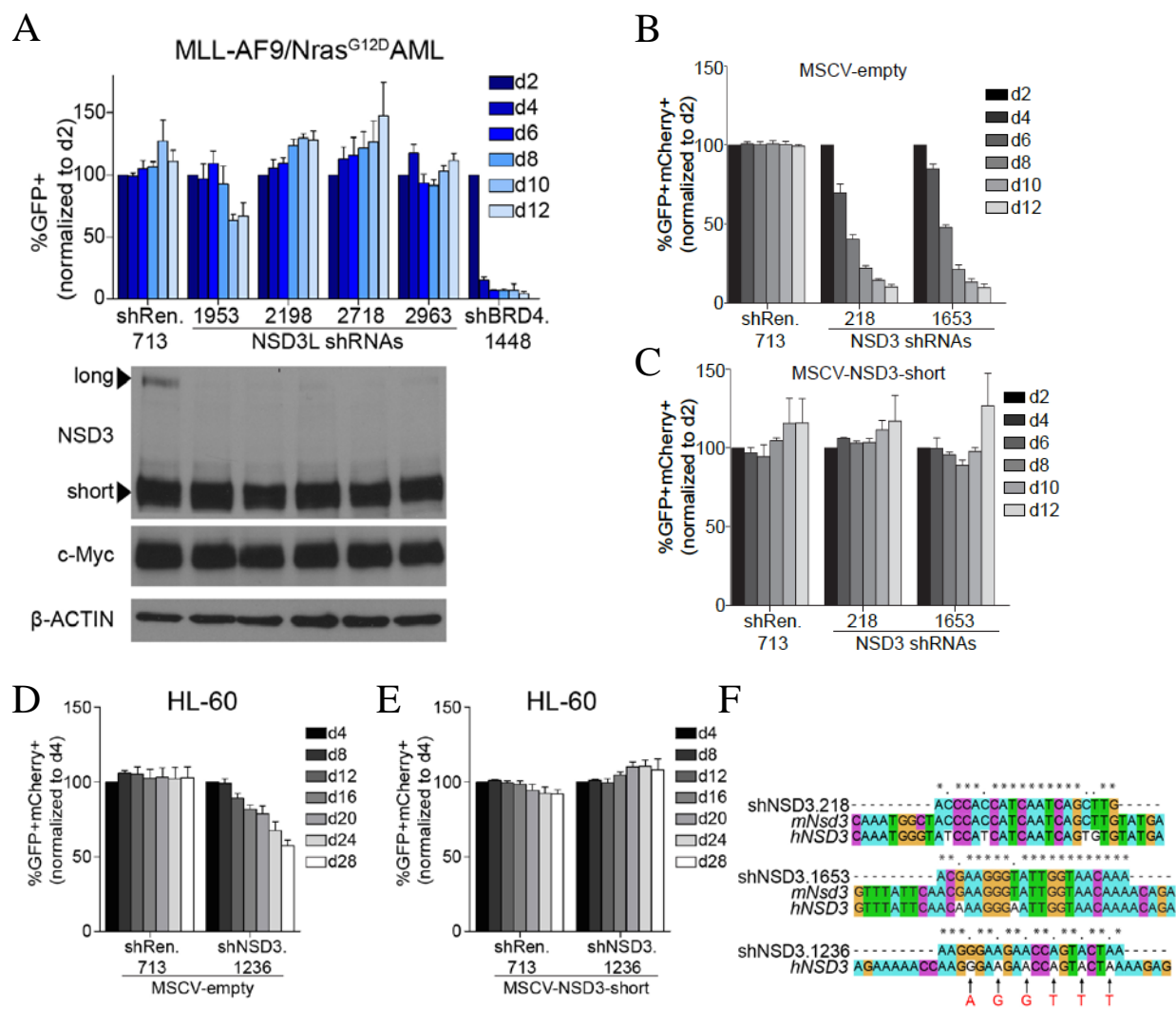
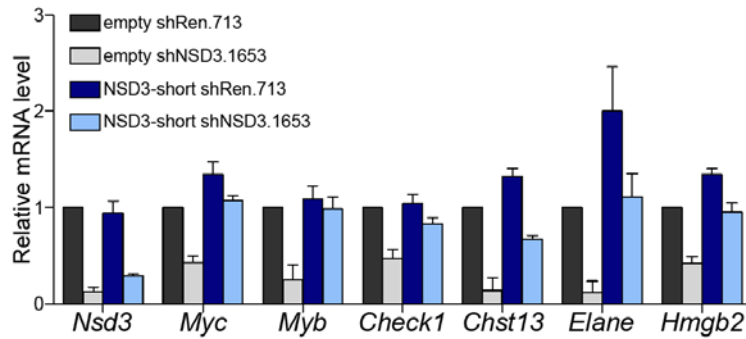


Figure 2.8 A short isoform of NSD3 is essential in AML.

(A) (top) Competition-based assays to evaluate the effect of NSD3L LMN shRNAs on RN2 cell proliferation. GFP percentages are normalized to d2 measurements. (bottom) Western blotting analysis of whole cell lysates prepared from RN2 cells transduced with the indicated TRMPV-Neo constructs following 48 hours of dox treatment. A representative experiment of three biological replicates is shown. (B-D) Competition-based assay evaluating the effect of the human NSD3-short cDNA (which is not recognized by the murine shRNAs and is expressed with the PIG vector linked to GFP) on the proliferation arrest induced by NSD3 shRNAs (expressed using the LMN-mCherry vector). Results were normalized to the d2 percentage of GFP+mCherry+ cells. All error bars represent the SEM for n=3. (F) Sequence alignments of mouse and human NSD3/WHSC1L1 sequence with indicated shRNAs. shNSD3.218 and shNSD3.1653 target the mouse NSD3 and shNSD3.1236 targets the human NSD3. For cDNA/shRNA rescue experiments in HL-60 cells, we made silent substitutions of human NSD3 cDNA as shown in red.

A



B

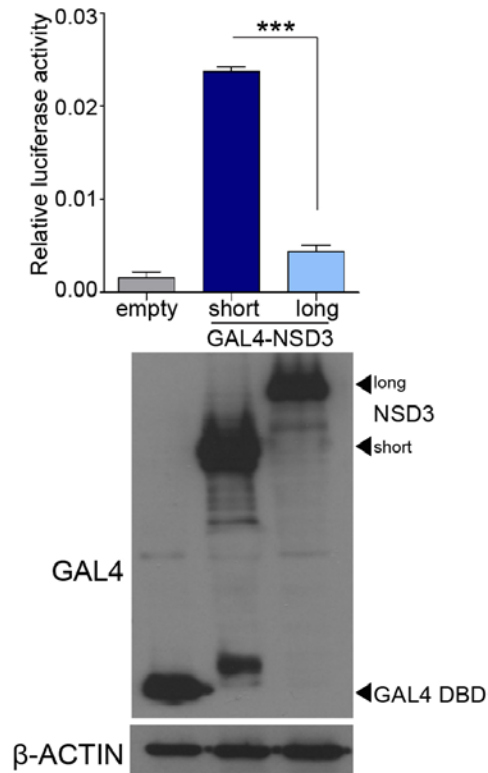


Figure 2.9 NSD3-short is essential for transcriptional activation.

(A) RT-qPCR analysis to evaluate effects of NSD3 knockdown on indicated gene expression in RN2 cells transduced with the FLAG-NSD3-short construct or empty vector. Indicated TRMPV-Neo shRNAs were induced by dox for 48 hours. Results are normalized to *Gapdh*. (B) (top) Luciferase reporter assay. (bottom) Western blotting analysis of HEK293T cells transfected with the indicated plasmids from (top). Western blotting experiments shown are a representative experiment of at least three independent biological replicates. . All error bars in this figure represent SEM for n=3. ***p<0.001, two-tailed Student's t-test.

Chapter 3: NSD3-short Binds Directly to the BRD4 ET Domain

As a putative ET-interacting protein, prior studies have shown that NSD3 can associate with BRD4 in nuclear lysates, however, the nature of this interaction and its functional relevance remains unclear (Rahman et al. 2011; French et al. 2014). With a series of thorough experiments, I identified the binding regions between NSD3 and BRD4 and confirmed the direct interaction between them.

3.1 NSD3 is an ET-domain associated protein

In order to confirm the presence of the BRD4-NSD3 complex in a leukemia context, I performed reciprocal IP of endogenous BRD4 (with an antibody targeting BRD4-long) or NSD3 (with an antibody targeting NSD3-long and -short) from human AML cell line NOMO-1 nuclear lysates followed by Western blotting. The association between BRD4 and both isoforms of NSD3 was confirmed in this cell type (Figure 3.1A).

I also confirmed NSD3 is an ET-domain associated protein. After transient expression of different FLAG-tagged BRD4 constructs in HEK293T cells for 48 hours, nuclear lysate was prepared for IP experiments. Western blotting indicated the ET domain-containing region pulled down NSD3-long and -short as efficiently as BRD4-short, but not the fragment containing bromodomains (Figure 3.1B and C). Taken together, the ET domain of BRD4 is sufficient for NSD3 interaction (Figure 3.1B and C) and the common region within NSD3-long and -short binds the ET domain.

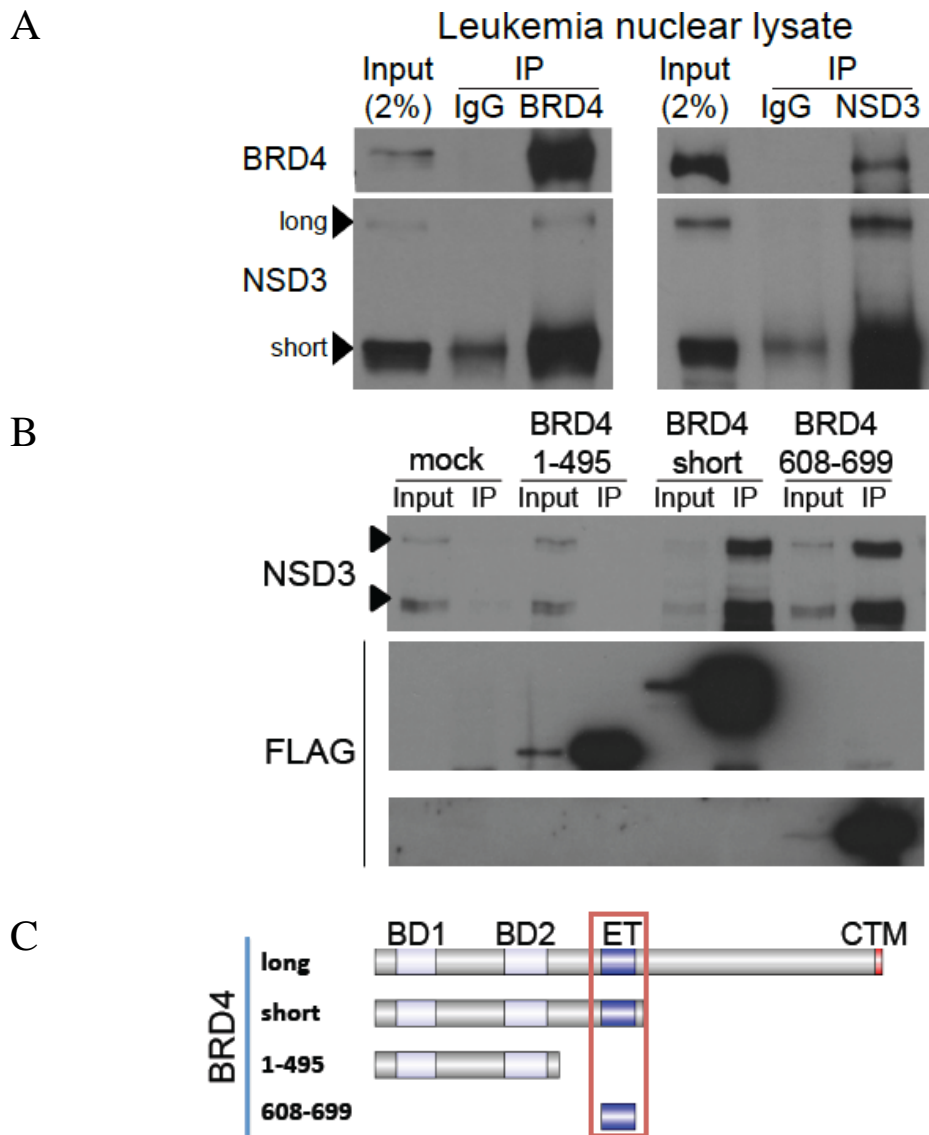


Figure 3.1 NSD3-short is an ET-domain associated protein.

(A) Immunoprecipitation followed by Western blotting performed with the indicated antibodies. The nuclear lysate was prepared from the human AML cell line NOMO-1. IP: immunoprecipitation, IgG: isotype control immunoglobulin. Note: a background band appears in the control IP at ~70 kDa, which is near the NSD3-short band. Shown is a representative experiment of three independent biological replicates. (B) FLAG-tag IP-Western blotting of transiently expressed constructs indicated. (C) Domain architectures of human BRD4 to indicate NSD3 binding domain.

3.2 NSD3-short 100-263 is a BRD4 interacting domain

Further, I mapped the region of NSD3-short that associates with BRD4 with FLAG IP experiments. First, FLAG-tagged BRD4 ET domains were transiently expressed in HEK293T cell for 48 hours. After extensive washes, FLAG-ET was immobilized on agarose beads followed by incubation with purified GST-tagged fragments of NSD3-short expressed in *E. coli*. Unbound NSD3 fragments were washed out and then bound NSD3 fragments were detected by Western blotting (Figure 3.2A). Pull-down experiments revealed that the BRD4-binding region resides between amino acids 100 to 263 of NSD3 (Figure 3.2B-D). Due to the limitation of protein purity in this assay, the direct interaction between BRD4 and NSD3 was proven by a more stringent assay (discussed later).

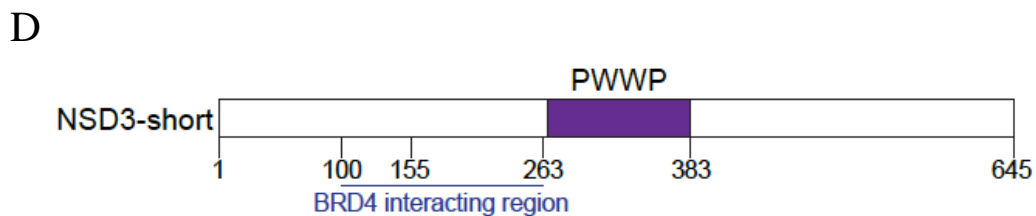
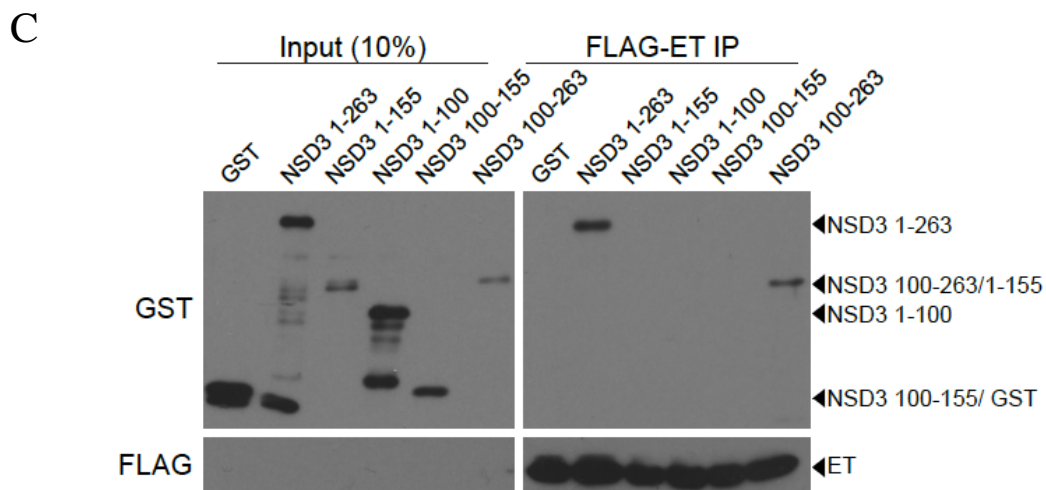
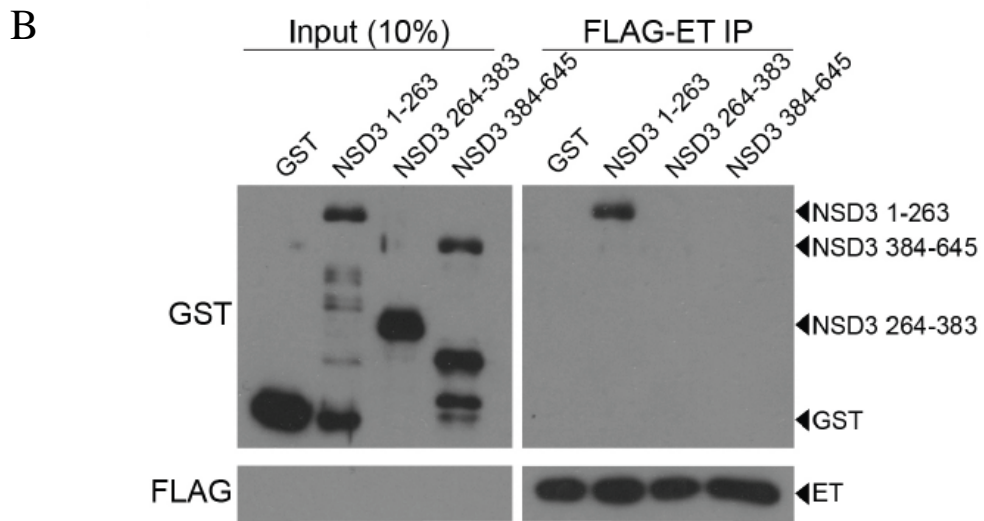
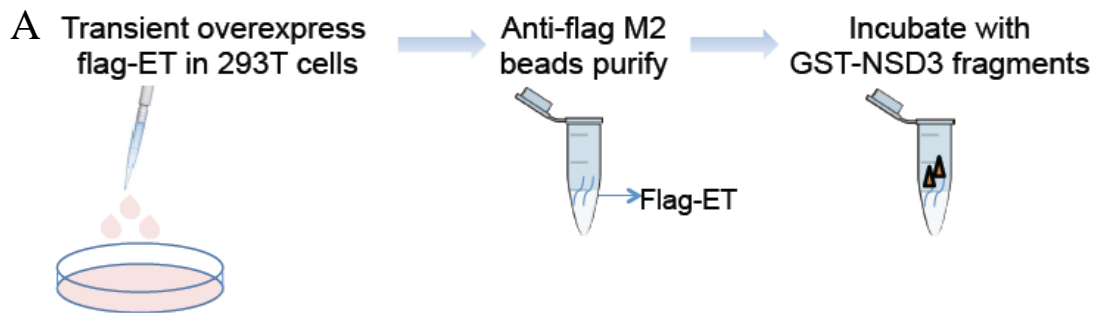


Figure 3.2 NSD3-short 100-263 is BRD4 interacting domain.

(A) Workflow for FLAG pull-down assays to identify BRD4 interacting region of NSD3 (B and C) FLAG-BRD4 ET domain pull-down assays evaluating interactions with the indicated GST-NSD3 fragments. FLAG-BRD4 ET domain was expressed in HEK293T followed by immobilization on anti-FLAG agarose beads and extensive washing. ET immobilized beads were then incubated with purified GST-NSD3 fragments expressed in *E. coli*. A representative experiment of three biological replicates is shown. D) Diagram of NSD3-short fragments evaluated in the BRD4 ET pull-down assay.

3.3 NSD3-short 100-263 Binds BRD4 ET-domain directly

In order to investigate whether NSD3 directly binds BRD4, I collaborated with Jonathan Ipsaro from Dr. Leemor Joshua-Tor's lab at Cold Spring Harbor Laboratory (CSHL). After copurification of Strep₂SUMO-BRD4 ET with untagged NSD3 (100-263) from Sf9 cells with a Strep-Tactin (IBA) column, a gel filtration separation step was performed for the elute. SDS-PAGE and Coomassie Blue staining revealed the purity of the recombinant protein and showed that the BRD4 ET and NSD3 100-263 could be copurified in an apparent 1:1 ratio (Figure 3.3A).

Surface plasmon resonance (SPR) analysis of purified BRD4 ET and NSD3 100-263 further validated the interaction between these proteins with an estimated dissociation constant of 2.1 μ M (Figure 3.3C and D). In this assay, Strep₂SUMO-BRD4 ET and Strep₂SUMO-NSD3 100-263 proteins were individually expressed in Sf9 cells and purified by affinity, ion exchange, and size exclusion chromatography. The final purity of these proteins was assessed by SDS-PAGE (Figure 3.3B). Strep₂SUMO-NSD3 100-263 (analyte) was diluted serially to the concentrations indicated and injected over a flow cell prepared with immobilized Strep₂SUMO-BRD4 ET (ligand). Injections began at a time corresponding to 0 seconds with an association phase of 60 seconds. At 60 seconds, application of NSD3 100-263 was stopped and a dissociation phase of 120 seconds followed. A representative concentration series is shown in Figure 3.3 C. Steady-state response values from the association phase of each injection were plotted as a function of analyte concentration and fit to determine the K_D (Figure 3.3D).

These experiments confirmed that NSD3-short directly binds to the BRD4 ET domain.

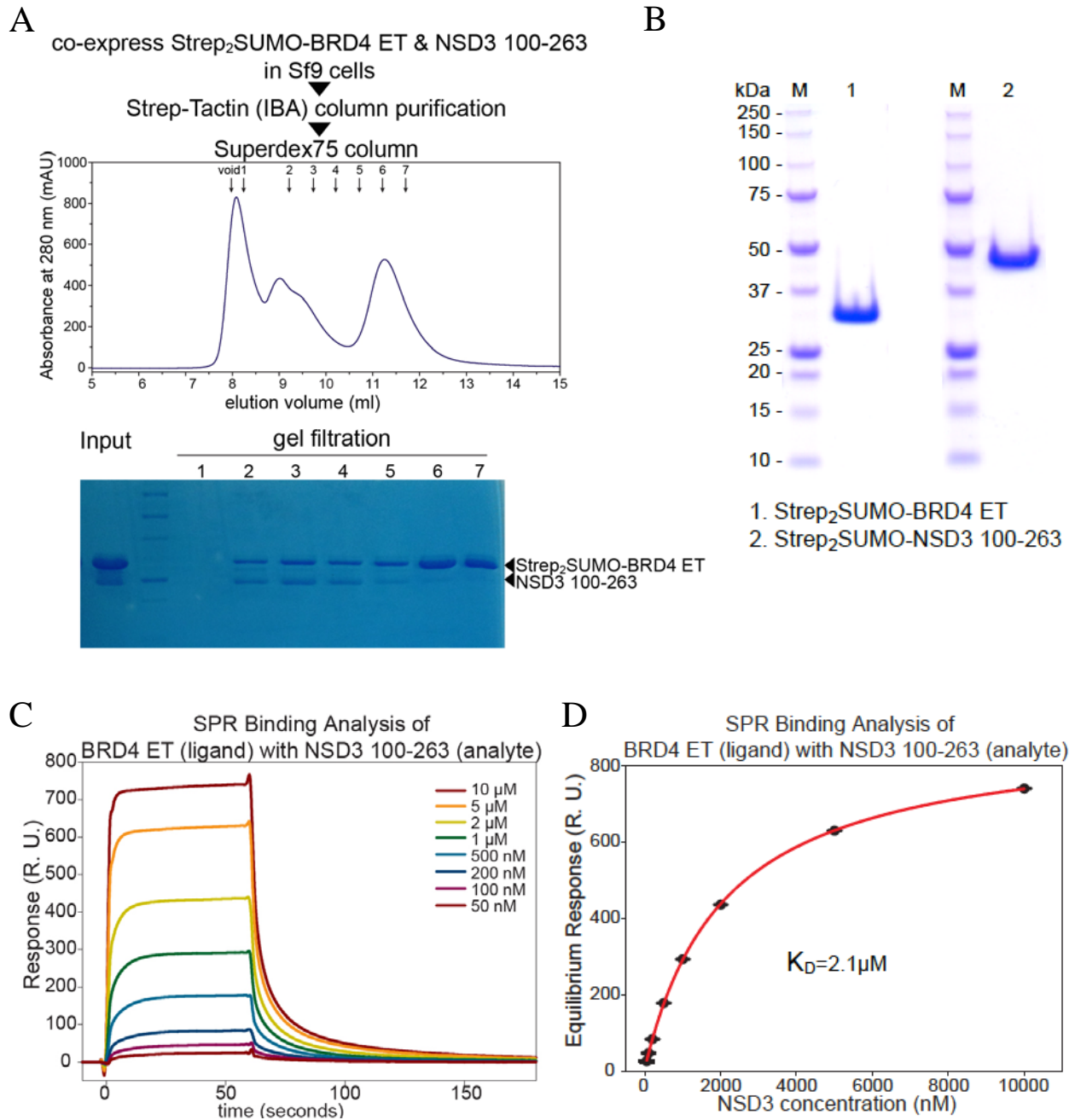


Figure 3.3 NSD3-short 100-263 binds BRD4 ET-domain directly. (A) Gel filtration separation of Strep₂SUMO-BRD4 ET with untagged NSD3 (100-263) copurified from Sf9 cells. (B) Recombinant protein purity was assessed by SDS-PAGE and Coomassie Blue staining. (C) Surface plasmon resonance sensorgrams of BRD4 ET-NSD3 binding. One representative concentration series is shown. (D) Binding affinity of the BRD4 ET-NSD3 interaction as determined by surface plasmon resonance using purified proteins. Steady-state response values from the association phase of each injection were plotted as a function of analyte concentration and fit to determine the K_D . Points indicate the average of three technical replicates with error bars representing the standard deviation.

3.4 Dissociation of NSD3 from BRD4 impairs ET domain functions

To demonstrate that NSD3 is a BRD4 effector in AML maintenance, I sought to test whether the dissociation of NSD3 leads to the functional impairment of BRD4. To answer this question, I performed structure-guided mutagenesis on the ET surface and assayed the impact on NSD3 binding *in vitro*. Although the structure of the BRD4 ET domain has been published (PDB: 2JNS) (Lin et al. 2008) (Figure 3.4D), NSD3 binding surface remained elusive. While alanine substitutions at 26 different charged residues had no effect on the NSD3 interaction, replacement of three hydrophobic residues with bulkier side chains (L630W, I654Q, or F656W) was each sufficient to disrupt NSD3 binding (Figure 3.4A-C). All three of these residues localize to a single hydrophobic groove on the surface of the ET domain, which is the likely binding surface for NSD3 (Figure 3.4D).

I next evaluated whether the three ET domain point mutations that disrupt NSD3 binding also resulted in a defect in BRD4-dependent transcriptional activation. HEK293T cells were co-transfected with p9xGAL4-UAS-luciferase (firefly) reporter and the indicated GAL4 fusion expression plasmids expressing Renilla luciferase from a constitutive promoter. When fused to the DNA binding domain of GAL4, the BRD4 ET domain activated transcription of a plasmid-based luciferase reporter harboring GAL4 recognition motifs upstream of a minimal promoter (Figure 3.4E). In contrast to the wild-type ET domain, the L630W, I654Q, and F656W substitutions each led to reduced transcriptional activation (Figure 3.4E). While we cannot rule out that the three ET mutations compromise the interaction with multiple binding partners, these results support the functional importance of the NSD3-BRD4 interaction for transcriptional activation.

However, I failed to evaluate whether these three point mutations could lead to functional impairment of full-length BRD4 in supporting AML cell proliferation as overexpression of full-length BRD4, either with or without mutations, resulted in severe cell proliferation arrest in RN2 cells when the MSCV vector was used.

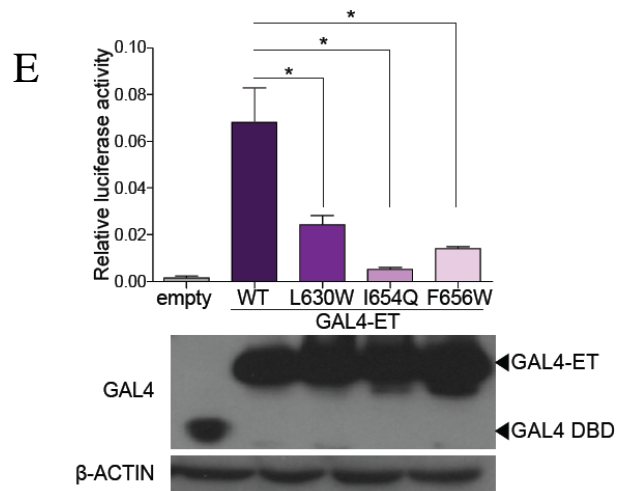
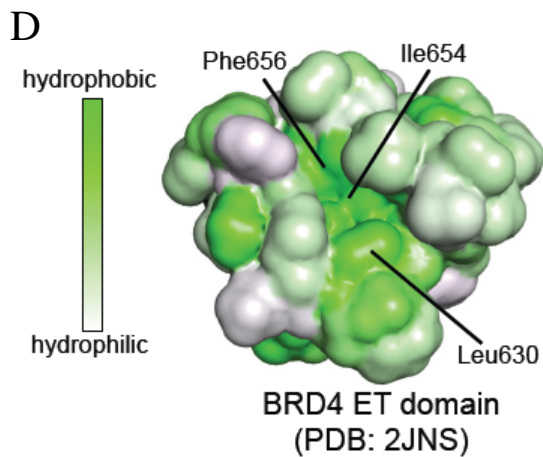
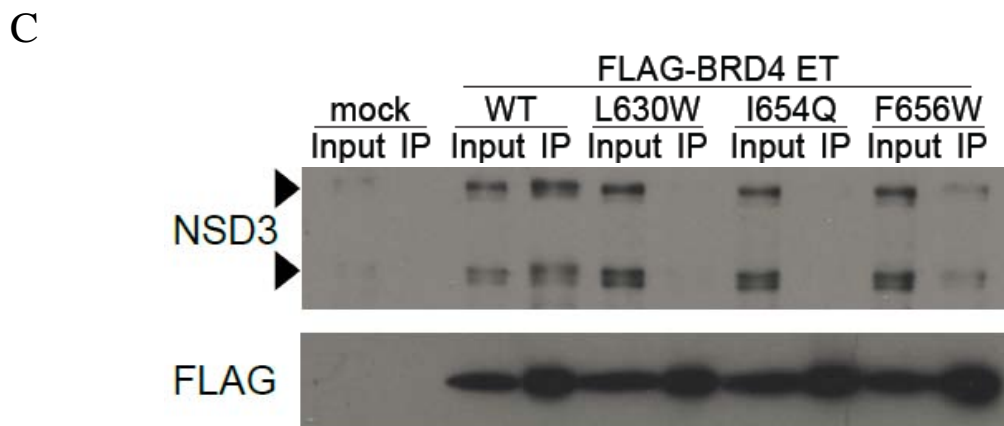
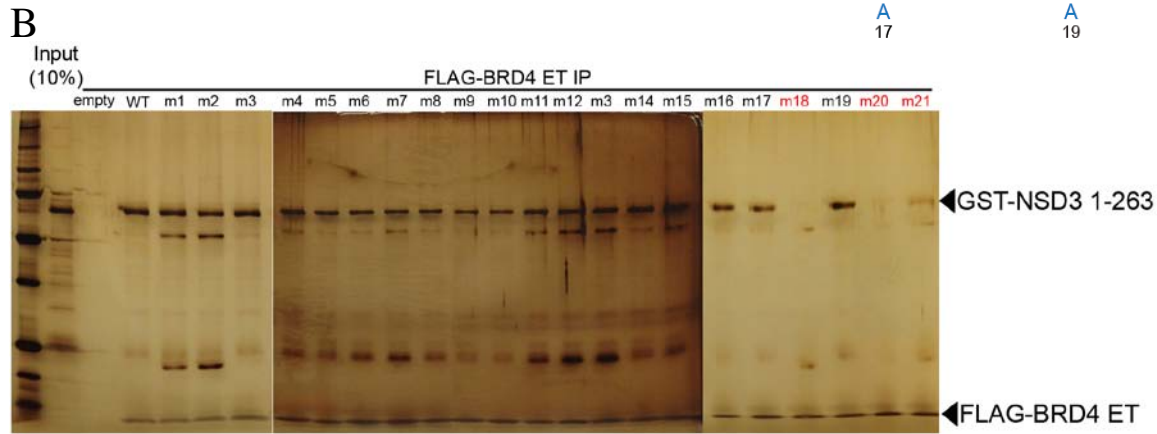
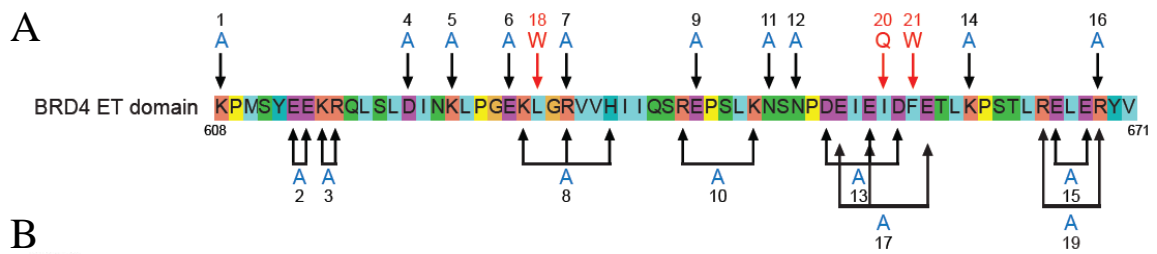


Figure 3.4 Dissociation of NSD3 from BRD4 impairs ET domain functions. (A) The amino acid sequence of the human BRD4 ET domain indicating the surface residues that were subjected to mutagenesis. Combinations of mutations were used in some cases in an attempt to disrupt specific clusters of charged residues. (B) In vitro FLAG-BRD4 ET domain binding assays with GST-NSD3 1-263. Silver staining was used to visualize pull-down products. (C) IP of the indicated FLAG-BRD4 ET domains expressed transiently in HEK293T cells followed by Western blotting with the indicated antibodies. (D) The molecular surface of the BRD4 ET domain (PDB: 2JNS) with hydrophobicity indicated in green (Lin et al. 2008). (E) (top) Luciferase reporter assay evaluating the activation function of the indicated GAL4-ET domain fusions on a minimal plasmid-based reporter harboring GAL4 recognition sequences. Plots indicate firefly luciferase activity normalized to the Renilla luciferase control. * $p < 0.05$, two-tailed Student's t-test. (bottom) Western blotting analysis of HEK293T cells transfected with the indicated plasmids shown in the top panel. All IP-Western and Western blotting experiments shown are a representative experiment of at least three independent biological replicates. All error bars represent SEM for $n=3$.

Chapter 4: NSD3-short Is an Adaptor Protein that Links BRD4 to the CHD8 Chromatin Remodeling Enzyme

Since NSD3-short lacks the lysine methyltransferase activity present on the long isoform, it is reasonable to investigate whether NSD3-short functions as a structural adaptor protein that links BRD4 to other regulators. Through a series of experiments, I demonstrated that NSD3-short links BRD4 to the CHD8 chromatin remodeler to support the leukemia cell state.

4.1 CHD8 is required for AML cell proliferation

In order to identify NSD3-short associated proteins, I performed unbiased IP-mass spectrometry analysis. Nuclear extracts were prepared from HEK293T cells after transient transfection for 48 hours with either an empty murine stem cell virus (MSCV) vector (for mock IP) or an MSCV vector expressing FLAG tagged NSD3-short. Nuclear extracts were incubated with anti-FLAG antibody overnight, followed by incubation with Protein G Dynabeads for 2 hours. After extensive washes, proteins were eluted using 3X FLAG peptide from beads. Samples were then precipitated using trichloroacetic acid and washed with acetone. Mass spectrometry and data analysis was performed at the Taplin Biological Mass Spectrometry Facility at Harvard University.

As expected, NSD3-short and BRD4 were among the top five proteins recovered in this analysis (Figure 4.1A). The other highly enriched proteins found associated with NSD3-short included BPTF, BOD1L, and CHD8 (Figure 4.1A). To examine the relevance of these factors in leukemia cells, shRNA-based targeting of each protein was performed and the effect on RN2 cell proliferation was measured. Notably, knockdown of CHD8 resulted in a proliferation arrest

whereas knockdown of BPTF or BOD1L resulted in no significant phenotype (Figure 4.1B). The dependency of CHD8 in RN2 cells was repeatedly investigated and the knockdown efficiency of shRNAs was evaluated with both RT-qPCR and Western blotting (Figure 4.1C-F). Consistent with the hypothesis that CHD8 may be relevant to NSD3-short and BRD4 in AML, c-Myc expression is also decreased upon CHD8 knockdown in RN2 cells (Figure 4.1C and D).

CHD8 is a member of the SNF2 family of chromatin remodeling ATPases, which, to our knowledge, has not previously been linked to BRD4, NSD3, or to leukemia maintenance. Due to the large size of *Chd8*, I was unable to perform cDNA rescue experiments to validate that the proliferation arrest observed using shRNAs was due to on-target CHD8 knockdown. Therefore, I performed negative selection CRISPR-Cas9 mutagenesis scanning of all *Chd8* coding exons with a multiplexed library of 903 single guide RNAs (sgRNAs), which is a method for revealing functionally important domains of large proteins (Shi et al. 2015b).

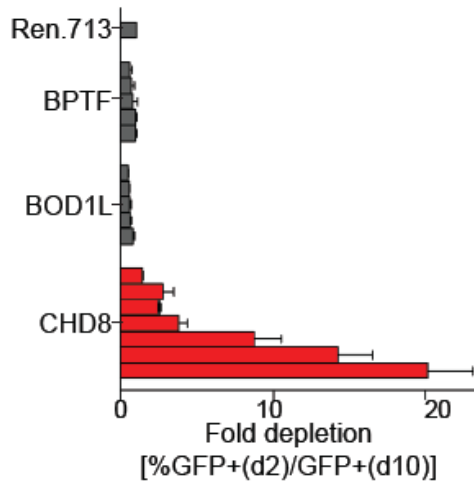
In this experiment, as previously described (Shi et al. 2015b), a Cas9 expressing RN2 cell line was generated with an MSCV construct expressing 53xFLAG tagged human -codon optimized Cas9. sgRNAs were designed to target all possible protospacer adjacent motif (PAM) NGG sequences on the plus or minus strand of the protein-coding region. sgRNAs were excluded from the library if they were predicted to have off-target cutting sites in the genome. Lentivirus of pooled sgRNAs was transduced into RN2 cells expressing Cas9. Then the genomic DNA was extracted at the first and last time points. The pooled screening libraries were constructed as described previously to maintain at least 500× sgRNA library representation (Shi et al. 2015b). Read counts for each sgRNA were normalized to the counts of the negative control *Rosa26* sgRNA to compare the differential representation of individual sgRNAs between day 2 and day 12 time points (Figure 4.2A). Deep sequencing revealed that severe proliferation arrest

of RN2 cells correlated with CRISPR-based targeting of exons encoding the chromodomains and the ATPase domain of CHD8, but not with targeting of the BRK domains (Figure 4.2B). The requirement of the ATPase domain in AML was then validated by a GFP depletion assay with individual sgRNAs (Figure 4.2C). This analysis also revealed a region of functional importance located between the ATPase and BRK domains at residues 1440-1750, which has not been annotated in published database (Figure 4.2B). These results validated CHD8 as a leukemia dependency and led us to hypothesize that NSD3-short performs an essential role in this disease by linking CHD8 to BRD4.

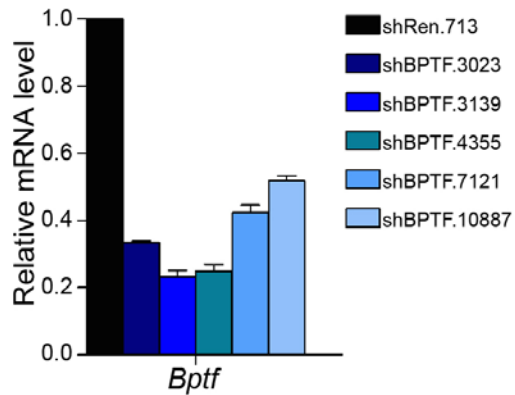
A

IP Mass-Spec		
protein	matching peptides	
	mock IP	NSD3 -short IP
NSD3-short	0	142
BPTF	0	19
BOD1L	0	18
BRD4	0	13
CHD8	0	11

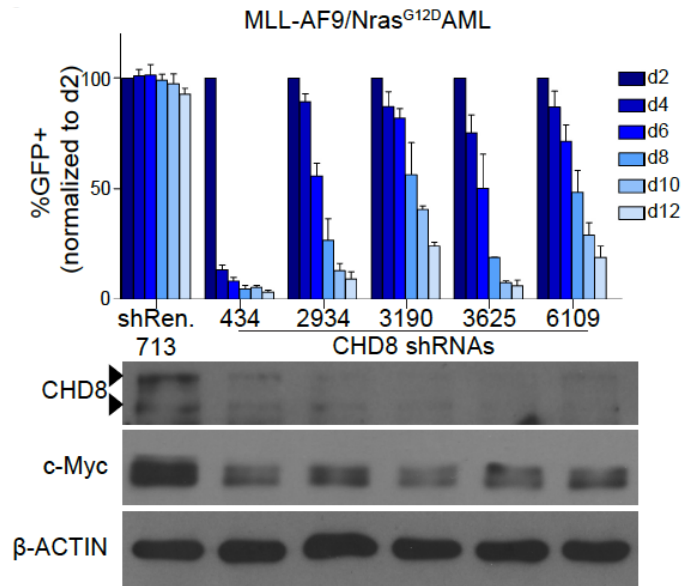
B



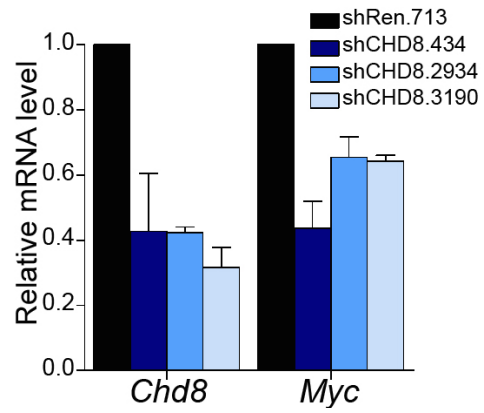
E



C



D



F

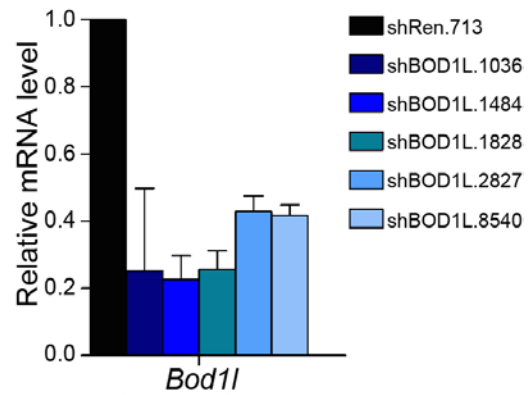


Figure 4.1 CHD8 is required for AML cell proliferation.

(A) Mass spectrometry analysis of proteins identified using anti-FLAG IP performed with nuclear lysates prepared from HEK293T cells transfected with FLAG-NSD3-short or empty vector (for mock IP). The list was ranked by the total number of matched peptides recovered. (B) Competition-based assay in RN2 cells evaluating the effect of LMN shRNAs targeting the indicated proteins. Each bar represents the average fold-decrease in the percentage of GFP+ cells over 8 days for individual shRNAs. (C) (top) Competition-based assays to evaluate the effect of CHD8 LMN shRNAs on RN2 cell proliferation. GFP percentages are normalized to d2 measurements. (bottom) Western blotting analysis of whole cell lysates prepared from RN2 cells transduced with the indicated TRMPV-Neo constructs following 48 hours of dox treatment. A representative experiment of three biological replicates is shown. (D) RT-qPCR analysis performed on RNA prepared from RN2 cells expressing the indicated TRMPV-Neo shRNAs following 48 hours of dox treatment. Results are normalized to *Gapdh*. (E-F) RT-qPCR analysis performed on RNA prepared from RN2 cells expressing the indicated LMN-shRNAs. Measurements for the indicated genes were normalized to *Gapdh*. All error bars represent SEM for n=3.

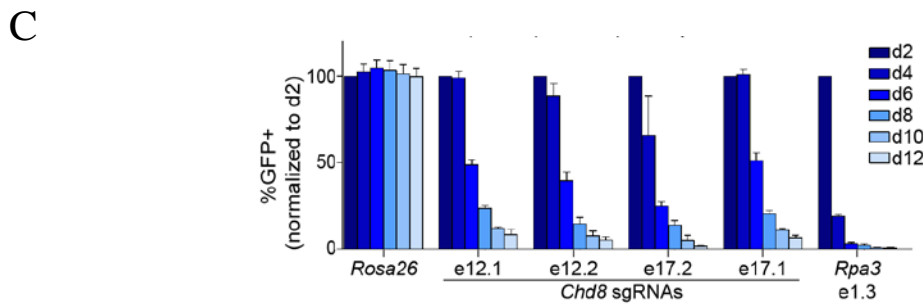
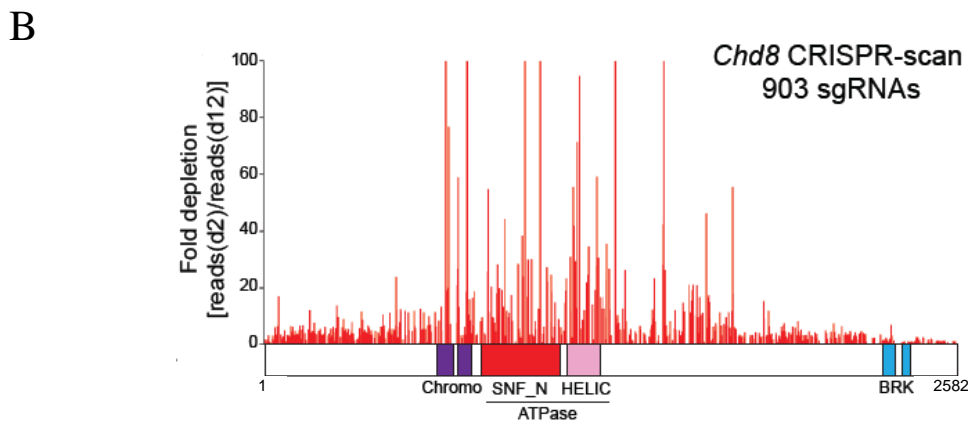
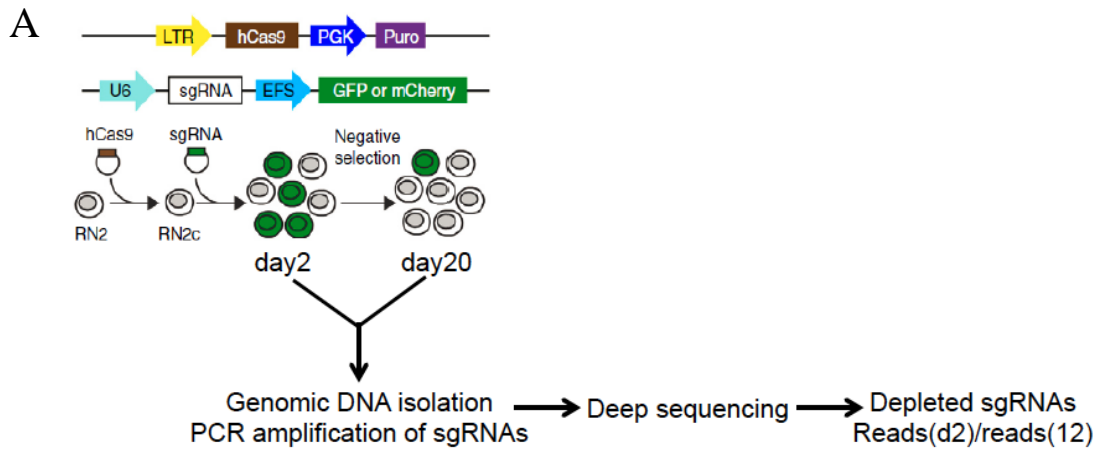


Figure 4.2 CRISPR-scanning of exons encoding *Chd8* in AML.

(A) Workflow of CRISPR-scanning experiment (B) CRISPR-scanning of *Chd8* with all possible sgRNAs. Deep sequencing based measurement of the impact of 903 *Chd8* sgRNAs on the proliferation of Cas9-expressing RN2 cells. The location of each sgRNA relative to the CHD8 protein is indicated along the x axis. Shown is a representative experiment of two biological replicates. (C) Competition-based assay data from RN2-Cas9 cells for the indicated LRG sgRNAs, which are linked to a GFP reporter. The GFP percentage over 12 days for individual sgRNAs is plotted, normalized to day 2 measurements.

4.2 CHD8 is required for maintaining the undifferentiated state of AML cells

Next, to examine whether CHD8 suppression leads to similar phenotypic effects observed upon NSD3 and BRD4 deficiency in AML cells, differentiation states of AML cells were evaluated after CHD8 knockdown by shRNAs or knock out by CRISPR-Cas9. Using flow cytometry, a decrease in the expression of c-Kit and an increase in Mac-1 on the cell surface was observed upon CHD8 knockdown or knockout, suggesting a myeloid differentiation phenotype also associated with BRD4 suppression (Figure 4.3A) (Zuber et al. 2011b). Moreover, targeting of the CHD8 ATPase domain by sgRNAs led RN2 cells to undergo morphological changes associated with terminal myeloid differentiation, which was prevented if c-Myc was expressed ectopically from a retroviral promoter (Figure 4.3B). The above results indicate the CHD8 suppression caused the same phenotypic changes in RN2 cells as targeting NSD3 or BRD4.

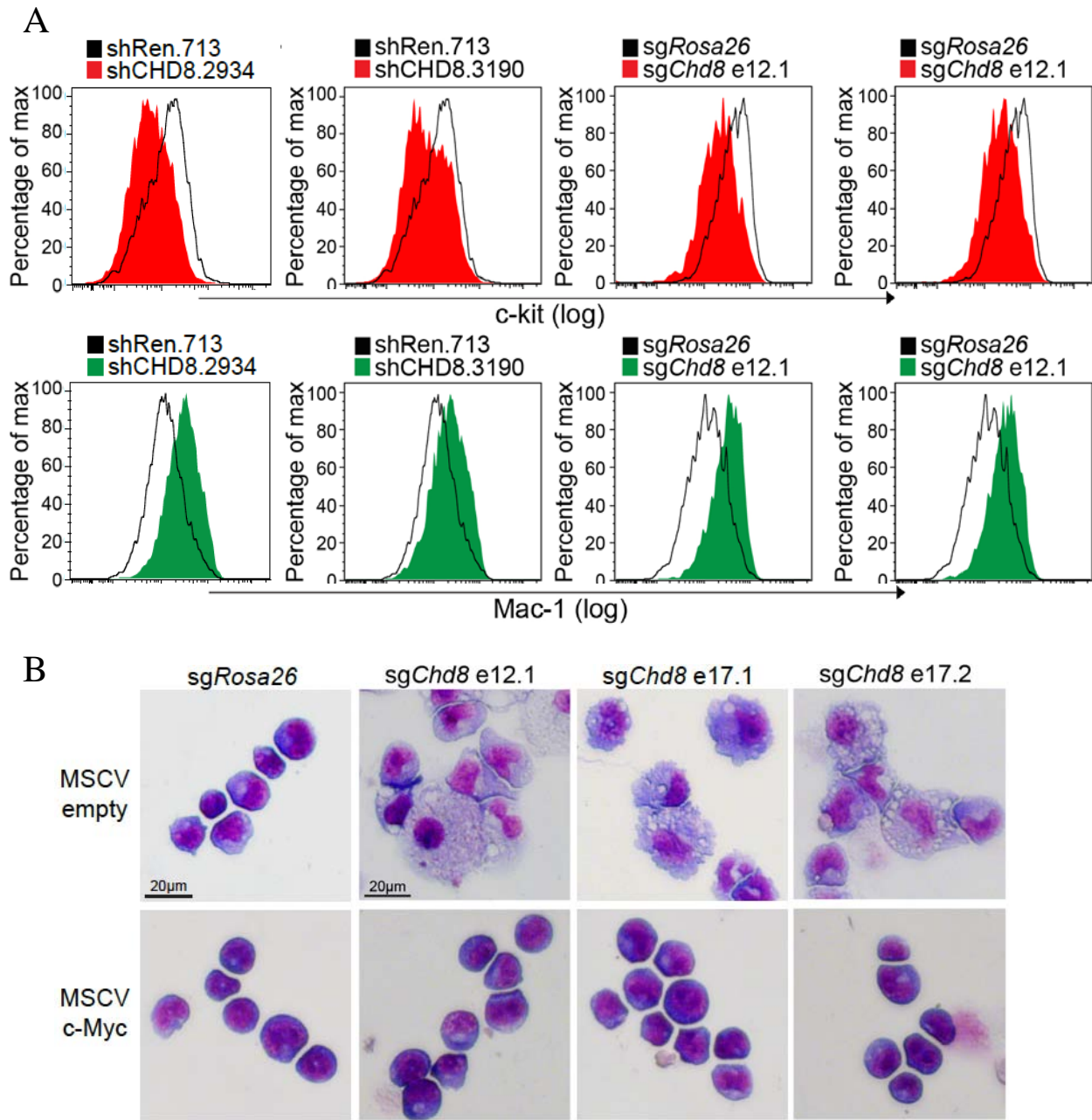


Figure 4.3 CHD8 is required for maintaining the undifferentiated state of AML cell. (A) Flow cytometry analysis of c-Kit and Mac-1 stained RN2 cells following TRMPV-Neo shRNA induction with dox for 4 days or Cas9-expressing RN2 cells transduced with LRG sgRNA for 5 days. Gating was performed on dsRed+/shRNA+ cells or GFP+/sgRNA+ cells. A representative experiment of three biological replicates is shown. (B) Light microscopy of May-Grünwald/Giemsa-stained RN2 cells expressing the indicated *Chd8* sgRNAs, in the presence or absence of ectopic c-Myc expression. For sgRNA experiments, an RN2 line stably expressing Cas9 was used. Cells were imaged 6 days following transduction with the indicated LRG sgRNAs. Imaging was performed with a 40x objective.

4.3 CHD8 regulates a similar global gene profile with NSD3 and BRD4 in AML

Finally, RNA-Seq was performed to evaluate the global gene regulatory profile of CHD8 in AML. RNA-Seq data was obtained from RN2 cells upon CHD8 suppression either by CRISPR-Cas9 knockout or shRNA knockdown. Gene expression in RN2-Cas9 cells expressing two independent *Chd8* sgRNAs was compared to that expressing a *Rosa26* sgRNA, while RN2 cells expressing two independent CHD8 shRNAs were compared to that expressing a Ren.713 shRNA. Log₂ fold changes of gene expression were ranked and ran into GSEA.

Targeting of CHD8 led to similar changes in the global gene expression profile as compared to NSD3 and BRD4 suppression in RN2 cells (Figure 4.4A and B, F and G) (Zuber et al. 2011b). A significant upregulation of a macrophage signature and downregulation of a LSC signature upon CHD8 suppression were also showed by GSEA (Somerville et al. 2009) (Figure 4.4C and D, H and I), suggesting a role of CHD8 to maintain an undifferentiated state of AML cells, akin to BRD4 and NSD3. Moreover, a decrease of a Myc signature was also observed when targeting CHD8 (Schuhmacher et al. 2001) (Figure 4.4E and J). RNA-Seq analysis confirmed that BRD4, NSD3, and CHD8 perform overlapping gene regulatory functions in AML, consistent with the idea that these factors act in the same pathway.

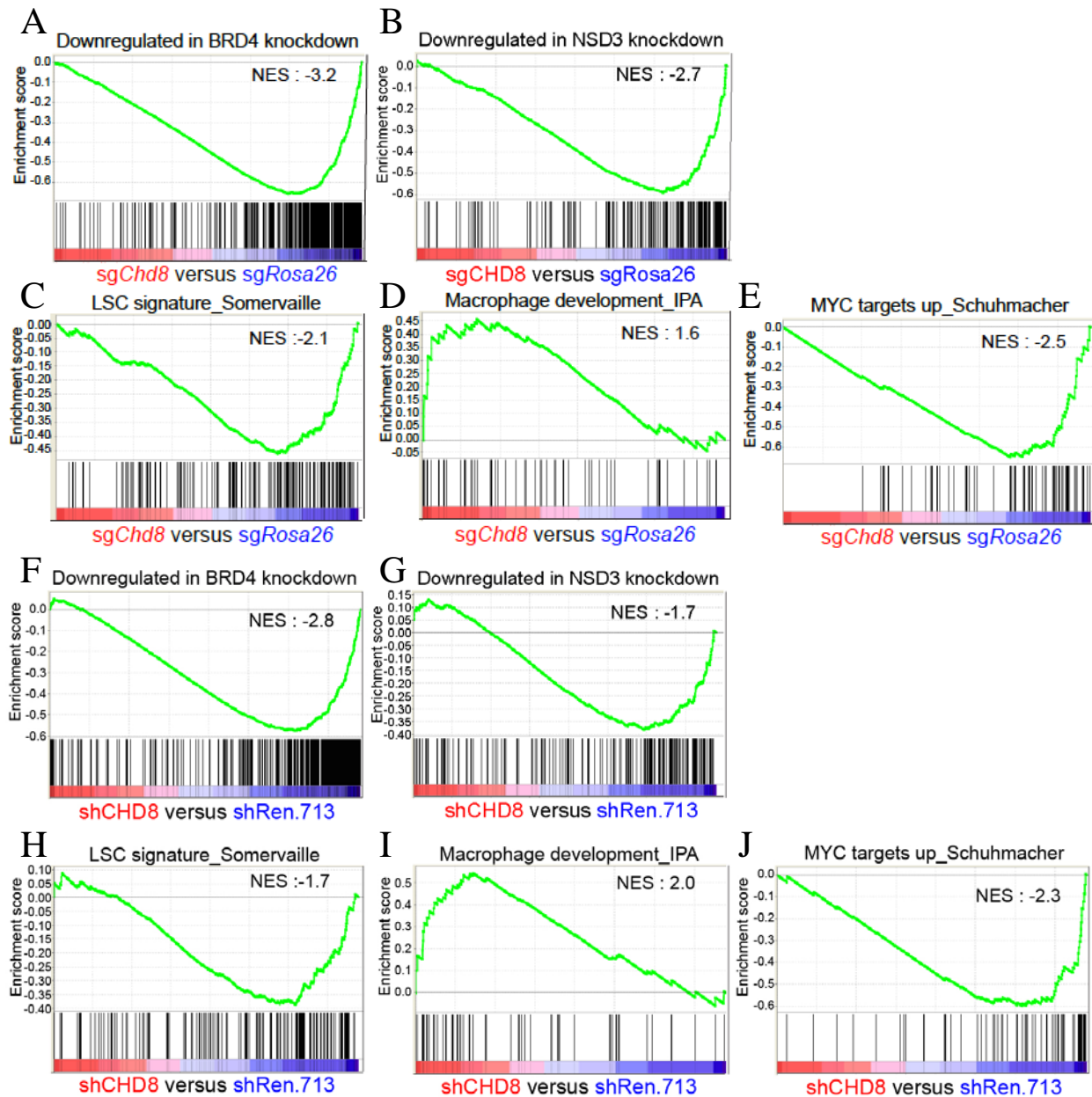


Figure 4.4 CHD8 regulates a similar global gene profile with NSD3 and BRD4 in AML. GSEA of RNA-Seq data obtained from (A-E) RN2-Cas9 cells expressing *Chd8* LRG sgRNAs (4 days following transduction). Two independent *Chd8* sgRNAs were compared to a *Rosa26* sgRNA (F-J) RN2 cells expressing CHD8 TRMPV-Neo shRNAs (induced with dox for 48 hours). Two independent CHD8 shRNAs were compared to a Ren.713 shRNA in this analysis. For each of the indicated gene sets shown, the FDR and nominal p-value were <0.01.

4.4 NSD3-short bridges BRD4 to the CHD8 chromatin remodeler

To confirm the association among BRD4, NSD3 and CHD8 in a leukemia context, I performed reciprocal IP experiments of endogenous proteins from leukemia nuclear extracts (Figure 4.5A). To further investigate the CHD8 binding region on NSD3-short, IP-Western blotting was performed with anti-FLAG antibodies in nuclear lysates prepared from RN2 cells stably expressing the indicated FLAG-NSD3 constructs or empty vector (Figure 4.4B). The deletion analysis identified a critical requirement for residues 384-645 (C-terminal to the PWWP domain) and a partial requirement for residues 280-342 in mediating the CHD8 interaction (Figure 4.4B). This data reveals that NSD3-short contains two independent binding regions for BRD4 and CHD8. In these experiments, deletion of residues 100-263 of NSD3-short reduced, but did not abolish, the interaction with BRD4 (Figure 4.5B). This may be due to the indirect BRD4 association under these conditions, since wide type NSD3 was also pulled down by NSD3-short del (100-263) in this assay (data not shown).

By evaluating various truncated forms of FLAG-BRD4 in IP assays, I also mapped the CHD8 interaction region to the ET domain on BRD4, which raises the possibility that NSD3-short could act as the bridge that links BRD4 to CHD8 (Figure 4.5C). This was further supported by IP experiments with FLAG tagged ET domain with or without point mutations, as shown in Figure 3.4C. All of the three mutations on the BRD4 ET domain, which were previously shown to disrupt NSD3-BRD4 interaction, were able to dissociate CHD8 from the BRD4 ET domain as well (Figure 4.5D). These results strongly suggest that NSD3-short acts as the intermediary between BRD4 and CHD8.

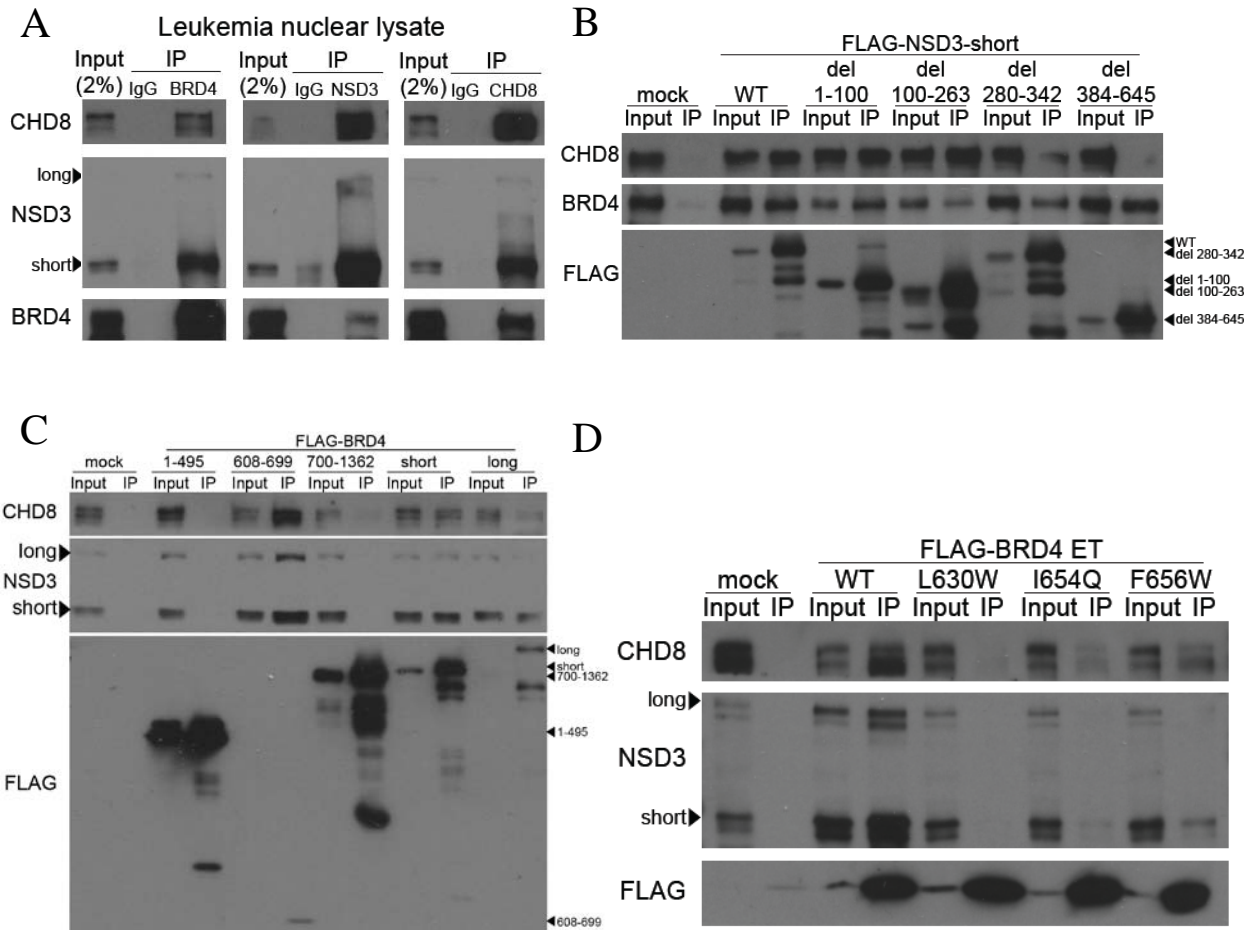


Figure 4.5 NSD3-short bridges BRD4 to the CHD8 chromatin remodeler. (A) Endogenous IP-Western blotting performed with the indicated antibodies and nuclear lysates prepared from NOMO-1 cells. (B) IP-Western blotting performed with anti-FLAG antibodies and nuclear lysates prepared from RN2 cells stably expressing the indicated FLAG-NSD3 constructs or empty vector. (C) FLAG-tag IP-Western blotting of transiently expressed constructs indicated. Plasmids were transfected into HEK293T cells, followed by nuclear lysate preparation at 48 hours. For constructs 1-495 and 608-699 BRD4 fragments contain an N-terminal FLAG tag. For 700-1362, BRD4-short, and BRD4-long, an N-terminal 3XFLAG tag was used. The 609-699 region encompasses the ET domain. (D) IP of the indicated FLAG-BRD4 ET domains expressed transiently in HEK293T cells followed by Western blotting with the indicated antibodies.

Chapter 5: BRD4 Recruits NSD3 and CHD8 to Super-Enhancer

Regions at Oncogene Loci

Genetic and biochemical evidence described so far supports a model in which NSD3-short bridges physical interactions between BRD4 and CHD8 to maintain an AML cell state. However, it is unclear whether these three chromatin regulators indeed co-occupy chromatin regions to execute their functions. Results obtained from ChIP assays in this study suggest that BRD4 recruits NSD3 to BRD4 occupied chromatin loci, which in turn facilitates recruitment of the CHD8 chromatin remodeler.

5.1 BRD4, NSD3, and CHD8 colocalize at active promoters and enhancers across the AML genome

To further corroborate the presence of BRD4-NSD3-CHD8 complexes in AML, ChIP-Seq was performed to compare the genomic localization of all three factors in RN2 cells. A density plot analysis of genomic intervals surrounding 5,135 high-confidence BRD4-occupied promoter and enhancers revealed a similar enrichment pattern of NSD3 and CHD8 across these locations (Figure 5.1A) (Roe et al. 2015). H3K27ac and H3K4me3 datasets described previously (Shi et al. 2013a) were used to confirm the active promoter and enhancer regions.

BRD4 has been shown previously to regulate *Myc* expression in AML cells via a super-enhancer (with individual enhancer constituents E1 to E5) located 1.7 megabases downstream of the *Myc* promoter (Shi et al. 2013b). The E1-E5 super-enhancer and the *Myc* promoter were found to exhibit high levels of BRD4, NSD3, and CHD8 in an overlapping pattern of enrichment, whereas the intervening regions exhibited lower occupancy (Figure 5.2A).

Additionally, I observed similarities among the enrichment of BRD4, NSD3, and CHD8 at *Myb*, *Cdk6*, *Cd47*, and *Bcl2* loci (Figure 5.2B-E). Collectively, these experiments show that BRD4, NSD3, and CHD8 occupy similar locations across the genome of leukemia cells.

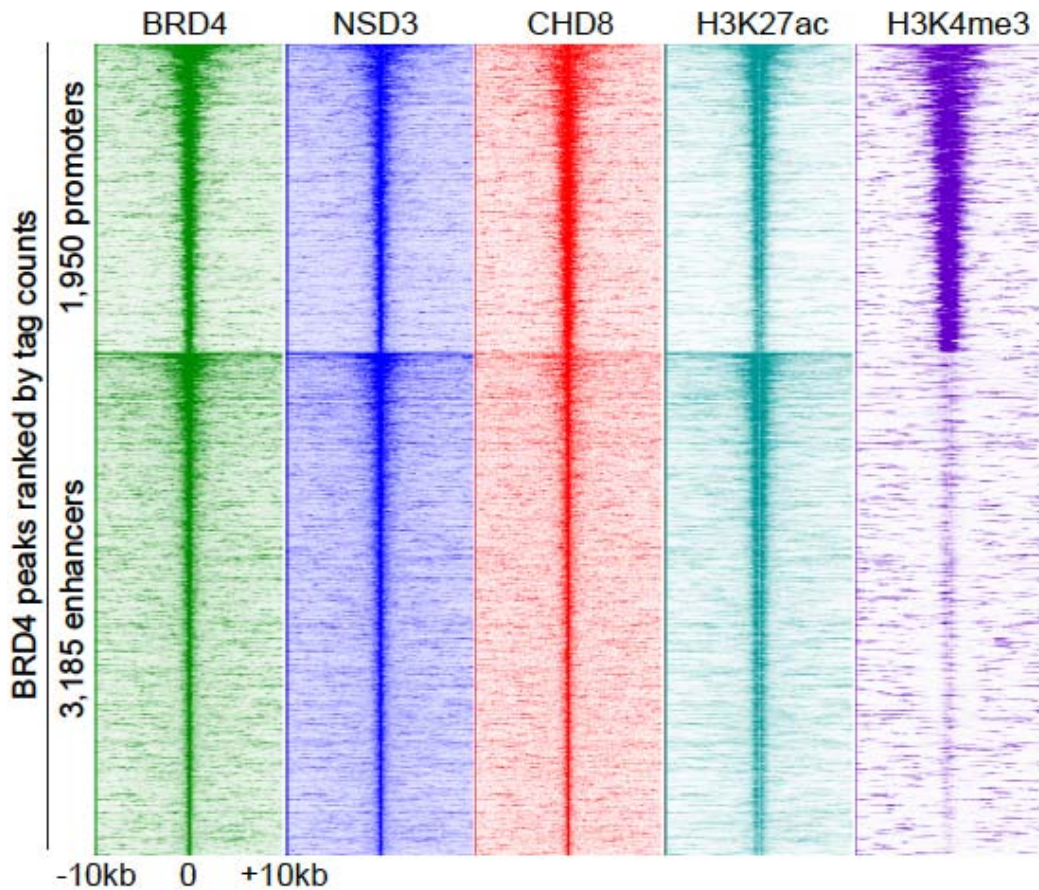


Figure 5.1 Genomewide colocalization of BRD4, NSD3, and CHD8 at active promoters and enhancers across the AML genome.

Density plot analysis comparing ChIP-Seq datasets obtained using the indicated antibodies. Indicated is a 20 kilobase interval surrounding 1,950 BRD4-occupied promoters and 3,185 BRD4-occupied enhancers, identified previously as high-confidence BRD4 occupied sites (Roe et al. 2015). H3K27ac and H3K4me3 datasets from RN2 were described previously (Shi et al. 2013a). Each row represents a single peak.

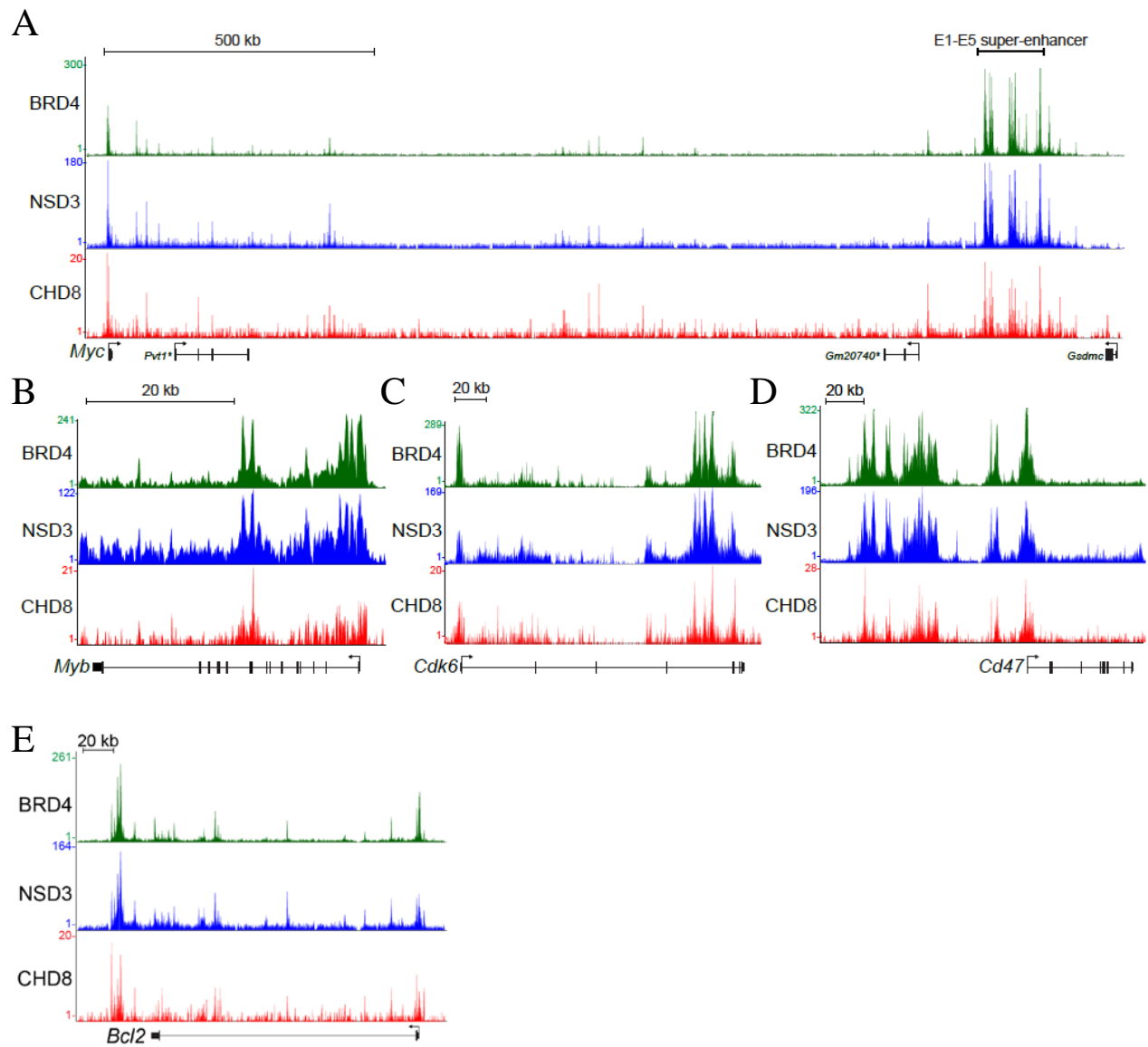


Figure 5.2 Colocalization of BRD4, NSD3, and CHD8 at oncogene loci. (A-E) ChIP-Seq occupancy profiles with the indicated antibodies at various loci. The y-axis reflects the number of cumulative tag counts in the vicinity of each region. Validated transcript models from the mm9 genome assembly are depicted below. The asterisks indicate non-coding RNAs.

5.2 BRD4 recruits NSD3 and CHD8 to the *Myc* +1.7 Mb super-enhancer region

Next, I performed ChIP-qPCR experiments to investigate whether BRD4, NSD3, and CHD8 associate with chromatin in an interdependent manner. Using the ectopically expressed FLAG-tagged NSD3-short, I confirmed the association of this isoform with the *Myc* E1-E5 super-enhancer using ChIP with anti-FLAG antibodies (Figure 5.3A). Deletion of the BRD4 interacting region of NSD3-short (100-263) led to a complete loss of its genomic occupancy while deletion of the CHD8 interacting region (384-645) or deletion of the (1-100) had no effect (Figure 5.3B-D). Unexpectedly, the classic W284A mutation within the PWWP domain failed to disrupt NSD3-short chromatin occupancy at the E1-E5 *Myc* super-enhancer (Figure 5.3E). This raises the possibility of a post-recruitment function of the NSD3-short PWWP domain. Collectively, these results indicate that the interaction with BRD4 is the principal means by which NSD3-short is recruited to chromatin.

ChIP-qPCR analysis was also performed following the exposure of RN2 cells to 500 nM JQ1 for 6 hours. As expected, exposure to JQ1 led to the rapid release of BRD4 from the *Myc* E1-E5 super-enhancer and super-enhancers at other oncogene loci (Figure 5.4A, Figure 5.5A). Importantly, under these conditions JQ1 also caused the eviction of NSD3 and CHD8 from these same regions (Figure 5.5B and C, Figure 5.6B and C). These effects were not limited to RN2 cells, as JQ1 also released BRD4, NSD3, and CHD8 from the *MYC* super-enhancer in human AML cells (NOMO-1 line) and from the *Myc* super-enhancer in murine B-ALL cells (Figure 5.6D-I). To evaluate the specific contribution of BRD4 to these effects, I performed ChIP-qPCR in RN2 cells following conditional BRD4 knockdown using a dox regulated shRNA, which confirmed a BRD4 requirement for NSD3 and CHD8 chromatin occupancy (Figure 5.5D-F).

Knockdown of NSD3 also led to significant reductions in CHD8 occupancy, but had no effect on BRD4 (Figure 5.5G-I). Taken together, these findings support the model that BRD4 tethers NSD3 to chromatin, which in turn recruits the CHD8 chromatin-remodeling enzyme.

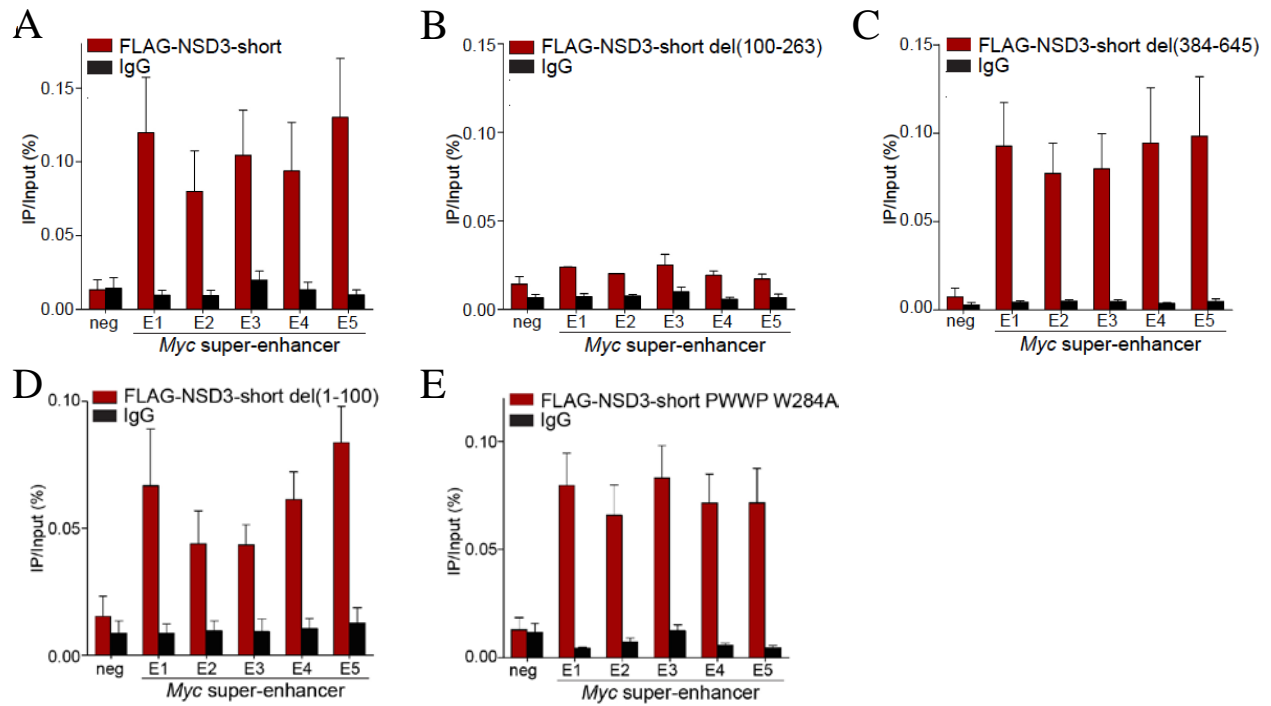


Figure 5.3 Recruitment of NSD3-short is solely dependent on BRD4 interacting region. (A-E) ChIP-qPCR analysis at the E1-E5 *Myc* super-enhancer region evaluating the occupancy of the indicated FLAG-NSD3-short constructs using anti-FLAG antibody or control IgG. All error bars represent the SEM of three independent biological replicates.

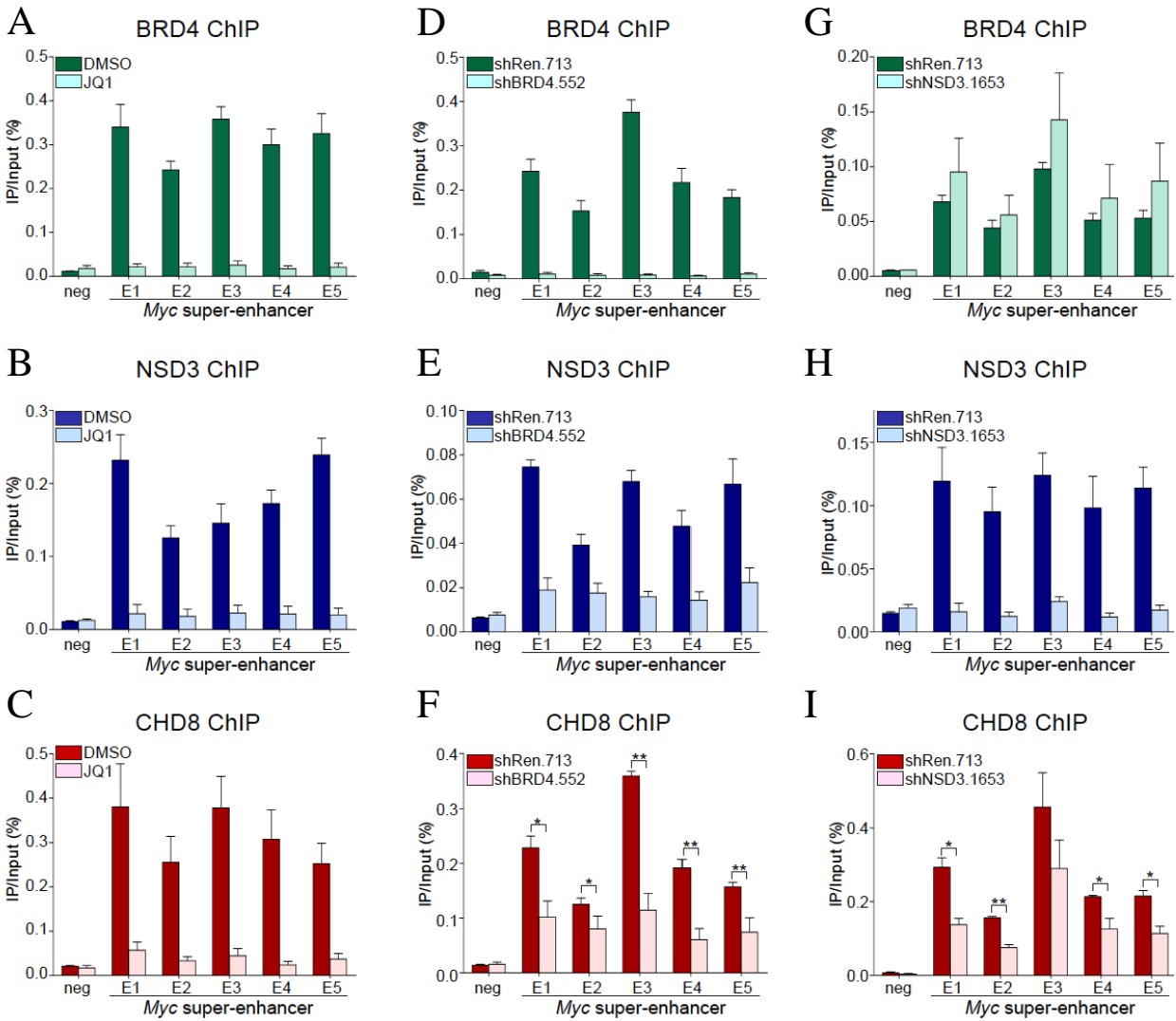


Figure 5.4 BRD4 recruits NSD3 and CHD8 to the Myc +1.7 Mb super-enhancer region in AML.

(A-C) ChIP-qPCR analysis with the indicated antibodies in RN2 cells treated with DMSO vehicle or 500 nM JQ1 for 6 hours. (D-I) ChIP-qPCR analysis with the indicated antibodies in RN2 cells transduced with the indicated TRMPV-Neo shRNA constructs and treated with dox for 48 hours. All error bars represent the SEM of three independent biological replicates.

* $p < 0.05$, ** $p < 0.01$, two-tailed Student's t-test.

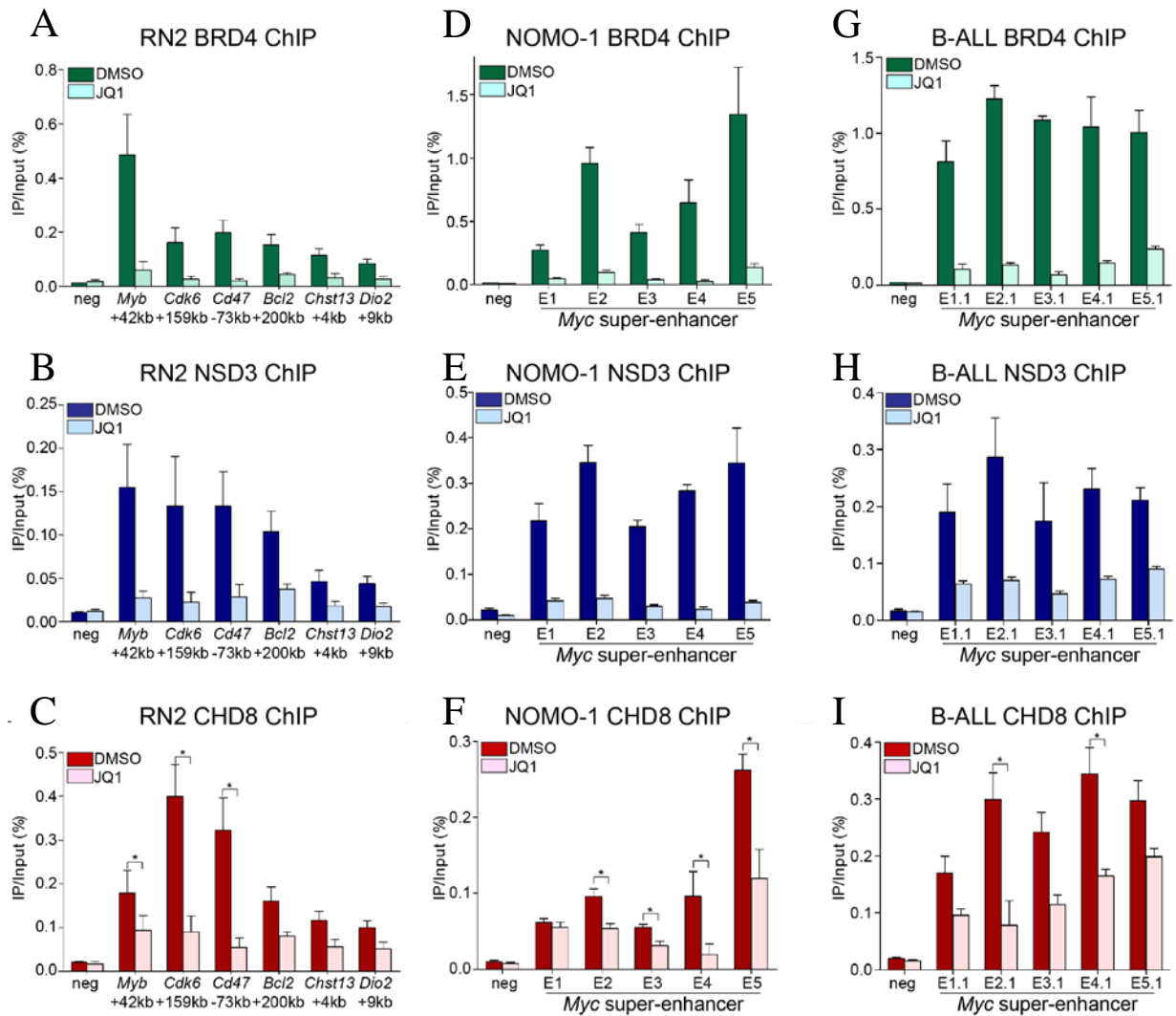


Figure 5.5 BRD4 recruits NSD3 and CHD8 to the super-enhancer regions at oncogene loci. (A-C) ChIP-qPCR analysis with the indicated antibodies in RN2 cells treated with DMSO vehicle or 500 nM JQ1 for 6 hours. (D-F) ChIP-qPCR analysis with the indicated antibodies in NOMO-1 cells treated with DMSO vehicle or 1 μ M JQ1 for 6 hours. (G-I) ChIP-qPCR analysis with the indicated antibodies in B-ALL cells treated with DMSO vehicle or 500 nM JQ1 for 6 hours. We used a modified set of qPCR primers to measure BRD4 occupancy at the E1-E5 region in B-ALL cells, based on BRD4 ChIP-Seq analysis performed in this cell type (data not shown). All error bars represent the SEM of three independent biological replicates. * $p < 0.05$, two-tailed Student's t-test.

Chapter 6: NSD3-short Uses Four Distinct Interaction Surfaces to Sustain AML Cell Proliferation

NSD3-short is an uncharacterized protein that lacks almost all the important annotated domains. Yet, it supports AML cell proliferation. How does NSD3-short perform this function? To answer this question, I carried out a series of experiments and identified functionally important regions in NSD3-short.

6.1 NSD3-short uses a PWWP reader module to sustain AML cell proliferation

First, I employed the shRNA/cDNA rescue assay described earlier to evaluate how mutating different regions of NSD3-short influenced the proliferation of RN2 cells. While a wild-type NSD3-short cDNA was able to complement the knockdown of endogenous NSD3, a deletion of amino acids 100-263 (the BRD4 interacting region) or 384-645 (the CHD8 interacting region) resulted in a functionally defective NSD3 protein despite being expressed at normal levels (Figure 6.1A-E). Knockdown efficiency of NSD3 shRNAs was validated with Western blotting in RN2 cell lines expressing the indicated NSD3 cDNAs (Figure 6.1H). These findings suggest that NSD3-short requires interactions with both BRD4 and CHD8 to maintain leukemia cell proliferation.

Next, we asked whether the essential function of NSD3-short in AML requires its PWWP domain, which has been shown previously to interact with H3K36 methylated peptides (Vermeulen et al. 2010; Wu et al. 2011; Sankaran et al. 2016). Methyl-lysine recognition by PWWP domains requires an aromatic cage, which can be perturbed by substituting the second

tryptophan of the PWWP motif with alanine (Figure 6.2A) (Qin and Min 2014). When introduced into the PWWP motif of NSD3-short (W284A), this mutation resulted in a loss-of-function in the shRNA/cDNA rescue assay, without impairing the interaction of NSD3-short with BRD4 and CHD8 or the stability of NSD3-short protein (Figure 6.1A and F, Figure 6.2B). A CRISPR-based targeting of NSD3 in the human AML cell line MOLM-13 further supports the role of this PWWP domain in leukemia maintenance (Figure 6.2C). ChIP analysis revealed that H3K36 di-methylation broadly correlated with NSD3-short occupancy at the *Myc* E1-E5 super-enhancer (Figure 6.2D and E). However, I could not detect an obvious enrichment of H3K36 mono- or tri-methylation occupancy at this super-enhancer region. These data suggest that NSD3-short requires H3K36-methyl recognition via its PWWP domain to carry out its essential function in AML and the PWWP domain is a potential drug target in leukemia.

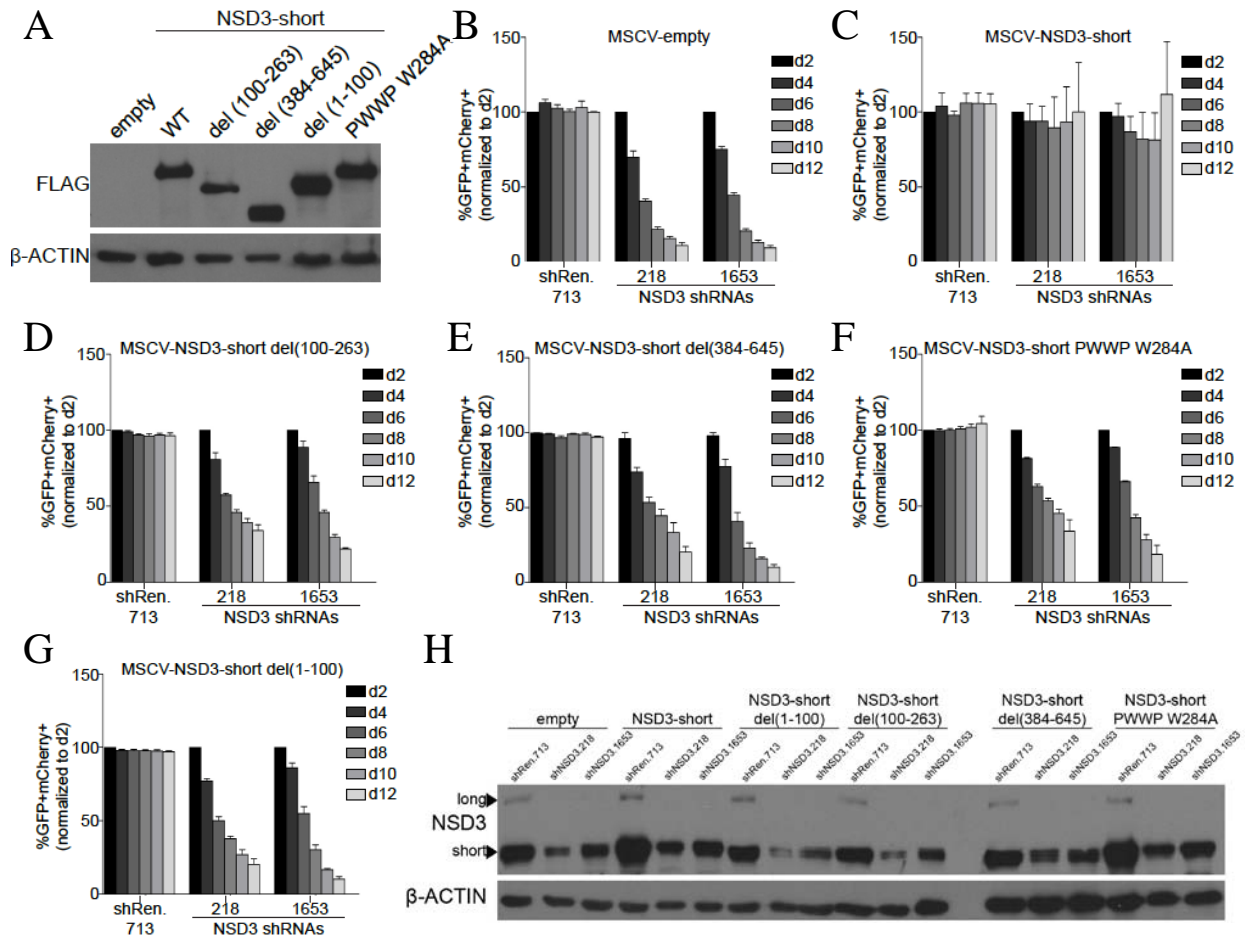


Figure 6.1 NSD3-short uses four distinct regions to sustain AML cell proliferation. (A) Western blotting analysis of whole cell lysates prepared from RN2 cells transduced with the indicated PIG retroviral expression constructs. A representative experiment of three independent biological replicates is shown. (B-G) Competition-based assay tracking the abundance of GFP+mCherry+ cells during culturing of transduced RN2 cells. GFP is linked to the indicated cDNA and mCherry is linked to the indicated LMN shRNA. Plotted is the average of three independent biological replicates, normalized to d2. (H) Western blotting analysis of whole cell lysates prepared from RN2 cells stably expressing indicated FLAG-NSD3 constructs or empty vector (mock) to evaluate knockdown efficiency of indicated TRMPV-Neo shRNA constructs. shRNAs were induced by dox for 48 hours. A representative experiment of three biological replicates is shown. All error bars represent SET for n=3.

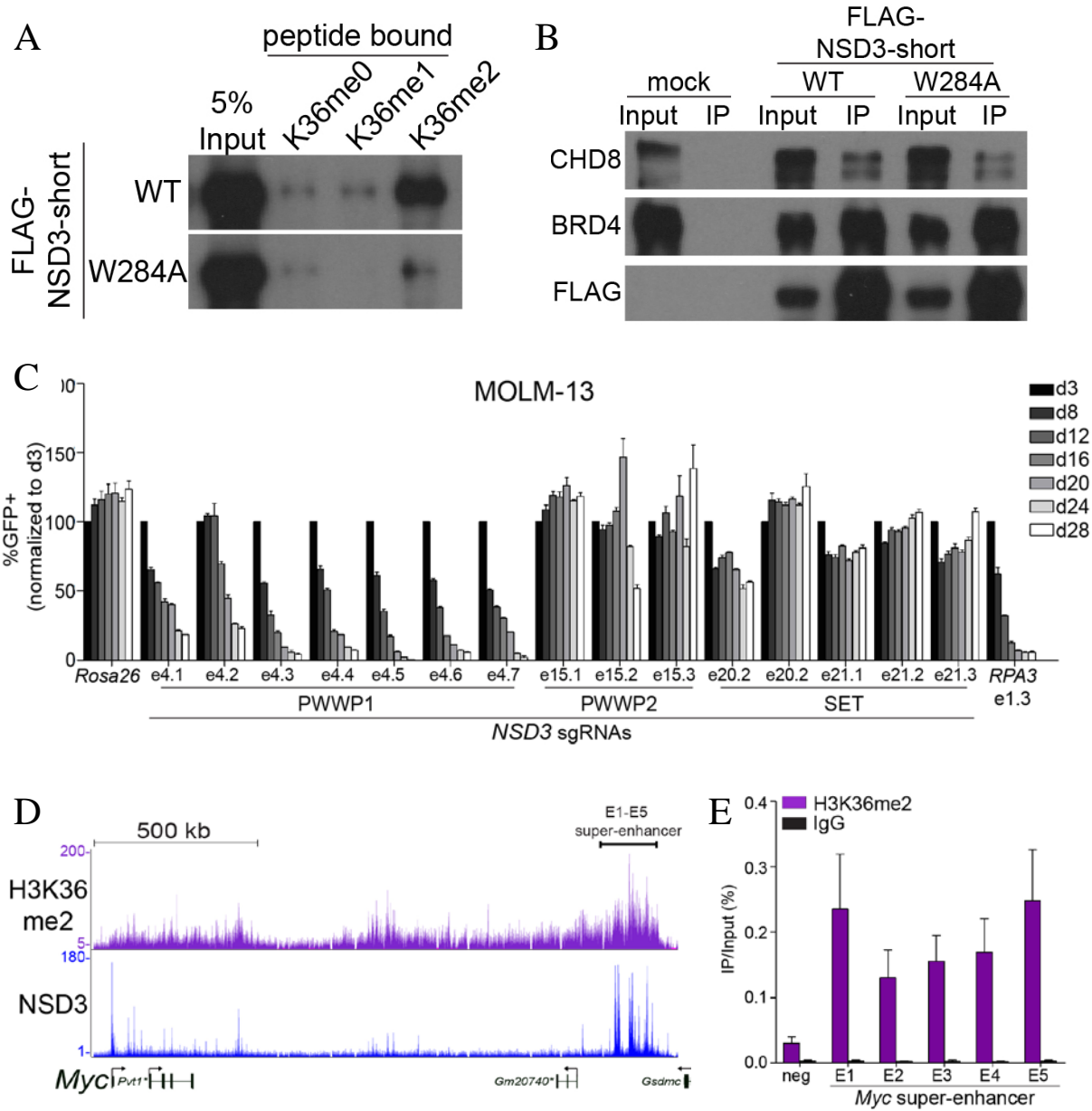


Figure 6.2 Functions of the PWWP domain within NSD3-short.

(A) Peptide-pull-down assay was carried out using nuclear lysates prepared from HEK293T cells transfected with FLAG-NSD3-short (wild-type or W284A mutant). The bound FLAG-NSD3-short with indicated biotinylated peptides bound to streptavidin beads was analyzed by anti-FLAG western blotting. (B) IP using anti-FLAG antibodies and nuclear lysates prepared from RN2 transduced with FLAG-NSD3-short (wild-type or W284A mutant) or empty vector (mock), followed by Western blotting for CHD8, BRD4, and FLAG-NSD3. (C) Competition-based assay data from MOLM-13-Cas9 cells for the indicated LRG sgRNAs, which are linked to a GFP reporter. The GFP percentage over 28 days for individual sgRNAs is plotted, normalized to day 3 measurements. (D) ChIP-Seq occupancy profiles with the indicated antibodies at *Myc* loci. The y-axis reflects the number of cumulative tag counts in the vicinity of each region. Validated transcript models from the mm9 genome assembly are depicted below. The asterisk indicates non-coding RNAs. (E) ChIP-qPCR analysis at the E1-E5 *Myc* super-enhancer region evaluating the enrichment of H3K36me2. All error bars represent the SEM of three independent biological replicates.

6.2 NSD3-short possesses an acidic transactivation domain

The N-terminal 100 amino acids of NSD3-short is dispensable for its association with BRD4 and CHD8 (Figure 4.5B), however, deleting this region compromised the function of NSD3-short in RN2 cells (Figure 6.1G). Interestingly, the 1-100 region of NSD3 is highly enriched for acidic amino acids (pI: 3.4), in contrast to the rest of NSD3-short (pI: 9.6). Since other transcription activation domains (TADs) are known to be enriched for acidic residues (e.g. VP16 and GCN4), the 1-100 region of NSD3 may function as a TAD (Sigler 1988). Using the GAL4-fusion based reporter assay described above, I observed that the activation function of GAL4-NSD3-short is significantly reduced upon deleting the first 100 amino acids of NSD3 (Figure 6.3A). Expression levels of each GAL4 fusions were validated (Figure 6.3B). In addition, a fusion of GAL4 with the 1-100 region of NSD3 alone led to potent transcriptional activation (~1,300 fold), thus confirming this region of NSD3 as a TAD (Figure 6.3A). It was also observed that the 1-100 region promoted transcriptional activation to a much greater extent than full length NSD3-short. This could be because the TAD region alone is more exposed to other cofactors. IP-mass spectrometry experiments failed to identify proteins associated with the NSD3 TAD (data not shown). Since many TADs are known to bind to multiple cofactors with low affinity, it is most likely that the functionally relevant ligand(s) of the NSD3 TAD were not retained under these purification conditions.

These experiments collectively indicate that NSD3-short utilizes four independent interaction surfaces to perform its essential function in leukemia cells: a BRD4 interacting region, a CHD8 interacting region, a PWWP domain-mediated interaction with H3K36 methylation, and an acidic TAD (Figure 6.3C).

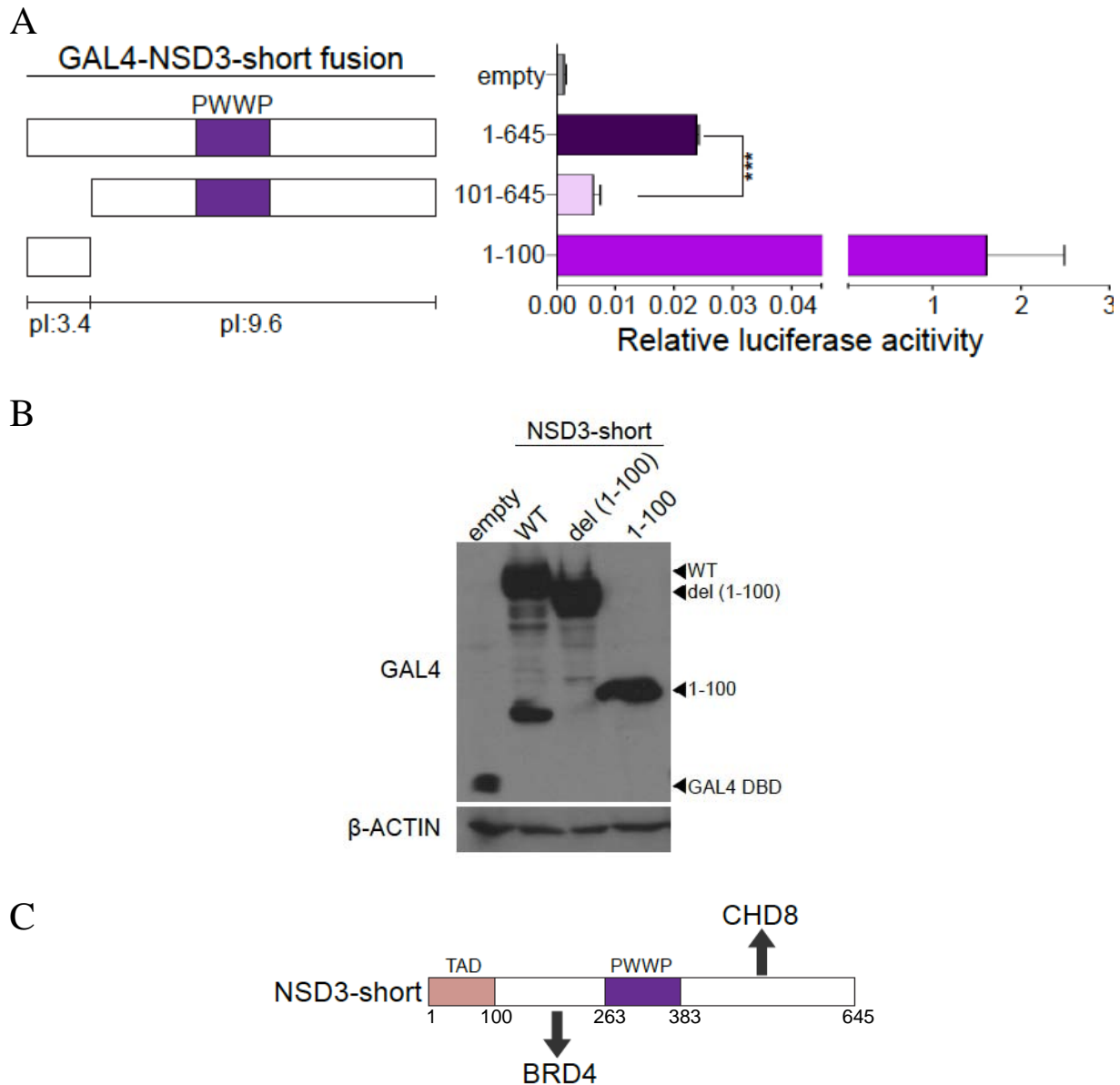


Figure 6.3 NSD3-short possesses an acidic transactivation domain.

(A) Luciferase reporter assay evaluating the activation function of the indicated GAL4-NSD3 fusions on a minimal plasmid-based reporter harboring GAL4 DNA-binding domain recognition sequences. HEK293T cells were co-transfected with p9xGAL4-UAS-luciferase (firefly) reporter and the indicated GAL4 fusion expression plasmids expressing Renilla luciferase from a constitutive promoter. Plots indicate firefly luciferase activity normalized to the Renilla luciferase control. (B) Western blotting analysis of HEK293T cells transfected with the indicated plasmids. A representative experiment of three biological replicates is shown. (C) Diagram of the functionally important surfaces of NSD3-short. All error bars in this figure represent SEM for $n=3$. *** $p<0.001$, two-tailed Student's t-test.

6.3 CRISPR-Cas9 scanning of exons encoding NSD3-short in AML

To further support the model that NSD3-short contains four functional important regions, I performed the CRISPR-Cas9 scanning of *Nsd3* in RN2 cells. As shown in Figure 6.4A, severe proliferation arrest of RN2 cells was correlated with CRISPR-based targeting of exons encoding across NSD3-short.

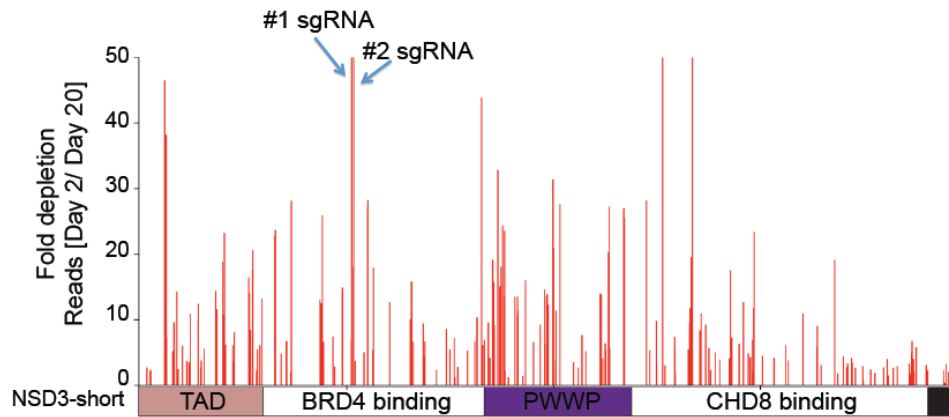
Within the exons encoding the BRD4 binding region, I noticed that two sgRNAs located close to each other presented the highest depletion fold depletion during RN2 cell culturing (50 was used as the cutoff for fold depletion in this assay) (Figure 6.4A). The targeting DNA sequence nearby was analyzed and translated into protein sequence (Figure 6.4B). The NSD3 peptide (152-163), of which DNA coding sequence is close to the cutting sites of these two sgRNAs, is one of the three peptides predicted to bind the BRD4 ET domain (Zhang *et al.*, 2016, *Structure*, in press). The other two peptides are NSD3 211-222 and NSD3 594-606 (Zhang *et al.*, 2016, *Structure*, in press). A common “KI motif” shared by these peptides is considered important for the ET interaction (Zhang *et al.*, 2016, *Structure*, in press). To test whether the “KI motif” of peptide (152-163) is required for NSD3 to bind the BRD4 ET domain, GST pull-down assays were performed. In HEK293T cells, I over-expressed wild type FLAG-NSD3-short or mutant fragments containing a “KI to AA” or “KIK to AAA” mutation within the three predicated peptides respectively. Next, GST tagged ET domain immobilized beads were incubated with HEK293T cells nuclear extract to pull down the indicated FLAG tagged NSD3-short. Western blotting with anti-FLAG antibody revealed that only mutation within peptide (152-163) disrupted the interaction between FLAG-NSD3-short and the GST-ET domain (Figure 6.5A), suggesting amino acids 152-163 within NSD3-short are essential for binding BRD4. NMR structure of the complex containing NSD3 152-163 and BRD4 ET was achieved later on

(Zhang *et al.*, 2016, *Structure*, in press), confirming the binding surfaces between NSD3 and BRD4.

Furthermore, I carried out functional analysis with shRNA/cDNA rescue assay and found that despite being expressed at normal levels, K156A/I157A led to a functionally defective NSD3 protein in supporting RN2 cell proliferation (Figure 6.5B-E).

These data suggest that CRISPR-scanning of exons encoding a protein can nominate functional hotspots at very high resolution. However, validations for more hotspots are needed. Careful characterization may also be required for scored sgRNAs targeting specific regions, such as RNA splicing machinery occupied sites and enhancer regions.

A



B

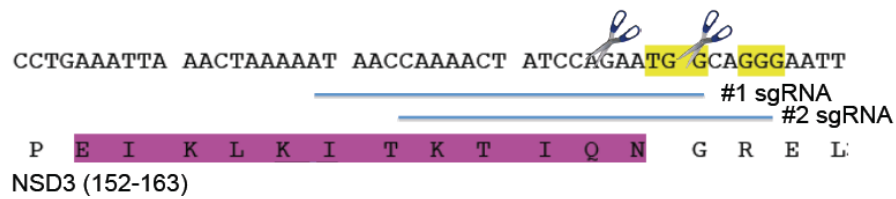


Figure 6.4 CRISPR-Cas9 scanning of exons encoding *Nsd3-short* in AML. (A) CRISPR-scan of exons encoding *Nsd3-short* with all possible sgRNAs. Deep sequencing based measurement of the impact of 212 *Nsd3* sgRNAs on the proliferation of Cas9-expressing RN2 cells. The location of each sgRNA relative to the NSD3-short protein is indicated along the x axis. Shown is a representative experiment of two biological replicates. (B) DNA and corresponding protein sequences close to the cutting sites of the indicated sgRNAs. NSD3 (152-163) peptide is colored by dark pink.

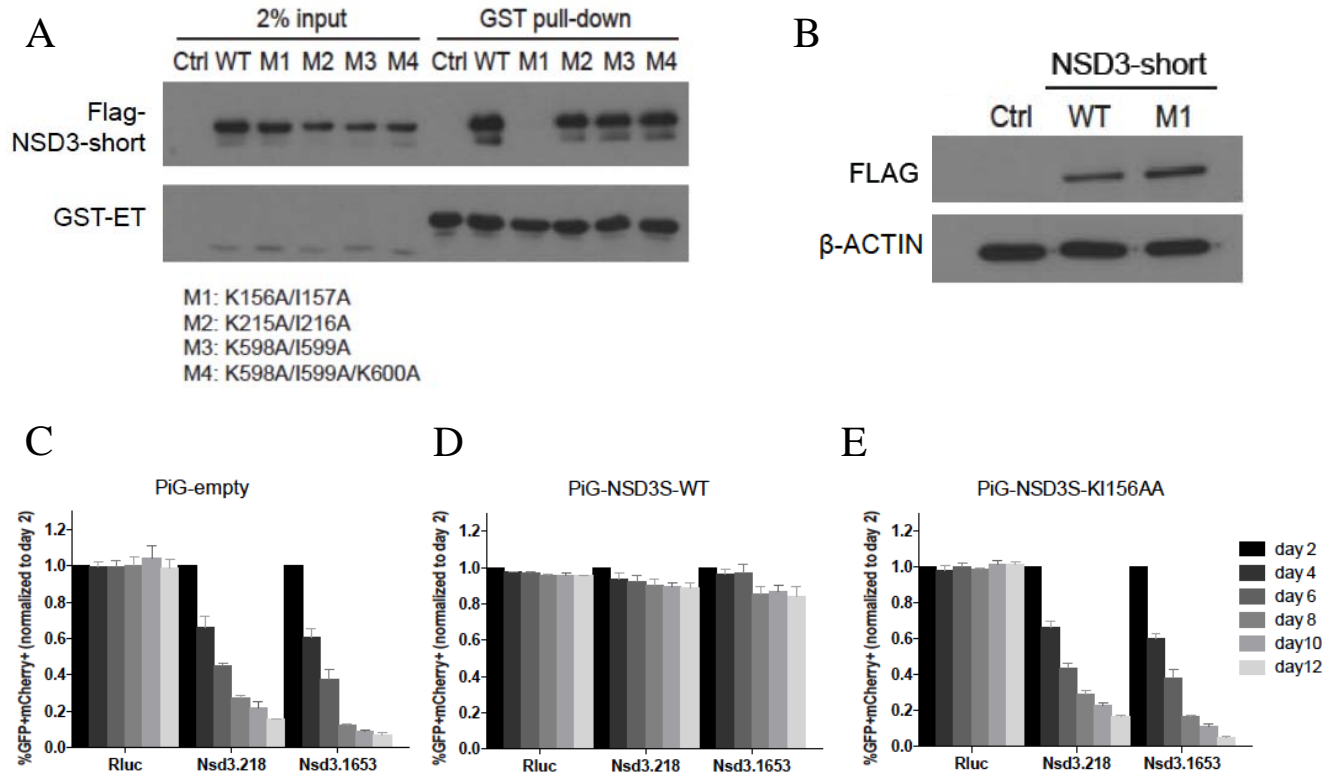


Figure 6.5 Dissociation of BRD4 with point mutation impacts NSD3-short function in AML. (A) Identification of the BRD4 ET domain binding site in NSD3-short by GST-BRD4 ET domain pull-down assays evaluating interactions with various FLAG-NSD3-short constructs carrying different mutations, as indicated. GST-ET domain immobilized beads were incubated with HEK293T cells expressing the wild-type FLAG-NSD3-short or corresponding mutant fragments of M1, M2, M3, and M4 that contain double or triple Ala mutations of K156A/I157A, K215A/I216A, K598A/I599A, and K598A/I599A/K600A, respectively. (B) Western blotting analysis of whole cell lysates prepared from RN2 cells transduced with the indicated PiG retroviral expression constructs. (C-E) K156A/I157A (M1) impairs NSD3-short function in sustaining leukemia cell proliferation. Competition-based assay tracking the abundance of GFP+mCherry+ cells during culturing of transduced RN2 cells. GFP is linked to the indicated cDNA and mCherry is linked to the indicated LMN shRNA. Plotted is the average of three independent biological replicates, normalized to d2. All error bars represent SEM.

Chapter 7: Conclusions and Perspectives

7.1 Summary

This study aims to investigate the mechanisms underlying the therapeutic effects of BET inhibitors in leukemia and has revealed several features of BRD4-mediated transcriptional activation, which are at least in part, via ET domain-mediated recruitment of NSD3-short and CHD8. The reliance of BRD4 on NSD3-short, and not NSD3-long, for transcriptional activation is totally unexpected, since the short isoform lacks the catalytic SET domain and six of the chromatin reader domains found on the long isoform. To explain this observation, I have shown that NSD3-short utilizes four discrete surfaces to maintain the proliferative state of leukemia cells. This includes an interaction with BRD4, an interaction with CHD8, a PWWP-mediated interaction with H3K36 methylation, and an N-terminal acidic transactivation domain. While NSD3-long is likely to have important roles in other contexts (Zhou et al. 2010; Jacques-Fricke and Gammill 2014), my findings demonstrate that NSD3-short can function as an adaptor protein that coordinates multiple regulatory machineries on chromatin to allow BRD4-dependent transcriptional activation (Figure 7.1).

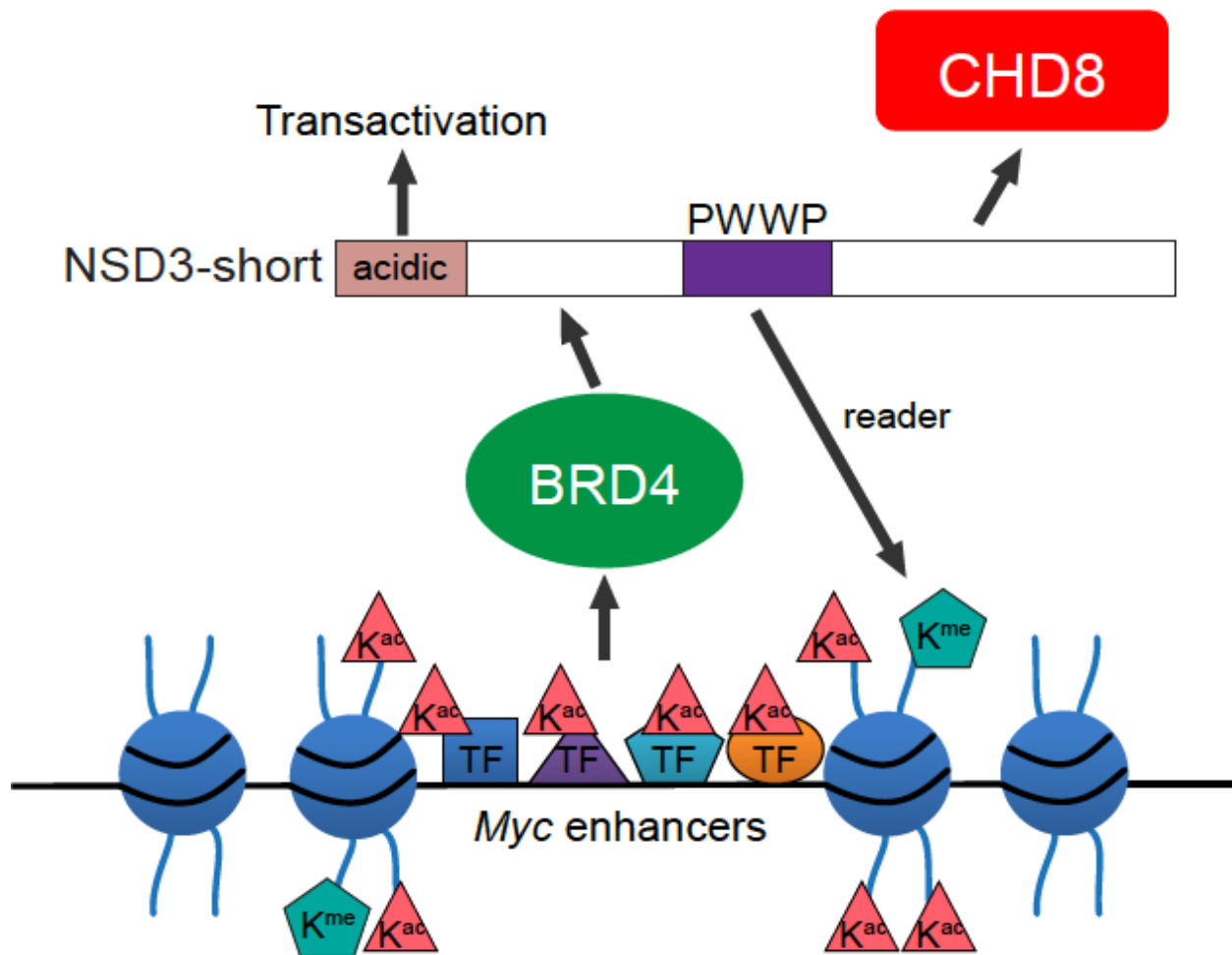


Figure 7.1 Model for NSD3-short functions in AML maintenance. A short isoform of NSD3 that lacks catalytic activity is essential in leukemia cells. NSD3-short functions as an adaptor protein that bridges the BET protein BRD4 with the chromatin-remodeling enzyme CHD8. NSD3-short also uses a PWWP module and an acidic activation domain to maintain AML cell state.

7.2 Discussions

Modification of chromatin is a key regulatory mechanism that contributes to chromatin structure and gene-specific transcriptional control. The chromatin regulatory apparatus encompasses a diverse array of enzymatic (histone modifiers and nucleosome remodeling complexes) and non-enzymatic (e.g. chromatin reader proteins) machineries that function in concert with sequence-specific DNA binding proteins to influence gene expression. BRD4, a chromatin reader protein, is a validated drug target in blood malignancies, by sustaining an aberrant oncogenic transcriptional program. This study uses structure-guided protein biochemistry and genetic dissection of regulator machineries with point mutations in conjunction with epigenomic analyses to provide a comprehensive molecular definition of the downstream components of the BRD4 pathway in leukemia maintenance. Thus, a host of new drug discovery opportunities for next-generation agents has been revealed.

7.2.1 BRD4 in AML maintenance

AML is an aggressive blood malignancy, in which immature leukemia blasts hijack the normal hematopoietic system. Leukemogenesis has been linked to the aberrant chromatin (Redner et al. 1999; Krivtsov and Armstrong 2007; Chen et al. 2010). An RNAi screen performed in our lab revealed an epigenetic vulnerability for targeting the chromatin regulator BRD4 in AML (Zuber et al. 2011b).

BRD4 belongs to the BET family of transcriptional coactivators, which use tandem bromodomain modules to recognize acetyl-lysine side chains on various nuclear proteins (Wu and Chiang 2007; Shi and Vakoc 2014). Original studies demonstrated a critical role for histone tail acetylation in tethering BRD4 to chromatin (Dey et al. 2003), however evidence suggests

that acetylation of TFs is also a major mechanism that directs BRD4 to enhancer and promoter regions across the genome (Huang et al. 2009; Brown et al. 2014; Shi et al. 2014; Roe et al. 2015). When bound to regulatory elements, BRD4 activates transcription of nearby genes, in part via the direct interaction of its CTD with the kinase P-TEFb (Jang et al. 2005; Yang et al. 2005; Bisgrove et al. 2007).

Emerging evidence has demonstrated that the ET domain of BRD4 is required for its function by linking BRD4 to other transcription regulators. Prior studies performed in non-hematopoietic cell types have suggested that the demethylase protein JMJD6 can also interact with the ET domain of BRD4 to allow transcriptional activation (Rahman et al. 2011; Liu et al. 2013). Demethylase protein JMJD6 was found to be recruited to enhancer regions by BRD4, where it erased the repressive histone mark (H4R3me1 and H4R3me2) and released the inhibitory regulation of P-TEFb by demethylating 7SK (Liu et al. 2013). The long-range interaction between promoters and enhancers via chromatin looping allows the enhancer bound BRD4/ JMJD6 complex to associate with the P-TEFb complex and regulate poise release at promoter-proximal region.

However, we have performed extensive shRNA and CRISPR-based targeting of JMJD6 in leukemia cells and failed to reveal an effect on cell viability or proliferation (Shi et al. 2015b). Hence, in leukemia cells it appears that NSD3-short is the relevant ET domain-binding partner that supports BRD4-dependent transcriptional activation. This then raises the possibility that different cell types utilize distinct ET-interacting partners of BRD4 to promote transcription. The presence of cell type-specific BRD4 effector proteins may underlie the well-described context-specific gene expression changes induced by BET inhibitors (Shi and Vakoc 2014). Since our prior CRISPR-scan of *Brd4* has implicated the ET and CTD regions as essential for leukemia

maintenance (Shi et al. 2015b), it is likely that BRD4 employs both NSD3-short/CHD8 and P-TEFb as distinct effectors to activate its downstream target genes.

Moreover, functional correlation between the Mediator complex and BRD4 has been identified in AML as well (Bhagwat et al. 2016). This indicates that Mediator could also act as a BRD4 effector to activate gene transcription in AML. Further studies addressing the binding surfaces between BRD4 and the Mediator complex may help us to better understand the BRD4 pathway.

7.2.2 Functions of the PWWP domain in NSD3-short

While the reader function of the NSD3-short PWWP domain is essential to support leukemia cell proliferation, it is surprising to find that this domain was dispensable for NSD3-short recruitment to the *Myc* super-enhancer region, which instead is dependent on the BRD4 interaction. This result implies a post-recruitment function for this chromatin reader module. It is possible that the PWWP module interacts with additional non-histone ligands to promote gene activation. However, our IP-MS analysis comparing wild-type and W284A NSD3-short failed to identify PWWP-dependent interacting proteins. Alternatively, it is also possible that the PWWP interaction with H3K36-methyl allosterically regulates the NSD3-short adaptor function. A recent study has demonstrated that the interaction of the Rpd3S complex with the nucleosome results in a conformational change that modulates its H3K36-methyl recognition function (Ruan et al. 2015). It will be worthwhile in future studies to evaluate whether the PWWP-mediated interaction with H3K36-methylated nucleosomes, or other binding interactions of NSD3, alter the conformation of NSD3-short and the functional output of its interacting partners.

7.2.3 Functions of NSD3-long

Previous studies have associated NSD3-long with neural crest specification and migration via its H3K36 methyltransferase activity (Jacques-Fricke and Gammill 2014). In this study, while NSD3-short was proven to be the essential isoform for transcriptional activation and AML maintenance, a few questions remain to be answered regarding the functions of NSD3-long.

First, although knockdown NSD3-long alone has little impact on RN2 cells (Figure 2.8A), it is hard to exclude the redundant functions performed by the more abundant isoform NSD3-short. An shRNA/cDNA rescue assay failed to support the sufficiency for NSD3-long to maintain RN2 cell proliferation (data not shown), but this could be due to a low expression level of NSD3-long driven by MSCV promoter or the limitation of the retroviral packaging ability for large constructs. This experiment could be revisited with lentiviral overexpression of NSD3-long.

Secondly, according to a GAL4-luciferase reporter assay, NSD3-long activates transcriptional activation to a much less extent than NSD3-short (Figure 2.9B). This raises the question whether the C-terminal region of NSD3-long has inhibitory functions and whether there is competition for binding functional partners between NSD3-short and -long. In this case, RNA splicing machinery controlling the expression of these two isoforms may impact the leukemia maintenance phenotype.

7.2.4 Interactions between NSD3 and BET family proteins other than BRD4

The putative NSD3 binding surface mapped in this study is conserved across BET family proteins. Indeed, NSD3 can interact with BRD2 and BRD3 as well (data not shown) (Rahman et

al. 2011). The molecular mechanisms demonstrated in this study may have broader implications in other disease contexts dependent on BET proteins besides BRD4.

7.3 Perspectives and future directions

BET inhibitors have been under investigation in a variety of pre-clinical studies and clinical trials (Table 1.2 and 1.3). The therapeutic activity of BET inhibitors is very promising in patients with acute myeloid leukemia (Berthon et al. 2016) and lymphoma (Amorim et al. 2016). However, due to the broad functions of BET family proteins, pharmaceutical interventions for BET proteins present side effects in pre-clinical models including induction of autism like behaviors (Sullivan et al. 2015), long-term memory defect (Korb et al. 2015) and susceptibility to influenza virus infection (Wienerroither et al. 2014). Additionally, the impact on male spermatogenesis by BRDT inhibition should also be taken into consideration (Berkovits and Wolgemuth 2011) (Matzuk et al. 2012). In this study, I mapped a hydrophobic patch as a putative NSD3 binding surface, which was later confirmed by NMR structure of ET-NSD3 (152-163) complex through a collaboration with Ming-Ming Zhou's lab (Zhang *et al.*, 2016, *Structure*, in press). Small molecules targeting this hydrophobic region could generate great selectivity towards leukemia cells, by dissociating NSD3 and CHD8 from BRD4 at the same time.

The oncogenic mechanism of NSD3-short described here is in stark contrast to its homolog NSD2, which is an oncoprotein in B lymphoid cancers. Chromosomal translocations found in multiple myeloma lead to the overexpression of NSD2, which utilizes its catalytic SET domain to elevate the global level of H3K36 di-methylation across the genome (Kuo et al. 2011; Popovic et al. 2014). Moreover, a subset of acute lymphoblastic leukemias acquire point mutations of the NSD2 SET domain that lead to increased methyltransferase activity (Jaffe et al. 2013; Oyer et al. 2014). NSD3 is known to be a much weaker H3K36 methyltransferase than

NSD2 in biochemical assays (Li et al. 2009), which might underlie the reliance of NSD3 on protein-protein interactions instead of catalysis to execute its transcriptional functions.

Nevertheless, the PWWP domain of NSD3-short interacts with H3K36 methylation, which raises the possibility that NSD3-short operates downstream of NSD2 to support a common pathway of malignant transformation.

While this study establishes a role for NSD3-short in maintaining the growth of AML, it is interesting to note that NSD3 is a putative oncoprotein in other forms of cancer. The most common genetic mechanism of NSD3/*WHSC1L1* deregulation is via 8p11-12 genomic amplifications, which occur in breast and lung cancers (Tonon et al. 2005; Yang et al. 2010). This raises the interesting possibility that the adaptor model of NSD3-short defined here in AML will be relevant to the pathogenesis of 8p11-12-amplified epithelial cancers (Yang et al. 2010). This provides a rationale to consider targeting the adaptor functionalities of NSD3, instead of its methyltransferase activity, as a therapeutic approach in these cancers. Since other chromatin reader domains (e.g. bromodomains and MBT domains) have proven to be amenable to direct chemical inhibition, the PWWP module of NSD3-short provides an attractive target for future drug development (Filippakopoulos et al. 2010; James et al. 2013).

This study, for the first time, links CHD8 to the BRD4-NSD3 complex and AML maintenance. CHD8 is best known for its role in neurodevelopment and as one of the most commonly mutated genes in autism spectrum disorders (Bernier et al. 2014). CHD8 has been shown previously to interact with the androgen receptor and with c-Myc, which are also TFs known to interact with BRD4 (Menon et al. 2010; Wu et al. 2013a; Asangani et al. 2014; Dingar et al. 2015). Moreover, CHD8 is also known to promote Wnt signaling by directly activating β -catenin target genes (Thompson et al. 2008). The CRISPR-scanning of *Chd8* in this study

suggests that targeting of CHD8, potentially via chemical inhibition of its chromodomains or ATPase activity, would suppress cancer-promoting transcriptional pathways in various malignancies. More detailed investigations of the binding nature and surfaces between NSD3 and CHD8, as well as how CHD8 regulates chromatin structure, may lead to a better understanding of CHD8 functions.

Chapter 8: Extended Materials and Methods

8.1 Cell culture

The Tet-On competent murine AML cell line RN2 was derived from a MLL-AF9/Nras^{G12D} transplantation-based animal model and was cultured *ex vivo* in RPMI1640 supplemented with 10% fetal bovine serum (FBS) and 1% penicillin/streptomycin (Zuber et al. 2011a). Murine B-ALL cells, driven by BCR-ABL and p19^{Arf} inactivation (Williams et al. 2006), were cultured in RPMI1640 supplemented with 10% FBS, 1% penicillin/streptomycin and 0.055 mM 2-Mercaptoethanol. HL-60, MOLM-13, and NOMO-1 human AML cell lines were cultured in RPMI1640 supplemented with 10% FBS and 1% penicillin/streptomycin. HEK293T and ecotropic Plat-E viral packaging cells were cultured in DMEM supplemented with 10% FBS and 1% penicillin/streptomycin. All retroviral packaging was performed with Plat-E cells according to established procedures (Morita et al. 2000). All lentiviral packaging was performed with HEK293T cells following standard procedures similar to previously described (Shi et al. 2015b). RN2 cells stably expressing Cas9 (RN2c cells) were described previously (Shi et al. 2015b).

8.2 Cell lines and plasmids

The Tet-ON competent murine MLL-AF9/NrasG12D AML cell line (RN2) used in this study was developed and characterized previously (Zuber et al. 2011a). For shRNA-based competition assays in murine cells, the LMN-GFP or LMN-mCherry shRNA retroviral vectors were used (MSCV-miR30-shRNA-PGKp-NeoR-IRES-GFP/mCherry). For shRNA-based competition assays in human leukemia cells, MLS-GFP shRNA retroviral vectors were used

(MSCV-miR30-shRNA-SV40p-GFP). TRMPV-Neo constructs were used for dox inducible shRNA expression in RN2 cells (Zuber et al. 2011a). Cells were treated with 1 µg/ml dox wherever indicated. For CRISPR-Cas9 based targeting of CHD8 and NSD3, the LRG lentiviral vector was used to express the sgRNA (U6-sgRNA-EFS-GFP) in either RN2 or MOLM-13 cells that stably express Cas9 (Shi et al. 2015b).

For c-Myc cDNA rescue experiments, the murine Myc cDNA was cloned into the PIG vector (MSCV-PGKp-Puro-IRES-GFP). For all retroviral and transfection-based expression of NSD3-short, a PIG vector was used containing the human NSD3-short cDNA (#31357; Addgene) with a C-terminal 3XFLAG. FLAG-tagged human BRD4 1-495 and 608-699 fragments were expressed using the pcDNA3 vector. FLAG-tagged human BRD4 700-1362, short, and long fragments were expressed using PIG. For GAL4-fusion experiments, human NSD3 or BRD4 ET domain fragments were cloned in-frame and C-terminal to the GAL4 DNA binding domain in the pFN26A (BIND) hRluc-neo Flexi Vector (Promega). Constructs with point mutations were generated by overlap PCR. For bacterial expression of GST-NSD3 fragment, NSD3-short cDNA sequences were PCR cloned into a pGEX-4T1 vector (#28-9545-49; GE Healthcare). For baculoviral expression, the BRD4 ET domain (608-699) and NSD3 100-263 coding sequences were cloned with an N-terminal Strep2-SUMO tag into the vector pFL. Untagged NSD3 100-263 coding sequence was cloned into the vector pSPL. All of the cloning procedures were performed using the In-Fusion cloning system (#638909; Clontech) or using SLIC (Sequence- and Ligation-Independent Cloning).

8.3 Competition assay to measure cell proliferation

For shRNA-based competition assays, RN2 cells were retrovirally transduced with the indicated LMN shRNA vectors (which express the shRNA and GFP from constitutive promoters), followed by tracking of GFP percentages using a Guava Easycyte HT instrument (Millipore) over time in culture. shRNA-induced proliferation arrest was monitored by GFP-negative cells outcompeting GFP-positive cells, which is represented in several plots as fold depletion [$\%GFP^{+}(d2)/\%GFP^{+}(d12)$]. For evaluating effects of specific cDNAs on shRNA-induced phenotypes in leukemia cells, RN2 or HL60 cells were first retrovirally transduced with PIG (empty or with a cDNA), followed by puromycin (1 μ g/ml) selection for 3-7 days. Subsequently, LMN-shRNAs-mCherry vectors were retrovirally transduced and the GFP+mCherry+ double positive population of cells were tracked over time using a BD LSR II flow cytometer. Complete shRNA sequences are provided in Table 8.3.

Table 8.1 List of shRNAs sequence.

human shRNA	97mer shRNA sequence
NSD3.1236	TGCTGTTGACAGTGAGCGAAAGGGAAGAACCAGTACTAAATAGTGAAGCCACA GATGTATTTAGTACTGGTTCTTCCCTTGTGCCTACTGCCTCGGA
NSD3.1399	TGCTGTTGACAGTGAGCGACAGCTTGAGGTTTCATACTAAATAGTGAAGCCACAG ATGTATTTAGTATGAACCTCAAGCTGGTGCCTACTGCCTCGGA
mouse shRNA	97mer shRNA sequence
Ren.713	TGCTGTTGACAGTGAGCGCAGGAATTATAATGCTTATCTATAGTGAAGCCACAG ATGTATAGATAAGCATTATAATTCCTATGCCTACTGCCTCGGA
BRD4.1448	TGCTGTTGACAGTGAGCGACACAATCAAGTCTAACTAGATAGTGAAGCCACAG ATGTATCTAGTTTAGACTTGATTGTGCTGCCTACTGCCTCGGA
NSD3.218	TGCTGTTGACAGTGAGCGCACCCACCATCAATCAGCTTGTTAGTGAAGCCACAG ATGTAACAAGCTGATTGATGGTGGGTATGCCTACTGCCTCGGA
NSD3.1019	TGCTGTTGACAGTGAGCGCACAAAGGTCATGAACAGTATATAGTGAAGCCACAG ATGTATATACTGTTTCATGACCTTTGTATGCCTACTGCCTCGGA
NSD3.1653	TGCTGTTGACAGTGAGCGCACGAAGGGTATTGGTAACAAATAGTGAAGCCACA GATGTATTTGTTACCAATACCCTTCGTTTGCCTACTGCCTCGGA
NSD3L.1953	TGCTGTTGACAGTGAGCGCAACGAGTATGTCGGTGAATTATAGTGAAGCCACAG ATGTATAATTCACCGACATACTCGTTTTGCCTACTGCCTCGGA
NSD3L.2198	TGCTGTTGACAGTGAGCGAAGGGATGGAGTTAACGTTTAATAGTGAAGCCACAG ATGTATTAACGTTAACTCCATCCCTGTGCCTACTGCCTCGGA
NSD3L.2718	TGCTGTTGACAGTGAGCGCTCCCAAGATAGTGGAGAAGAATAGTGAAGCCACA GATGTATTCTTCTCCACTATCTTGGGATTGCCTACTGCCTCGGA
NSD3L.2963	TGCTGTTGACAGTGAGCGCCAGTGTCTTTGCAATCAGCAATAGTGAAGCCACAG ATGTATTGCTGATTGCAAAGACACTGATGCCTACTGCCTCGGA
NSD3L.3042	TGCTGTTGACAGTGAGCGCTACGATCAGTGTAAGCCTAATAGTGAAGCCACAG ATGTATTAGGCTTTACACTGATCGTATTGCCTACTGCCTCGGA
CHD8.434	TGCTGTTGACAGTGAGCGACCCAGTAATACTGGAGGACAATAGTGAAGCCACA GATGTATTGTCTCCAGTATTACTGGGGTGCCTACTGCCTCGGA
CHD8.2934	TGCTGTTGACAGTGAGCGCCAGGGACACCGTTACAAAATATAGTGAAGCCACAG ATGTATATTTTGTAAACGGTGTCCCTGTTGCCTACTGCCTCGGA
CHD8.3190	TGCTGTTGACAGTGAGCGCCAGAGCTATTTTAGAGAAGAATAGTGAAGCCACAG ATGTATTCTTCTCTAAAATAGCTCTGTTGCCTACTGCCTCGGA
CHD8.3265	TGCTGTTGACAGTGAGCGCCACAATGATGGAGCTACGAAATAGTGAAGCCACA GATGTATTTTCGTAGCTCCATCATTGTGTTGCCTACTGCCTCGGA
CHD8.6109	TGCTGTTGACAGTGAGCGACCGACTCACCTACAAGACTATAGTGAAGCCACAG ATGTATAGTCTTGTGAGGTGAGTCGGTGCCTACTGCCTCGGA
CHD8.6761	TGCTGTTGACAGTGAGCGCACAGTTCAGATCAAAGATGAATAGTGAAGCCACAG ATGTATTCATCTTTGATCTGAAGTGTATGCCTACTGCCTCGGA

8.4 RT-qPCR

Total RNA was extracted from PBS-washed cell pellets using TRIzol reagent (Invitrogen) following the manufacturer's instructions. DNase I treatment was performed to eliminate contaminating genomic DNA after RNA isolation. cDNA was synthesized using the Q-Script cDNA SuperMix (Quanta BioScience), followed by qPCR with SYBR green (ABI) on an ABI 7900HT. All results were quantified using the delta Ct method with *Gapdh* as the control gene for normalization. All RT primer sequences are listed in the Table 8.2.

Table 8.2 Primers used for RT-qPCR for mouse genes.

Gene	Primer sequence
m <i>Gapdh</i> RT_F	TTCACCACCATGGAGAAGGC
m <i>Gapdh</i> RT_R	CCCTTTTGGCTCCACCCT
m <i>Nsd3</i> RT_F	TCCTTACCAGCCTCCATCAC
m <i>Nsd3</i> RT_R	CCCATCTCCTGTTGCATTCT
m <i>Chd8</i> RT_F1	GGCAGTCCAAGTGCTTCTTC
m <i>Chd8</i> RT_R1	TTGGCCTGGACTCTCTGACT
m <i>Chd8</i> RT_F2	CAGTATGAGGGGCACAGCTT
m <i>Chd8</i> RT_R2	GGGAGCCTCTTCTGGACTCT
m <i>Myc</i> RT_F	GCCGATCAGCTGGAGATGA
m <i>Myc</i> RT_R	GTCGTCAGGATCGCAGATGAAG
m <i>Myb</i> RT_F	GCTGAAGAAGCTGGTGG AAC
m <i>Myb</i> RT_R	CAACGCTTCGGACCATATTT
m <i>Check1</i> RT_F	ATTCTATGGCCACAGGAGGG
m <i>Check1</i> RT_R	ATAAACCACCCCTGCCATGA
m <i>Chst13</i> RT_F	CAGTGTTTCGTTGAAGGGCTC
m <i>Chst13</i> RT_R	TTGTGTGCCCAAGAAGATGC
m <i>Elane</i> RT_F	TGGCCTCAGAGATTGTTGGT
m <i>Elane</i> RT_R	TACCTGCACTGACCGGAAAT
m <i>Hmgb2</i> RT_F	GAACACCCAGGCCTGTCTAT
m <i>Hmgb2</i> RT_R	TTCCTGCTTCACTTTTGCCC
m <i>Bod11</i> RT_F	TGAGGCTGCTGTTGAAAATG
m <i>Bod11</i> RT_R	AGCTGCTGCTGGTTTTGAAT
m <i>Bptf</i> RT_F	GGTAAGAAACTGGGCCAACA
m <i>Bptf</i> RT_R	CCCTTCAGGTACCCCTTAGC

8.5 Protein lysate preparation for Western blotting

500,000 live cells were collected and lysed using 2x Laemmli Sample Buffer (#161-0737, BIO-RAD), supplemented with Beta-mercaptoethanol. The lysate was resuspended using 1 ml syringe and 26 ½ gauge needle until smooth and then was heated to 95 degree for 7 min. About 10% of extract was loaded into each well. Protein extracts were resolved by SDS-polyacrylamide gel electrophoresis and then transferred to nitrocellulose membrane at 90 V for 1-2 hours for immunoblotting.

8.6 May-Grünwald-Giemsa Cytospin staining

RN2 cells were transduced with individual TRMPV-Neo shRNAs (selected with G418), followed by treatment with dox for 4 days. For CRISPR-Cas9 targeting of *Chd8*, RN2c cells were lentivirally transduced with LRG sgRNAs and analyzed on day 6 post infection. RN2 cells were cytospun onto glass slides followed by staining with May-Grünwald (#019K4368; Sigma-Aldrich) and Giemsa (#010M4338; Sigma-Aldrich), following the manufacturer's instruction. Images were collected with a Zeiss Observer Microscope using a 40x objective.

8.7 c-Kit/Mac-1 staining and flow cytometry

RN2 cells transduced with TRMPV-Neo constructs were treated with dox for 4 days to induce shRNA expression or RN2c cells transduced with LRG sgRNAs were analyzed on day 5 post infection. Cells were collected in FACS buffer (5% FBS, 0.05% NaN₃ in PBS) and incubated with c-Kit or Mac-1 antibody (1:200) for 1 hour at 4°C. Stained cells were analyzed with an LSR II flow cytometer and data analysis was performed with Flowjo software. Gating was performed on dsRed+/shRNA+ or GFP+/sgRNA+ live cells.

8.8 Immunoprecipitation

PBS-washed cell pellets were resuspended in Buffer A2 (10 mM Hepes-KOH pH 7.9, 1.5 mM MgCl₂, 10 mM KCl) and incubated on ice for 30 minutes to allow hypotonic cell membrane lysis. Nuclei were spun down at 4900 rcf for 5 minutes and resuspended in Buffer C2 (20 mM Hepes-KOH pH 7.9, 25% glycerol, 420 mM NaCl, 1.5 mM MgCl₂, 0.2 mM EDTA) and incubated on ice for 30 minutes. Samples were then centrifuged at 18000 rcf for 10 minutes and the supernatant (nuclear extract) was then diluted with Buffer C2_No salt (20 mM Hepes-KOH pH 7.9, 25% glycerol, 1.5 mM MgCl₂, 0.2 mM EDTA) to reduce NaCl concentration to 150 mM. For endogenous IP, 1 mg of nuclear extracts was incubated with 2 µg antibody overnight at 4°C, followed by incubation with 25 µl Protein A Dynabeads (#10002D; Life Technologies) for 2 hours at 4°C. Beads were then washed three times with 1 ml TBS (50 mM Tris-Cl, pH 7.5, 150 mM NaCl) plus 0.5% NP-40 and one additional wash with TBS (no NP-40). Material was eluted from beads by adding Laemmli Sample Buffer and boiling for 5 minutes. For FLAG-IP, 1 mg nuclear extracts was incubated with 25 µl of anti-FLAG pre-conjugated agarose beads (#A2220; Sigma-Aldrich) for 2 hours at 4°C. Washing conditions were the same as for endogenous IP, however protein complexes were eluted using 3X FLAG peptide (#F4799; Sigma-Aldrich). For FLAG-IP-Western performed in RN2 cells, nuclear extracts were treated with Benzonase (#E1014, Sigma-Aldrich) for 2 hours at 4°C before incubation with anti-FLAG beads.

8.9 FLAG-NSD3-short IP-mass spectrometry

Nuclear extracts were prepared as described above from HEK293T cells after transient transfection for 48 hours with either an empty MSCV vector (for mock IP) or an MSCV vector expressing FLAG tagged NSD3-short. 4 mg of nuclear extracts were used as starting material to

incubate with 8 μg of anti-FLAG antibody overnight, followed by incubation with 100 μl Protein G Dynabeads (#10004D; Life Technologies) for 2 hours. Beads were washed three times in 1 ml TBS plus 0.5% NP-40 and then with 1 ml TBS. Proteins were eluted using 3X FLAG peptide from beads. Samples were then precipitated using trichloroacetic acid and washed with acetone.

Mass spectrometry and data analysis was performed at the Taplin Biological Mass Spectrometry Facility at Harvard University. Samples were resuspended in 50 μl 50 mM ammonium bicarbonate with about 5 $\text{ng}/\mu\text{l}$ trypsin. The extracts were then dried in a speed-vac for around 1 hour. The samples were then stored at 4°C until analysis. On the day of analysis the samples were reconstituted in 5-10 μl of HPLC solvent A (2.5% acetonitrile, 0.1% formic acid). A nano-scale reverse-phase HPLC capillary column was created by packing 2.6 μm C18 spherical silica beads into a fused silica capillary (100 μm inner diameter x ~25 cm length) with a flame-drawn tip (Shevchenko et al. 1996). After equilibrating the column, each sample was loaded via a Famos auto sampler (LC Packings) onto the column. A gradient was formed and peptides were eluted with increasing concentrations of solvent B (97.5% acetonitrile, 0.1% formic acid). As peptides eluted they were subjected to electrospray ionization and then entered into an LTQ Orbitrap Velos Pro ion-trap mass spectrometer (Thermo Fisher Scientific). Peptides were detected, isolated, and fragmented to produce a tandem mass spectrum of specific fragment ions for each peptide. Peptide sequences (and hence protein identity) were determined by matching protein databases with the acquired fragmentation pattern by the software program, Sequest (ThermoFisher) (Eng et al. 1994). All databases include a reversed version of all the sequences and the data were filtered to between a one and two percent false discovery rate (FDR) and no peptide detected in mock IP sample. Complete IP-MS data can be found in appendix A.

8.10 FLAG-NSD3-short IP iTRAQ mass spectrometry

Analysis was performed at the CSHL Proteomics Shared Resource. Tryptic Digestion and iTRAQ Labeling – The beads for NSD3-short IP and mock IP samples were reconstituted with 20 μ l of 50mM triethylammonium bicarbonate buffer (TEAB). Protease Max Surfactant was added to a final concentration of 0.1% and tris(2-carboxyethyl)phosphine (TCEP) was added to a final concentration of 5 mM. Samples were then heated to 55°C for 20min, allowed to cool to room temperature and methyl methanethiosulfonate (MMTS) was added to a final concentration of 10 mM. Samples were incubated at room temperature for 20 min to complete blocking of free sulfhydryl groups. 2 μ g of sequencing grade trypsin (Promega) was then added to the samples to digest overnight at 37°C. After digestion the supernatant was removed from the beads and was dried in speed-vac. Peptides were reconstituted in 50 μ l of 0.5 M TEAB/70% ethanol and labeled with 8-plex iTRAQ reagent for 2 hours at room temperature essentially according to previous study (Ross et al. 2004). Labeled samples were then acidified to pH 4 using formic acid, combined and concentrated in speed-vac until ~10 μ l remained.

2-Dimensional Fractionation – Peptides were fractionated using a high-low pH reverse phase separation strategy adapted from previous study (Gilar et al. 2005). For the first (high pH) dimension, peptides were fractionated on a 10cm x 1.0mm column packed with Gemini 3 μ m C18 resin (Phenomenex) at a flow rate of 100 μ l/min. Mobile phase A consisted of 20 mM ammonium formate pH 10 and mobile phase B consisted of 90% acetonitrile/20 mM ammonium formate pH 10. Samples were reconstituted with 50 μ l of mobile phase A and the entire sample injected onto the column. Peptides were separated using a 35 minutes linear gradient from 5% B to 70% B and then increasing mobile phase to 95% B for 10 minutes. Fractions were collected every minute for 40 minutes and were then combined into 8 fractions using the concatenation

strategy described by (Wang et al. 2011). Each of the 8 fractions was then separately injected into the mass spectrometer using capillary reverse phase LC at low pH.

Mass Spectrometry - An Orbitrap Velos Pro mass spectrometer (Thermo Scientific), equipped with a nano-ion spray source was coupled to an EASY-nLC system (Thermo Scientific). The nano-flow LC system was configured with a 180 μm I.D. fused silica capillary trap column containing 3 cm of Aqua 5 μm C18 material (Phenomenex), and a self-pack PicoFrit™ 100 μm analytical column with an 8 μm emitter (New Objective) packed to 15 cm with Aqua 3 μm C18 material (Phenomenex). Mobile phase A consisted of 2% acetonitrile; 0.1% formic acid and mobile phase B consisted of 90% acetonitrile; 0.1% formic Acid. 3 μl of each sample dissolved in mobile phase A, were injected through the autosampler onto the trap column. Peptides were then separated using the following linear gradient steps at a flow rate of 400 nl/min: 5% B for 1 min, 5% B to 35% B over 70 min, 35% B to 75% B over 15 min, held at 75% B for 8 min, 75% B to 8% B over 1 min and the final 5 min held at 8% B. Eluted peptides were directly electrosprayed into the Orbitrap Velos Pro mass spectrometer with the application of a distal 2.3 kV spray voltage and a capillary temperature of 275 °C. Each full-scan mass spectrum (Res=60,000; 380-1700 m/z) was followed by MS/MS spectra for the top 12 masses. High-energy collisional dissociation (HCD) was used with the normalized collision energy set to 35 for fragmentation, the isolation width set to 1.2 and activation time of 0.1. A duration of 70 seconds was set for the dynamic exclusion with an exclusion list size of 500, repeat count of 1 and exclusion mass width of 10ppm. We used monoisotopic precursor selection for charge states 2+ and greater, and all data were acquired in profile mode.

Database Searching - Peaklist files were generated by Mascot Distiller (Matrix Science). Protein identification and quantification was carried using Mascot 2.4 (Perkins et al. 1999)

against the UniProt human sequence database (89,005 sequences; 35,230,190 residues). Methylthiolation of cysteine and N-terminal and lysine iTRAQ modifications were set as fixed modifications, methionine oxidation and deamidation (NQ) as variable. Trypsin was used as cleavage enzyme with one missed cleavage allowed. Mass tolerance was set at 30 ppm for intact peptide mass and 0.3 Da for fragment ions. Search results were rescored to give a final 1% FDR using a randomized version of the same Uniprot Human database. Protein-level iTRAQ ratios were calculated as intensity weighted, using only peptides with expectation values < 0.05. As this was a protein IP experiment, no global ratio normalization was applied. Protein enrichment was then calculated by dividing the true sample protein ratios with the corresponding mock IP sample ratios, with values 1.25 used as a cutoff for enrichment. Complete iTRAQ data can be found in appendix B.

8.11 Peptide pull-down assay

Nuclear extracts were prepared as described above from HEK293T cells after transient transfection with an MSCV vector expressing FLAG tagged NSD3-short wild-type or W284A mutant for 48 hours. 2 µg Biotinylated histone H3 peptides (aa27-45) (EpiCypher) were incubated with 20 µl streptavidin-coated magnetic beads (Invitrogen) in 500 µl peptide binding buffer (50 mM Tris-HCl, PH 7.4, 150 mM NaCl, 0.05% NP-40+ protease inhibitor cocktail) at 4°C for 3 hours. The bound beads were washed three times in 1 ml of binding buffer and then incubated with 0.5 mg nuclear extract at 4°C for 2 hours. To remove non-specific binding, the beads were washed in 1 ml washing buffer (50 mM Tris-HCl, 150 mM NaCl, 0.5% NP-40) for four times and followed by final wash with 1 ml TBS (50 mM Tris-HCl, 150 mM NaCl). The

bound proteins were eluted by 2x Laemmli Sample Buffer (supplemented with Beta-mercaptoethanol) and analyzed by SDS-PAGE and anti-FLAG Western blotting.

8.12 GAL4 luciferase reporter assay

Plasmids encoding the GAL4 DNA-binding domain (DBD) fusions (modified from pFN26A (BIND) hRluc-neo Flexi® Vector, #E1380; Promega) were co-transfected with pGL4.35[luc2P/9XGAL4UAS/Hygro] Vector (#E1370; Promega) into HEK293T for 48 hours. Luciferase activity was measured with Dual Luciferase Reporter Assay System (#E1910; Promega) following the manufacturer's instructions. All the data shown represent Firefly luciferase activity normalized to the internal Renilla luciferase activity, the latter of which was expressed via a constitutive promoter on the pFN26A plasmid.

8.13 Expression and purification of recombinant GST-NSD3 fragments from bacteria

0.2 mM IPTG (#10724815; Roche) was added to a culture of *E.coli* when the OD600 was 0.6-0.8 and then was returned to a 30°C incubator for 3 hours. Cells were spun down at 7200 rcf at 4°C for 5 minutes and resuspended in BC500 buffer (20 mM Tris-HCl, PH 8.0, 500 mM KCl, 0.5 mM EDTA, 1% NP-40, 20% glycerol, 1 mM DTT, 0.5 mM PMSF, 2 µl/ml Protease Inhibitor Cocktail (#P8340; Sigma-Aldrich)) plus 2 mg/ml of lysozyme (#L6876; Sigma-Aldrich). After incubation at room temperature for 5 minutes, 1% Triton-X 100 was added and cells were further lysed with sonication (5 seconds on/off at 40% amplitude) for 2 minutes. Cells were spun down at 14,000 rcf for 10 minutes and then the supernatant was incubated with GST-sepharose 4B beads (#17-0756-01; GE Healthcare) overnight at 4°C. After four washes with

BC500 and one wash with PBS (supplemented with 20% glycerol, 1% NP-40 and 0.5 mM PMSF), proteins were eluted with Reduced Glutathione Solution (10 mM glutathione dissolved in 50 mM Tris, pH 8, #G4251; Sigma-Aldrich) and stored at -80 °C.

8.14 Cloning, expression, and purification of recombinant proteins from Sf9 cells

The BRD4 ET domain (608-699) and NSD3 100-263 were expressed in the baculoviral-induced insect cell culture system (Bieniossek et al. 2008). These constructs included an N-terminal Strep₂-SUMO tag that allowed for affinity purification and enhanced solubility of the recombinant protein. After expression, cells were harvested by centrifugation at ~1,000g, resuspended in lysis buffer (50 mM Tris, pH 8.0, 0.1 M KCl, 1 mM dithiothreitol (DTT)) (~20 mL per liter culture), and lysed by sonication. The cell lysate was clarified by ultracentrifugation at 140,000g for 45 min and the supernatant was applied to a Strep-Tactin (IBA) column equilibrated with lysis buffer. The bound proteins were washed with lysis buffer, further washed with lysis buffer containing 2 mM ATP, and finally eluted in lysis buffer containing 5 mM D-desthiobiotin.

The eluted proteins were then further purified by ion exchange chromatography using a MonoS 5/50 GL column (GE Healthcare) equilibrated with 25 mM MES, pH 6.5, and 2 mM DTT. Bound proteins were fractionated by elution using a linear gradient of NaCl from 0 to 1 M. Fractions corresponding to the target protein were pooled, concentrated, and purified further by gel filtration using a Superdex75 column equilibrated with 20 mM Tris, pH 8.0, 150 mM NaCl, and 2 mM DTT. The purified protein was concentrated to 1–5 mg/mL and stored at -80°C until

needed. Typical yields were 0.5–2 mg of purified protein (>98% purity as assessed by SDS–PAGE, 260/280 is around 0.6) per liter culture.

8.15 Surface plasmon resonance

The binding affinity of Strep₂SUMO-NSD3 100-263 for Strep₂SUMO-BRD4 ET was measured with a Biacore X100 equipped with a CM5 biosensor. After sensor surface activation for covalent amine coupling, the purified Strep₂SUMO-BRD4 ET was diluted in 10 mM sodium acetate, pH 5.0, to a concentration of 1 nM and applied to the active flow cell surface until 1000 Response Units (R.U.) of material were immobilized. Subsequently, the remaining activated sites on the sensor surface were quenched by injecting ethanolamine. The sensor chip was equilibrated with HEPES buffered saline with surfactant P20 (HBS-P: 10 mM HEPES, pH 7.4; 0.15 M NaCl; 0.005% (vol/vol) surfactant P20; GE) that thereafter served as the system running buffer.

Purified Strep₂SUMO-NSD3 100-263 (analyte) was diluted serially in HBS-P to the concentrations indicated and maintained at room temperature (~23°C) until the time of injection. Injections were performed in parallel, with the analyte being applied over both the active and reference flow cells simultaneously at a flow rate of 30 µl/min at a sensor temperature of 25°C. Injections were performed in triplicate; association and dissociation phases were 60 seconds each. Following each injection, an additional dissociation time of 60 seconds and a wash injection (HBS-P mixed with 5 M NaCl in a ratio of 4:1 for a final NaCl concentration of 1 M) were performed to ensure complete dissociation of the analyte.

Data were analyzed with the Biacore X100 evaluation software package (version 2.0.1) after reference flow cell and blank subtraction. Steady-state responses for each sensorgram were then used to calculate the K_D .

8.16 Molecular Graphics

Molecular graphics were created with PyMOL version 1.7.4.0 based on the structure of the BRD4 ET domain from *Mus musculus* (PDB ID: 2JNS). Since mouse and human BRD4 have an identical amino acid sequence in the 608-671 region, we have labeled amino acids in this structure using the human numbering system.

8.17 CRISPR-Cas9 targeting of *Chd8* and *Nsd3*

Cas9 was expressed RN2 and MOLM-13 cell line were generated with MSCV construct expressing 5' 3xFLAG tagged human-codon optimized Cas9, described previously (Ross et al. 2004) (#65655; Addgene). All sgRNAs were designed with <http://crispr.mit.edu/> and inserted into the U6-sgRNA-EFS-GFP vector (#65656; Addgene). For sgRNA lentivirus packaging, HEK293T cells were transfected with sgRNA:pVSVg:psPAX2 plasmids in a 4:2:3 ratio by using PEI reagent (#23966; Polysciences) following standard procedures. GFP percentages were measured by Guava EasyCyte flow HT instrument (Millipore) over time after infection. Complete sgRNA sequences are given in Table 8.3.

Table 8.3 List of sgRNAs sequences.

	mouse sgRNA sequences
<i>Chd8_e12.1</i>	TCAATCGCCTTCTTGCAGG
<i>Chd8_e12.2</i>	ACGCTCCCAGTTAGTAATGG
<i>Chd8_e17.1</i>	GTCGATAGCAGCTTGTCGA
<i>Chd8_e17.2</i>	CGTATTGATGGGCGAGTTAG
<i>Rosa26</i>	GAAGATGGGCGGGAGTCTTC
<i>Rpa3_e1.3</i>	GCTGGCGTTGACGCGCGCTT
	human sgRNA sequences
<i>NSD3_e4.1</i>	CCAAGGTGGGAACCTATCCT
<i>NSD3_e4.2</i>	TTCAGGTTGGCGATCTTGTG
<i>NSD3_e4.3</i>	AGGTGGGAACCTATCCTTGG
<i>NSD3_e4.4</i>	CCAAGGATAGGTTCCACCT
<i>NSD3_e4.5</i>	GGATCACTTGAAACCATACA
<i>NSD3_e4.6</i>	AGGTGGGAACCTATCCTTGG
<i>NSD3_e4.7</i>	CTATCCTTGGTGGCCTTGTA
<i>NSD3_e15.1</i>	TTGGTTCTCATGACTACTAC
<i>NSD3_e15.2</i>	CCAGGGCCTTAAACATGACT
<i>NSD3_e15.3</i>	AGTCCCCCAAGTCATGTTTA
<i>NSD3_e20.1</i>	ATTAGTTACACTGTTCTCGT
<i>NSD3_e20.2</i>	AATTAGTTACACTGTTCTCG
<i>NSD3_e21.1</i>	ATAATTGATGCCGGCCCAA
<i>NSD3_e21.2</i>	TTGGGCCGGCATCAATTATA
<i>NSD3_e21.3</i>	GTGAATGGAGATGTTTCGAGT
<i>RPA3_e1.3</i>	GATGAATTGAGCTAGCATGC

For comprehensive mutagenesis of *Chd8* and *Nsd3* exons, sgRNAs were designed to target all possible PAM NGG sequences on the plus or minus strand of the protein-coding region. sgRNAs were excluded from the library if they were predicted to have off-target cutting sites in the genome. Single stranded oligos were synthesized through array platform (Customarray), PCR amplified, and then Gibson cloned into a Bsmbl-digested LRG sgRNA lentiviral expression vector (#65656; Addgene). The Gibson ligation product was transformed into electrocompetent cells (#C6400-3, Invitrogen) to ensure at least 300x library coverage of each sgRNA designs. The overall quality of the pooled sgRNA library was measured through deep sequencing (data not shown).

Lentivirus of pooled sgRNAs targeting *Chd8* and *Nsd3* was produced as described above and the viral titer was measured through a serial dilutions. To ensure that a single sgRNA was transduced per cell, the viral volume for infection was chosen to achieve a multiplicity of infection (MOI) of 0.3–0.4. To maintain the representation of each sgRNA, at least 1000 leukemia cells transduced with each individual sgRNAs were maintained throughout the entire culture period. The genomic DNA was extracted at the indicated time points with QiAamp DNA mini kit (#51304; Qiagen), following the manufacturer's instructions. The pooled screening libraries were constructed as described previously (Shi et al. 2015b). Briefly, multiple independent PCR reactions were set up to amplify the sgRNA cassette to maintain at least 500x sgRNA library representation using the 2X Phusion Master Mix (#F-548; Thermo Scientific). PCR products were pooled and subjected to Illumina MiSeq library construction and sequencing. The sequence data were trimmed to contain only the sgRNA sequence before mapped to the reference sgRNA library allowing no mismatch. The read counts were then calculated for each individual sgRNA. To compare the differential representation of individual sgRNAs between day

2 and day 12 time points, read counts for each sgRNA were normalized to the counts of the negative control *Rosa26* sgRNA. Complete sgRNA sequences for pool screening are provided in appendix C.

8.18 Chromatin immunoprecipitation

For each IP, 10 million cells were crosslinked with 1% formaldehyde for 20 min at room temperature. 0.125 M glycine was used to quench the reaction. Cells were lysed sequentially with cell lysis buffer (10 mM Tris, pH 8.0, 10 mM NaCl, 0.2% NP-40) and nuclei lysis buffer (50 mM Tris, pH 8.0, 10 mM EDTA, 1% SDS). After spun down at 1400g for 5 minutes, pellets were resuspended and sonicated in IP dilution buffer (20 mM Tris, pH 8.0, 2 mM EDTA, 150 mM NaCl, 1% Triton X-100, 0.01% SDS). Each sample was incubated with 2 µg antibody overnight at 4°C and then precipitated using Protein A Dynabeads (#10002D; Life Technologies) or Protein G Dynabeads for 2 hours at 4°C. Eluted samples were reversed crosslink in 65°C overnight and digested with RNase A and Proteinase K. ChIP-qPCR were performed with SYBR green (ABI) on an ABI 7900HT. An input standard curve dilution series of the pre-immunoprecipitated genomic DNA was used to normalize for the differences of start cell number and the amplification efficiency of various primer sets. All results were quantified as IP signal/Input. All ChIP-qPCR primer sequences are provided in Table 8.4.

Table 8.4 Primers used for ChIP-qPCR.

Gene	Mouse ChIP-qPCR primer sequence
Negative ChIP F	AACCTCACACACAACAAGCTG
Negative ChIP R	TGTGATAGGGAGAATGCTTGC
RN2 <i>Myc</i> E1_F	ACGCTCAGAGTGCTTTCCAT
RN2 <i>Myc</i> E1_R	GTGGTGTGGGGTGGCTAATA
RN2 <i>Myc</i> E2_F	AACCATAAAAAGCCGTGGTG
RN2 <i>Myc</i> E2_R	GCTGCTCGGTCATTTCTCTT
RN2 <i>Myc</i> E3_F	GAACAGGAAGCTGGGGAAAT
RN2 <i>Myc</i> E3_R	TGCAAGGAGGCTTTTCCTAA
RN2 <i>Myc</i> E4_F	CACATGTGGTCCACTCCAAG
RN2 <i>Myc</i> E4_R	CCAACCCTCTTGTCTTTCCA
RN2 <i>Myc</i> E5_F	GCAACAGCAAGAACCAGTGA
RN2 <i>Myc</i> E5_R	TGCTTCTCCTGAACCACCTT
B-ALL <i>Myc</i> E1.1_F	CCTGCTGGGGTTTCTACTCA
B-ALL <i>Myc</i> E1.1_R	GGCACGGTAAGCTTGTTAGC
B-ALL <i>Myc</i> E2.1_F	TCTGTTGCACAGGTCTCTGG
B-ALL <i>Myc</i> E2.1_R	TCAGGGTCACCCAAGTCTTC
B-ALL <i>Myc</i> E3.1_F	CATATACCACAGGGGGCAAT
B-ALL <i>Myc</i> E3.1_R	TGAGAGACCGCATGGTAAGA
B-ALL <i>Myc</i> E4.1_F	GAACAGGAAGCTGGGGAAAT
B-ALL <i>Myc</i> E4.1_R	TGCAAGGAGGCTTTTCCTAA
B-ALL <i>Myc</i> E5.1_F	CACATGTGGTCCACTCCAAG
B-ALL <i>Myc</i> E5.1_R	CCAACCCTCTTGTCTTTCCA
<i>Bcl2</i> +200kb_F	CCAACCAGAGGCCATACTGT
<i>Bcl2</i> +200kb_R	GCCTTGACTTGGACCTGTGT
<i>Cd47</i> -73kb_F	ACCCTTTCTCCTTCGTGGTT
<i>Cd47</i> -73kb_R	ATCTCTCCCCGGTCTGACTT
<i>Cdk6</i> +159kb_F	TCCAGCGTCCTCATAAATCC
<i>Cdk6</i> +159kb_R	GCTGGGGAACTCTCTCTCCT
<i>Myb</i> +42kb_F	GCTGGTGAGGCACTTTCTTC
<i>Myb</i> +42kb_R	TTCTGTTTGGGAGAACACC
<i>Chst13</i> +4kb_F	TCAGCCTACACTTCCAGCAA
<i>Chst13</i> +4kb_R	CACCTGAGGCTCTGACCTAG
<i>Dio2</i> +9kb_F	GACCGAGAAGCAGAGATGGA
<i>Dio2</i> +9kb_R	CAGACTCACCAGCCCATGTA
Gene	Human ChIP-qPCR primer sequence
<i>MYC</i> neg_F	GGTCAGGCCAACTTGATTGT
<i>MYC</i> neg_R	AATTTGTGTTGGGCCACATT
<i>MYC</i> E1_F	AGGAGCCCACCTTCTCATTT
<i>MYC</i> E1_R	ACATTGCAAGAGTGGCTGTG
<i>MYC</i> E2_F	AGGAAGTGGCTTTCACATGC
<i>MYC</i> E2_R	GCGTGCAAAAAGAGAGAAACC
<i>MYC</i> E3_F	TGGCAGTGGTCACAGTTCTC
<i>MYC</i> E3_R	CTCTGCACCTTGAGCATTGA
<i>MYC</i> E4_F	TTCCAGAGACCTCTGCCAGT
<i>MYC</i> E4_R	AGAGTCGGGTGTTGATTG
<i>MYC</i> E5_F	CAATACTTTCCGGCCATTTTC
<i>MYC</i> E5_R	GACGTTGGCCACTTCATCTT

8.19 RNA-Seq and ChIP-Seq library construction

For RNA-Seq, total RNA was prepared using TRIzol reagent according to the manufacturer's protocol. Libraries were constructed with the TruSeq Sample Prep Kit v2 (Illumina) following the manufacturer's protocol. 2 µg of total RNA was used for Poly-A selection and fragmentation, subsequently followed by cDNA synthesis, end repairing, dA tailing, adapter ligation and library amplification. For the second replicate of RNA-Seq with NSD3 knockdown, libraries were constructed with "not-so-random" primer-based RNA-Seq library preparation method according to protocols described previously (Armour et al. 2009). 1 µg of total RNA was used for first-strand synthesis with Superscript III system (#18080044; Life Technologies) and then performed second-strand synthesis with Klenow fragment (#M0212L; NEB). The final PCR amplification was performed with Expand High Fidelity Plus PCR system (#11732641001; Roche). For ChIP-Seq, 100 million cells and 10 µg antibodies were used for each IP. DNA was prepared as described above in chromatin immunoprecipitation. ChIP-Seq libraries were constructed with TruSeq ChIP Sample Prep Kit (Illumina) according to the manufacturer's instructions. The quantity and quality of all libraries were determined using a Bioanalyzer (Agilent Technologies). Barcoded libraries were sequenced in a multiplexed fashion with two to four libraries at equal molar ratio, using an Illumina HiSeq 2000 platform with single end reads of 50 bases.

8.20 RNA-Seq analysis

With Tophat software, raw reads were mapped to the mouse genome (mm9) allowing no mismatch. Then differentially expressed genes were analyzed with Cuffdiff software and structural RNAs were masked. reads per kilobase per million (RPKM) from control (shRen.713

or *sgRosa26*) and biological replicates of shRNAs knockdown or sgRNAs knockout samples were used to calculate fold change with log₂ scale. During this step, only genes with OK test status and RPKM above 5 were considered (For library constructed with “not-so-random” primer-based preparation method, only genes with OK test status were considered).

Differentially expressed gene lists were further analyzed using GSEA with weighted GSEA Preranked tool following the instructions found at www.broadinstitute.org/gsea/index.jsp. 1000 gene set permutations were applied (Subramanian et al. 2005). The LSC gene set (Somerville et al. 2009) and MYC target gene set (Schuhmacher et al. 2001) were obtained from prior studies. The macrophage development gene set was obtained from the Ingenuity Pathway Analysis (IPA) software (Ingenuity). The BRD4 gene set signature represents the top 500 downregulated genes identified previously following BRD4 knockdown in RN2 cells using microarrays (Zuber et al. 2011b). All the gene sets used here are provided in appendix D.

8.21 ChIP-Seq analysis

With Bowtie software, raw reads were mapped to the mouse genome (mm9) allowing 2 mismatches. Model based analysis of ChIP-Seq (MACS) software was used to identify ChIP-Seq peaks. A p value threshold of enrichment of 1e-5 was used for identifying significant peaks within each dataset. For BRD4 peaks, a FDR of less than 1%, and 10-fold enrichment relative to input control cutoffs were applied as well. ChIP-Seq signals were normalized to the number of total mapped reads. For read-density calculation with ChIP-Seq enriched regions, heatmap matrices were created by counting tags using 20 kb window size with 20 bp bin. Data from a previous study (Roe et al. 2015) were used to define BRD4 peaks at promoter and enhancer regions. ChIP-Seq data sets of H3K4me3 and H3K27ac were obtained from a previous study

(Shi et al. 2013b). Visualization of heatmap matrices were done by using Java TreeView 1.1.6r4 (<http://jtreeview.sourceforge.net>).

8.22 Accession numbers

The accession number for the raw and processed sequencing data reported in this paper is GEO: GSE71186, with the subseries accession numbers GEO: GSE71183 for ChIP-Seq and GEO: GSE71185 for RNAseq, respectively.

8.23 Animal studies

All mouse experiments were approved by the Cold Spring Harbor animal care and use committee. For conditional RNAi experiments in vivo, Tet-ON MLL-AF9/Nras^{G12D} leukemia cells were transduced with TRMPV-Neo shRNA constructs and transplanted by tail-vein injection of 1×10^6 cells into sub-lethally (5.5 Gy) irradiated B6/SJL(CD45.1) recipient mice, as described previously (Zuber et al. 2011b). Animals were treated with dox in both drinking water (2 mg/ml with 2% sucrose; Sigma-Aldrich) and food (625 mg/kg, Harlan laboratories) to induce shRNAs expression. For whole-body bioluminescent imaging, mice were intraperitoneally injected with 50 mg/kg D-Luciferin (Goldbio) and analysed using an IVIS Spectrum system (Caliper LifeSciences) 10 minutes later.

8.24 Antibodies

β -actin HRP (#A3854; Sigma-Aldrich) and Myc (#1472-1; Epitomics) were used for western blotting; FLAG (#F1804; Sigma-Aldrich), BRD4 (#A301-985A; Bethyl), CHD8 (#A301-224A; Bethyl) and NSD3 (polyclonal antibody made in house raised against the peptide:

PTDYYHSEIPNTRPHEC) were used for western blotting, immunoprecipitation and ChIP assays; control IgG (#I8140; Sigma-Aldrich) was used for immunoprecipitation and ChIP; H3K36me2 (#39255; Active Motif) was used for ChIP; APC-labeled c-Kit (#105811; biolegend) and Mac-1 (#101211; biolegend) were used for flow cytometry.

Bibliography

Albrecht BK, Gehling VS, Hewitt MC, Vaswani RG, Cote A, Leblanc Y, Nasveschuk CG, Bellon S, Bergeron L, Campbell R et al. 2016. Identification of a Benzoisoxazoloazepine Inhibitor (CPI-0610) of the Bromodomain and Extra-Terminal (BET) Family as a Candidate for Human Clinical Trials. *Journal of medicinal chemistry* **59**: 1330-1339.

Alekseyenko AA, Walsh EM, Wang X, Grayson AR, Hsi PT, Kharchenko PV, Kuroda MI, French CA. 2015. The oncogenic BRD4-NUT chromatin regulator drives aberrant transcription within large topological domains. *Genes & development* **29**: 1507-1523.

Alsarraj J, Faraji F, Geiger TR, Mattaini KR, Williams M, Wu J, Ha NH, Merlino T, Walker RC, Bosley AD et al. 2013. BRD4 short isoform interacts with RRP1B, SIPA1 and components of the LINC complex at the inner face of the nuclear membrane. *PloS one* **8**: e80746.

Althoff K, Beckers A, Bell E, Nortmeyer M, Thor T, Sprussel A, Lindner S, De Preter K, Florin A, Heukamp LC et al. 2015. A Cre-conditional MYCN-driven neuroblastoma mouse model as an improved tool for preclinical studies. *Oncogene* **34**: 3357-3368.

Ambrosini G, Sawle AD, Musi E, Schwartz GK. 2015. BRD4-targeted therapy induces Myc-independent cytotoxicity in Gnaq/11-mutant uveal melanoma cells. *Oncotarget* **6**: 33397-33409.

Amin HM, Yang Y, Shen Y, Estey EH, Giles FJ, Pierce SA, Kantarjian HM, O'Brien SM, Jilani I, Albitar M. 2005. Having a higher blast percentage in circulation than bone marrow: clinical implications in myelodysplastic syndrome and acute lymphoid and myeloid leukemias. *Leukemia* **19**: 1567-1572.

Amorim S, Stathis A, Gleeson M, Iyengar S, Magarotto V, Leleu X, Morschhauser F, Karlin L, Broussais F, Rezai K. 2016. Bromodomain inhibitor OTX015 in patients with lymphoma or multiple myeloma: a dose-escalation, open-label, pharmacokinetic, phase 1 study. *The Lancet Haematology*.

Anand P, Brown JD, Lin CY, Qi J, Zhang R, Artero PC, Alaiti MA, Bullard J, Alazem K, Margulies KB et al. 2013. BET bromodomains mediate transcriptional pause release in heart failure. *Cell* **154**: 569-582.

Angrand PO, Apiou F, Stewart AF, Dutrillaux B, Losson R, Chambon P. 2001. NSD3, a new SET domain-containing gene, maps to 8p12 and is amplified in human breast cancer cell lines. *Genomics* **74**: 79-88.

Armour CD, Castle JC, Chen R, Babak T, Loerch P, Jackson S, Shah JK, Dey J, Rohl CA, Johnson JM et al. 2009. Digital transcriptome profiling using selective hexamer priming for cDNA synthesis. *Nature methods* **6**: 647-649.

- Asangani IA, Dommeti VL, Wang X, Malik R, Cieslik M, Yang R, Escara-Wilke J, Wilder-Romans K, Dhanireddy S, Engelke C et al. 2014. Therapeutic targeting of BET bromodomain proteins in castration-resistant prostate cancer. *Nature* **510**: 278-282.
- Bailey D, Jahagirdar R, Gordon A, Hafiane A, Campbell S, Chatur S, Wagner GS, Hansen HC, Chiacchia FS, Johansson J et al. 2010. RVX-208: a small molecule that increases apolipoprotein A-I and high-density lipoprotein cholesterol in vitro and in vivo. *Journal of the American College of Cardiology* **55**: 2580-2589.
- Baker EK, Taylor S, Gupte A, Sharp PP, Walia M, Walsh NC, Zannettino AC, Chalk AM, Burns CJ, Walkley CR. 2015. BET inhibitors induce apoptosis through a MYC independent mechanism and synergise with CDK inhibitors to kill osteosarcoma cells. *Scientific reports* **5**: 10120.
- Bamborough P, Diallo H, Goodacre JD, Gordon L, Lewis A, Seal JT, Wilson DM, Woodrow MD, Chung CW. 2012. Fragment-based discovery of bromodomain inhibitors part 2: optimization of phenylisoxazole sulfonamides. *Journal of medicinal chemistry* **55**: 587-596.
- Bandopadhyay P, Bergthold G, Nguyen B, Schubert S, Gholamin S, Tang Y, Bolin S, Schumacher SE, Zeid R, Masoud S et al. 2014. BET bromodomain inhibition of MYC-amplified medulloblastoma. *Clinical cancer research : an official journal of the American Association for Cancer Research* **20**: 912-925.
- Bandukwala HS, Gagnon J, Togher S, Greenbaum JA, Lamperti ED, Parr NJ, Molesworth AM, Smithers N, Lee K, Witherington J et al. 2012. Selective inhibition of CD4+ T-cell cytokine production and autoimmunity by BET protein and c-Myc inhibitors. *Proceedings of the National Academy of Sciences of the United States of America* **109**: 14532-14537.
- Baratta MG, Schinzel AC, Zwang Y, Bandopadhyay P, Bowman-Colin C, Kutt J, Curtis J, Piao H, Wong LC, Kung AL et al. 2015. An in-tumor genetic screen reveals that the BET bromodomain protein, BRD4, is a potential therapeutic target in ovarian carcinoma. *Proceedings of the National Academy of Sciences of the United States of America* **112**: 232-237.
- Barrett E, Brothers S, Wahlestedt C, Beurel E. 2014. I-BET151 selectively regulates IL-6 production. *Biochimica et biophysica acta* **1842**: 1549-1555.
- Belkina AC, Nikolajczyk BS, Denis GV. 2013. BET protein function is required for inflammation: Brd2 genetic disruption and BET inhibitor JQ1 impair mouse macrophage inflammatory responses. *Journal of immunology* **190**: 3670-3678.
- Bennett JM, Catovsky D, Daniel MT, Flandrin G, Galton DA, Gralnick HR, Sultan C. 1976. Proposals for the classification of the acute leukaemias. French-American-British (FAB) co-operative group. *British journal of haematology* **33**: 451-458.
- Berkovits BD, Wolgemuth DJ. 2011. The first bromodomain of the testis-specific double bromodomain protein Brdt is required for chromocenter organization that is modulated by genetic background. *Developmental biology* **360**: 358-368.

Bernier R, Golzio C, Xiong B, Stessman HA, Coe BP, Penn O, Witherspoon K, Gerds J, Baker C, Vulto-van Silfhout AT et al. 2014. Disruptive CHD8 mutations define a subtype of autism early in development. *Cell* **158**: 263-276.

Bernt KM, Zhu N, Sinha AU, Vempati S, Faber J, Krivtsov AV, Feng Z, Punt N, Daigle A, Bullinger L et al. 2011. MLL-rearranged leukemia is dependent on aberrant H3K79 methylation by DOT1L. *Cancer cell* **20**: 66-78.

Berthon C, Raffoux E, Thomas X, Vey N, Gomez-Roca C, Yee K, Taussig DC, Rezai K, Roumier C, Herait P. 2016. Bromodomain inhibitor OTX015 in patients with acute leukaemia: a dose-escalation, phase 1 study. *The Lancet Haematology*.

Bhadury J, Nilsson LM, Muralidharan SV, Green LC, Li Z, Gesner EM, Hansen HC, Keller UB, McLure KG, Nilsson JA. 2014. BET and HDAC inhibitors induce similar genes and biological effects and synergize to kill in Myc-induced murine lymphoma. *Proceedings of the National Academy of Sciences of the United States of America* **111**: E2721-2730.

Bhagwat AS, Roe J-S, Mok BYL, Hohmann AF, Shi J, Vakoc CR. 2016. BET Bromodomain Inhibition Releases the Mediator Complex from Select cis-Regulatory Elements. *Cell reports*.

Bieniossek C, Richmond TJ, Berger I. 2008. MultiBac: multigene baculovirus-based eukaryotic protein complex production. *Current protocols in protein science / editorial board, John E Coligan [et al]* **Chapter 5**: Unit 5 20.

Bihani T, Ezell SA, Ladd B, Grosskurth SE, Mazzola AM, Pietras M, Reimer C, Zinda M, Fawell S, D'Cruz CM. 2015. Resistance to everolimus driven by epigenetic regulation of MYC in ER+ breast cancers. *Oncotarget* **6**: 2407-2420.

Bisgrove DA, Mahmoudi T, Henklein P, Verdin E. 2007. Conserved P-TEFb-interacting domain of BRD4 inhibits HIV transcription. *Proceedings of the National Academy of Sciences of the United States of America* **104**: 13690-13695.

Boi M, Gaudio E, Bonetti P, Kwee I, Bernasconi E, Tarantelli C, Rinaldi A, Testoni M, Cascione L, Ponzoni M et al. 2015. The BET Bromodomain Inhibitor OTX015 Affects Pathogenetic Pathways in Preclinical B-cell Tumor Models and Synergizes with Targeted Drugs. *Clinical cancer research : an official journal of the American Association for Cancer Research* **21**: 1628-1638.

Brondfield S, Umesh S, Corella A, Zuber J, Rappaport AR, Gaillard C, Lowe SW, Goga A, Kogan SC. 2015. Direct and indirect targeting of MYC to treat acute myeloid leukemia. *Cancer chemotherapy and pharmacology* **76**: 35-46.

Brown JD, Lin CY, Duan Q, Griffin G, Federation AJ, Paranal RM, Bair S, Newton G, Lichtman AH, Kung AL et al. 2014. NF-kappaB directs dynamic super enhancer formation in inflammation and atherogenesis. *Molecular cell* **56**: 219-231.

Cancer Genome Atlas Research N. 2013. Genomic and epigenomic landscapes of adult de novo acute myeloid leukemia. *The New England journal of medicine* **368**: 2059-2074.

- Cassileth PA, Harrington DP, Hines JD, Oken MM, Mazza JJ, McGlave P, Bennett JM, O'Connell MJ. 1988. Maintenance chemotherapy prolongs remission duration in adult acute nonlymphocytic leukemia. *Journal of clinical oncology : official journal of the American Society of Clinical Oncology* **6**: 583-587.
- Ceribelli M, Kelly PN, Shaffer AL, Wright GW, Xiao W, Yang Y, Mathews Griner LA, Guha R, Shinn P, Keller JM et al. 2014. Blockade of oncogenic I κ B kinase activity in diffuse large B-cell lymphoma by bromodomain and extraterminal domain protein inhibitors. *Proceedings of the National Academy of Sciences of the United States of America* **111**: 11365-11370.
- Chaidos A, Caputo V, Gouvedenou K, Liu B, Marigo I, Chaudhry MS, Rotolo A, Tough DF, Smithers NN, Bassil AK et al. 2014. Potent antimyeloma activity of the novel bromodomain inhibitors I-BET151 and I-BET762. *Blood* **123**: 697-705.
- Chan SC, Selth LA, Li Y, Nyquist MD, Miao L, Bradner JE, Raj GV, Tilley WD, Dehm SM. 2015. Targeting chromatin binding regulation of constitutively active AR variants to overcome prostate cancer resistance to endocrine-based therapies. *Nucleic acids research* **43**: 5880-5897.
- Chapuy B, McKeown MR, Lin CY, Monti S, Roemer MG, Qi J, Rahl PB, Sun HH, Yeda KT, Doench JG et al. 2013. Discovery and characterization of super-enhancer-associated dependencies in diffuse large B cell lymphoma. *Cancer cell* **24**: 777-790.
- Chen C, Liu Y, Lu C, Cross JR, Morris JPt, Shroff AS, Ward PS, Bradner JE, Thompson C, Lowe SW. 2013. Cancer-associated IDH2 mutants drive an acute myeloid leukemia that is susceptible to Brd4 inhibition. *Genes & development* **27**: 1974-1985.
- Chen C, Liu Y, Rappaport AR, Kitzing T, Schultz N, Zhao Z, Shroff AS, Dickins RA, Vakoc CR, Bradner JE et al. 2014. MLL3 is a haploinsufficient 7q tumor suppressor in acute myeloid leukemia. *Cancer cell* **25**: 652-665.
- Chen J, Odenike O, Rowley JD. 2010. Leukaemogenesis: more than mutant genes. *Nature reviews Cancer* **10**: 23-36.
- Cheng Z, Gong Y, Ma Y, Lu K, Lu X, Pierce LA, Thompson RC, Muller S, Knapp S, Wang J. 2013. Inhibition of BET bromodomain targets genetically diverse glioblastoma. *Clinical cancer research : an official journal of the American Association for Cancer Research* **19**: 1748-1759.
- Cho H, Herzka T, Zheng W, Qi J, Wilkinson JE, Bradner JE, Robinson BD, Castillo-Martin M, Cordon-Cardo C, Trotman LC. 2014. RapidCaP, a novel GEM model for metastatic prostate cancer analysis and therapy, reveals myc as a driver of Pten-mutant metastasis. *Cancer discovery* **4**: 318-333.
- Da Costa D, Agathangelou A, Perry T, Weston V, Petermann E, Zlatanou A, Oldreive C, Wei W, Stewart G, Longman J et al. 2013. BET inhibition as a single or combined therapeutic approach in primary paediatric B-precursor acute lymphoblastic leukaemia. *Blood cancer journal* **3**: e126.

Dawson MA, Gudgin EJ, Horton SJ, Giotopoulos G, Meduri E, Robson S, Cannizzaro E, Osaki H, Wiese M, Putwain S et al. 2014. Recurrent mutations, including NPM1c, activate a BRD4-dependent core transcriptional program in acute myeloid leukemia. *Leukemia* **28**: 311-320.

Dawson MA, Kouzarides T. 2012. Cancer epigenetics: from mechanism to therapy. *Cell* **150**: 12-27.

Dawson MA, Prinjha RK, Dittmann A, Giotopoulos G, Bantscheff M, Chan WI, Robson SC, Chung CW, Hopf C, Savitski MM et al. 2011. Inhibition of BET recruitment to chromatin as an effective treatment for MLL-fusion leukaemia. *Nature* **478**: 529-533.

de Greef GE, van Putten WL, Boogaerts M, Huijgens PC, Verdonck LF, Vellenga E, Theobald M, Jacky E, Lowenberg B, Dutch-Belgian Hemato-Oncology Co-operative Group H et al. 2005. Criteria for defining a complete remission in acute myeloid leukaemia revisited. An analysis of patients treated in HOVON-SAKK co-operative group studies. *British journal of haematology* **128**: 184-191.

De Raedt T, Beert E, Pasmant E, Luscan A, Brems H, Ortonne N, Helin K, Hornick JL, Mautner V, Kehrer-Sawatzki H et al. 2014. PRC2 loss amplifies Ras-driven transcription and confers sensitivity to BRD4-based therapies. *Nature* **514**: 247-251.

Delmore JE, Issa GC, Lemieux ME, Rahl PB, Shi J, Jacobs HM, Kastiris E, Gilpatrick T, Paranal RM, Qi J et al. 2011. BET bromodomain inhibition as a therapeutic strategy to target c-Myc. *Cell* **146**: 904-917.

Devaiah BN, Lewis BA, Cherman N, Hewitt MC, Albrecht BK, Robey PG, Ozato K, Sims RJ, 3rd, Singer DS. 2012. BRD4 is an atypical kinase that phosphorylates serine2 of the RNA polymerase II carboxy-terminal domain. *Proceedings of the National Academy of Sciences of the United States of America* **109**: 6927-6932.

Devaraj SG, Fiskus W, Shah B, Qi J, Sun B, Iyer SP, Sharma S, Bradner JE, Bhalla KN. 2015. HEXIM1 induction is mechanistically involved in mediating anti-AML activity of BET protein bromodomain antagonist. *Leukemia*.

Dey A, Chitsaz F, Abbasi A, Misteli T, Ozato K. 2003. The double bromodomain protein Brd4 binds to acetylated chromatin during interphase and mitosis. *Proceedings of the National Academy of Sciences of the United States of America* **100**: 8758-8763.

Dhalluin C, Carlson JE, Zeng L, He C, Aggarwal AK, Zhou MM. 1999. Structure and ligand of a histone acetyltransferase bromodomain. *Nature* **399**: 491-496.

Ding N, Hah N, Yu RT, Sherman MH, Benner C, Leblanc M, He M, Liddle C, Downes M, Evans RM. 2015. BRD4 is a novel therapeutic target for liver fibrosis. *Proceedings of the National Academy of Sciences of the United States of America*.

Dingar D, Kalkat M, Chan PK, Srikumar T, Bailey SD, Tu WB, Coyaud E, Ponzielli R, Kolyar M, Jurisica I et al. 2015. BioID identifies novel c-MYC interacting partners in cultured cells and xenograft tumors. *Journal of proteomics* **118**: 95-111.

- Dohner H, Weisdorf DJ, Bloomfield CD. 2015. Acute Myeloid Leukemia. *The New England journal of medicine* **373**: 1136-1152.
- Donner AJ, Ebmeier CC, Taatjes DJ, Espinosa JM. 2010. CDK8 is a positive regulator of transcriptional elongation within the serum response network. *Nature structural & molecular biology* **17**: 194-201.
- Eng JK, McCormack AL, Yates JR. 1994. An approach to correlate tandem mass spectral data of peptides with amino acid sequences in a protein database. *Journal of the American Society for Mass Spectrometry* **5**: 976-989.
- Falini B, Tiacci E, Martelli MP, Ascani S, Pileri SA. 2010. New classification of acute myeloid leukemia and precursor-related neoplasms: changes and unsolved issues. *Discovery medicine* **10**: 281-292.
- Feng Q, Zhang Z, Shea MJ, Creighton CJ, Coarfa C, Hilsenbeck SG, Lanz R, He B, Wang L, Fu X et al. 2014. An epigenomic approach to therapy for tamoxifen-resistant breast cancer. *Cell research* **24**: 809-819.
- Filippakopoulos P, Knapp S. 2014. Targeting bromodomains: epigenetic readers of lysine acetylation. *Nature reviews Drug discovery* **13**: 337-356.
- Filippakopoulos P, Qi J, Picaud S, Shen Y, Smith WB, Fedorov O, Morse EM, Keates T, Hickman TT, Felleter I et al. 2010. Selective inhibition of BET bromodomains. *Nature* **468**: 1067-1073.
- Fiskus W, Sharma S, Qi J, Valenta JA, Schaub LJ, Shah B, Peth K, Portier BP, Rodriguez M, Devaraj SG et al. 2014. Highly active combination of BRD4 antagonist and histone deacetylase inhibitor against human acute myelogenous leukemia cells. *Molecular cancer therapeutics* **13**: 1142-1154.
- French CA. 2012. Pathogenesis of NUT midline carcinoma. *Annual review of pathology* **7**: 247-265.
- French CA, Rahman S, Walsh EM, Kuhnle S, Grayson AR, Lemieux ME, Grunfeld N, Rubin BP, Antonescu CR, Zhang S et al. 2014. NSD3-NUT fusion oncoprotein in NUT midline carcinoma: implications for a novel oncogenic mechanism. *Cancer discovery* **4**: 928-941.
- French CA, Ramirez CL, Kolmakova J, Hickman TT, Cameron MJ, Thyne ME, Kutok JL, Toretsky JA, Tadavarthy AK, Kees UR et al. 2008. BRD-NUT oncoproteins: a family of closely related nuclear proteins that block epithelial differentiation and maintain the growth of carcinoma cells. *Oncogene* **27**: 2237-2242.
- Gallagher SJ, Mijatov B, Gunatilake D, Tiffen JC, Gowrishankar K, Jin L, Pupo GM, Cullinane C, Prinjha RK, Smithers N et al. 2014. The epigenetic regulator I-BET151 induces BIM-dependent apoptosis and cell cycle arrest of human melanoma cells. *The Journal of investigative dermatology* **134**: 2795-2805.

Gamsjaeger R, Webb SR, Lamonica JM, Billin A, Blobel GA, Mackay JP. 2011. Structural basis and specificity of acetylated transcription factor GATA1 recognition by BET family bromodomain protein Brd3. *Molecular and cellular biology* **31**: 2632-2640.

Garcia PL, Miller AL, Kreitzburg KM, Council LN, Gamblin TL, Christein JD, Heslin MJ, Arnoletti JP, Richardson JH, Chen D et al. 2015. The BET bromodomain inhibitor JQ1 suppresses growth of pancreatic ductal adenocarcinoma in patient-derived xenograft models. *Oncogene*.

Garraway LA, Lander ES. 2013. Lessons from the cancer genome. *Cell* **153**: 17-37.

Gautschi JaM, R. 2014. PHARMACEUTICAL FORMULATION CONTAINING THIENOTRIAZOLODIAZEPINE COMPOUNDS. ONCOETHIX SA (Avenue de l'Elysee 32, Lausanne, CH-1006, CH).

Gilar M, Olivova P, Daly AE, Gebler JC. 2005. Two-dimensional separation of peptides using RP-RP-HPLC system with different pH in first and second separation dimensions. *Journal of separation science* **28**: 1694-1703.

Gopalakrishnan R, Matta H, Tolani B, Triche T, Jr., Chaudhary PM. 2015. Immunomodulatory drugs target IKZF1-IRF4-MYC axis in primary effusion lymphoma in a cereblon-dependent manner and display synergistic cytotoxicity with BRD4 inhibitors. *Oncogene*.

Gosmini R, Nguyen VL, Toum J, Simon C, Brusq JM, Krysa G, Mirguet O, Riou-Eymard AM, Boursier EV, Trottet L et al. 2014. The discovery of I-BET726 (GSK1324726A), a potent tetrahydroquinoline ApoA1 up-regulator and selective BET bromodomain inhibitor. *Journal of medicinal chemistry* **57**: 8111-8131.

Grayson AR, Walsh EM, Cameron MJ, Godec J, Ashworth T, Ambrose JM, Aserlind AB, Wang H, Evan GI, Kluk MJ et al. 2014. MYC, a downstream target of BRD-NUT, is necessary and sufficient for the blockade of differentiation in NUT midline carcinoma. *Oncogene* **33**: 1736-1742.

Harris NL, Jaffe ES, Diebold J, Flandrin G, Muller-Hermelink HK, Vardiman J, Lister TA, Bloomfield CD. 1999. The World Health Organization classification of neoplastic diseases of the hematopoietic and lymphoid tissues. Report of the Clinical Advisory Committee meeting, Airlie House, Virginia, November, 1997. *Annals of oncology : official journal of the European Society for Medical Oncology / ESMO* **10**: 1419-1432.

Hayden MS, Ghosh S. 2012. NF-kappaB, the first quarter-century: remarkable progress and outstanding questions. *Genes & development* **26**: 203-234.

He C, Li F, Zhang J, Wu J, Shi Y. 2013. The methyltransferase NSD3 has chromatin-binding motifs, PHD5-C5HCH, that are distinct from other NSD (nuclear receptor SET domain) family members in their histone H3 recognition. *The Journal of biological chemistry* **288**: 4692-4703.

Heinemann A, Cullinane C, De Paoli-Iseppi R, Wilmott JS, Gunatilake D, Madore J, Strbenac D, Yang JY, Gowrishankar K, Tiffen JC et al. 2015. Combining BET and HDAC inhibitors

synergistically induces apoptosis of melanoma and suppresses AKT and YAP signaling. *Oncotarget* **6**: 21507-21521.

Hensel T, Giorgi C, Schmidt O, Calzada-Wack J, Neff F, Buch T, Niggli FK, Schafer BW, Burdach S, Richter GH. 2015. Targeting the EWS-ETS transcriptional program by BET bromodomain inhibition in Ewing sarcoma. *Oncotarget*.

Henssen A, Thor T, Odersky A, Heukamp L, El-Hindy N, Beckers A, Speleman F, Althoff K, Schafers S, Schramm A et al. 2013. BET bromodomain protein inhibition is a therapeutic option for medulloblastoma. *Oncotarget* **4**: 2080-2095.

Henssen AG, Althoff K, Odersky A, Beckers A, Koche R, Speleman F, Schaefer S, Bell E, Nortmeyer M, Westermann F et al. 2015. Targeting MYCN-driven transcription by BET-bromodomain inhibition. *Clinical cancer research : an official journal of the American Association for Cancer Research*.

Hsin JP, Manley JL. 2012. The RNA polymerase II CTD coordinates transcription and RNA processing. *Genes & development* **26**: 2119-2137.

Hu Y, Zhou J, Ye F, Xiong H, Peng L, Zheng Z, Xu F, Cui M, Wei C, Wang X et al. 2015. BRD4 inhibitor inhibits colorectal cancer growth and metastasis. *International journal of molecular sciences* **16**: 1928-1948.

Huang B, Yang XD, Zhou MM, Ozato K, Chen LF. 2009. Brd4 coactivates transcriptional activation of NF-kappaB via specific binding to acetylated RelA. *Molecular and cellular biology* **29**: 1375-1387.

Jacques-Fricke BT, Gammill LS. 2014. Neural crest specification and migration independently require NSD3-related lysine methyltransferase activity. *Molecular biology of the cell* **25**: 4174-4186.

Jaffe JD, Wang Y, Chan HM, Zhang J, Huether R, Kryukov GV, Bhang HE, Taylor JE, Hu M, Englund NP et al. 2013. Global chromatin profiling reveals NSD2 mutations in pediatric acute lymphoblastic leukemia. *Nature genetics* **45**: 1386-1391.

Jahagirdar R, Zhang H, Azhar S, Tobin J, Attwell S, Yu R, Wu J, McLure KG, Hansen HC, Wagner GS et al. 2014. A novel BET bromodomain inhibitor, RVX-208, shows reduction of atherosclerosis in hyperlipidemic ApoE deficient mice. *Atherosclerosis* **236**: 91-100.

James LI, Barsyte-Lovejoy D, Zhong N, Krichevsky L, Korboukh VK, Herold JM, MacNevin CJ, Norris JL, Sagum CA, Tempel W et al. 2013. Discovery of a chemical probe for the L3MBTL3 methyllysine reader domain. *Nature chemical biology* **9**: 184-191.

Jang MK, Mochizuki K, Zhou M, Jeong HS, Brady JN, Ozato K. 2005. The bromodomain protein Brd4 is a positive regulatory component of P-TEFb and stimulates RNA polymerase II-dependent transcription. *Molecular cell* **19**: 523-534.

Jenuwein T, Allis CD. 2001. Translating the histone code. *Science* **293**: 1074-1080.

Jiang YW, Veschambre P, Erdjument-Bromage H, Tempst P, Conaway JW, Conaway RC, Kornberg RD. 1998. Mammalian mediator of transcriptional regulation and its possible role as an end-point of signal transduction pathways. *Proceedings of the National Academy of Sciences of the United States of America* **95**: 8538-8543.

Kannan A, Lin Z, Shao Q, Zhao S, Fang B, Moreno MA, Vural E, Stack BC, Jr., Suen JY, Kannan K et al. 2015. Dual mTOR inhibitor MLN0128 suppresses Merkel cell carcinoma (MCC) xenograft tumor growth. *Oncotarget*.

Khmelnitsky YL, Mozhaev VV, Cotterill IC, Michels PC, Boudjabi S, Khlebnikov V, Madhava Reddy M, Wagner GS, Hansen HC. 2013. In vitro biosynthesis, isolation, and identification of predominant metabolites of 2-(4-(2-hydroxyethoxy)-3,5-dimethylphenyl)-5,7-dimethoxyquinazolin-4(3H)-one (RVX-208). *European journal of medicinal chemistry* **64**: 121-128.

Kim SM, Kee HJ, Eom GH, Choe NW, Kim JY, Kim YS, Kim SK, Kook H, Kook H, Seo SB. 2006. Characterization of a novel WHSC1-associated SET domain protein with H3K4 and H3K27 methyltransferase activity. *Biochemical and biophysical research communications* **345**: 318-323.

Kim YJ, Bjorklund S, Li Y, Sayre MH, Kornberg RD. 1994. A multiprotein mediator of transcriptional activation and its interaction with the C-terminal repeat domain of RNA polymerase II. *Cell* **77**: 599-608.

Knoechel B, Roderick JE, Williamson KE, Zhu J, Lohr JG, Cotton MJ, Gillespie SM, Fernandez D, Ku M, Wang H et al. 2014. An epigenetic mechanism of resistance to targeted therapy in T cell acute lymphoblastic leukemia. *Nature genetics* **46**: 364-370.

Korb E, Herre M, Zucker-Scharff I, Darnell RB, Allis CD. 2015. BET protein Brd4 activates transcription in neurons and BET inhibitor Jq1 blocks memory in mice. *Nature neuroscience* **18**: 1464-1473.

Krivtsov AV, Armstrong SA. 2007. MLL translocations, histone modifications and leukaemia stem-cell development. *Nature reviews Cancer* **7**: 823-833.

Kuo AJ, Cheung P, Chen K, Zee BM, Kioi M, Lauring J, Xi Y, Park BH, Shi X, Garcia BA et al. 2011. NSD2 links dimethylation of histone H3 at lysine 36 to oncogenic programming. *Molecular cell* **44**: 609-620.

Lamonica JM, Deng W, Kadauke S, Campbell AE, Gamsjaeger R, Wang H, Cheng Y, Billin AN, Hardison RC, Mackay JP et al. 2011. Bromodomain protein Brd3 associates with acetylated GATA1 to promote its chromatin occupancy at erythroid target genes. *Proceedings of the National Academy of Sciences of the United States of America* **108**: E159-168.

Lamonica JM, Vakoc CR, Blobel GA. 2006. Acetylation of GATA-1 is required for chromatin occupancy. *Blood* **108**: 3736-3738.

Langdon CG, Wiedemann N, Held MA, Mamillapalli R, Iyidogan P, Theodosakis N, Platt JT, Levy F, Vuagniaux G, Wang S et al. 2015. SMAC mimetic Debio 1143 synergizes with taxanes, topoisomerase inhibitors and bromodomain inhibitors to impede growth of lung adenocarcinoma cells. *Oncotarget* **6**: 37410-37425.

Latchman DS. 1997. Transcription factors: an overview. *The international journal of biochemistry & cell biology* **29**: 1305-1312.

Lee DH, Qi J, Bradner JE, Said JW, Doan NB, Forscher C, Yang H, Koeffler HP. 2015a. Synergistic effect of JQ1 and rapamycin for treatment of human osteosarcoma. *International journal of cancer Journal international du cancer* **136**: 2055-2064.

Lee S, Rellinger EJ, Kim KW, Craig BT, Romain CV, Qiao J, Chung DH. 2015b. Bromodomain and extraterminal inhibition blocks tumor progression and promotes differentiation in neuroblastoma. *Surgery* **158**: 819-826.

Lee TI, Young RA. 2013. Transcriptional regulation and its misregulation in disease. *Cell* **152**: 1237-1251.

Li GQ, Guo WZ, Zhang Y, Seng JJ, Zhang HP, Ma XX, Zhang G, Li J, Yan B, Tang HW et al. 2015. Suppression of BRD4 inhibits human hepatocellular carcinoma by repressing MYC and enhancing BIM expression. *Oncotarget*.

Li Y, Trojer P, Xu CF, Cheung P, Kuo A, Drury WJ, 3rd, Qiao Q, Neubert TA, Xu RM, Gozani O et al. 2009. The target of the NSD family of histone lysine methyltransferases depends on the nature of the substrate. *The Journal of biological chemistry* **284**: 34283-34295.

Lin YJ, Umehara T, Inoue M, Saito K, Kigawa T, Jang MK, Ozato K, Yokoyama S, Padmanabhan B, Guntert P. 2008. Solution structure of the extraterminal domain of the bromodomain-containing protein BRD4. *Protein science : a publication of the Protein Society* **17**: 2174-2179.

Liu R, Zhong Y, Li X, Chen H, Jim B, Zhou MM, Chuang PY, He JC. 2014. Role of transcription factor acetylation in diabetic kidney disease. *Diabetes* **63**: 2440-2453.

Liu W, Ma Q, Wong K, Li W, Ohgi K, Zhang J, Aggarwal AK, Rosenfeld MG. 2013. Brd4 and JMJD6-associated anti-pause enhancers in regulation of transcriptional pause release. *Cell* **155**: 1581-1595.

Lochrin SE, Price DK, Figg WD. 2014. BET bromodomain inhibitors--a novel epigenetic approach in castration-resistant prostate cancer. *Cancer biology & therapy* **15**: 1583-1585.

Long J, Li B, Rodriguez-Blanco J, Pastori C, Volmar CH, Wahlestedt C, Capobianco A, Bai F, Pei XH, Ayad NG et al. 2014. The BET bromodomain inhibitor I-BET151 acts downstream of smoothed protein to abrogate the growth of hedgehog protein-driven cancers. *The Journal of biological chemistry* **289**: 35494-35502.

Loosveld M, Castellano R, Gon S, Goubard A, Crouzet T, Pouyet L, Prebet T, Vey N, Nadel B, Collette Y et al. 2014. Therapeutic targeting of c-Myc in T-cell acute lymphoblastic leukemia, T-ALL. *Oncotarget* **5**: 3168-3172.

Loven J, Hoke HA, Lin CY, Lau A, Orlando DA, Vakoc CR, Bradner JE, Lee TI, Young RA. 2013. Selective inhibition of tumor oncogenes by disruption of super-enhancers. *Cell* **153**: 320-334.

Lucio-Eterovic AK, Carpenter PB. 2011. An open and shut case for the role of NSD proteins as oncogenes. *Transcription* **2**: 158-161.

Mathis D, Benoist C. 2009. Aire. *Annual review of immunology* **27**: 287-312.

Matzuk MM, McKeown MR, Filippakopoulos P, Li Q, Ma L, Agno JE, Lemieux ME, Picaud S, Yu RN, Qi J et al. 2012. Small-molecule inhibition of BRDT for male contraception. *Cell* **150**: 673-684.

Mazur PK, Herner A, Mello SS, Wirth M, Hausmann S, Sanchez-Rivera FJ, Lofgren SM, Kuschma T, Hahn SA, Vangala D et al. 2015. Combined inhibition of BET family proteins and histone deacetylases as a potential epigenetics-based therapy for pancreatic ductal adenocarcinoma. *Nature medicine* **21**: 1163-1171.

Mele DA, Salmeron A, Ghosh S, Huang HR, Bryant BM, Lora JM. 2013. BET bromodomain inhibition suppresses TH17-mediated pathology. *The Journal of experimental medicine* **210**: 2181-2190.

Meloche J, Potus F, Vaillancourt M, Bourgeois A, Johnson I, Deschamps L, Chabot S, Ruffenach G, Henry S, Breuils-Bonnet S et al. 2015. Bromodomain-Containing Protein 4: The Epigenetic Origin of Pulmonary Arterial Hypertension. *Circulation research* **117**: 525-535.

Meng S, Zhang L, Tang Y, Tu Q, Zheng L, Yu L, Murray D, Cheng J, Kim SH, Zhou X et al. 2014. BET Inhibitor JQ1 Blocks Inflammation and Bone Destruction. *Journal of dental research* **93**: 657-662.

Menon T, Yates JA, Bochar DA. 2010. Regulation of androgen-responsive transcription by the chromatin remodeling factor CHD8. *Molecular endocrinology* **24**: 1165-1174.

Mertz JA, Conery AR, Bryant BM, Sandy P, Balasubramanian S, Mele DA, Bergeron L, Sims RJ, 3rd. 2011. Targeting MYC dependence in cancer by inhibiting BET bromodomains. *Proceedings of the National Academy of Sciences of the United States of America* **108**: 16669-16674.

Miyoshi S, Ooike, S., Iwata, K., Hikawa, H., Sugahara, K. 2010. ANTITUMOR AGENT. Mitsubishi Tanabe Pharma Corporation EP2239264.

Morita S, Kojima T, Kitamura T. 2000. Plat-E: an efficient and stable system for transient packaging of retroviruses. *Gene therapy* **7**: 1063-1066.

- Moros A, Rodriguez V, Saborit-Villarroya I, Montraveta A, Balsas P, Sandy P, Martinez A, Wiestner A, Normant E, Campo E et al. 2014. Synergistic antitumor activity of lenalidomide with the BET bromodomain inhibitor CPI203 in bortezomib-resistant mantle cell lymphoma. *Leukemia* **28**: 2049-2059.
- Nadeem A, Al-Harbi NO, Al-Harbi MM, El-Sherbeeney AM, Ahmad SF, Siddiqui N, Ansari MA, Zoheir KM, Attia SM, Al-Hosaini KA et al. 2015. Imiquimod-induced psoriasis-like skin inflammation is suppressed by BET bromodomain inhibitor in mice through RORC/IL-17A pathway modulation. *Pharmacological research* **99**: 248-257.
- Neff T, Armstrong SA. 2013. Recent progress toward epigenetic therapies: the example of mixed lineage leukemia. *Blood* **121**: 4847-4853.
- Nicholls SJ, Gordon A, Johannson J, Ballantyne CM, Barter PJ, Brewer HB, Kastelein JJ, Wong NC, Borgman MR, Nissen SE. 2012. ApoA-I induction as a potential cardioprotective strategy: rationale for the SUSTAIN and ASSURE studies. *Cardiovascular drugs and therapy / sponsored by the International Society of Cardiovascular Pharmacotherapy* **26**: 181-187.
- Nicodeme E, Jeffrey KL, Schaefer U, Beinke S, Dewell S, Chung CW, Chandwani R, Marazzi I, Wilson P, Coste H et al. 2010. Suppression of inflammation by a synthetic histone mimic. *Nature* **468**: 1119-1123.
- Ott CJ, Kopp N, Bird L, Paranal RM, Qi J, Bowman T, Rodig SJ, Kung AL, Bradner JE, Weinstock DM. 2012. BET bromodomain inhibition targets both c-Myc and IL7R in high-risk acute lymphoblastic leukemia. *Blood* **120**: 2843-2852.
- Oyer JA, Huang X, Zheng Y, Shim J, Ezponda T, Carpenter Z, Allegretta M, Okot-Kotber CI, Patel JP, Melnick A et al. 2014. Point mutation E1099K in MMSET/NSD2 enhances its methyltransferase activity and leads to altered global chromatin methylation in lymphoid malignancies. *Leukemia* **28**: 198-201.
- Pastori C, Daniel M, Penas C, Volmar CH, Johnstone AL, Brothers SP, Graham RM, Allen B, Sarkaria JN, Komotar RJ et al. 2014. BET bromodomain proteins are required for glioblastoma cell proliferation. *Epigenetics* **9**: 611-620.
- Patel AJ, Liao CP, Chen Z, Liu C, Wang Y, Le LQ. 2014. BET bromodomain inhibition triggers apoptosis of NF1-associated malignant peripheral nerve sheath tumors through Bim induction. *Cell reports* **6**: 81-92.
- Perkins DN, Pappin DJ, Creasy DM, Cottrell JS. 1999. Probability-based protein identification by searching sequence databases using mass spectrometry data. *Electrophoresis* **20**: 3551-3567.
- Peterson P, Org T, Rebane A. 2008. Transcriptional regulation by AIRE: molecular mechanisms of central tolerance. *Nature reviews Immunology* **8**: 948-957.
- Picaud S, Wells C, Felletar I, Brotherton D, Martin S, Savitsky P, Diez-Dacal B, Philpott M, Bountra C, Lingard H et al. 2013. RVX-208, an inhibitor of BET transcriptional regulators with

selectivity for the second bromodomain. *Proceedings of the National Academy of Sciences of the United States of America* **110**: 19754-19759.

Popovic R, Martinez-Garcia E, Giannopoulou EG, Zhang Q, Zhang Q, Ezponda T, Shah MY, Zheng Y, Will CM, Small EC et al. 2014. Histone methyltransferase MMSET/NSD2 alters EZH2 binding and reprograms the myeloma epigenome through global and focal changes in H3K36 and H3K27 methylation. *PLoS genetics* **10**: e1004566.

Prinjha RK, Witherington J, Lee K. 2012. Place your BETs: the therapeutic potential of bromodomains. *Trends in pharmacological sciences* **33**: 146-153.

Puissant A, Frumm SM, Alexe G, Bassil CF, Qi J, Chanthery YH, Nekritz EA, Zeid R, Gustafson WC, Greninger P et al. 2013. Targeting MYCN in neuroblastoma by BET bromodomain inhibition. *Cancer discovery* **3**: 308-323.

Qin S, Min J. 2014. Structure and function of the nucleosome-binding PWWP domain. *Trends in biochemical sciences* **39**: 536-547.

Qiu H, Jackson AL, Kilgore JE, Zhong Y, Chan LL, Gehrig PA, Zhou C, Bae-Jump VL. 2015. JQ1 suppresses tumor growth through downregulating LDHA in ovarian cancer. *Oncotarget* **6**: 6915-6930.

Rahman S, Sowa ME, Ottinger M, Smith JA, Shi Y, Harper JW, Howley PM. 2011. The Brd4 extraterminal domain confers transcription activation independent of pTEFb by recruiting multiple proteins, including NSD3. *Molecular and cellular biology* **31**: 2641-2652.

Rajagopalan V, Vaidyanathan M, Janardhanam VA, Bradner JE. 2014. Pre-clinical analysis of changes in intra-cellular biochemistry of glioblastoma multiforme (GBM) cells due to c-Myc silencing. *Cellular and molecular neurobiology* **34**: 1059-1069.

Ram O, Goren A, Amit I, Shoresh N, Yosef N, Ernst J, Kellis M, Gymrek M, Issner R, Coyne M et al. 2011. Combinatorial patterning of chromatin regulators uncovered by genome-wide location analysis in human cells. *Cell* **147**: 1628-1639.

Redner RL, Wang J, Liu JM. 1999. Chromatin remodeling and leukemia: new therapeutic paradigms. *Blood* **94**: 417-428.

Roderick JE, Tesell J, Shultz LD, Brehm MA, Greiner DL, Harris MH, Silverman LB, Sallan SE, Gutierrez A, Look AT et al. 2014. c-Myc inhibition prevents leukemia initiation in mice and impairs the growth of relapsed and induction failure pediatric T-ALL cells. *Blood* **123**: 1040-1050.

Roe JS, Mercan F, Rivera K, Pappin DJ, Vakoc CR. 2015. BET Bromodomain Inhibition Suppresses the Function of Hematopoietic Transcription Factors in Acute Myeloid Leukemia. *Molecular cell* **58**: 1028-1039.

- Rosati R, La Starza R, Veronese A, Aventin A, Schwienbacher C, Vallespi T, Negrini M, Martelli MF, Mecucci C. 2002. NUP98 is fused to the NSD3 gene in acute myeloid leukemia associated with t(8;11)(p11.2;p15). *Blood* **99**: 3857-3860.
- Ross PL, Huang YN, Marchese JN, Williamson B, Parker K, Hattan S, Khainovski N, Pillai S, Dey S, Daniels S et al. 2004. Multiplexed protein quantitation in *Saccharomyces cerevisiae* using amine-reactive isobaric tagging reagents. *Molecular & cellular proteomics : MCP* **3**: 1154-1169.
- Roy N, Malik S, Villanueva KE, Urano A, Lu X, Von Figura G, Seeley ES, Dawson DW, Collisson EA, Hebrok M. 2015. Brg1 promotes both tumor-suppressive and oncogenic activities at distinct stages of pancreatic cancer formation. *Genes & development* **29**: 658-671.
- Ruan C, Lee CH, Cui H, Li S, Li B. 2015. Nucleosome contact triggers conformational changes of Rpd3S driving high-affinity H3K36me nucleosome engagement. *Cell reports* **10**: 204-215.
- Sankaran SM, Wilkinson AW, Gozani O. 2016. A PWWP domain of histone-lysine N-methyltransferase NSD2 binds to dimethylated Lys36 of histone H3 and regulates NSD2 function at chromatin. *The Journal of biological chemistry*.
- Sartor GC, Powell SK, Brothers SP, Wahlestedt C. 2015. Epigenetic Readers of Lysine Acetylation Regulate Cocaine-Induced Plasticity. *The Journal of neuroscience : the official journal of the Society for Neuroscience* **35**: 15062-15072.
- Schroder S, Cho S, Zeng L, Zhang Q, Kaehlcke K, Mak L, Lau J, Bisgrove D, Schnolzer M, Verdin E et al. 2012. Two-pronged binding with bromodomain-containing protein 4 liberates positive transcription elongation factor b from inactive ribonucleoprotein complexes. *The Journal of biological chemistry* **287**: 1090-1099.
- Schuhmacher M, Kohlhuber F, Holzel M, Kaiser C, Burtscher H, Jarsch M, Bornkamm GW, Laux G, Polack A, Weidle UH et al. 2001. The transcriptional program of a human B cell line in response to Myc. *Nucleic acids research* **29**: 397-406.
- Segura MF, Fontanals-Cirera B, Gaziel-Sovran A, Guijarro MV, Hanniford D, Zhang G, Gonzalez-Gomez P, Morante M, Jubierre L, Zhang W et al. 2013. BRD4 sustains melanoma proliferation and represents a new target for epigenetic therapy. *Cancer research* **73**: 6264-6276.
- Sengupta D, Kannan A, Kern M, Moreno MA, Vural E, Stack B, Jr., Suen JY, Tackett AJ, Gao L. 2015. Disruption of BRD4 at H3K27Ac-enriched enhancer region correlates with decreased c-Myc expression in Merkel cell carcinoma. *Epigenetics* **10**: 460-466.
- Shahbazi J, Liu PY, Atmadibrata B, Bradner JE, Marshall GM, Lock RB, Liu T. 2016. The bromodomain inhibitor JQ1 and the histone deacetylase inhibitor panobinostat synergistically reduce N-Myc expression and induce anticancer effects. *Clinical cancer research : an official journal of the American Association for Cancer Research*.
- Shao Q, Kannan A, Lin Z, Stack BC, Jr., Suen JY, Gao L. 2014. BET protein inhibitor JQ1 attenuates Myc-amplified MCC tumor growth in vivo. *Cancer research* **74**: 7090-7102.

- Shevchenko A, Wilm M, Vorm O, Mann M. 1996. Mass spectrometric sequencing of proteins silver-stained polyacrylamide gels. *Analytical chemistry* **68**: 850-858.
- Shi J, Cao J, Zhou BP. 2015a. Twist-BRD4 complex: potential drug target for basal-like breast cancer. *Current pharmaceutical design* **21**: 1256-1261.
- Shi J, Vakoc CR. 2014. The mechanisms behind the therapeutic activity of BET bromodomain inhibition. *Molecular cell* **54**: 728-736.
- Shi J, Wang E, Milazzo JP, Wang Z, Kinney JB, Vakoc CR. 2015b. Discovery of cancer drug targets by CRISPR-Cas9 screening of protein domains. *Nature biotechnology* **33**: 661-667.
- Shi J, Wang E, Zuber J, Rappaport A, Taylor M, Johns C, Lowe SW, Vakoc CR. 2013a. The Polycomb complex PRC2 supports aberrant self-renewal in a mouse model of MLL-AF9;Nras(G12D) acute myeloid leukemia. *Oncogene* **32**: 930-938.
- Shi J, Wang Y, Zeng L, Wu Y, Deng J, Zhang Q, Lin Y, Li J, Kang T, Tao M et al. 2014. Disrupting the interaction of BRD4 with diacetylated Twist suppresses tumorigenesis in basal-like breast cancer. *Cancer cell* **25**: 210-225.
- Shi J, Whyte WA, Zepeda-Mendoza CJ, Milazzo JP, Shen C, Roe JS, Minder JL, Mercan F, Wang E, Eckersley-Maslin MA et al. 2013b. Role of SWI/SNF in acute leukemia maintenance and enhancer-mediated Myc regulation. *Genes & development* **27**: 2648-2662.
- Shu S, Lin CY, He HH, Witwicky RM, Tabassum DP, Roberts JM, Janiszewska M, Jin Huh S, Liang Y, Ryan J et al. 2016. Response and resistance to BET bromodomain inhibitors in triple-negative breast cancer. *Nature*.
- Siegel RL, Miller KD, Jemal A. 2015. Cancer statistics, 2015. *CA: a cancer journal for clinicians* **65**: 5-29.
- Sigler PB. 1988. Transcriptional activation. Acid blobs and negative noodles. *Nature* **333**: 210-212.
- Somervaille TC, Matheny CJ, Spencer GJ, Iwasaki M, Rinn JL, Witten DM, Chang HY, Shurtleff SA, Downing JR, Cleary ML. 2009. Hierarchical maintenance of MLL myeloid leukemia stem cells employs a transcriptional program shared with embryonic rather than adult stem cells. *Cell stem cell* **4**: 129-140.
- Spiltoir JJ, Stratton MS, Cavasin MA, Demos-Davies K, Reid BG, Qi J, Bradner JE, McKinsey TA. 2013. BET acetyl-lysine binding proteins control pathological cardiac hypertrophy. *Journal of molecular and cellular cardiology* **63**: 175-179.
- Stathis A, Zucca E, Bekradda M, Gomez-Roca C, Delord JP, de La Motte Rouge T, Uro-Coste E, de Braud F, Pelosi G, French CA. 2016. Clinical Response of Carcinomas Harboring the BRD4-NUT Oncoprotein to the Targeted Bromodomain Inhibitor OTX015/MK-8628. *Cancer discovery*.

Stonestrom AJ, Hsu SC, Jahn KS, Huang P, Keller CA, Giardine BM, Kadauke S, Campbell AE, Evans P, Hardison RC et al. 2015. Functions of BET proteins in erythroid gene expression. *Blood* **125**: 2825-2834.

Stratikopoulos EE, Dendy M, Szabolcs M, Khaykin AJ, Lefebvre C, Zhou MM, Parsons R. 2015. Kinase and BET Inhibitors Together Clamp Inhibition of PI3K Signaling and Overcome Resistance to Therapy. *Cancer cell* **27**: 837-851.

Subramanian A, Tamayo P, Mootha VK, Mukherjee S, Ebert BL, Gillette MA, Paulovich A, Pomeroy SL, Golub TR, Lander ES et al. 2005. Gene set enrichment analysis: a knowledge-based approach for interpreting genome-wide expression profiles. *Proceedings of the National Academy of Sciences of the United States of America* **102**: 15545-15550.

Sullivan JM, Badimon A, Schaefer U, Ayata P, Gray J, Chung CW, von Schimmelmann M, Zhang F, Garton N, Smithers N et al. 2015. Autism-like syndrome is induced by pharmacological suppression of BET proteins in young mice. *The Journal of experimental medicine* **212**: 1771-1781.

Sun B, Shah B, Fiskus W, Qi J, Rajapakshe K, Coarfa C, Li L, Devaraj SG, Sharma S, Zhang L et al. 2015a. Synergistic activity of BET protein antagonist-based combinations in mantle cell lymphoma cells sensitive or resistant to ibrutinib. *Blood* **126**: 1565-1574.

Sun Y, Wang Y, Toubai T, Oravec-Wilson K, Liu C, Mathewson N, Wu J, Rossi C, Cummings E, Wu D et al. 2015b. BET bromodomain inhibition suppresses graft-versus-host disease after allogeneic bone marrow transplantation in mice. *Blood* **125**: 2724-2728.

Tang X, Peng R, Phillips JE, Deguzman J, Ren Y, Apparsundaram S, Luo Q, Bauer CM, Fuentes ME, DeMartino JA et al. 2013a. Assessment of Brd4 inhibition in idiopathic pulmonary fibrosis lung fibroblasts and in vivo models of lung fibrosis. *The American journal of pathology* **183**: 470-479.

Tang X, Peng R, Ren Y, Apparsundaram S, Deguzman J, Bauer CM, Hoffman AF, Hamilton S, Liang Z, Zeng H et al. 2013b. BET bromodomain proteins mediate downstream signaling events following growth factor stimulation in human lung fibroblasts and are involved in bleomycin-induced pulmonary fibrosis. *Molecular pharmacology* **83**: 283-293.

Tang Y, Gholamin S, Schubert S, Willardson MI, Lee A, Bandopadhyay P, Bergthold G, Masoud S, Nguyen B, Vue N et al. 2014. Epigenetic targeting of Hedgehog pathway transcriptional output through BET bromodomain inhibition. *Nature medicine* **20**: 732-740.

Thompson BA, Tremblay V, Lin G, Bochar DA. 2008. CHD8 is an ATP-dependent chromatin remodeling factor that regulates beta-catenin target genes. *Molecular and cellular biology* **28**: 3894-3904.

Tolani B, Gopalakrishnan R, Punj V, Matta H, Chaudhary PM. 2014. Targeting Myc in KSHV-associated primary effusion lymphoma with BET bromodomain inhibitors. *Oncogene* **33**: 2928-2937.

- Tonon G, Wong KK, Maulik G, Brennan C, Feng B, Zhang Y, Khattry DB, Protopopov A, You MJ, Aguirre AJ et al. 2005. High-resolution genomic profiles of human lung cancer. *Proceedings of the National Academy of Sciences of the United States of America* **102**: 9625-9630.
- Tough DF, Prinjha RK, Tak PP. 2015. Epigenetic mechanisms and drug discovery in rheumatology. *Clinical medicine* **15 Suppl 6**: s64-71.
- Trabucco SE, Gerstein RM, Evens AM, Bradner JE, Shultz LD, Greiner DL, Zhang H. 2015. Inhibition of bromodomain proteins for the treatment of human diffuse large B-cell lymphoma. *Clinical cancer research : an official journal of the American Association for Cancer Research* **21**: 113-122.
- Venkataraman S, Alimova I, Balakrishnan I, Harris P, Birks DK, Griesinger A, Amani V, Cristiano B, Remke M, Taylor MD et al. 2014. Inhibition of BRD4 attenuates tumor cell self-renewal and suppresses stem cell signaling in MYC driven medulloblastoma. *Oncotarget* **5**: 2355-2371.
- Vermeulen M, Eberl HC, Matarese F, Marks H, Denissov S, Butter F, Lee KK, Olsen JV, Hyman AA, Stunnenberg HG et al. 2010. Quantitative interaction proteomics and genome-wide profiling of epigenetic histone marks and their readers. *Cell* **142**: 967-980.
- Wang Y, Yang F, Gritsenko MA, Wang Y, Clauss T, Liu T, Shen Y, Monroe ME, Lopez-Ferrer D, Reno T et al. 2011. Reversed-phase chromatography with multiple fraction concatenation strategy for proteome profiling of human MCF10A cells. *Proteomics* **11**: 2019-2026.
- Wei S, Sun Y, Sha H. 2015. Therapeutic targeting of BET protein BRD4 delays murine lupus. *International immunopharmacology* **29**: 314-319.
- Wienerroither S, Rauch I, Rosebrock F, Jamieson AM, Bradner J, Muhar M, Zuber J, Muller M, Decker T. 2014. Regulation of NO synthesis, local inflammation, and innate immunity to pathogens by BET family proteins. *Molecular and cellular biology* **34**: 415-427.
- Williams RT, Roussel MF, Sherr CJ. 2006. Arf gene loss enhances oncogenicity and limits imatinib response in mouse models of Bcr-Abl-induced acute lymphoblastic leukemia. *Proceedings of the National Academy of Sciences of the United States of America* **103**: 6688-6693.
- Winter GE, Buckley DL, Paulk J, Roberts JM, Souza A, Dhe-Paganon S, Bradner JE. 2015. DRUG DEVELOPMENT. Phthalimide conjugation as a strategy for in vivo target protein degradation. *Science* **348**: 1376-1381.
- Wong C, Laddha SV, Tang L, Vosburgh E, Levine AJ, Normant E, Sandy P, Harris CR, Chan CS, Xu EY. 2014. The bromodomain and extra-terminal inhibitor CPI203 enhances the antiproliferative effects of rapamycin on human neuroendocrine tumors. *Cell death & disease* **5**: e1450.

- Wu H, Zeng H, Lam R, Tempel W, Amaya MF, Xu C, Dombrovski L, Qiu W, Wang Y, Min J. 2011. Structural and histone binding ability characterizations of human PWWP domains. *PLoS one* **6**: e18919.
- Wu SY, Chiang CM. 2007. The double bromodomain-containing chromatin adaptor Brd4 and transcriptional regulation. *The Journal of biological chemistry* **282**: 13141-13145.
- Wu SY, Lee AY, Lai HT, Zhang H, Chiang CM. 2013a. Phospho switch triggers Brd4 chromatin binding and activator recruitment for gene-specific targeting. *Molecular cell* **49**: 843-857.
- Wu X, Qi J, Bradner JE, Xiao G, Chen LF. 2013b. Bromodomain and extraterminal (BET) protein inhibition suppresses human T cell leukemia virus 1 (HTLV-1) Tax protein-mediated tumorigenesis by inhibiting nuclear factor kappaB (NF-kappaB) signaling. *The Journal of biological chemistry* **288**: 36094-36105.
- Wyce A, Degenhardt Y, Bai Y, Le B, Korenchuk S, Crouthame MC, McHugh CF, Vessella R, Creasy CL, Tummino PJ et al. 2013a. Inhibition of BET bromodomain proteins as a therapeutic approach in prostate cancer. *Oncotarget* **4**: 2419-2429.
- Wyce A, Ganji G, Smitheman KN, Chung CW, Korenchuk S, Bai Y, Barbash O, Le B, Craggs PD, McCabe MT et al. 2013b. BET inhibition silences expression of MYCN and BCL2 and induces cytotoxicity in neuroblastoma tumor models. *PLoS one* **8**: e72967.
- Xiao Y, Liang L, Huang M, Qiu Q, Zeng S, Shi M, Zou Y, Ye Y, Yang X, Xu H. 2015. Bromodomain and extra-terminal domain bromodomain inhibition prevents synovial inflammation via blocking IkappaB kinase-dependent NF-kappaB activation in rheumatoid fibroblast-like synoviocytes. *Rheumatology*.
- Xu C, Buczkowski KA, Zhang Y, Asahina H, Beauchamp EM, Terai H, Li YY, Meyerson M, Wong KK, Hammerman PS. 2015. NSCLC Driven by DDR2 Mutation Is Sensitive to Dasatinib and JQ1 Combination Therapy. *Molecular cancer therapeutics* **14**: 2382-2389.
- Xu Y, Vakoc CR. 2014. Brd4 is on the move during inflammation. *Trends in cell biology* **24**: 615-616.
- Yang Z, Yik JH, Chen R, He N, Jang MK, Ozato K, Zhou Q. 2005. Recruitment of P-TEFb for stimulation of transcriptional elongation by the bromodomain protein Brd4. *Molecular cell* **19**: 535-545.
- Yang ZQ, Liu G, Bollig-Fischer A, Giroux CN, Ethier SP. 2010. Transforming properties of 8p11-12 amplified genes in human breast cancer. *Cancer research* **70**: 8487-8497.
- Yates JW, Wallace HJ, Jr., Ellison RR, Holland JF. 1973. Cytosine arabinoside (NSC-63878) and daunorubicin (NSC-83142) therapy in acute nonlymphocytic leukemia. *Cancer chemotherapy reports Part 1* **57**: 485-488.
- Yoshida H, Bansal K, Schaefer U, Chapman T, Rioja I, Proekt I, Anderson MS, Prinjha RK, Tarakhovskiy A, Benoist C et al. 2015. Brd4 bridges the transcriptional regulators, Aire and P-

TEFb, to promote elongation of peripheral-tissue antigen transcripts in thymic stromal cells. *Proceedings of the National Academy of Sciences of the United States of America* **112**: E4448-4457.

Zhang G, Liu R, Zhong Y, Plotnikov AN, Zhang W, Zeng L, Rusinova E, Gerona-Nevarro G, Moshkina N, Joshua J et al. 2012. Down-regulation of NF-kappaB transcriptional activity in HIV-associated kidney disease by BRD4 inhibition. *The Journal of biological chemistry* **287**: 28840-28851.

Zhang QG, Qian J, Zhu YC. 2015. Targeting bromodomain-containing protein 4 (BRD4) benefits rheumatoid arthritis. *Immunology letters* **166**: 103-108.

Zhou Q, Li T, Price DH. 2012. RNA polymerase II elongation control. *Annual review of biochemistry* **81**: 119-143.

Zhou X, Fan LX, Peters DJ, Trudel M, Bradner JE, Li X. 2015. Therapeutic targeting of BET bromodomain protein, Brd4, delays cyst growth in ADPKD. *Human molecular genetics* **24**: 3982-3993.

Zhou Z, Thomsen R, Kahns S, Nielsen AL. 2010. The NSD3L histone methyltransferase regulates cell cycle and cell invasion in breast cancer cells. *Biochemical and biophysical research communications* **398**: 565-570.

Zou Z, Huang B, Wu X, Zhang H, Qi J, Bradner J, Nair S, Chen LF. 2014. Brd4 maintains constitutively active NF-kappaB in cancer cells by binding to acetylated RelA. *Oncogene* **33**: 2395-2404.

Zuber J, McJunkin K, Fellmann C, Dow LE, Taylor MJ, Hannon GJ, Lowe SW. 2011a. Toolkit for evaluating genes required for proliferation and survival using tetracycline-regulated RNAi. *Nature biotechnology* **29**: 79-83.

Zuber J, Shi J, Wang E, Rappaport AR, Herrmann H, Sison EA, Magoon D, Qi J, Blatt K, Wunderlich M et al. 2011b. RNAi screen identifies Brd4 as a therapeutic target in acute myeloid leukaemia. *Nature* **478**: 524-528.

Appendix

A. IP-MS results

Gene Symbol	Unique_empty	Total_empty	Unique_NSD3 short	Total_NSD3 short	Unique_NSD3 short_W284A	Total_NSD3 short_W284A
WHSC1L1	0	0	19	142	20	54
BPTF	0	0	15	19	20	29
BOD1L1	0	0	13	18	16	19
BRD4	0	0	7	13	4	5
CHD8	0	0	9	11	10	16
DBN1	0	0	8	11	7	7
SNRPA	0	0	3	10	3	4
KCNC4	0	0	1	10	0	0
LUZP1	0	0	7	9	11	11
YEATS2	0	0	8	9	11	11
KHDRBS1	0	0	3	9	8	10
PELP1	0	0	5	9	2	2
AHNAK	0	0	8	8	8	9
SIN3A	0	0	6	8	9	10
DOCK7	0	0	7	7	18	20
TNKS1BP1	0	0	6	7	13	17
SCRIB	0	0	5	7	10	12
EPB41L2	0	0	5	7	7	10
IRS4	0	0	4	7	9	10
SRRM1	0	0	5	7	6	7
RBM26	0	0	6	7	5	6
ANLN	0	0	4	7	6	8
CEP170	0	0	4	6	15	19
CTNND1	0	0	6	6	8	10
CABIN1	0	0	6	6	6	7
SETD2	0	0	6	6	4	5
BAP18	0	0	4	6	5	6
MRE11A	0	0	3	6	5	6
KPNA2	0	0	4	6	4	6
GPR158	0	0	1	6	1	6
TJP1	0	0	4	5	3	3
PKN2	0	0	5	5	7	7
CDC73	0	0	4	5	8	8
ANK3	0	0	3	5	7	7
HNRPLL	0	0	3	5	6	9
FIP1L1	0	0	4	5	6	8
C17orf85	0	0	3	5	5	7
FLNB	0	0	4	4	8	8
MLL2	0	0	3	4	14	14
CDK12	0	0	3	4	8	8
GATAD2B	0	0	3	4	7	9
BRD8	0	0	4	4	7	11
EPS15L1	0	0	4	4	7	8
RBBP4	0	0	2	4	6	7
ASH2L	0	0	3	4	6	6
HIRA	0	0	4	4	3	4
ZC3H18	0	0	3	4	3	4
PPP1R10	0	0	2	4	4	5

DMAPI	0	0	3	4	4	5
MYL6	0	0	4	4	2	2
EIF3D	0	0	3	4	3	4
POLR2B	0	0	3	4	2	2
SP3	0	0	2	4	0	0
SHROOM3	0	0	1	4	0	0
SRP72	0	0	3	3	10	14
EIF4G1	0	0	3	3	10	13
MKI67	0	0	3	3	9	9
PRPF40A	0	0	3	3	8	9
EP400	0	0	3	3	9	10
ARID3B	0	0	3	3	8	11
MTA1	0	0	3	3	6	6
MGA	0	0	2	3	6	7
ADNP	0	0	2	3	5	5
GTF3C5	0	0	3	3	5	5
CENPF	0	0	3	3	4	5
SRSF11	0	0	3	3	4	6
ARID3A	0	0	3	3	4	5
CALM1	0	0	2	3	2	2
DDX42	0	0	3	3	3	3
UBE2S	0	0	2	3	4	4
SGOL2	0	0	3	3	4	5
NCOA6	0	0	3	3	3	3
ITSN1	0	0	2	3	2	3
ZBTB2	0	0	3	3	2	2
DYNC1I2	0	0	2	3	3	5
CDC27	0	0	2	3	3	3
UBN1	0	0	2	3	2	2
POLE3	0	0	3	3	1	1
EDC3	0	0	2	3	2	3
DNAJA2	0	0	2	3	1	1
EIF4A1	0	0	2	3	2	3
SENP3	0	0	2	3	1	1
INTS2	0	0	2	3	1	1
CBX3	0	0	1	3	0	0
LRRK1	0	0	2	3	1	1
SDCBP	0	0	2	3	0	0
PRB3	0	0	1	3	1	1
SAV	0	0	1	3	0	0
ACTL6A	0	0	2	2	7	8
OGT	0	0	2	2	7	7
DDX5	0	0	2	2	5	14
RBM25	0	0	2	2	6	7
KDM6A	0	0	2	2	6	8
ZNF24	0	0	2	2	6	10
PPP1R12A	0	0	2	2	3	3
FUBP1	0	0	2	2	6	7
ANKHD1	0	0	2	2	5	6
ACTN4	0	0	2	2	0	0
LIN54	0	0	2	2	5	6
NFRKB	0	0	2	2	4	4
EIF3G	0	0	2	2	4	4
SRSF6	0	0	2	2	2	3
KIAA1967	0	0	1	2	3	7
IRF2BP2	0	0	1	2	4	5
QKI	0	0	2	2	4	4

RFX5	0	0	2	2	3	3
FUBP3	0	0	2	2	4	4
MYBL2	0	0	2	2	3	3
REPS1	0	0	2	2	2	4
GABPA	0	0	1	2	3	3
YAP1	0	0	1	2	3	3
WDR5	0	0	2	2	3	5
NFATC2IP	0	0	2	2	3	4
BRCA1	0	0	2	2	3	4
CNOT3	0	0	2	2	3	4
ASF1A	0	0	2	2	3	3
NKAP	0	0	2	2	3	3
LARS	0	0	2	2	3	3
CXXC1	0	0	2	2	3	4
GIGYF2	0	0	2	2	3	3
POLR2A	0	0	2	2	3	3
RPAP3	0	0	2	2	2	2
ANKRD17	0	0	1	2	3	3
ZNF687	0	0	2	2	3	3
CPSF7	0	0	2	2	2	2
TMOD3	0	0	2	2	0	0
TPM1	0	0	2	2	0	0
SNX3	0	0	2	2	2	3
HNRNPH2	0	0	1	2	2	3
NPLOC4	0	0	2	2	1	2
RAD51AP1	0	0	2	2	2	2
NUDT21	0	0	2	2	1	2
PPP1CA	0	0	2	2	1	1
KANSL3	0	0	1	2	2	2
CUX1	0	0	2	2	2	2
NOP2	0	0	2	2	0	0
TIAL1	0	0	2	2	1	1
TF	0	0	2	2	0	0
FGFR1OP	0	0	1	2	1	2
DNTTIP2	0	0	1	2	1	2
ZNF238	0	0	1	2	1	1
RPS8	0	0	1	2	1	2
CTBP1	0	0	1	2	1	1
ZKSCAN4	0	0	1	2	0	0
ANXA1	0	0	1	2	0	0
CIC	0	0	1	2	0	0
GNAI2	0	0	1	2	0	0
PTK2	0	0	1	2	0	0
PNISR	0	0	1	2	0	0
SMC2	0	0	1	1	6	6
MTA2	0	0	1	1	6	7
EPRS	0	0	1	1	6	9
SMARCA4	0	0	1	1	6	6
CNOT1	0	0	1	1	6	6
DDX46	0	0	1	1	5	6
SART1	0	0	1	1	5	5
KIAA0284	0	0	1	1	5	7
RNF40	0	0	1	1	5	5
GTF3C2	0	0	1	1	4	6
ZHX2	0	0	1	1	4	4
RFX7	0	0	1	1	4	4
MED1	0	0	1	1	3	4

ZC3H14	0	0	1	1	4	4
WHSC2	0	0	1	1	4	4
NCOR1	0	0	1	1	3	3
HNRPDL	0	0	1	1	3	4
ATF7IP	0	0	1	1	3	3
RPSA	0	0	1	1	1	2
WAPAL	0	0	1	1	3	4
CCT4	0	0	1	1	3	3
THOC2	0	0	1	1	3	4
MPP5	0	0	1	1	2	2
XRN2	0	0	1	1	3	3
MKL1	0	0	1	1	3	3
ZBTB33	0	0	1	1	3	4
SMARCA1	0	0	1	1	3	4
PRRC2C	0	0	1	1	3	3
CUX1	0	0	1	1	2	2
CNOT2	0	0	1	1	3	3
YTHDF2	0	0	1	1	3	3
SMC3	0	0	1	1	2	2
SKP1	0	0	1	1	2	2
PLEKHA5	0	0	1	1	3	3
ZMYM3	0	0	1	1	3	3
CCT6A	0	0	1	1	2	4
SAP30BP	0	0	1	1	2	3
EHMT1	0	0	1	1	2	4
YJ005	0	0	1	1	1	1
CHAF1B	0	0	1	1	2	3
SPECC1L	0	0	1	1	1	1
TAF6	0	0	1	1	1	1
NMD3	0	0	1	1	2	3
UBAP2	0	0	1	1	2	2
SMARCB1	0	0	1	1	2	2
ORC2	0	0	1	1	2	2
RFC2	0	0	1	1	2	2
FLJ22184	0	0	1	1	2	3
THOC6	0	0	1	1	2	2
LIMA1	0	0	1	1	0	0
ZNF639	0	0	1	1	2	2
EP300	0	0	1	1	2	2
POLR2C	0	0	1	1	2	3
KDM1A	0	0	1	1	2	3
VPS72	0	0	1	1	2	2
PRPF31	0	0	1	1	2	3
UNK	0	0	1	1	1	2
WIZ	0	0	1	1	2	2
CCNT1	0	0	1	1	2	3
SMAD2	0	0	1	1	2	2
ERH	0	0	1	1	1	1
TCERG1	0	0	1	1	2	2
TBL1XR1	0	0	1	1	2	2
ZNF638	0	0	1	1	2	2
CHD6	0	0	1	1	2	2
KAT7	0	0	1	1	2	2
CEP76	0	0	1	1	0	0
COIL	0	0	1	1	2	2
DNAJA1	0	0	1	1	2	2
RAD50	0	0	1	1	2	2

TLE3	0	0	1	1	2	2
MAP7D3	0	0	1	1	2	2
Asun	0	0	1	1	2	2
SNW1	0	0	1	1	2	2
SNRPA1	0	0	1	1	2	2
ATXN10	0	0	1	1	1	1
DDX41	0	0	1	1	1	1
TOX4	0	0	1	1	1	1
CDSN	0	0	1	1	1	1
WDR82	0	0	1	1	1	1
SATB2	0	0	1	1	1	1
HNRNPH1	0	0	1	1	1	1
SNRPC	0	0	1	1	1	1
INTS4	0	0	1	1	1	1
LIN9	0	0	1	1	1	1
STXBP1	0	0	1	1	1	1
DES	0	0	1	1	1	1
DAZAP1	0	0	1	1	1	1
PRPH	0	0	1	1	1	1
HIC2	0	0	1	1	1	1
EYA3	0	0	1	1	1	1
RING1	0	0	1	1	1	1
NCOA2	0	0	1	1	1	2
TADA3	0	0	1	1	1	2
PRKAR2A	0	0	1	1	1	1
GMEB1	0	0	1	1	1	2
FRG1	0	0	1	1	1	1
INTS5	0	0	1	1	1	1
WDR77	0	0	1	1	1	1
CDC16	0	0	1	1	1	1
MCRS1	0	0	1	1	1	2
DPY30	0	0	1	1	1	1
ADD3	0	0	1	1	1	1
CDK11A	0	0	1	1	1	1
CIRBP	0	0	1	1	0	0
SNX12	0	0	1	1	1	1
ARPC1A	0	0	1	1	1	1
ACTG1	0	0	1	1	1	1
MOB1A	0	0	1	1	0	0
KPNA6	0	0	1	1	1	2
ASXL1	0	0	1	1	1	1
HEXIM1	0	0	1	1	1	1
PRSS1	0	0	1	1	0	0
MBD3	0	0	1	1	1	1
CWF19L2	0	0	1	1	1	1
GPRASP2	0	0	1	1	1	1
CHRAC1	0	0	1	1	1	1
CHD1	0	0	1	1	1	1
GCFC2	0	0	1	1	1	1
ARHGEF2	0	0	1	1	1	1
RPS28	0	0	1	1	1	1
DDB1	0	0	1	1	1	1
RPS10P5	0	0	1	1	1	1
TFPT	0	0	1	1	1	1
PDIA6	0	0	1	1	0	0
TOX3	0	0	1	1	1	1
RBM12B	0	0	1	1	0	0

MED14	0	0	1	1	1	1
NUP62	0	0	1	1	0	0
PHF21A	0	0	1	1	1	1
DLG1	0	0	1	1	0	0
GFP	0	0	1	1	1	1
FN1	0	0	1	1	1	1
C19orf47	0	0	1	1	1	1
RPL7A	0	0	1	1	0	0
DCAF7	0	0	1	1	1	1
SPP1	0	0	1	1	1	1
CPSF3L	0	0	1	1	1	1
GATA4	0	0	1	1	1	1
TUBA4A	0	0	1	1	1	1
CSR2BP	0	0	1	1	1	1
RAN	0	0	1	1	0	0
NDUFV1	0	0	1	1	0	0
ATP2B1	0	0	1	1	1	1
ZCCHC8	0	0	1	1	1	1
ARFGAP2	0	0	1	1	0	0
SCYL2	0	0	1	1	0	0
ZKSCAN3	0	0	1	1	0	0
CST1	0	0	1	1	0	0
NAPB	0	0	1	1	0	0
FGA	0	0	1	1	0	0
IGHA2	0	0	1	1	0	0
TOM1	0	0	1	1	0	0
YTHDF1	0	0	1	1	0	0
SENP5	0	0	1	1	0	0
C12orf57	0	0	1	1	0	0
DNAJB6	0	0	1	1	0	0
LIN7C	0	0	1	1	0	0
GPN3	0	0	1	1	0	0
THBS1	0	0	1	1	0	0
INTS1	0	0	1	1	0	0
CA6	0	0	1	1	0	0
AVID	0	0	1	1	0	0
DNAH8	0	0	1	1	0	0
MYCBP2	0	0	1	1	0	0
ZMYND8	0	0	1	1	0	0
DPYSL2	0	0	1	1	0	0
DMBT1	0	0	1	1	0	0
DNAJC10	0	0	1	1	0	0
DNAH1	0	0	1	1	0	0
TANC2	0	0	1	1	0	0
HV320	0	0	1	1	0	0
GLTSCR1	0	0	1	1	0	0
MYBBP1A	0	0	1	1	0	0
SIDT2	0	0	1	1	0	0
ESF1	0	0	1	1	0	0
COL4A1	0	0	1	1	0	0
MAP4K3	0	0	1	1	0	0
NUDT13	0	0	1	1	0	0
DYNC1H1	0	0	0	0	18	20
GTF3C1	0	0	0	0	10	11
BCOR	0	0	0	0	9	10
PAWR	0	0	0	0	3	3
EDC4	0	0	0	0	8	9

FAM21A	0	0	0	0	6	6
CIC	0	0	0	0	6	6
SRP54	0	0	0	0	5	6
SMC4	0	0	0	0	6	7
KIF20B	0	0	0	0	6	7
KDM3B	0	0	0	0	5	5
LMO7	0	0	0	0	6	6
MLL	0	0	0	0	6	6
HNRNPCL1	0	0	0	0	5	6
RANGAP1	0	0	0	0	5	6
CHAMP1	0	0	0	0	3	4
CDKN2AIP	0	0	0	0	5	6
ZMYM2	0	0	0	0	5	5
MPRIP	0	0	0	0	3	3
QSER1	0	0	0	0	5	5
SEC16A	0	0	0	0	5	5
U2AF2	0	0	0	0	4	5
SLC1A2	0	0	0	0	4	4
TJP2	0	0	0	0	3	3
WTAP	0	0	0	0	3	5
LARP1	0	0	0	0	4	5
IARS	0	0	0	0	4	5
ELF1	0	0	0	0	4	5
MLL3	0	0	0	0	4	5
CAMSAP1	0	0	0	0	3	4
IRF2BPL	0	0	0	0	4	5
CREBBP	0	0	0	0	4	4
TRRAP	0	0	0	0	4	4
ELF2	0	0	0	0	4	4
MACF1	0	0	0	0	4	4
ARCN1	0	0	0	0	4	4
HNRNPUL1	0	0	0	0	3	4
MAP4	0	0	0	0	3	4
AMOTL1	0	0	0	0	3	3
EIF3B	0	0	0	0	3	4
ZNHIT1	0	0	0	0	3	3
SCAF4	0	0	0	0	3	5
PPP1R9B	0	0	0	0	2	3
CASKIN2	0	0	0	0	3	3
SMARCC2	0	0	0	0	3	5
ARID1A	0	0	0	0	3	3
DDX6	0	0	0	0	3	3
ERCC6L	0	0	0	0	3	5
IRF2BP1	0	0	0	0	3	5
PLEC	0	0	0	0	2	2
DGCR14	0	0	0	0	3	4
INTS3	0	0	0	0	3	4
NUP153	0	0	0	0	3	4
CCT8	0	0	0	0	2	2
FOXK1	0	0	0	0	3	4
DCPIA	0	0	0	0	3	4
ZNF318	0	0	0	0	3	4
HELLS	0	0	0	0	3	3
PNN	0	0	0	0	2	2
COPB1	0	0	0	0	3	3
TCP1	0	0	0	0	3	3
ZHX1	0	0	0	0	3	3

QRICH1	0	0	0	0	3	3
HMGXB4	0	0	0	0	3	3
NUP214	0	0	0	0	3	3
CEP170P1	0	0	0	0	3	3
CHD7	0	0	0	0	3	3
MAP1S	0	0	0	0	3	3
CGGBP1	0	0	0	0	2	2
KANSL1	0	0	0	0	3	3
AGFG1	0	0	0	0	2	2
SPAG9	0	0	0	0	2	3
ATRX	0	0	0	0	1	2
KPNA3	0	0	0	0	1	1
UIMC1	0	0	0	0	2	3
GTF3C3	0	0	0	0	2	4
HIST1H2BA	0	0	0	0	2	2
HDAC2	0	0	0	0	2	3
BRIP1	0	0	0	0	2	3
CCT7	0	0	0	0	2	3
OXSRI	0	0	0	0	2	3
TRPS1	0	0	0	0	2	3
EP400NL	0	0	0	0	2	2
NASP	0	0	0	0	2	2
TP53BP1	0	0	0	0	2	2
ZEB1	0	0	0	0	2	3
SYMPK	0	0	0	0	2	3
OTUD4	0	0	0	0	2	2
ANKRD11	0	0	0	0	2	2
MORF4L1	0	0	0	0	2	2
FANCI	0	0	0	0	2	3
PABPN1	0	0	0	0	2	2
TRA2B	0	0	0	0	2	2
NKRF	0	0	0	0	2	2
PAGR1	0	0	0	0	2	2
HTATSF1	0	0	0	0	1	1
RBM4	0	0	0	0	2	2
ARHGAP17	0	0	0	0	2	2
SLU7	0	0	0	0	2	2
CTBP2	0	0	0	0	2	2
ZFR	0	0	0	0	2	2
MLLT4	0	0	0	0	2	2
KIF23	0	0	0	0	2	2
CKAP2	0	0	0	0	1	1
ZNF295	0	0	0	0	2	2
RPS20	0	0	0	0	2	2
LRWD1	0	0	0	0	2	2
SKA1	0	0	0	0	2	2
BAZ1A	0	0	0	0	1	1
TCF25	0	0	0	0	2	2
SMARCE1	0	0	0	0	2	2
NR2C2	0	0	0	0	2	2
BCCIP	0	0	0	0	2	2
PAXIP1	0	0	0	0	2	2
CLASP1	0	0	0	0	2	2
SAP130	0	0	0	0	2	2
PCF11	0	0	0	0	2	2
PRR12	0	0	0	0	2	2
ADD1	0	0	0	0	1	1

GTPBP1	0	0	0	0	2	2
WNK1	0	0	0	0	1	1
CNN3	0	0	0	0	2	2
LRCH2	0	0	0	0	2	2
RPRD2	0	0	0	0	2	2
CDCA5	0	0	0	0	2	2
PPFIA1	0	0	0	0	2	2
RAVER2	0	0	0	0	2	2
COPA	0	0	0	0	2	2
BAG6	0	0	0	0	2	2
ZFHX4	0	0	0	0	2	2
MKL2	0	0	0	0	2	2
SALL1	0	0	0	0	2	2
CDC37	0	0	0	0	2	2
TLN1	0	0	0	0	2	2
ZMYM4	0	0	0	0	2	2
ZEB2	0	0	0	0	2	2
PUM1	0	0	0	0	2	2
TAF5	0	0	0	0	2	2
AIP	0	0	0	0	2	2
SRSF9	0	0	0	0	1	1
CDC42EP1	0	0	0	0	2	2
CCT3	0	0	0	0	2	2
CDK9	0	0	0	0	1	1
RAD18	0	0	0	0	2	2
SRSF10	0	0	0	0	2	2
KATNB1	0	0	0	0	2	2
PRTN3	0	0	0	0	2	2
SRP19	0	0	0	0	1	18
SYNGR1	0	0	0	0	1	1
SF3A3	0	0	0	0	1	1
EP400NL	0	0	0	0	1	2
PPP1CC	0	0	0	0	1	1
EEA1	0	0	0	0	1	1
G3BP1	0	0	0	0	1	1
RDBP	0	0	0	0	1	1
MAP3K7	0	0	0	0	1	2
VWA9	0	0	0	0	1	2
USP28	0	0	0	0	1	2
PDXDC1	0	0	0	0	1	2
VCPIP1	0	0	0	0	1	1
EIF3A	0	0	0	0	1	1
ACTR1A	0	0	0	0	1	2
ILF2	0	0	0	0	1	2
CHAF1A	0	0	0	0	1	2
NAP1L1	0	0	0	0	1	1
EIF3C	0	0	0	0	1	1
RREB1	0	0	0	0	1	2
SREK1	0	0	0	0	1	1
FASN	0	0	0	0	1	2
GTF3C6	0	0	0	0	1	1
INTS6	0	0	0	0	1	2
USP19	0	0	0	0	1	2
NUSAP1	0	0	0	0	1	2
KARS	0	0	0	0	1	2
NOB1	0	0	0	0	1	2
AIMP2	0	0	0	0	1	2

SMCHD1	0	0	0	0	1	1
FTSJD2	0	0	0	0	1	1
LRRC40	0	0	0	0	1	2
ZBTB43	0	0	0	0	1	2
RPLP1	0	0	0	0	1	2
LSM3	0	0	0	0	1	1
RAI14	0	0	0	0	1	1
BPTF	0	0	0	0	1	1
MEN1	0	0	0	0	1	1
GTF2IRD2	0	0	0	0	1	1
NRF1	0	0	0	0	1	1
KAT8	0	0	0	0	1	2
INA	0	0	0	0	1	1
INADL	0	0	0	0	1	1
GUCY1B2	0	0	0	0	1	1
EIF2A	0	0	0	0	1	2
NR2F1	0	0	0	0	1	1
TAF10	0	0	0	0	1	1
AKAP8	0	0	0	0	1	1
DNM1L	0	0	0	0	1	1
PHF8	0	0	0	0	1	1
ZNHIT6	0	0	0	0	1	1
USP10	0	0	0	0	1	1
HNRNPC	0	0	0	0	1	1
DCTN2	0	0	0	0	1	1
CCT5	0	0	0	0	1	1
ILF3	0	0	0	0	1	1
ZC3H13	0	0	0	0	1	1
COPG1	0	0	0	0	1	1
POU3F2	0	0	0	0	1	1
USO1	0	0	0	0	1	1
POLR1C	0	0	0	0	1	1
TP53	0	0	0	0	1	1
PPP6R1	0	0	0	0	1	1
WBP7	0	0	0	0	1	1
ZNF598	0	0	0	0	1	1
PIAS4	0	0	0	0	1	1
HAUS6	0	0	0	0	1	1
CDYL	0	0	0	0	1	1
NCAPD2	0	0	0	0	1	1
ZC3HC1	0	0	0	0	1	1
YKT6	0	0	0	0	1	1
TBC1D15	0	0	0	0	1	1
TH1L	0	0	0	0	1	1
COPZ1	0	0	0	0	1	1
DHX9	0	0	0	0	1	1
CHD4	0	0	0	0	1	1
SF3B4	0	0	0	0	1	1
CIC	0	0	0	0	1	1
ANK3	0	0	0	0	1	1
ASXL2	0	0	0	0	1	1
CPSF1	0	0	0	0	1	1
TOPBP1	0	0	0	0	1	1
RNF2	0	0	0	0	1	1
MAGED2	0	0	0	0	1	1
BBX	0	0	0	0	1	1
RANBP2	0	0	0	0	1	1

QARS	0	0	0	0	1	1
DST	0	0	0	0	1	1
SIX4	0	0	0	0	1	1
NUP50	0	0	0	0	1	1
JUN	0	0	0	0	1	1
LRCH3	0	0	0	0	1	1
ADAR	0	0	0	0	1	1
PRRC2A	0	0	0	0	1	1
RAVER1	0	0	0	0	1	1
TAB1	0	0	0	0	1	1
SSRP1	0	0	0	0	1	1
CIZ1	0	0	0	0	1	1
SUGP2	0	0	0	0	1	1
C9orf40	0	0	0	0	1	1
UPF3B	0	0	0	0	1	1
ALS2CR12	0	0	0	0	1	1
HUWE1	0	0	0	0	1	1
PICALM	0	0	0	0	1	1
SMARCD2	0	0	0	0	1	1
INO80	0	0	0	0	1	1
CEP55	0	0	0	0	1	1
TOE1	0	0	0	0	1	1
AHSA1	0	0	0	0	1	1
SMARCD1	0	0	0	0	1	1
USP1	0	0	0	0	1	1
HOXB9	0	0	0	0	1	1
SMTN	0	0	0	0	1	1
XRN1	0	0	0	0	1	1
RFC4	0	0	0	0	1	1
AKAP8L	0	0	0	0	1	1
KPNA1	0	0	0	0	1	1
SPAG5	0	0	0	0	1	1
PRPF38A	0	0	0	0	1	1
CECR2	0	0	0	0	1	1
KLF5	0	0	0	0	1	1
SPRTN	0	0	0	0	1	1
GGA3	0	0	0	0	1	1
HBS1L	0	0	0	0	1	1
PATL1	0	0	0	0	1	1
MYL6B	0	0	0	0	1	1
SAFB2	0	0	0	0	1	1
EYA1	0	0	0	0	1	1
CAMSAP3	0	0	0	0	1	1
NACC1	0	0	0	0	1	1
CSTF3	0	0	0	0	1	1
IWS1	0	0	0	0	1	1
NEK9	0	0	0	0	1	1
HSP90B1	0	0	0	0	1	1
PHF2	0	0	0	0	1	1
TAF2	0	0	0	0	1	1
ZZZ3	0	0	0	0	1	1
EPB41	0	0	0	0	1	1
ARHGEF6	0	0	0	0	1	1
UFD1L	0	0	0	0	1	1
RIPK1	0	0	0	0	1	1
PHF16	0	0	0	0	1	1
CCDC101	0	0	0	0	1	1

RFXAP	0	0	0	0	1	1
MAD1L1	0	0	0	0	1	1
NCOA3	0	0	0	0	1	1
TFDP1	0	0	0	0	1	1
AIMP1	0	0	0	0	1	1
SLK	0	0	0	0	1	1
SIX5	0	0	0	0	1	1
ARF1	0	0	0	0	1	1
ZHX3	0	0	0	0	1	1
CCDC6	0	0	0	0	1	1
FBRS	0	0	0	0	1	1
DPF2	0	0	0	0	1	1
SMARCA2	0	0	0	0	1	1
COBRA1	0	0	0	0	1	1
AFF4	0	0	0	0	1	1
WIZ	0	0	0	0	1	1
FXR1	0	0	0	0	1	1
KIF4A	0	0	0	0	1	1
ARHGEF1	0	0	0	0	1	1
MAGED1	0	0	0	0	1	1
LSM2	0	0	0	0	1	1
TAF4B	0	0	0	0	1	1
BANP	0	0	0	0	1	1
DCTN1	0	0	0	0	1	1
CACUL1	0	0	0	0	1	1
RAPGEF2	0	0	0	0	1	1
MICAL3	0	0	0	0	1	1
TNFRSF21	0	0	0	0	1	1
RASAL2	0	0	0	0	1	1
MPDZ	0	0	0	0	1	1
NXN	0	0	0	0	1	1
ATAD5	0	0	0	0	1	1
PSMD3	0	0	0	0	1	1
MYH7B	0	0	0	0	1	1
RARS	0	0	0	0	1	1
EPHB6	0	0	0	0	1	1
ALG3	0	0	0	0	1	1
PPP1CB	0	0	0	0	1	1
SYNE1	0	0	0	0	1	1
TIA1	0	0	0	0	1	1
RBM22	0	0	0	0	1	1
UTRN	0	0	0	0	1	1
PKLR	0	0	0	0	1	1
LRRC57	0	0	0	0	1	1
PBX2	0	0	0	0	1	1
ASPDH	0	0	0	0	1	1
LTN1	0	0	0	0	1	1

B. iTRAQ results

Gene Symbol	Mock IP signal	NSD3-short IP signal
Q9BZ95-3	1	11.49425287
H7BYY1	1	8.26446281
Q9Y608	1	7.874015748
Q5JU85	1	6.493506494
Q5VU59	1	6.134969325
P09496-2	1	5.714285714
I3L4U8	1	4.807692308
P47914	1	4.694835681
Q8N3R9	1	4.310344828
P01621	1	4.291845494
B4DEB1	1	4.032258065
F8VSE7	1	4.016064257
O00311	1	3.968253968
P33981	1	3.831417625
Q8N680	1	3.787878788
P01857	1	3.745318352
Q9ULV4	1	3.623188406
K7EJH0	1	3.597122302
J3QRS3	1	3.597122302
H7BYJ3	1	3.571428571
Q8IW35	1	3.496503497
O14974	1	3.436426117
P62805	1	3.436426117
Q8WWK9	1	3.311258278
Q7Z333	1	3.300330033
B4E1Y1	1	3.267973856
Q00587	1	3.25732899
Q14247	1	3.236245955
P08670	1	3.225806452
G3XAN1	1	3.164556962
M0QZD9	1	3.154574132
H0Y9P1	1	3.144654088
E7ENU7	1	3.134796238
Q8IY63	1	3.134796238
F5H8F7	1	3.115264798
B4DF64	1	3.105590062
Q4VCS5	1	3.086419753
F5GXS2	1	3.058103976
P62857	1	3.058103976
O14646	1	3.012048193
H0YIS7	1	2.976190476
P01700	1	2.96735905
Q14257	1	2.958579882
F8VQE1	1	2.941176471
Q8IX90	1	2.923976608
IIE4Y6	1	2.915451895
J3KN01	1	2.906976744
O75531	1	2.865329513
Q5HY54	1	2.840909091
P68032	1	2.83286119
Q6W2J9	1	2.816901408
P09234	1	2.816901408
Q562R1	1	2.816901408
Q9ULW0	1	2.808988764
F5H1T6	1	2.808988764
Q9BW19	1	2.793296089
Q9BY89	1	2.777777778

Q96ST2	1	2.770083102
Q9POK7	1	2.770083102
B0QYK0	1	2.747252747
G8JLA2	1	2.739726027
Q13395	1	2.732240437
P11940	1	2.732240437
J3KND3	1	2.717391304
Q5JXX1	1	2.7100271
Q2M1P5	1	2.7100271
H3BPL5	1	2.702702703
Q6WCQ1	1	2.702702703
P60709	1	2.688172043
Q8NFC6	1	2.659574468
P62888	1	2.652519894
P53999	1	2.638522427
B7Z7M6	1	2.631578947
Q00610	1	2.624671916
Q86V48	1	2.624671916
Q6P3W7	1	2.583979328
I3L4U9	1	2.577319588
Q13045-3	1	2.570694087
H0YKU1	1	2.564102564
E7EPB3	1	2.564102564
J3KMX5	1	2.53164557
Q5T8R3	1	2.518891688
C9JDG0	1	2.512562814
H0Y8L7	1	2.512562814
D6R9X2	1	2.506265664
Q6UXN9	1	2.506265664
Q96IZ0	1	2.506265664
Q9UGU5	1	2.5
Q9HCJ3	1	2.493765586
Q9UDY2	1	2.493765586
B8ZZG1	1	2.487562189
J3KRB3	1	2.475247525
Q9UGU0	1	2.475247525
J3KN11	1	2.469135802
Q01082	1	2.469135802
P35580	1	2.457002457
Q9HBE1-2	1	2.457002457
Q16643	1	2.444987775
Q5VTE0	1	2.444987775
Q14677	1	2.43902439
H0Y7A7	1	2.43902439
G3V1L9	1	2.421307506
Q9Y6J0	1	2.415458937
J3KPP4	1	2.392344498
P26373	1	2.392344498
E7EWD6	1	2.380952381
M0R2D9	1	2.380952381
M0QY61	1	2.375296912
Q9UI36	1	2.358490566
Q9C0D5	1	2.341920375
K7EME2	1	2.341920375
B4DX42	1	2.341920375
B7Z888	1	2.336448598
Q8NHS0	1	2.331002331
B4DX29	1	2.331002331
Q9POU4	1	2.314814815
Q6ZW49	1	2.309468822
J3KSS0	1	2.309468822

Q9C005	1	2.304147465
J3QL14	1	2.298850575
Q15149-3	1	2.293577982
F8VR50	1	2.293577982
Q9NXF1	1	2.293577982
H7C0C7	1	2.283105023
O43823	1	2.283105023
Q9UIV1	1	2.277904328
Q96RE7	1	2.267573696
Q9Y5A9	1	2.267573696
Q96R06	1	2.262443439
P27816	1	2.262443439
Q5EBL8	1	2.257336343
K7EPJ1	1	2.247191011
Q5SVZ6	1	2.247191011
I3L2R3	1	2.242152466
Q14126	1	2.227171492
Q9BPX5	1	2.222222222
P10644	1	2.2172949
F8WCF6	1	2.212389381
B1AK87	1	2.202643172
H0Y638	1	2.197802198
P23246	1	2.197802198
P05023	1	2.188183807
C9JZR2	1	2.188183807
F5H1U9	1	2.183406114
J3KP06	1	2.183406114
O75909	1	2.183406114
B3KVR1	1	2.183406114
P54198	1	2.173913043
O14654	1	2.159827214
Q96I18	1	2.145922747
Q5T5Y3	1	2.145922747
F8W115	1	2.145922747
Q9NYV4	1	2.136752137
Q96PU8	1	2.118644068
Q96EK4	1	2.109704641
Q15291	1	2.100840336
F8W726	1	2.100840336
O76094	1	2.096436059
Q2KHR3	1	2.096436059
Q6P1J9	1	2.092050209
P35579	1	2.087682672
E7ET07	1	2.083333333
Q9BT25	1	2.079002079
Q5VUJ6	1	2.079002079
P05386	1	2.074688797
H7BY16	1	2.074688797
Q3KQU3	1	2.070393375
P08107	1	2.066115702
E9PID9	1	2.06185567
Q01658	1	2.057613169
E9PDF6	1	2.057613169
P49790	1	2.049180328
P36578	1	2.049180328
Q15723	1	2.040816327
J3QRR5	1	2.040816327
J3KQR7	1	2.040816327
S4R2X9	1	2.032520325
O15020	1	2.02020202
Q5VUA4	1	2.02020202

F5H6S1	1	2.016129032
O15047	1	2.016129032
J3KP15	1	2.012072435
C9J2Y9	1	2.008032129
Q9NS91	1	2.008032129
H0Y449	1	1.996007984
P11021	1	1.996007984
A8MUD9	1	1.996007984
A6NG51	1	1.996007984
M0R165	1	1.992031873
C9J0M6	1	1.988071571
P11142	1	1.976284585
O00287	1	1.972386588
Q15058	1	1.964636542
P26368	1	1.964636542
Q5UIP0	1	1.960784314
F6WCX7	1	1.960784314
P06748	1	1.956947162
O75369	1	1.953125
Q96DT7	1	1.953125
Q6DN90	1	1.949317739
K7EJT8	1	1.949317739
F5H5C2	1	1.945525292
E9PB61	1	1.941747573
C9J6W2	1	1.930501931
O14545	1	1.930501931
Q92922	1	1.926782274
Q9H9A5	1	1.926782274
Q7Z2Z1	1	1.926782274
P52907	1	1.919385797
O15294	1	1.919385797
B3KTC7	1	1.915708812
P0CG12	1	1.908396947
Q9UK45	1	1.908396947
H7BY10	1	1.904761905
J3KNH7	1	1.904761905
F5H5Y3	1	1.904761905
J3KS31	1	1.904761905
Q5JR95	1	1.904761905
E7EMV2	1	1.901140684
H7BZT4	1	1.897533207
Q81WC1	1	1.897533207
H0YIZ6	1	1.893939394
Q7L4I2	1	1.890359168
P17028	1	1.886792453
F5GYC2	1	1.876172608
P09132	1	1.872659176
J3KQ70	1	1.872659176
E9PDP5	1	1.869158879
Q9UIU6	1	1.869158879
Q9NV56	1	1.851851852
H0Y2V6	1	1.84501845
Q8NHZ8	1	1.841620626
Q14686	1	1.834862385
P42695	1	1.828153565
Q6P9B9	1	1.828153565
M0QYZ2	1	1.824817518
Q9NZM4	1	1.824817518
O43683	1	1.821493625
P62140	1	1.821493625
C9JNW5	1	1.818181818

H3BPE7	1	1.818181818
P16989	1	1.814882033
Q14671	1	1.814882033
B7Z1R5	1	1.811594203
E2QRE6	1	1.811594203
H0Y612	1	1.808318264
Q14671-2	1	1.808318264
B1AKL4	1	1.805054152
B4DXZ6	1	1.805054152
J3KNE0	1	1.805054152
Q9Y2X3	1	1.805054152
A6NEM2	1	1.798561151
O75152	1	1.798561151
Q7LBC6	1	1.798561151
Q81Y67-2	1	1.792114695
P50750	1	1.792114695
U3KQC1	1	1.792114695
B4DVY1	1	1.788908766
P61964	1	1.788908766
H7C1A9	1	1.785714286
F8VYE8	1	1.785714286
P05387	1	1.782531194
F5H2U4	1	1.782531194
Q14008-2	1	1.776198934
Q96JP5	1	1.773049645
Q6PIW4	1	1.769911504
Q5T760	1	1.76366843
Q00341	1	1.76366843
Q96QC0	1	1.76056338
B3KQ25	1	1.76056338
B3KQH5	1	1.76056338
F5GZU3	1	1.757469244
J3QS39	1	1.748251748
O60216	1	1.742160279
G3V210	1	1.742160279
Q6P4R8	1	1.742160279
Q86Y82	1	1.739130435
H0YDS0	1	1.739130435
Q8N201	1	1.739130435
P09012	1	1.733102253
P46937	1	1.733102253
F8W6N3	1	1.730103806
Q96T58	1	1.727115717
H7C5Q0	1	1.727115717
Q9H8E8	1	1.727115717
O75175	1	1.724137931
Q9HCK8-2	1	1.724137931
O00571	1	1.721170396
Q6ULP2	1	1.721170396
Q9BZK7	1	1.721170396
P61160	1	1.718213058
P62266	1	1.712328767
Q2TAY7	1	1.712328767
P10398	1	1.709401709
Q8N0X7	1	1.706484642
H0YID1	1	1.706484642
Q3KRB8	1	1.706484642
B3KSY9	1	1.706484642
E9PCY4	1	1.703577513
P41208	1	1.700680272
B4E241	1	1.700680272

O75934	1	1.697792869
B4E1K0	1	1.694915254
Q06587	1	1.686340641
Q9H0H5	1	1.686340641
Q8WXA9-2	1	1.686340641
P13010	1	1.683501684
Q13322	1	1.683501684
K7EIS0	1	1.677852349
Q5JVM0	1	1.677852349
H7C3F9	1	1.675041876
Q69YQ0	1	1.675041876
F5H6E2	1	1.675041876
H0Y7K8	1	1.672240803
Q8IYH5	1	1.672240803
H3BP71	1	1.672240803
Q13242	1	1.672240803
F2Z2B9	1	1.672240803
P62136	1	1.672240803
Q12824	1	1.666666667
O43143	1	1.666666667
J3QRN6	1	1.661129568
H0Y390	1	1.661129568
O14976	1	1.658374793
Q2QGD7	1	1.658374793
P62995	1	1.652892562
P04908	1	1.644736842
F5H013	1	1.644736842
E7EX48	1	1.642036125
H0YNH8	1	1.639344262
M0QZN2	1	1.639344262
H7C2K2	1	1.633986928
P08579	1	1.628664495
P18583-10	1	1.628664495
H3BLZ8	1	1.628664495
P30153	1	1.62601626
Q9P2D1	1	1.623376623
O14776	1	1.618122977
Q9UHD2	1	1.615508885
Q7Z4H7-3	1	1.612903226
Q96KM6	1	1.607717042
Q9Y3B4	1	1.605136437
Q8IX12	1	1.6
Q14160	1	1.597444089
Q9NPJ6	1	1.592356688
G5E988	1	1.589825119
E9PK95	1	1.589825119
MOR210	1	1.589825119
P37108	1	1.589825119
P08621	1	1.587301587
O14686	1	1.584786054
Q15233	1	1.582278481
B5MCW3	1	1.579778831
Q96I24	1	1.579778831
P62316	1	1.579778831
P62701	1	1.579778831
P62304	1	1.577287066
F5GWU7	1	1.577287066
D6R9P3	1	1.57480315
O94927	1	1.572327044
F6S0T5	1	1.572327044
Q13151	1	1.572327044

P15924-2	1	1.569858713
X1WI28	1	1.564945227
E7ETA6	1	1.564945227
Q5SW96	1	1.564945227
Q96BN2	1	1.5625
P46821	1	1.557632399
B1AP46	1	1.557632399
Q12905	1	1.555209953
P54136	1	1.552795031
Q6ZWJ1	1	1.552795031
Q6NZ67	1	1.550387597
P38159	1	1.545595054
Q12948	1	1.543209877
Q9BZ17	1	1.540832049
P46777	1	1.540832049
G3V1Y1	1	1.538461538
P12270	1	1.538461538
H0YJV7	1	1.533742331
E7ETH6	1	1.533742331
P42166	1	1.531393568
J3KNE1	1	1.529051988
Q15648	1	1.529051988
Q6NZY4	1	1.526717557
G3V4C1	1	1.526717557
Q5W0B1	1	1.526717557
G8JLB6	1	1.524390244
Q9H9B1	1	1.524390244
Q6PKG0	1	1.524390244
Q8IVW6	1	1.522070015
Q7L014	1	1.522070015
Q9NV70	1	1.522070015
H3BT13	1	1.522070015
J3KMZ7	1	1.522070015
B7Z848	1	1.515151515
Q969J2	1	1.510574018
Q9Y6D9	1	1.510574018
Q09028	1	1.508295626
O75528	1	1.508295626
P01616	1	1.499250375
Q9H8M2	1	1.499250375
P52292	1	1.499250375
Q9C0C2	1	1.499250375
B4DZC3	1	1.497005988
O60306	1	1.492537313
Q15776	1	1.492537313
K7EP67	1	1.492537313
C9JAB2	1	1.490312966
Q86XI2	1	1.488095238
Q9UJX3-2	1	1.488095238
D3YTB1	1	1.485884101
Q6PF04	1	1.485884101
Q5T8P6	1	1.485884101
K7EL96	1	1.483679525
Q9ULM3	1	1.483679525
A6NHB5	1	1.481481481
O43172	1	1.481481481
A6NDA1	1	1.481481481
E1PSS2	1	1.477104874
Q7Z5K2	1	1.474926254
B5MC59	1	1.474926254
E9PC52	1	1.47275405

B4DLW8	1	1.47275405
P49368	1	1.47275405
P10244	1	1.468428781
P52597	1	1.464128843
O15037	1	1.459854015
P01859	1	1.459854015
O60264	1	1.459854015
Q5VY93	1	1.457725948
Q14676	1	1.455604076
G3V4F7	1	1.455604076
Q5JNZ5	1	1.455604076
H0YKN5	1	1.453488372
B3KRH1	1	1.449275362
O95983	1	1.449275362
Q9ULM6	1	1.449275362
Q16864	1	1.449275362
Q9UHX1-2	1	1.447178003
B4DQI6	1	1.447178003
O96019	1	1.445086705
E9PJI1	1	1.445086705
Q16513	1	1.443001443
U3KPZ7	1	1.443001443
Q9H2P0	1	1.443001443
P53621	1	1.44092219
H0YMU7	1	1.438848921
J3KN32	1	1.43472023
Q9NQ29	1	1.43472023
O95613	1	1.432664756
U3KQK0	1	1.432664756
H0YLR3	1	1.430615165
Q9NSI2	1	1.430615165
Q01081	1	1.430615165
H3BMM9	1	1.430615165
Q14669	1	1.428571429
Q12955-6	1	1.424501425
H0YBD0	1	1.418439716
Q9ULL5-3	1	1.418439716
P52272	1	1.418439716
K7EP82	1	1.418439716
B7Z5C0	1	1.416430595
Q5SY16	1	1.414427157
O94842	1	1.414427157
H0Y8G5	1	1.412429379
Q9NRZ9	1	1.412429379
Q9H981	1	1.410437236
E7EX29	1	1.410437236
P38919	1	1.408450704
P06396-2	1	1.406469761
H0Y3Y4	1	1.406469761
P0C0S5	1	1.404494382
P28066	1	1.404494382
P61981	1	1.404494382
Q9NYZ3	1	1.400560224
F5H4D6	1	1.398601399
H7C072	1	1.398601399
J3KNN5	1	1.398601399
A2A2E9	1	1.396648045
Q96PK6	1	1.396648045
Q6ZU65	1	1.39275766
Q5SY74	1	1.39275766
B4DVB8	1	1.388888889

B7Z632	1	1.388888889
P57740	1	1.386962552
D6RJ98	1	1.385041551
P17987	1	1.385041551
F5H2Z1	1	1.38121547
F8W617	1	1.38121547
P14866	1	1.379310345
Q8NAV1	1	1.379310345
Q96FJ2	1	1.377410468
O14519	1	1.377410468
Q92600	1	1.375515818
P46013	1	1.375515818
P09874	1	1.375515818
G3V1A4	1	1.375515818
O00629	1	1.373626374
Q13492	1	1.371742112
Q12906	1	1.371742112
F5H604	1	1.369863014
P42285	1	1.367989056
P14859	1	1.367989056
O15116	1	1.366120219
J3KTL2	1	1.36425648
O95747	1	1.36239782
Q15208	1	1.360544218
F8VP97	1	1.360544218
Q8IU81	1	1.356852103
Q96QD5	1	1.356852103
Q99856	1	1.35501355
F8W919	1	1.353179973
B7Z4B8	1	1.353179973
P52732	1	1.353179973
H3BUU5	1	1.353179973
Q5QPL9	1	1.353179973
P49207	1	1.353179973
P51991	1	1.351351351
Q04917	1	1.34589502
Q8WY36	1	1.34589502
P35658	1	1.34589502
K4DI95	1	1.344086022
A5YKK6	1	1.344086022
S4R341	1	1.340482574
Q15019	1	1.338688086
B7Z321	1	1.336898396
B9ZVT1	1	1.336898396
Q96EV2	1	1.331557923
P62258	1	1.328021248
G3V4T2	1	1.328021248
O75643	1	1.328021248
H0YJA2	1	1.324503311
B1AKI6	1	1.324503311
B1AHC8	1	1.324503311
A8MXP9	1	1.322751323
Q99996	1	1.321003963
Q9ULJ3	1	1.321003963
Q96L91-2	1	1.319261214
F8WCX5	1	1.317523057
Q9Y230	1	1.315789474
A2A3R5	1	1.314060447
D6RGK3	1	1.312335958
O75533	1	1.312335958
Q6P2Q9	1	1.308900524

B4DJ07	1	1.307189542
F5GY88	1	1.305483029
Q8NCM8	1	1.305483029
P51532-2	1	1.303780965
O75376	1	1.303780965
Q13148	1	1.303780965
Q09472	1	1.302083333
Q12830	1	1.297016861
P46940	1	1.295336788
J3QTQ0	1	1.288659794
Q96N67	1	1.288659794
Q8WWH5	1	1.288659794
M0R1T5	1	1.287001287
Q5T8U3	1	1.283697047
Q9H307	1	1.283697047
Q8WXI9	1	1.282051282
H0YDT0	1	1.282051282
H0Y5B5	1	1.280409731
H0Y760	1	1.280409731
Q9UQ13	1	1.275510204
P62310	1	1.27388535
Q9UNY4	1	1.27388535
B7Z5N7	1	1.27388535
Q9Y265	1	1.272264631
P80748	1	1.272264631
P0CG05	1	1.27064803
F8WJN3	1	1.267427123
Q9BTC0-1	1	1.267427123
Q9Y383	1	1.267427123
Q9H4L7-2	1	1.265822785
P52756	1	1.265822785
P22670	1	1.262626263
F5H669	1	1.261034048
M0QYC1	1	1.261034048
P22626	1	1.256281407
B4DPJ8	1	1.254705144
Q86TB9	1	1.254705144
F5H7W5	1	1.253132832
Q09666	1	1.251564456
Q9Y6X8	1	1.25

C. sgRNAs sequences used in pool screening

	<i>Chd8</i> sgRNAs for CRIRPR scan
Chd8_CDS_7749.0	TTTGATGACCCAAACTTATT
Chd8_CDS_7749.1	TGACCCAAACTTATTTGGCC
Chd8_CDS_7749.100	CATTGCTAGGGCCCGGCCA
Chd8_CDS_7749.1000	GGTGTGATGTCTGCAAGAC
Chd8_CDS_7749.1001	TTGATGTCTGCAAGACAGGC
Chd8_CDS_7749.1002	TGATGTCTGCAAGACAGGCT
Chd8_CDS_7749.1003	GTCTGCAAGACAGGCTGGGC
Chd8_CDS_7749.1005	CTGGGCTGGCTGCTCCTGGC
Chd8_CDS_7749.1006	GGCTGGCTGCTCCTGGCTGG
Chd8_CDS_7749.1007	GCTGGCTGCTCCTGGCTGGT
Chd8_CDS_7749.1008	CTCCTGGCTGGTGGGCTGAG
Chd8_CDS_7749.1009	CTGAGTGGTATAATCATGCA
Chd8_CDS_7749.101	ATTGCTAGGGCCCGGCCAG
Chd8_CDS_7749.1010	GGTATAATCATGCAAGGTTA
Chd8_CDS_7749.1011	TCATGCAAGGTTAAGGATTC
Chd8_CDS_7749.1012	AAGGTTAAGGATTCTGGAGC
Chd8_CDS_7749.1014	AGCTGGAGCTGTGGATTCTT
Chd8_CDS_7749.1015	GCTGGAGCTGTGGATTCTTT
Chd8_CDS_7749.1016	GGATTCTTTGGGAAGTTCAG
Chd8_CDS_7749.1017	TCAGTGAAGCTGTTTCCTC
Chd8_CDS_7749.1018	GTGGAAGCTGTTTCCTCTGG
Chd8_CDS_7749.1019	GAAGCTGTTTCCTCTGGTGG
Chd8_CDS_7749.102	CATACCTCGAGTCCTGAATG
Chd8_CDS_7749.1020	TTTCCTCTGGTGGAGGAACC
Chd8_CDS_7749.1022	ATCTTGGTTCATCTGATCCA
Chd8_CDS_7749.1023	TCCAAGGAGTCCAGAGAGCT
Chd8_CDS_7749.1024	CAGTCCAAGTGCTTCTTCAA
Chd8_CDS_7749.1025	AGTCCAAGTGCTTCTTCAAT
Chd8_CDS_7749.1026	GTCCAAGTGCTTCTTCAATG
Chd8_CDS_7749.1027	TGTCATCAGTCAGAGAGTCC
Chd8_CDS_7749.1028	GAGTCCAGCCAAATAAGTT
Chd8_CDS_7749.1029	AGTCCAGGCCAAATAAGTTT
Chd8_CDS_7749.103	AGGATGAGCTGCCTAGTGTG
Chd8_CDS_7749.1030	GTCATCAAAAAGATCCATGA
Chd8_CDS_7749.1031	TCATCAAAAAGATCCATGAT
Chd8_CDS_7749.1032	CATCAAAAAGATCCATGATG
Chd8_CDS_7749.104	GCTGCCTAGTGTCCGCCAG
Chd8_CDS_7749.105	GCCTAGTGTCCGGCCAGAGG
Chd8_CDS_7749.106	TAGTGTCCGGCCAGAGGAGG
Chd8_CDS_7749.107	AGTGTCCGGCCAGAGGAGGA
Chd8_CDS_7749.108	AGGAGGGTGAAAAGAAACGC
Chd8_CDS_7749.109	AAACGCAGGAAGAAGAGCAG
Chd8_CDS_7749.110	AACGCAGGAAGAAGAGCAGT
Chd8_CDS_7749.111	ACGCAGGAAGAAGAGCAGTG
Chd8_CDS_7749.113	GAGCAGTGGGAAAGGCTGA
Chd8_CDS_7749.114	CAGTGGGAAAGGCTGAAGG
Chd8_CDS_7749.115	TGCTGCTGCCTCCAAAACGA
Chd8_CDS_7749.116	GCTGCTGCCTCCAAAACGAA
Chd8_CDS_7749.119	ATCGTCTGCAAACTCTGACG
Chd8_CDS_7749.12	ATGGTGGAGGTGGTGATGTG
Chd8_CDS_7749.120	TTATGCCTGCACAATCGCCC
Chd8_CDS_7749.121	TATGCCTGCACAATCGCCCC
Chd8_CDS_7749.122	GCCTGCACAATCGCCCCGGG

Chd8_CDS_7749.123	TAAGCGAAAAAATATACAG
Chd8_CDS_7749.125	AAAGATAACAGACGATGAAG
Chd8_CDS_7749.126	GATAACAGACGATGAAGAGG
Chd8_CDS_7749.129	GAGGAGGAGGTCGATGTAAC
Chd8_CDS_7749.13	GAATTCATCAGCAAGTGACC
Chd8_CDS_7749.130	GAACCAGTGCAAGAGCCTGA
Chd8_CDS_7749.131	TCCTTCCATGCAGTCTTTG
Chd8_CDS_7749.132	TGAAGAAGATGCAGCTATTG
Chd8_CDS_7749.134	TCCTTCTGGACAATACACTG
Chd8_CDS_7749.136	CTCTTATCTGCACTGTGAGT
Chd8_CDS_7749.137	GTGGGCAACGATCTCCCAGC
Chd8_CDS_7749.138	AACGATCTCCCAGCTGGAGA
Chd8_CDS_7749.139	CCCAGCTGGAGAAGGATAAG
Chd8_CDS_7749.14	TGACCTGGTTCCTCCACCAG
Chd8_CDS_7749.140	GGATCCACCAGAACTAAAA
Chd8_CDS_7749.141	AAAACGGTTCAAAACAAAAA
Chd8_CDS_7749.142	TTTCAATCCAGACTACGTAG
Chd8_CDS_7749.143	CAATCCAGACTACGTAGAGG
Chd8_CDS_7749.144	CAGACTACGTAGAGGTGGAT
Chd8_CDS_7749.145	CGTAGAGGTGGATAGGATAC
Chd8_CDS_7749.146	CGAGTCTCACAGTGTGACA
Chd8_CDS_7749.147	CACAGTGTGACAAGGATAA
Chd8_CDS_7749.149	TAATTTACTACCTGGTAAAA
Chd8_CDS_7749.15	TACCACTCAGCCCACCAGCC
Chd8_CDS_7749.150	ATGGTGCTCTCTGCCCTATG
Chd8_CDS_7749.151	TGCCCTATGAGGACAGTACG
Chd8_CDS_7749.152	GCCCTATGAGGACAGTACGT
Chd8_CDS_7749.153	CAGTACGTGGGAGCTAAAAAG
Chd8_CDS_7749.154	GCTAAAAGAGGATGTTGATG
Chd8_CDS_7749.155	CTAAAAGAGGATGTTGATGA
Chd8_CDS_7749.156	ATGTTGATGAGGGCAAGATT
Chd8_CDS_7749.157	TGTTGATGAGGGCAAGATTC
Chd8_CDS_7749.158	GCAAGATTCGGGAATTTAAA
Chd8_CDS_7749.159	AATTTAAACGGATCCAGTCA
Chd8_CDS_7749.16	CAGACATCAACACCAACAGC
Chd8_CDS_7749.160	CAAGGCACCCAGAAGTGA
Chd8_CDS_7749.161	AAGGCACCCAGAAGTGA
Chd8_CDS_7749.163	ATCGTCCACAGGCAAATGCC
Chd8_CDS_7749.166	TAAAAACAGAAACCAATTAC
Chd8_CDS_7749.167	TTACGGGAATATCAGTTAGA
Chd8_CDS_7749.168	TACGGGAATATCAGTTAGAA
Chd8_CDS_7749.169	ACGGGAATATCAGTTAGAAG
Chd8_CDS_7749.17	ACCAACAGCAGGACTCTTGC
Chd8_CDS_7749.170	ATCAGTTAGAAGGGGTCAAC
Chd8_CDS_7749.171	TCAACTGGCTCCTCTTTAAT
Chd8_CDS_7749.172	TCCTCTTTAATTGGTATAAC
Chd8_CDS_7749.174	CTGCATCCTGGCTGATGAAA
Chd8_CDS_7749.175	TGCATCCTGGCTGATGAAAT
Chd8_CDS_7749.176	CCTGGCTGATGAAATGGGAT
Chd8_CDS_7749.177	CTGGCTGATGAAATGGGATT
Chd8_CDS_7749.178	TCAGTCAATCGCCTTCTTGC
Chd8_CDS_7749.179	GTCAATCGCCTTCTTGCAGG
Chd8_CDS_7749.18	CTTGCAGGTCTCCAAGAGCC
Chd8_CDS_7749.180	TTGCAGGAGGTATATAATGT
Chd8_CDS_7749.181	GTATATAATGTAGGCATCCA
Chd8_CDS_7749.182	AGGCATCCATGGTCCCTTTT
Chd8_CDS_7749.183	CATTGTCCACCATTACTAAC

Chd8_CDS_7749.184	ATTGTCCACCATTACTAACT
Chd8_CDS_7749.185	GGGAGCGTGAATTCAATACA
Chd8_CDS_7749.186	ATGAACACTATTGTGTACCA
Chd8_CDS_7749.187	TATTGTGTACCATGGCAGCC
Chd8_CDS_7749.188	ACCATGGCAGCCTGGCCAGC
Chd8_CDS_7749.189	AAATGTACTGTAAAGACTCA
Chd8_CDS_7749.19	AGCCAGGAGATCTTGAGCCA
Chd8_CDS_7749.190	AATGTACTGTAAAGACTCAC
Chd8_CDS_7749.193	CTGAGCTTCGTGAAATTGAA
Chd8_CDS_7749.194	TTATCATTGATGAAGCCCAT
Chd8_CDS_7749.195	ACTTGATAGTCTCAAGCACA
Chd8_CDS_7749.196	TAGTCTCAAGCACATGGACC
Chd8_CDS_7749.197	GAGCATAAAAGTGTACTCAC
Chd8_CDS_7749.198	AGCATAAAAGTGTACTCACA
Chd8_CDS_7749.199	ACCGTTACAAAATACCGTAG
Chd8_CDS_7749.2	GACTGATGACAGCTTTAATC
Chd8_CDS_7749.20	GCCAGGAGATCTTGAGCCAA
Chd8_CDS_7749.200	G TTCAGTCTACTGCATTCT
Chd8_CDS_7749.201	CTCAGAATCAGAATTCCTTA
Chd8_CDS_7749.202	TCAGAATTCCTTAAGGATTT
Chd8_CDS_7749.203	CAGAATTCCTTAAGGATTTT
Chd8_CDS_7749.204	AGAATTCCTTAAGGATTTTG
Chd8_CDS_7749.205	TTTTGGGGATCTCAAGACCG
Chd8_CDS_7749.206	GGATCTCAAGACCGAGGAGC
Chd8_CDS_7749.208	TTCTAAAAGCCAATGATGCTG
Chd8_CDS_7749.209	GATGCTGAGGAGACTCAAAG
Chd8_CDS_7749.21	GAGCCAAGGGAATCCTTTCA
Chd8_CDS_7749.210	AGAGGATGTTGAAAAAAATT
Chd8_CDS_7749.211	AAAAAATTGGCTCCCAAAC
Chd8_CDS_7749.212	AATTTCTCCTTCCTTTCCAA
Chd8_CDS_7749.213	ATTTCTCCTTCCTTTCCAAA
Chd8_CDS_7749.215	TCCTTCCTTTCCAAAGGGGC
Chd8_CDS_7749.216	TAATCTACTGAACACAATGA
Chd8_CDS_7749.217	AATCACCCGTACCTCATCAA
Chd8_CDS_7749.218	TGCAGAAGAGAAAATCCTGA
Chd8_CDS_7749.219	AGAAAATCCTGATGGAATTT
Chd8_CDS_7749.22	AGCCAAGGGAATCCTTTTCAT
Chd8_CDS_7749.220	GAAAATCCTGATGGAATTTT
Chd8_CDS_7749.221	ACCTCAAGATTTCCACCTGC
Chd8_CDS_7749.222	AGATTTCCACCTGCAGGCTA
Chd8_CDS_7749.223	TCCACCTGCAGGCTATGGTT
Chd8_CDS_7749.224	CAGGCTATGGTTCGGTCAGC
Chd8_CDS_7749.225	T TACTTCCAAAGCTTAAAGC
Chd8_CDS_7749.226	CTTCCAAAGCTTAAAGCTGG
Chd8_CDS_7749.227	AGTTCTGATCTTCTCCAGA
Chd8_CDS_7749.228	GGTACGCTGTCTAGACATTC
Chd8_CDS_7749.229	ACGCTGTCTAGACATTCTGG
Chd8_CDS_7749.23	TTCATGGGTGTCTCTGCCAC
Chd8_CDS_7749.230	TGGAGGATTATCTGATCCAG
Chd8_CDS_7749.231	AGGATTATCTGATCCAGAGG
Chd8_CDS_7749.232	TACTTATATGAACGTATTGA
Chd8_CDS_7749.233	ACTTATATGAACGTATTGAT
Chd8_CDS_7749.234	CGTATTGATGGGCGAGTTAG
Chd8_CDS_7749.235	TTCTTGCTATGTACCCGTGC
Chd8_CDS_7749.236	TTGCTATGTACCCGTGCTGG
Chd8_CDS_7749.237	TGTACCCGTGCTGGTGGACT
Chd8_CDS_7749.238	GTATTATCTTTGATTTCAGAC

Chd8_CDS_7749.239	GAATCCACAGAATGACCTGC
Chd8_CDS_7749.24	GGTGTCTCCCCAGTAATAC
Chd8_CDS_7749.240	CAAGCACGTTGTCATCGAAT
Chd8_CDS_7749.241	TGGACAGAGCAAAGCTGTGA
Chd8_CDS_7749.242	TGATAAAGCTAGCCTCAAGT
Chd8_CDS_7749.243	GATAAAGCTAGCCTCAAGTT
Chd8_CDS_7749.244	AGCTAGCCTCAAGTTGGGAT
Chd8_CDS_7749.245	GCTGTGCTTCAGTCCATGAG
Chd8_CDS_7749.246	TGCTTCAGTCCATGAGTGGT
Chd8_CDS_7749.247	GCTTCAGTCCATGAGTGGTC
Chd8_CDS_7749.248	CAGTCCATGAGTGGTCGGGA
Chd8_CDS_7749.249	GGTCGGGATGGCAACATTAC
Chd8_CDS_7749.25	GTCTCCCCAGTAATACTGG
Chd8_CDS_7749.250	AAGAGATTGAAGATCTCTTA
Chd8_CDS_7749.251	ATTGAAGATCTCTTAAGGAA
Chd8_CDS_7749.252	CTTAAGGAAAGGTGCCTATG
Chd8_CDS_7749.253	AGGTGCCTATGCGGCCATAA
Chd8_CDS_7749.254	TGCCTATGCGGCCATAATGG
Chd8_CDS_7749.255	CATAATGGAGGAAGACGATG
Chd8_CDS_7749.256	ATAATGGAGGAAGACGATGA
Chd8_CDS_7749.257	TGAGGGTTCTAAGTTTTGTG
Chd8_CDS_7749.258	GGGTTCTAAGTTTTGTGAGG
Chd8_CDS_7749.259	TAGATCAGATCTTACTGAGA
Chd8_CDS_7749.26	CCACCAAACCTCTCCGTCAC
Chd8_CDS_7749.260	ACCATCACTATTGAGTCTGA
Chd8_CDS_7749.261	CCATCACTATTGAGTCTGAA
Chd8_CDS_7749.262	ACTATTGAGTCTGAAGGGAA
Chd8_CDS_7749.263	GAAAGGTTCTACTTTTGCCA
Chd8_CDS_7749.264	GCTTTGTGCTTCTGAAAAT
Chd8_CDS_7749.265	AAATAGGACAGATATTTCCC
Chd8_CDS_7749.266	CCCTGGATGATCCAAACTTT
Chd8_CDS_7749.267	ATCCAAACTTTTGGCAAAAA
Chd8_CDS_7749.268	TCCAAACTTTTGGCAAAAAAT
Chd8_CDS_7749.269	TTGGCAAAAAATGGGCCAAAA
Chd8_CDS_7749.27	CTCCGTCACAGGCACCCATG
Chd8_CDS_7749.270	CAAAAAGGCAGACCTAGACA
Chd8_CDS_7749.271	TGATCGACACACCTCGAGTT
Chd8_CDS_7749.272	CACTTTCAAAGATGATGACC
Chd8_CDS_7749.273	CCTGGTTGAGTTTTCTGATT
Chd8_CDS_7749.275	CACGTTCCCGAAGACATGAC
Chd8_CDS_7749.276	CATGACCGGCATCACACCTA
Chd8_CDS_7749.277	ATGACCGGCATCACACCTAT
Chd8_CDS_7749.278	ATGGGCGCACTGACTGCTTC
Chd8_CDS_7749.279	TGGGCGCACTGACTGCTTCC
Chd8_CDS_7749.28	CACCCATGTGGCACAATTC
Chd8_CDS_7749.280	CCGGGTAGAAAAGCATCTCC
Chd8_CDS_7749.281	GAAAAGCATCTCCTGGTATA
Chd8_CDS_7749.286	TGGAGAGATATTTGTCTCA
Chd8_CDS_7749.287	TGTCTCACGGACGATTTAAG
Chd8_CDS_7749.288	TACTGTCTTCTACACTACCG
Chd8_CDS_7749.289	ACTGTCTTCTACACTACCGT
Chd8_CDS_7749.29	GTGGCACAAATTCAGGCCCA
Chd8_CDS_7749.290	CTGTCTTCTACACTACCGTG
Chd8_CDS_7749.291	AAAACATCAAAGCTTCATT
Chd8_CDS_7749.292	AAACATCAAAGCTTCATT
Chd8_CDS_7749.293	TTGATTAGCCCTGCTGAAAA
Chd8_CDS_7749.294	AAAGAATTGCAGAATCATT

Chd8_CDS_7749.295	CTGTCTATCCCTGTGCCCCG
Chd8_CDS_7749.296	TGTCTATCCCTGTGCCCCGT
Chd8_CDS_7749.297	CCCTGTGCCCCGTGGGCGTA
Chd8_CDS_7749.298	CCTGTGCCCCGTGGGCGTAA
Chd8_CDS_7749.299	CTGTGCCCCGTGGGCGTAAG
Chd8_CDS_7749.3	GACCCCATTTGAAGAAGCACT
Chd8_CDS_7749.30	CAGTACAGCTCAGCCCCTAG
Chd8_CDS_7749.300	AAGTACTTTTGACATTCATA
Chd8_CDS_7749.301	TTGACATTCATAAAGGCAGAC
Chd8_CDS_7749.302	TTCATAAAGGCAGACTGGATC
Chd8_CDS_7749.305	GATGCTCTACTACCTGAGAC
Chd8_CDS_7749.306	GCTCTACTACCTGAGACAGG
Chd8_CDS_7749.307	TACCTGAGACAGGAGGTTAT
Chd8_CDS_7749.308	ACAGGAGGTTATTGGAGACC
Chd8_CDS_7749.309	TATTGGAGACCAGGCAGAGA
Chd8_CDS_7749.31	ACAGCTCAGCCCCTAGTGGC
Chd8_CDS_7749.310	GACCAGGCAGAGAAGGTGTT
Chd8_CDS_7749.311	CAGGCAGAGAAGGTGTTAGG
Chd8_CDS_7749.313	GATTGACATATGGTTCCCAG
Chd8_CDS_7749.314	TGACATATGGTTCCCAGTGG
Chd8_CDS_7749.315	GTTCCCAGTGGTGGATCAGC
Chd8_CDS_7749.316	CCCAGTGGTGGATCAGCTGG
Chd8_CDS_7749.317	AGCTGGAGGTTCTACAACCT
Chd8_CDS_7749.318	TGGAGGTTCTACAACCTGG
Chd8_CDS_7749.319	GGAGGTTCTACAACCTGGT
Chd8_CDS_7749.32	CAGCTCAGCCCCTAGTGGCT
Chd8_CDS_7749.320	TACAACCTGGTGGGATAGTG
Chd8_CDS_7749.321	GCTGACAAATCCCTGCTCAT
Chd8_CDS_7749.322	CTCATTGGCGTTTTTAAGCA
Chd8_CDS_7749.323	ATGAGAAATACAATACCATG
Chd8_CDS_7749.324	TGAGAAATACAATACCATGA
Chd8_CDS_7749.325	TGCCTTGTGCTTCTAGAAA
Chd8_CDS_7749.326	TTGTGCTTCTAGAAAAGGC
Chd8_CDS_7749.327	GCTTCTAGAAAAGGCTGGC
Chd8_CDS_7749.328	CGCAGCAGAACATAGAGTGT
Chd8_CDS_7749.329	GTTGGATAATTTCTCCGACC
Chd8_CDS_7749.33	CTAGTGGCTGGGACAGCCAA
Chd8_CDS_7749.330	AATTTCTCCGACCTGGTAGA
Chd8_CDS_7749.331	ATTTCTCCGACCTGGTAGAA
Chd8_CDS_7749.333	TCCTGAATATAAACCCCTCC
Chd8_CDS_7749.334	CCTGAATATAAACCCCTCCA
Chd8_CDS_7749.335	ACCCCTCCAGGGTCTCCAA
Chd8_CDS_7749.336	TCCAAAGGACCCAGATGATG
Chd8_CDS_7749.338	GGGTGATCCCTTGATGATGA
Chd8_CDS_7749.339	TCCCTTGATGATGATGGATG
Chd8_CDS_7749.34	GTGGCTGGGACAGCCAACGG
Chd8_CDS_7749.340	GAGGAGATCTCAGTCATCGA
Chd8_CDS_7749.341	GATCTCAGTCATCGACGGAG
Chd8_CDS_7749.343	GCCCAGGTAACCAACAGCC
Chd8_CDS_7749.344	CCCAGGTAACCAACAGCCA
Chd8_CDS_7749.345	AACAGCCAGGGCATTTATTC
Chd8_CDS_7749.346	GGGCATTTATTCTGGCCTCC
Chd8_CDS_7749.347	CAGGCTCCGCCTCACAGCT
Chd8_CDS_7749.35	ACTTTTACCAAAGTGCTGAC
Chd8_CDS_7749.350	ACAAATGAAGATGGAGGCTG
Chd8_CDS_7749.351	AAGATGGAGGCTGCGGAACG
Chd8_CDS_7749.352	AGATGGAGGCTGCGGAACGT

Chd8_CDS_7749.353	GATGGAGGCTGCGGAACGTG
Chd8_CDS_7749.354	AGGCTGCGGAACGTGGGGAC
Chd8_CDS_7749.355	TTAAGCTCAAAGAAATCGCA
Chd8_CDS_7749.356	AGCTCAAAGAAATCGCAAGG
Chd8_CDS_7749.357	GCTCAAAGAAATCGCAAGGC
Chd8_CDS_7749.36	ACTGGTACACCCCTTCGACC
Chd8_CDS_7749.361	TACCGAGTAGTATCTACCTT
Chd8_CDS_7749.362	AGTAGTATCTACCTTTGGTG
Chd8_CDS_7749.363	CTGACAACATGCAGTTTCAC
Chd8_CDS_7749.364	TGACAACATGCAGTTTCACT
Chd8_CDS_7749.365	CTCCGCACTTTTGCTGCC
Chd8_CDS_7749.366	AGCCTTACCAAGTACTTCCA
Chd8_CDS_7749.367	CAAGTACTTCCATGGTTTGTG
Chd8_CDS_7749.368	TGCCGCCTTCCCCAGCTGC
Chd8_CDS_7749.369	TCACTGAAGAGAGAGCCTCG
Chd8_CDS_7749.37	CCAGGTGTATCCATTGTCTC
Chd8_CDS_7749.370	TTGAGTTGCTTCGACGCTTA
Chd8_CDS_7749.371	TGAGTTGCTTCGACGCTTAC
Chd8_CDS_7749.372	GCCACCCCTTTTAGAAGAT
Chd8_CDS_7749.373	CCCCCTTTTAGAAGATCGGC
Chd8_CDS_7749.374	CTGGCATTGTGTCAGCCTCC
Chd8_CDS_7749.375	CAGGTCTGAATTGCCAAA
Chd8_CDS_7749.376	GTCTTGAATTGCCCAAATGG
Chd8_CDS_7749.377	TCTTGAATTGCCCAAATGGT
Chd8_CDS_7749.378	TGGGAACCTGTCCGTCATGA
Chd8_CDS_7749.379	GGGAACCTGTCCGTCATGAT
Chd8_CDS_7749.38	TGTCTCTGGTAATACAGTGT
Chd8_CDS_7749.380	GGAACCTGTCCGTCATGATG
Chd8_CDS_7749.381	CATGATGGGGAGCTCCTACG
Chd8_CDS_7749.382	CTACGAGGAGCAGCCCGCCA
Chd8_CDS_7749.383	TACGAGGAGCAGCCCGCCAT
Chd8_CDS_7749.384	ACGAGGAGCAGCCCGCCATG
Chd8_CDS_7749.385	AACAGACTGCAACATCATGC
Chd8_CDS_7749.386	GGACCCAGACTTCTCTTTTC
Chd8_CDS_7749.387	GAATTATATGCAGAACCATC
Chd8_CDS_7749.388	TTATATGCAGAACCATCAGG
Chd8_CDS_7749.389	TATATGCAGAACCATCAGGC
Chd8_CDS_7749.39	TAATACAGTGTGGCCACGA
Chd8_CDS_7749.390	TCCTGTTGAAAAGTCACCTG
Chd8_CDS_7749.391	ACCTGAGGAAAAGTACTGTTC
Chd8_CDS_7749.392	TACTGTTGAGGTCCCCAATC
Chd8_CDS_7749.393	GAGTCTGACTTTAAAGTTAG
Chd8_CDS_7749.394	GACTTTAAAGTTAGAGGATG
Chd8_CDS_7749.395	AAAGTTAGAGGATGAGGTTG
Chd8_CDS_7749.396	TAGAGGATGAGGTTGTGGCT
Chd8_CDS_7749.397	CAAGACTATGAAGTACGCGT
Chd8_CDS_7749.398	CAGATACAGCTCCTCTGTCC
Chd8_CDS_7749.399	GAGTGTCCCACCAGTAAAC
Chd8_CDS_7749.4	ACTTGGACTGCCAAGCTCTC
Chd8_CDS_7749.40	GTGTTGGCCACGAAGGTCCC
Chd8_CDS_7749.400	TGTCCCACCAGTGAAACTGG
Chd8_CDS_7749.401	ACCAGTGAAACTGGAGGACG
Chd8_CDS_7749.402	GGATGATTCAGACTCTGAGC
Chd8_CDS_7749.403	TGACGAGAGTGAAGACGAGA
Chd8_CDS_7749.405	TCCCTTACTATGTCCCAAGA
Chd8_CDS_7749.406	GATGGATTCCCAAATGAAGA
Chd8_CDS_7749.407	CCCTGAGTTGCTGCTACTGC

Chd8_CDS_7749.409	AAGAGCCTCTGAATGGCCTA
Chd8_CDS_7749.41	TGTTGGCCACGAAGGTCCCT
Chd8_CDS_7749.410	CCGCATTGACCTCGTCTGCC
Chd8_CDS_7749.411	GTCTGCCAGGCTGTACTCTC
Chd8_CDS_7749.412	TCTGCCAGGCTGTACTCTCA
Chd8_CDS_7749.413	AGGCTGTACTCTCAGGAAAA
Chd8_CDS_7749.414	GGAAATGGCCTTCTAACC GC
Chd8_CDS_7749.415	GCCTTCTAACC GCCGAGCC
Chd8_CDS_7749.416	CGGAGCCAGGAAGTGACAGC
Chd8_CDS_7749.417	AGCCAGGAAGTGACAGCAGG
Chd8_CDS_7749.418	AGTGACAGCAGGAGGAATTT
Chd8_CDS_7749.419	GTGACAGCAGGAGGAATTTT
Chd8_CDS_7749.42	CACGAAGTCCCTGGGAACC
Chd8_CDS_7749.420	TGACAGCAGGAGGAATTTTG
Chd8_CDS_7749.421	GCAGGAGGAATTTGGGGCC
Chd8_CDS_7749.422	GACAGTCCCTCTTTGACCCC
Chd8_CDS_7749.423	TCTTTGACCCCAGGAGAAGA
Chd8_CDS_7749.424	CTTTGACCCCAGGAGAAGAT
Chd8_CDS_7749.425	TTTGACCCCAGGAGAAGATG
Chd8_CDS_7749.426	CCAGTCCCCACGCCACGAAG
Chd8_CDS_7749.427	AAGTGGCAGTGCAGCTTCCA
Chd8_CDS_7749.428	TGGCAGTGCAGCTTCCATGG
Chd8_CDS_7749.429	CAGTGCAGCTTCCATGGCGG
Chd8_CDS_7749.43	AAGCCGACCAGTAAAACAGC
Chd8_CDS_7749.430	AGCTTCCATGGCGGAGGAAG
Chd8_CDS_7749.431	GGCATCTGCAGTACCACAG
Chd8_CDS_7749.432	ATCTGCAGTACCACAGCGG
Chd8_CDS_7749.433	CGGCCAGTTTACGAAACTT
Chd8_CDS_7749.434	CAGTTTACGAAACTTCGCGC
Chd8_CDS_7749.435	TACGAAACTTCGGCGAGGCA
Chd8_CDS_7749.437	ATTCCAGAAGCATAGATTGA
Chd8_CDS_7749.439	ATTGATGGCTAATGGTGTA
Chd8_CDS_7749.44	GCTGGTCTCCAGCCAGTAA
Chd8_CDS_7749.440	TTGATGGCTAATGGTGTAAT
Chd8_CDS_7749.441	GCTAATGGTGTAATGGGAGA
Chd8_CDS_7749.45	CTGGTCTCCAGCCAGTAAA
Chd8_CDS_7749.450	AGAGCCTAATCACCTTGATC
Chd8_CDS_7749.451	TAATCACCTTGATCTGGACC
Chd8_CDS_7749.452	TTGATCTGGACCTGGAGACC
Chd8_CDS_7749.453	CCGGATCCCTGTCATCAATA
Chd8_CDS_7749.454	GATCCCTGTCATCAATAAGG
Chd8_CDS_7749.455	CCTGTCATCAATAAGGTGGA
Chd8_CDS_7749.456	TAAGGTGGATGGTACTTTGC
Chd8_CDS_7749.457	GGTGGATGGTACTTTGCTGG
Chd8_CDS_7749.458	GTGGATGGTACTTTGCTGGT
Chd8_CDS_7749.459	TACTTTGCTGGTGGGTGATG
Chd8_CDS_7749.46	GTAAAGGGTTCAGCTCCTGC
Chd8_CDS_7749.460	TGGGTGATGAGCCCCCTCGC
Chd8_CDS_7749.461	GGGTGATGAGGCCCTCGCC
Chd8_CDS_7749.462	TGATGAGGCCCTCGCCGGG
Chd8_CDS_7749.463	GGCCCCTCGCCGGGCGGAGC
Chd8_CDS_7749.464	GCCGGGCGGAGCTGGAGATG
Chd8_CDS_7749.465	GGAGCTGGAGATGTGGTTAC
Chd8_CDS_7749.466	GAGCTGGAGATGTGGTTACA
Chd8_CDS_7749.469	AGGAACGTAGAAAACAGAAG
Chd8_CDS_7749.47	TAAAGGGTTCAGCTCCTGCT
Chd8_CDS_7749.471	TAAGGCAGAATTGAACTGTT

Chd8_CDS_7749.472	AAGGCAGAATTGAACTGTTT
Chd8_CDS_7749.473	AGAATTGAACTGTTTGGGAA
Chd8_CDS_7749.474	CAGCCAGCGAACTCTAGAAA
Chd8_CDS_7749.475	AGCCAGCGAACTCTAGAAAT
Chd8_CDS_7749.478	ATGCTGAAACTGCGTTCAAC
Chd8_CDS_7749.479	TGCTGAAACTGCGTTCAACC
Chd8_CDS_7749.48	TCAGTCCTGCTGGGAATCC
Chd8_CDS_7749.480	GCGTTCAACCGGGTTTTGCC
Chd8_CDS_7749.481	CGTTCAACCGGGTTTTGCCA
Chd8_CDS_7749.482	CACCAGAGAACAGCAAGAAA
Chd8_CDS_7749.483	ACCAGAGAACAGCAAGAAAC
Chd8_CDS_7749.484	ACAGCAAGAAACGGGTCCGT
Chd8_CDS_7749.485	ACCAGACCTTTCTAAGATGA
Chd8_CDS_7749.486	TAAGATGATGGCCCTGATGC
Chd8_CDS_7749.487	AAGATGATGGCCCTGATGCA
Chd8_CDS_7749.488	ATGATGGCCCTGATGCAGGG
Chd8_CDS_7749.489	CTGATGCAGGGTGAAGCAC
Chd8_CDS_7749.49	CAGCTCCTGCTGGGAATCCT
Chd8_CDS_7749.490	TGATGCAGGGTGAAGCACT
Chd8_CDS_7749.491	CCTACAGTCTGTGTCGTCTC
Chd8_CDS_7749.492	CTACAGTCTGTGTCGTCTCT
Chd8_CDS_7749.493	GCCTTTTATGCCGTTTGTGA
Chd8_CDS_7749.494	CCTTTTATGCCGTTTGTGAT
Chd8_CDS_7749.496	CATCCAGGCTTGAGAACCAC
Chd8_CDS_7749.497	TCACCAGCTACTACCACCTC
Chd8_CDS_7749.498	CCACCTCTGGTACTGCCTTG
Chd8_CDS_7749.499	GTTACCAACACTGCAACCTG
Chd8_CDS_7749.5	GCCAAGCTCTCTGGACTCCT
Chd8_CDS_7749.50	AGCTCCTGCTGGGAATCCTG
Chd8_CDS_7749.500	ACCTGAGGACGATGATGAAG
Chd8_CDS_7749.502	AGAAGATGATGATTTATCTC
Chd8_CDS_7749.503	GAAGATGATGATTTATCTCA
Chd8_CDS_7749.504	AGGGCTATGACAGCTCAGAA
Chd8_CDS_7749.505	GGGCTATGACAGCTCAGAAC
Chd8_CDS_7749.506	TCAGTCGTCAGCATCTTCAC
Chd8_CDS_7749.507	ATCTTACTGGAGTCTGAGT
Chd8_CDS_7749.508	TCACTGGAGTCTGAGTTGGC
Chd8_CDS_7749.509	TCTGAGTTGGCTGGCATCAT
Chd8_CDS_7749.51	GCTGGGAATCCTGGGGCTGC
Chd8_CDS_7749.510	CTGAGTTGGCTGGCATCATA
Chd8_CDS_7749.511	TCCTTCTCATCATCGTCTC
Chd8_CDS_7749.512	TCGTCTCAGGTTGCAGTGT
Chd8_CDS_7749.513	TTGCAGTGTGGTAACCGCA
Chd8_CDS_7749.514	TAACCGCAAGGCAGTACCAG
Chd8_CDS_7749.515	CCGCAAGGCAGTACCAGAGG
Chd8_CDS_7749.516	GTACCAGAGGTGGTAGTAGC
Chd8_CDS_7749.517	GTGGTAGTAGCTGGTGAAGA
Chd8_CDS_7749.518	TGGTAGTAGCTGGTGAAGAA
Chd8_CDS_7749.519	TGGTGAAGAAGGGTAGCCAG
Chd8_CDS_7749.52	CTGGGAATCCTGGGGCTGCC
Chd8_CDS_7749.520	TAGCCAGTGGTTCTCAAGCC
Chd8_CDS_7749.521	CAGTGGTTCTCAAGCCTGGA
Chd8_CDS_7749.522	TTCTCAAGCCTGGATGGTGA
Chd8_CDS_7749.523	TCAAGCCTGGATGGTATGG
Chd8_CDS_7749.53	ACTGACGTCTACACCTACCC
Chd8_CDS_7749.536	GTGATGATGAAGCATGGTGC
Chd8_CDS_7749.537	ATGGTGCTGGAGTCTACATG

Chd8_CDS_7749.538	TGGTGCTGGAGTCTACATGA
Chd8_CDS_7749.539	GGTGCTGGAGTCTACATGAG
Chd8_CDS_7749.540	GTGCTGGAGTCTACATGAGG
Chd8_CDS_7749.541	GCTGCTGCACCCATCACAAA
Chd8_CDS_7749.542	CCCATCACAAACGGCATAAA
Chd8_CDS_7749.544	CCAGAGACGACACAGACTGT
Chd8_CDS_7749.545	GTTACTACTGCTGTGTTGAA
Chd8_CDS_7749.546	GAAAGGTGTTATGCAGAGAC
Chd8_CDS_7749.547	AAAGGTGTTATGCAGAGACA
Chd8_CDS_7749.548	CAGTGCTCCACCCTGCATC
Chd8_CDS_7749.549	AGTGCTTCCACCCTGCATCA
Chd8_CDS_7749.55	TGAATCGAAACGCATCACTT
Chd8_CDS_7749.550	TCAGGGCCATCATCTTAGAA
Chd8_CDS_7749.551	GCCATCATCTTAGAAAGGTC
Chd8_CDS_7749.552	AAAGGTCTGGTCTTGTCCTA
Chd8_CDS_7749.553	ACCCGTTTCTTGCTGTCTC
Chd8_CDS_7749.554	TTGCTGTTCTCTGGTGCAAC
Chd8_CDS_7749.555	TTCTCTGGTGCAACAGGCC
Chd8_CDS_7749.556	CAACAGGCCCTGGCAAAACC
Chd8_CDS_7749.557	TTCCATTCTAGAGTTCGC
Chd8_CDS_7749.558	CTAGAGTTCGCTGGCTGTAC
Chd8_CDS_7749.56	GTCCTTCAACAGCCACAGTC
Chd8_CDS_7749.562	CGGGGATCAACAGCAAACCTC
Chd8_CDS_7749.563	ACCACATCTCCAGCTCCGCC
Chd8_CDS_7749.564	ATCTCCAGCTCCGCCCGGCG
Chd8_CDS_7749.565	TCTCCAGCTCCGCCCGGCGA
Chd8_CDS_7749.566	CTCCAGCTCCGCCCGGCGAG
Chd8_CDS_7749.567	CCATCCACCTTATTGATGAC
Chd8_CDS_7749.568	CATCCACCTTATTGATGACA
Chd8_CDS_7749.569	CCTTATTGATGACAGGGATC
Chd8_CDS_7749.57	CTTCAACAGCCACAGTCCGG
Chd8_CDS_7749.570	CTTATTGATGACAGGGATCC
Chd8_CDS_7749.571	TGACAGGGATCCGGGTCTCC
Chd8_CDS_7749.572	GGGTCTCCAGGTCCAGATCA
Chd8_CDS_7749.573	AGGTCCAGATCAAGGTGATT
Chd8_CDS_7749.576	CTCGCCGAAGTTTCGTAAAC
Chd8_CDS_7749.577	TCGCCGAAGTTTCGTAAACT
Chd8_CDS_7749.578	CGTAAACTGGGCCCGCGCTG
Chd8_CDS_7749.579	AGATGCCTCTCCTCCGCCA
Chd8_CDS_7749.58	CCACAGTCCGGAGGTCCCCA
Chd8_CDS_7749.580	GAAGCTGCACTGCCACTTCG
Chd8_CDS_7749.581	TGCACTGCCACTTCGTGGCG
Chd8_CDS_7749.582	GCACTGCCACTTCGTGGCGT
Chd8_CDS_7749.583	CACTGCCACTTCGTGGCGTG
Chd8_CDS_7749.584	CCACTTCGTGGCGTGGGGAC
Chd8_CDS_7749.585	GGAGAGTCCCATCTTCTCC
Chd8_CDS_7749.586	GAGAGTCCCATCTTCTCCT
Chd8_CDS_7749.587	AGAGTCCCATCTTCTCCTG
Chd8_CDS_7749.588	ATCTTCTCCTGGGGTCAAAG
Chd8_CDS_7749.589	TCTTCTCCTGGGGTCAAAGA
Chd8_CDS_7749.59	CCGGAGGTCCCAAGGACAT
Chd8_CDS_7749.590	AAGAGGGACTGTCTAATAAA
Chd8_CDS_7749.591	CTGTCTAATAAATGGTTGCC
Chd8_CDS_7749.592	TTCTCTGCTGTCACTTCC
Chd8_CDS_7749.593	CTGCTGCACTTCTGGCTC
Chd8_CDS_7749.594	CTGCACTTCTGGCTCCGG
Chd8_CDS_7749.595	TCCTGGCTCCGGCGGTTAGA

Chd8_CDS_7749.596	ATTTCCCTGAGAGTACAGCC
Chd8_CDS_7749.597	AGAGTACAGCCTGGCAGACG
Chd8_CDS_7749.598	CCTGGCAGACGAGGTCAATG
Chd8_CDS_7749.6	TTGGATCAGATGAACCAAGA
Chd8_CDS_7749.60	GGACATCGGCATGTTGTGTT
Chd8_CDS_7749.601	TCCTGCAGTAGCAGCAACTC
Chd8_CDS_7749.602	CCTGCAGTAGCAGCAACTCA
Chd8_CDS_7749.603	CTGCAGTAGCAGCAACTCAG
Chd8_CDS_7749.604	ATTTGTTCTCCATCTTCATT
Chd8_CDS_7749.606	CTTCATTTGGGAATCCATCT
Chd8_CDS_7749.607	TTCATTTGGGAATCCATCTT
Chd8_CDS_7749.608	ATCCATCTTTGGGACATAGTA
Chd8_CDS_7749.61	GACATCGGCATGTTGTGTTA
Chd8_CDS_7749.610	GGGACATAGTAAGGGACAGA
Chd8_CDS_7749.611	CTCTCTTCATCATAGAGCTT
Chd8_CDS_7749.612	TCTCTTCATCATAGAGCTTT
Chd8_CDS_7749.613	CTTCATCATAGAGCTTTGGG
Chd8_CDS_7749.614	TTCATCATAGAGCTTTGGGC
Chd8_CDS_7749.615	CATAGAGCTTTGGGCGGGAC
Chd8_CDS_7749.616	GTCTTCACTCTCGTCAGTGC
Chd8_CDS_7749.617	ACTCTCGTCAGTGCTGGAGC
Chd8_CDS_7749.62	GTTGTGTAGGGAGTCTACC
Chd8_CDS_7749.624	TCCTCGTCTCCAGTTTCAC
Chd8_CDS_7749.625	TCGTCCTCCAGTTTCACTGG
Chd8_CDS_7749.626	CGTCCTCCAGTTTCACTGGT
Chd8_CDS_7749.627	GTTTCACTGGTGGGACACTC
Chd8_CDS_7749.628	TTTCACTGGTGGGACACTCC
Chd8_CDS_7749.629	GGTGGGACACTCCGGGACAG
Chd8_CDS_7749.63	ACCAGGCAAGATAGTGTAC
Chd8_CDS_7749.630	GCGTACTTCATAGTCTTGTG
Chd8_CDS_7749.631	CATAGTCTTGTGAGGTGAGT
Chd8_CDS_7749.632	TAAAGTCAGACTCTCCAGAT
Chd8_CDS_7749.633	AAAGTCAGACTCTCCAGATT
Chd8_CDS_7749.634	AAGTCAGACTCTCCAGATTG
Chd8_CDS_7749.636	TCCTCAGGTGACTTTTCAAC
Chd8_CDS_7749.637	GACTTTTCAACAGGAGCATC
Chd8_CDS_7749.638	ACTTTTCAACAGGAGCATCT
Chd8_CDS_7749.639	CAACAGGAGCATCTGGGCGC
Chd8_CDS_7749.64	CCAGGCAAGATAGTGTTACA
Chd8_CDS_7749.640	AACAGGAGCATCTGGGCGCA
Chd8_CDS_7749.641	ACAGGAGCATCTGGGCGCAG
Chd8_CDS_7749.642	GCATCTGGGCGCAGGGGTGA
Chd8_CDS_7749.643	TGATGGTGAAGCAGTACGTG
Chd8_CDS_7749.644	CAGTACGTGAGGTACACTGC
Chd8_CDS_7749.645	GTACACTGCTGGTGCAGCAG
Chd8_CDS_7749.646	CTGCTGGTGCAGCAGTGGAG
Chd8_CDS_7749.647	GTGGAGTGGAGCATCGCGAC
Chd8_CDS_7749.648	TGGAGTGGAGCATCGCGACA
Chd8_CDS_7749.649	CAGCTGATGCTCCCGCTGA
Chd8_CDS_7749.65	GACTCAAGCCAAGAATGCC
Chd8_CDS_7749.650	GGTCTGCATATAATTCATA
Chd8_CDS_7749.651	GTTCTGCATATAATTCATAC
Chd8_CDS_7749.652	GCAGCCAGAAAAGAGAAGTC
Chd8_CDS_7749.653	CAGCCAGAAAAGAGAAGTCT
Chd8_CDS_7749.654	GCATGATGTGCAGTCTGTT
Chd8_CDS_7749.655	AGTCTGTTGGCTACCCCA
Chd8_CDS_7749.656	CTGTTTGGCTACCCCATGG

Chd8_CDS_7749.657	TGTTTGGCTCACCCCATGGC
Chd8_CDS_7749.658	CATGGCGGGCTGCTCCTCGT
Chd8_CDS_7749.659	GTAGGAGCTCCCCATCATGA
Chd8_CDS_7749.66	ACTCAAGCCAAGAATGCCCA
Chd8_CDS_7749.660	AGCTCCCCATCATGACGGAC
Chd8_CDS_7749.661	ACGGACAGGTTCCCACCATT
Chd8_CDS_7749.662	CGGACAGGTTCCCACCATT
Chd8_CDS_7749.663	CATTTGGGCAATTCAAGACC
Chd8_CDS_7749.664	TTGGGCAATTCAAGACCTGG
Chd8_CDS_7749.665	ATGCCAGCCGATCTTCTAAA
Chd8_CDS_7749.666	TGCCAGCCGATCTTCTAAA
Chd8_CDS_7749.667	GCCAGCCGATCTTCTAAAAG
Chd8_CDS_7749.668	CCAGCCGATCTTCTAAAAGG
Chd8_CDS_7749.669	GCCGATCTTCTAAAAGGGGG
Chd8_CDS_7749.67	CTCAAGCCAAGAATGCCCAG
Chd8_CDS_7749.670	AGCGTCGAAGCAACTCAATT
Chd8_CDS_7749.671	AATTCGGTAGAGAGTCCCTCG
Chd8_CDS_7749.672	CGAGGCTCTCTTTCAGTGA
Chd8_CDS_7749.673	GAGGCTCTCTTTCAGTGAT
Chd8_CDS_7749.674	ATGGGCTCAATGAACAGATT
Chd8_CDS_7749.675	TGGGCTCAATGAACAGATTA
Chd8_CDS_7749.676	TCAATGAACAGATTAGGGTC
Chd8_CDS_7749.677	ATGAACAGATTAGGGTCTGG
Chd8_CDS_7749.68	AGTAGTAACTATTCAGCTGC
Chd8_CDS_7749.682	CATCACCAGCAGCTGGGGGA
Chd8_CDS_7749.683	CACCAGCAGCTGGGGGAAGG
Chd8_CDS_7749.684	GCGGCACACTTGTCGACACA
Chd8_CDS_7749.685	GACACATGGCCACAAAACCA
Chd8_CDS_7749.686	CACAAAACCATGGAAGTACT
Chd8_CDS_7749.687	AACCATGGAAGTACTTGGTA
Chd8_CDS_7749.688	TTTCATCTGTTTTTTGTCC
Chd8_CDS_7749.689	TGTCCAGGCGAGCAAAAGTG
Chd8_CDS_7749.69	GACCCTGTCTCTGTGCAGC
Chd8_CDS_7749.690	CAGTGAAACTGCATGTTGTC
Chd8_CDS_7749.691	AGTGAAACTGCATGTTGTCA
Chd8_CDS_7749.692	AGGGTCATACTCCACACCAA
Chd8_CDS_7749.693	CACCAAAGGTAGATACTACT
Chd8_CDS_7749.694	TGCGATTCTTTGAGCTTAA
Chd8_CDS_7749.695	TAAAGGCTGCTCACATCGT
Chd8_CDS_7749.696	CTTCACATCGTCGGCGTCTC
Chd8_CDS_7749.697	TCTCTGTAGCTGCGTTGAT
Chd8_CDS_7749.698	TGCGTTGATAGGCTGTTACT
Chd8_CDS_7749.699	GTTGATAGGCTGTTACTAGG
Chd8_CDS_7749.7	GATCAGATGAACCAAGATGG
Chd8_CDS_7749.70	TGTGCAGCAGGCTCAGATAA
Chd8_CDS_7749.700	GCGGCGAAGCCTAGCTGTG
Chd8_CDS_7749.701	GCGGCGAAGCCTAGCTGTGA
Chd8_CDS_7749.702	GCGAAGCCTAGCTGTGAGGG
Chd8_CDS_7749.703	CTAGCTGTGAGGGCGGAGCC
Chd8_CDS_7749.704	GCTGTGAGGGCGGAGCCTGG
Chd8_CDS_7749.705	GGAGGCCAGAATAAATGCC
Chd8_CDS_7749.706	GCCCTGGCTGTTGAGTTACC
Chd8_CDS_7749.707	CCCTGGCTGTTGAGTTACCT
Chd8_CDS_7749.708	CTCCTCATCCATCATCATCA
Chd8_CDS_7749.709	TCCTCATCCATCATCATCAA
Chd8_CDS_7749.71	GTGCAGCAGGCTCAGATAAT
Chd8_CDS_7749.713	TCATCATCTGGGTCCTTTGG

Chd8_CDS_7749.714	CTGGGTCCTTTGGAGGACCC
Chd8_CDS_7749.715	GGTCCTTTGGAGGACCCTGG
Chd8_CDS_7749.716	GTCCTTTGGAGGACCCTGGA
Chd8_CDS_7749.717	TCCTTTGGAGGACCCTGGAG
Chd8_CDS_7749.718	CCCTGGAGGGGTTTATATTC
Chd8_CDS_7749.72	TGCAGCAGGCTCAGATAATG
Chd8_CDS_7749.721	CACTCTATGTTCTGCTGCGA
Chd8_CDS_7749.722	GCTGCGATGGCTTTGTGATC
Chd8_CDS_7749.723	CTGGCCTGCCAGCCTTTTCT
Chd8_CDS_7749.724	AGCCTTTTCTAGGAAGCACA
Chd8_CDS_7749.725	TTTTCTAGGAAGCACAAGGC
Chd8_CDS_7749.726	TTTTCTAGGAAGCACAAGGCA
Chd8_CDS_7749.727	CAAGGCAGGGTCTGCCCTCA
Chd8_CDS_7749.728	GCTTAAAAACGCCAATGAGC
Chd8_CDS_7749.729	CTTAAAAACGCCAATGAGCA
Chd8_CDS_7749.73	CAGGCTCAGATAATGGGGCC
Chd8_CDS_7749.730	TCACTATCCCACCAAGTTGT
Chd8_CDS_7749.731	ACCTCCAGCTGATCCACCAC
Chd8_CDS_7749.732	CCTCCAGCTGATCCACCACT
Chd8_CDS_7749.735	CTCCTAACACCTTCTCTGCC
Chd8_CDS_7749.736	CTCCAATAACCTCCTGTCTC
Chd8_CDS_7749.737	GTCTCAGGTAGTAGAGCATC
Chd8_CDS_7749.738	GCTTCTTATAACTCTCATCT
Chd8_CDS_7749.739	TCATCTTGGAACAGAGTATC
Chd8_CDS_7749.74	ATGGGGCCAGGCCAAAACCC
Chd8_CDS_7749.740	CATCTTGGAACAGAGTATCA
Chd8_CDS_7749.741	GAGTATCAGGGTTGTATTC
Chd8_CDS_7749.742	CTTTTTTCCCCTTACGCCCA
Chd8_CDS_7749.743	TTTTTTCCCCTTACGCCCAC
Chd8_CDS_7749.744	TTTTTTCCCCTTACGCCACG
Chd8_CDS_7749.745	CCCTTACGCCACGGGGCAC
Chd8_CDS_7749.746	CCTTACGCCACGGGGCACA
Chd8_CDS_7749.747	TTTGTCTTGCCATTTTCAGC
Chd8_CDS_7749.748	TTGTCTTGCCATTTTCAGCA
Chd8_CDS_7749.749	TTTTGATGTTTTTCATCCCA
Chd8_CDS_7749.75	TGGGGCCAGGCCAAAACCCA
Chd8_CDS_7749.750	AGTGTAGAAGACAGTACACG
Chd8_CDS_7749.751	TAGAAGACAGTACACGAGGA
Chd8_CDS_7749.752	GACAGTACACGAGGATGGCA
Chd8_CDS_7749.754	CCAGGAGATGCTTTTCTACC
Chd8_CDS_7749.755	GAAGCAGTCAGTGCGCCCAT
Chd8_CDS_7749.756	TGCGCCCATAGGTGTGATGC
Chd8_CDS_7749.757	TGTGATGCCGGTCATGTCTT
Chd8_CDS_7749.758	GTGATGCCGGTCATGTCTTC
Chd8_CDS_7749.759	CGGTCATGTCTTCGGGAACG
Chd8_CDS_7749.76	ACTTTCTGTACCGTCAAGA
Chd8_CDS_7749.760	CCAAATCAGAAAACCAACC
Chd8_CDS_7749.761	CGAGTCTGTTCCGAACCTCG
Chd8_CDS_7749.762	TATTCAGCAGATCCATGTCT
Chd8_CDS_7749.763	CATGTCTAGGTCTGCCTTTT
Chd8_CDS_7749.764	GCCCATTTTTGCCAAAAGTT
Chd8_CDS_7749.768	CCCTTCAGACTCAATAGTGA
Chd8_CDS_7749.769	AGACTCAATAGTGATGGTTG
Chd8_CDS_7749.77	CAAGATGGTGCTGCAGCCAC
Chd8_CDS_7749.770	CTCATCGTCTTCTCCATTA
Chd8_CDS_7749.771	TTCCTCCATTATGGCCGCAT
Chd8_CDS_7749.773	GTTGCCATCCCACCCTCA

Chd8_CDS_7749.774	CTTTATCCAATCCCAACTTG
Chd8_CDS_7749.775	ATCAAACATCTCTCTCAT
Chd8_CDS_7749.776	AGGAATTACGAGTGATGAGT
Chd8_CDS_7749.777	CAATTCGATGACAACGTGCT
Chd8_CDS_7749.778	AATTCGATGACAACGTGCTT
Chd8_CDS_7749.781	GTCTGAATCAAAGATAATAC
Chd8_CDS_7749.782	TAATACCAAGTCCACCAGCA
Chd8_CDS_7749.783	AATACCAAGTCCACCAGCAC
Chd8_CDS_7749.784	TACATAGCAAGAAGACAAAG
Chd8_CDS_7749.786	CTGAGTCAGGCTTGCTAAAG
Chd8_CDS_7749.787	GGTCGATAGCAGCTTGTCTGA
Chd8_CDS_7749.789	TGTCTAGACAGCGTACCATC
Chd8_CDS_7749.790	GTCTAGACAGCGTACCATCT
Chd8_CDS_7749.791	GGGAGAAGATCAGAACTTTA
Chd8_CDS_7749.792	TGGCCACCAGCTTTAAGCTT
Chd8_CDS_7749.793	CTGACCGAACCATAGCCTGC
Chd8_CDS_7749.794	ACCGAACCATAGCCTGCAGG
Chd8_CDS_7749.795	GCCTGCAGGTGGAAATCTTG
Chd8_CDS_7749.796	GGAAATCTTGAGGTATAATA
Chd8_CDS_7749.797	AAGCTTCCCGAAATTCATC
Chd8_CDS_7749.8	CAGATGAACCAAGATGGTGG
Chd8_CDS_7749.801	ATCATTGTGTTCAAGTAGATT
Chd8_CDS_7749.802	GTTCAGTAGATTAGGCATAT
Chd8_CDS_7749.803	ATTGGTATGACCTGCCCTT
Chd8_CDS_7749.804	TATGACCTGCCCTTTGGAA
Chd8_CDS_7749.805	ACCTGCCCTTTGGAAAGGA
Chd8_CDS_7749.806	TAGCTCTGTAGTATTTCTTC
Chd8_CDS_7749.807	GTAGTATTTCTTCTGGATGT
Chd8_CDS_7749.808	TTCAATAATAGTTTCCTGTT
Chd8_CDS_7749.809	TCAATAATAGTTTCCTGTTT
Chd8_CDS_7749.81	TCTTCTCAGGGAGCCTCTTC
Chd8_CDS_7749.810	TTGAGTCTCCTCAGCATCAT
Chd8_CDS_7749.811	CAGCATCATTGGCTTTAGAA
Chd8_CDS_7749.813	TGAGATCCCCAAAATCCTTA
Chd8_CDS_7749.814	CTTAAGGAATTCTGATTCTG
Chd8_CDS_7749.815	TTAAGGAATTCTGATTCTGA
Chd8_CDS_7749.816	TAAGGAATTCTGATTCTGAG
Chd8_CDS_7749.817	GATTCTGAGGGGAAGTCTGAGA
Chd8_CDS_7749.818	TAGACTGAACAGTTCCCTCTA
Chd8_CDS_7749.819	TCCTCTACGGTATTTTGTA
Chd8_CDS_7749.821	TATCAAGTAGCTTGCAATTA
Chd8_CDS_7749.822	AATTACGGTTCTTCAGCCTA
Chd8_CDS_7749.823	ATTACGGTTCTTCAGCCTAT
Chd8_CDS_7749.824	CATTCAATTTACGAAGCTC
Chd8_CDS_7749.825	TGACAAAATCATCTCAAAG
Chd8_CDS_7749.826	CATCTCAAAGTGGTGATCA
Chd8_CDS_7749.827	GCATCAAACCTATATGCACC
Chd8_CDS_7749.828	CATCAAACCTATATGCACCA
Chd8_CDS_7749.829	ACTTATATGCACCAGGGATG
Chd8_CDS_7749.83	AGTTCTAAGTGCCAGTGAAG
Chd8_CDS_7749.830	TACAGTACATTTCATACTGC
Chd8_CDS_7749.831	CATACTGCTGGATCATCTGC
Chd8_CDS_7749.832	CTGCTGGATCATCTGCCGGC
Chd8_CDS_7749.833	GGATCATCTGCCGGCTGGCC
Chd8_CDS_7749.834	GCCGGCTGGCCAGGCTGCCA
Chd8_CDS_7749.835	TTCACGCTCCCAGTTAGTAA
Chd8_CDS_7749.836	ACGCTCCCAGTTAGTAATGG

Chd8_CDS_7749.837	CAGTTAGTAATGGTGGACAA
Chd8_CDS_7749.838	CAATGGAGCAATGACCAAAA
Chd8_CDS_7749.839	AATGGAGCAATGACCAAAA
Chd8_CDS_7749.84	AGCTGTGCCCTCATACTGC
Chd8_CDS_7749.840	CAATGACCAAAAAGGGACCA
Chd8_CDS_7749.841	ATTATATACCTCCTGCAAGA
Chd8_CDS_7749.842	CCAATCCCATTTCATCAGCC
Chd8_CDS_7749.844	CTAACTGATATCCCCTAAT
Chd8_CDS_7749.845	TGATAACTCCAATTTCTTCC
Chd8_CDS_7749.846	TTCTTCCAGGCATTTGCCTG
Chd8_CDS_7749.849	TCAGTTCTGGGTGCCTTGAC
Chd8_CDS_7749.85	GCTGTGCCCTCATACTGCA
Chd8_CDS_7749.850	CTCCCACGTAAGTCTCAT
Chd8_CDS_7749.851	TCCCACGTAAGTCTCATA
Chd8_CDS_7749.852	GCAGAGAGCACCATTTTACC
Chd8_CDS_7749.853	TTTACCAGGTAGTAAATTAC
Chd8_CDS_7749.854	CTATCCACCTCTACGTAGTC
Chd8_CDS_7749.855	TCTACGTAGTCTGGATTGAA
Chd8_CDS_7749.856	TTTTGAACCGTTTTAGTTTC
Chd8_CDS_7749.857	TGAACCGTTTTAGTTCTGG
Chd8_CDS_7749.858	TCCTCTATCCTTCTCCAGC
Chd8_CDS_7749.859	CCTCTTATCCTTCTCCAGCT
Chd8_CDS_7749.86	CCTCATACTGCAGGGAAGAC
Chd8_CDS_7749.860	GCCTCAGTGTATTGTCCAGA
Chd8_CDS_7749.861	CTCTTTCTTCACAACCTCGCA
Chd8_CDS_7749.862	ATAGCTGCATCTTCTTCACT
Chd8_CDS_7749.865	GAAGGAAGAGTCTCGCCATC
Chd8_CDS_7749.866	TCGCCATCAGGCTCTTGAC
Chd8_CDS_7749.867	TCAGGCTCTTGCACTGGTTC
Chd8_CDS_7749.868	CAGGCTCTTGCACTGGTTCT
Chd8_CDS_7749.869	GCTCTTGCACTGGTTCTGGG
Chd8_CDS_7749.87	CTCATACTGCAGGGAAGACT
Chd8_CDS_7749.870	TTGCACTGGTTCTGGGAGGA
Chd8_CDS_7749.871	TGCACTGGTTCTGGGAGGAT
Chd8_CDS_7749.872	TGGTTCTGGGAGGATGGGCT
Chd8_CDS_7749.873	GGTTCTGGGAGGATGGGCTC
Chd8_CDS_7749.874	AGGATGGGCTCGGGTTTTAT
Chd8_CDS_7749.875	CGTCTGTTATCTTTATATCC
Chd8_CDS_7749.876	TATATTTTTTTCGCTTAACT
Chd8_CDS_7749.877	ATTTTTTTCGCTTAACTTGG
Chd8_CDS_7749.879	TGCTGCTCTCTCGTCTCC
Chd8_CDS_7749.88	TACTGCAGGGAAGACTGGGA
Chd8_CDS_7749.880	GCTGCTCTCTCGTCTCCC
Chd8_CDS_7749.881	CTGCTCTCTCGTCTCCC
Chd8_CDS_7749.882	TCCTCCCGGGCGATTGTGC
Chd8_CDS_7749.883	TTTCTCTCTTGCCACTAC
Chd8_CDS_7749.884	CTTGCCCACTACAGGAGTGA
Chd8_CDS_7749.885	CTTACTCTTGCCCTTCGTTT
Chd8_CDS_7749.886	ACTCTTGCCCTTCGTTTGG
Chd8_CDS_7749.887	GCAGCAGTCTTGCTCTTCTT
Chd8_CDS_7749.888	TTCTTTTACCCTCCTCCTC
Chd8_CDS_7749.889	TTTACCCTCCTCCTCCTGGC
Chd8_CDS_7749.890	TCCTCCTCTGGCCGGACT
Chd8_CDS_7749.891	TAGGCAGCTCATCCTCATC
Chd8_CDS_7749.892	TCATCCTCATTGAGGACTCG
Chd8_CDS_7749.893	AGGTATGTTTTGCTCGCCCC
Chd8_CDS_7749.894	TGTTTTGCTCGCCCCCTGGCC

Chd8_CDS_7749.895	GTTTTGCTCGCCCCTGGCCC
Chd8_CDS_7749.896	CCTGGCCCGGGCCCTAGCAA
Chd8_CDS_7749.898	TTTTCTGGTGCTCCAACCTG
Chd8_CDS_7749.899	CCAGTCTTCCCTGCAGTATG
Chd8_CDS_7749.9	ATGAACCAAGATGGTGGAGG
Chd8_CDS_7749.90	CTGGGATGGAGGAGAACC GC
Chd8_CDS_7749.900	CAGTCTTCCCTGCAGTATGA
Chd8_CDS_7749.901	AGTCTTCCCTGCAGTATGAG
Chd8_CDS_7749.902	GTATGAGGGGCACAGCTTGC
Chd8_CDS_7749.903	TATGAGGGGCACAGCTTGCT
Chd8_CDS_7749.904	ATGAGGGGCACAGCTTGCTG
Chd8_CDS_7749.905	CACAGCTTGCTGGGGATGAC
Chd8_CDS_7749.906	ACAGCTTGCTGGGGATGACA
Chd8_CDS_7749.907	TGACAGGGCTGCCACTTAC
Chd8_CDS_7749.908	AACCACAGAGAGTCCAGAAG
Chd8_CDS_7749.91	GATGGAGGAGAACC GCAGGT
Chd8_CDS_7749.910	GGCTGCAGCACCATCTTGAG
Chd8_CDS_7749.911	GGTACAGAAAGTCTTGCCC
Chd8_CDS_7749.912	GTACAGAAAGTCTTGCCCT
Chd8_CDS_7749.913	AAAGTCTTGCCCTGGGTTT
Chd8_CDS_7749.914	CTCTGCCCTGGGTTTTGGCC
Chd8_CDS_7749.915	TATCTGAGCCTGCTGCACAG
Chd8_CDS_7749.916	GAGCCTGCTGCACAGAGGAC
Chd8_CDS_7749.917	AGCCTGCTGCACAGAGGACA
Chd8_CDS_7749.918	TGCACAGAGGACAGGGTCAA
Chd8_CDS_7749.919	CAGAGGACAGGGTCAACGGC
Chd8_CDS_7749.920	AGAGGACAGGGTCAACGGCT
Chd8_CDS_7749.921	CAGGGTCAACGGCTGGGCTG
Chd8_CDS_7749.922	AGGGTCAACGGCTGGGCTGA
Chd8_CDS_7749.923	GTCAACGGCTGGGCTGAGGG
Chd8_CDS_7749.924	AACGGCTGGGCTGAGGGTGG
Chd8_CDS_7749.925	TGGGCTGAGGGTGGCGGCTG
Chd8_CDS_7749.926	GAGGGTGGCGGCTGCGGCTG
Chd8_CDS_7749.928	TGTGGCTGTGGTTGTGATGA
Chd8_CDS_7749.929	GGCTGTGGTTGTGATGATGG
Chd8_CDS_7749.93	AGAGAAAGCAAATCGGATTG
Chd8_CDS_7749.930	GGTTGTGATGATGGAGGCTG
Chd8_CDS_7749.931	ATGGAGGCTGAGGTACAATC
Chd8_CDS_7749.932	ACAATCTGGATTTTCTGCTG
Chd8_CDS_7749.933	CAGCTGAATAGTTACTACTT
Chd8_CDS_7749.934	TGAATAGTTACTACTTTGGC
Chd8_CDS_7749.935	CTACTTTGGCAGGCTGCCCC
Chd8_CDS_7749.936	TACTTTGGCAGGCTGCCCCCT
Chd8_CDS_7749.937	AGGCTGCCCTGGGCATTCT
Chd8_CDS_7749.938	GGCATTCTTGGCTTGAGTCA
Chd8_CDS_7749.939	CTTGAGTCAAGGCTGCTAGC
Chd8_CDS_7749.94	AGCAAATCGGATTGTGGCAG
Chd8_CDS_7749.940	CCCTGTAACACTATCTTGCC
Chd8_CDS_7749.941	ACACAACATGCCGATGTCCT
Chd8_CDS_7749.942	CACAACATGCCGATGTCCTT
Chd8_CDS_7749.943	ACAACATGCCGATGTCCTTG
Chd8_CDS_7749.944	CCGATGTCCTTGGGGACCTC
Chd8_CDS_7749.945	CCTTGGGGACCTCCGACTG
Chd8_CDS_7749.946	CTCCGACTGTGGCTGTTGA
Chd8_CDS_7749.95	TTGTGGCAGAGGCCATTGCT
Chd8_CDS_7749.950	GTAGACGTCAAGTGAACCTGC
Chd8_CDS_7749.951	AGTGTAACCTGCAGGCTTCAG

Chd8_CDS_7749.952	GTGTAAGTGCAGGCTTCAGT
Chd8_CDS_7749.953	TGTAAGTGCAGGCTTCAGTG
Chd8_CDS_7749.954	GTAAGTGCAGGCTTCAGTGG
Chd8_CDS_7749.955	TGCAGGCTTCAGTGGGGGCC
Chd8_CDS_7749.956	AGTGGGGGCCCGGCAGCCCC
Chd8_CDS_7749.957	GCAGCCCCAGGATTCCCAGC
Chd8_CDS_7749.958	GCAGGAGCTGAACCCTTTAC
Chd8_CDS_7749.959	GAGCTGAACCCTTTACTGGC
Chd8_CDS_7749.96	TGTGGCAGAGGCCATTGCTA
Chd8_CDS_7749.960	CTGAACCCTTTACTGGCTGG
Chd8_CDS_7749.961	TGGAGGACCAGCTGTTTTAC
Chd8_CDS_7749.962	GGACCAGCTGTTTTACTGGT
Chd8_CDS_7749.963	AGCTGTTTTACTGGTCGGCT
Chd8_CDS_7749.964	GTTTTACTGGTCGGCTTGGC
Chd8_CDS_7749.965	CAATGCGCTGAACAGCAGCC
Chd8_CDS_7749.966	TGAACAGCAGCCTGGTTCCC
Chd8_CDS_7749.967	GAACAGCAGCCTGGTTCCCA
Chd8_CDS_7749.968	CTGGTCCCAGGGACCTTCG
Chd8_CDS_7749.969	CACTGTATTACCAGAGACAA
Chd8_CDS_7749.97	CAGAGGCCATTGCTAGGGCC
Chd8_CDS_7749.970	CCAGAGACAATGGATACACC
Chd8_CDS_7749.971	CAATGGATACACCTGGTCGA
Chd8_CDS_7749.972	AATGGATACACCTGGTCGAA
Chd8_CDS_7749.973	ATGGATACACCTGGTCGAAG
Chd8_CDS_7749.974	GGGTGTACCAGTCAGCACTT
Chd8_CDS_7749.975	AAAAGTACTTTCCACCGT
Chd8_CDS_7749.976	CGTTGGCTGTCCCAGCCACT
Chd8_CDS_7749.977	GTTGGCTGTCCCAGCCACTA
Chd8_CDS_7749.978	TTGGCTGTCCCAGCCACTAG
Chd8_CDS_7749.979	CACTAGGGGCTGAGCTGTAC
Chd8_CDS_7749.98	AGAGGCCATTGCTAGGGCCC
Chd8_CDS_7749.980	GAGCTGTACTGGTGATACCT
Chd8_CDS_7749.981	AGCTGTACTGGTGATACCTT
Chd8_CDS_7749.982	GGGCCTGAATTTGTGCCACA
Chd8_CDS_7749.983	GGCCTGAATTTGTGCCACAT
Chd8_CDS_7749.984	TGCCACATGGGTGCCTGTGA
Chd8_CDS_7749.985	CACATGGGTGCCTGTGACGG
Chd8_CDS_7749.986	GTGCCTGTGACGGAGGAGTT
Chd8_CDS_7749.987	CCTGTGACGGAGGAGTTTGG
Chd8_CDS_7749.988	GCTTTAAGAATAACAATCTT
Chd8_CDS_7749.989	ATCTTAGGAGCTGACTGAGA
Chd8_CDS_7749.99	CCATTGCTAGGGCCCCGGGCC
Chd8_CDS_7749.990	TGGTTGCTCCTCCAGTATTAC
Chd8_CDS_7749.991	GGTTGCTCCTCCAGTATTACT
Chd8_CDS_7749.992	GTTGCTCCTCCAGTATTACTG
Chd8_CDS_7749.993	TTGCTCCTCCAGTATTACTGG
Chd8_CDS_7749.994	ATTACTGGGGGAGACACCTG
Chd8_CDS_7749.995	GTGGCAGAGACACCCATGAA
Chd8_CDS_7749.996	CACCCATGAAAAGGATTCCCT
Chd8_CDS_7749.997	TCCCTTGGCTCAAGATCTCC
Chd8_CDS_7749.998	GCTCAAGATCTCCTGGCTCT
Chd8_CDS_7749.999	ACCTGCAAGAGTCTCTGCTGT
	Nsd3 sgRNAs for CRIRPR scan
Nsd3s_CDS_81.0	GTCGCGGACCGAGGAGCGC
Nsd3s_CDS_81.1	TCGCGGACCGAGGAGCGCA
Nsd3s_CDS_81.6	TGACAGAGCCCTGCGCTCCT
Nsd3_CDS_4341.0	TTCTCTTCTCTTCATGCA

Nsd3_CDS_4341.2	CTCTTTCATGCAAGGGATCA
Nsd3_CDS_4341.3	TCTTTCATGCAAGGGATCAT
Nsd3s_CDS_81.5	TTCCTCTTTCGCTCGGAGGA
Nsd3s_CDS_81.2	CTCCGTCTCCGCAGCGAAAG
Nsd3s_CDS_81.4	CACAGTTTCTCTTTCGCTG
Nsd3_CDS_4341.540	GCCGAGTCAATGAGTTGAGG
Nsd3_CDS_4341.539	TTGGCCGAGTCAATGAGTTG
Nsd3_CDS_4341.4	ACCACCTCAACTCATTGACT
Nsd3s_CDS_81.3	CGCAGCGAAAGAGGAAACTG
Nsd3_CDS_4341.5	TGACTCGGCAACATCCGCC
Nsd3_CDS_4341.538	GGCATCCTCCTGGCGGATGT
Nsd3_CDS_4341.6	CTCGGCCAACATCCGCCAGG
Nsd3_CDS_4341.537	TATCAAAGGCATCCTCCTGG
Nsd3_CDS_4341.536	GGTTATCAAAGGCATCCTCC
Nsd3_CDS_4341.535	AATGTCACTGTGGTTATCAA
Nsd3_CDS_4341.534	CATCTTCAACAATGTCACTG
Nsd3_CDS_4341.7	CACAGTGACATTGTTGAAGA
Nsd3_CDS_4341.8	AGTGACATTGTTGAAGATGG
Nsd3_CDS_4341.533	AAGTAGCTTCAAAGGGTGTC
Nsd3_CDS_4341.532	AAAGTAGCTTCAAAGGGTGT
Nsd3_CDS_4341.531	TGTTGCAAAGTAGCTTCAA
Nsd3_CDS_4341.530	TTGTTGCAAAGTAGCTCAA
Nsd3_CDS_4341.9	TTTGAAGCTACTTTGCAACA
Nsd3_CDS_4341.529	GGAAGGTCTTCTGTTGTAGG
Nsd3_CDS_4341.528	GGAGGAAGGTCTTCTGTTGT
Nsd3_CDS_4341.527	AGCCATTTGTGAGCGGAGGA
Nsd3_CDS_4341.10	GACCTTCTCCGCTCACAAA
Nsd3_CDS_4341.526	GGGTAGCCATTTGTGAGCGG
Nsd3_CDS_4341.525	GGTGGGTAGCCATTTGTGAG
Nsd3_CDS_4341.524	CATACAAGCTGATTGATGGT
Nsd3_CDS_4341.523	TCATACAAGCTGATTGATGG
Nsd3_CDS_4341.522	GTTTCATACAAGCTGATTGA
Nsd3_CDS_4341.521	CTGATTATATGGCGGGTATT
Nsd3_CDS_4341.520	TGGGATACTGATTATATGGC
Nsd3_CDS_4341.519	TTGGGATACTGATTATATGG
Nsd3_CDS_4341.518	CCATTGGGATACTGATTATA
Nsd3_CDS_4341.11	CCATATAATCAGTATCCCAA
Nsd3_CDS_4341.12	CATATAATCAGTATCCCAAT
Nsd3_CDS_4341.517	AAACCGTTGGCTGACCCATT
Nsd3_CDS_4341.516	AAAACCGTTGGCTGACCCAT
Nsd3_CDS_4341.13	TATCCCAATGGGTCAGCCAA
Nsd3_CDS_4341.14	AATGGGTCAGCCAACGGTTT
Nsd3_CDS_4341.515	TCTAACTGCACCAAAACCGT
Nsd3_CDS_4341.514	CTGAATGGTAATAGTCAGTA
Nsd3_CDS_4341.513	TCTGAATGGTAATAGTCAGT
Nsd3_CDS_4341.512	TTGTGTTGGAATTTCTGAA
Nsd3_CDS_4341.511	ATTTTCATGTGGTCTTGTGTT
Nsd3_CDS_4341.15	CACAAGACCACATGAAATTC
Nsd3_CDS_4341.510	GGTTTTTCCAGAATTCATG
Nsd3_CDS_4341.496	TGTGGTACCGAAGGAGGAGG
Nsd3_CDS_4341.495	GTTTGTGGTACCGAAGGAGG
Nsd3_CDS_4341.494	ACAGTTTGTGGTACCGAAGG
Nsd3_CDS_4341.493	ATCACAGTTTGTGGTACCGA
Nsd3_CDS_4341.17	ACTGTGATTCCAAAGAAGAC
Nsd3_CDS_4341.491	TCGGGTGAGCCTGTCTTCTT
Nsd3_CDS_4341.490	GTTATTTTGTAGTTTAACTC
Nsd3_CDS_4341.489	GGTTATTTTGTAGTTTAACTC

Nsd3_CDS_4341.488	CCTGCCATTCTGGATAGTTT
Nsd3_CDS_4341.18	ATAACCAAACTATCCAGAA
Nsd3_CDS_4341.19	CCAAAATATCCAGAATGGC
Nsd3_CDS_4341.20	CAAAAATATCCAGAATGGCA
Nsd3_CDS_4341.487	CAAACAATTCCCTGCCATTC
Nsd3_CDS_4341.21	TTGTTTGAGTCTTCCCTTTG
Nsd3_CDS_4341.486	ATTTAAGAGGTCTCCACAAA
Nsd3_CDS_4341.485	CATTTAAGAGGTCTCCACAA
Nsd3_CDS_4341.484	TTGCCTGTACTTCATTTAAG
Nsd3_CDS_4341.22	AGACCTCTTAAATGAAGTAC
Nsd3_CDS_4341.23	GTCTAAGCATGAAAGCAGAA
Nsd3_CDS_4341.25	AGTCATCTCGATCCGAAGAG
Nsd3_CDS_4341.26	CATCTCGATCCGAAGAGCGG
Nsd3_CDS_4341.483	CTTGTGTGACCTCCGCTCTT
Nsd3_CDS_4341.27	CAAGATTCCCAAGCTAGAGC
Nsd3_CDS_4341.482	TGTCCCTCCGGCTCTAGCTT
Nsd3_CDS_4341.28	GATTTCCAAGCTAGAGCCGG
Nsd3_CDS_4341.481	CTGTCCCTCCGGCTCTAGCT
Nsd3_CDS_4341.29	ATTCCAAGCTAGAGCCGGA
Nsd3_CDS_4341.479	GCAGTGTCCACCCTCTCATT
Nsd3_CDS_4341.478	GGCTCTTCTTTGGCTTCTC
Nsd3_CDS_4341.477	TTGAGCACTGGCTCTTCTCT
Nsd3_CDS_4341.33	AGAAGAGCCAGTGCTCAAAG
Nsd3_CDS_4341.476	GGGATGGCCTCTTTGAGCAC
Nsd3_CDS_4341.34	AGTGCTCAAAGAGGCCATCC
Nsd3_CDS_4341.472	GTTGGAACAGAAGACAGTAT
Nsd3_CDS_4341.471	CCAGTGGATGTTTCTGTGTG
Nsd3_CDS_4341.35	CCAACAACAGAAACATCCAC
Nsd3_CDS_4341.470	AACCTGGAACCTAACACCAG
Nsd3_CDS_4341.36	ATCCACTGGTGTTAAGTTCC
Nsd3_CDS_4341.37	ACTGGTGTTAAGTTCCAGGT
Nsd3_CDS_4341.469	ACCAAACAAGATCACCAACC
Nsd3_CDS_4341.38	TCCAGGTTGGTGATCTTGTT
Nsd3_CDS_4341.39	TGGTGATCTTGTTTGGTCCA
Nsd3_CDS_4341.40	TGATCTTGTTTGGTCCAAGG
Nsd3_CDS_4341.41	GATCTTGTTTGGTCCAAGGT
Nsd3_CDS_4341.468	CCAAGGGTAGGTTCCACCT
Nsd3_CDS_4341.42	CCAAGGTGGGAACCTACCCT
Nsd3_CDS_4341.43	AGGTGGGAACCTACCCTTGG
Nsd3_CDS_4341.467	CATACAAGGCCACCAAGGGT
Nsd3_CDS_4341.466	AAACCATACAAGGCCACCAA
Nsd3_CDS_4341.465	GAAACCATACAAGGCCACCA
Nsd3_CDS_4341.44	CTACCCTTGGTGGCCTTGTA
Nsd3_CDS_4341.464	GGATCACTTGAAACCATACA
Nsd3_CDS_4341.45	TTCAAGTGATCCCCAGCTTG
Nsd3_CDS_4341.463	TTGGAATGGACCTCAAGCTG
Nsd3_CDS_4341.462	TTTGGAAATGGACCTCAAGCT
Nsd3_CDS_4341.461	TTTTGGAATGGACCTCAAGC
Nsd3_CDS_4341.460	CTCTTGTTGTTAATTTGGAA
Nsd3_CDS_4341.46	CATTCCAAAATTAACACAAG
Nsd3_CDS_4341.458	AAATTGGACATGATATTCCC
Nsd3_CDS_4341.456	CTGGCTGGTTGCTAAAAAAT
Nsd3_CDS_4341.49	TTTTTAGCAACCAGCCAGAG
Nsd3_CDS_4341.50	TTTTAGCAACCAGCCAGAGA
Nsd3_CDS_4341.455	GAACCCATGCCCTCTCTGGC
Nsd3_CDS_4341.51	GCAACCAGCCAGAGAGGGCA
Nsd3_CDS_4341.52	CAACCAGCCAGAGAGGGCAT

Nsd3_CDS_4341.454	TCATGAACCCATGCCCTCTC
Nsd3_CDS_4341.53	GGGCATGGGTTTCATGAGAAA
Nsd3_CDS_4341.54	GGCATGGGTTTCATGAGAAAC
Nsd3_CDS_4341.55	GGGTTTCATGAGAAACGGGTA
Nsd3_CDS_4341.56	GGTTCATGAGAAACGGGTAC
Nsd3_CDS_4341.57	AAACGGGTACGGGAATACAA
Nsd3_CDS_4341.58	GTATGAAGAGTTACTAGCCG
Nsd3_CDS_4341.453	GCTGGCTTGCTTGGCTGCCT
Nsd3_CDS_4341.452	AGAATGATTGCTGGCTTGCT
Nsd3_CDS_4341.451	TTGCTTTTCAGAATGATTGC
Nsd3_CDS_4341.450	GCACGTTCTCTCTGAGGTCG
Nsd3_CDS_4341.449	GGCACGTTCTCTCTGAGGTC
Nsd3_CDS_4341.448	GGGCACGTTCTCTCTGAGGT
Nsd3_CDS_4341.447	CATTGGGCACGTTCTCTCTG
Nsd3_CDS_4341.60	CTCAGAGAGAACGTGCCCAA
Nsd3_CDS_4341.61	TCAGAGAGAACGTGCCCAAT
Nsd3_CDS_4341.62	GAACGTGCCCAATGGGACAT
Nsd3_CDS_4341.446	AGCAATGCCAATGTCCCATT
Nsd3_CDS_4341.445	GAGCAATGCCAATGTCCCAT
Nsd3_CDS_4341.63	AGAAAGCATTGAAAATGACT
Nsd3_CDS_4341.64	GAAAGCATTGAAAATGACTC
Nsd3_CDS_4341.65	AGCATTGAAAATGACTCGGG
Nsd3_CDS_4341.66	CATTGATAAGCAGCCAGAAG
Nsd3_CDS_4341.444	GCTTGGGACGAAGCCTCTTC
Nsd3_CDS_4341.443	GGTAACATTCTTCTTTGCTT
Nsd3_CDS_4341.442	AGGTAACATTCTTCTTTGCT
Nsd3_CDS_4341.67	GAAGAATGTACCTCTAAGA
Nsd3_CDS_4341.441	TTTCTTGACTTCCGCTTAG
Nsd3_CDS_4341.440	AGCACAGATCTTGGTCTTCG
Nsd3_CDS_4341.439	CAGCACAGATCTTGGTCTTC
Nsd3_CDS_4341.438	TCAGCACAGATCTTGGTCTT
Nsd3_CDS_4341.436	TCCCCAGCATTGGTCTGTTC
Nsd3_CDS_4341.68	CAGCCAGAACAGACCAATGC
Nsd3_CDS_4341.69	AGCCAGAACAGACCAATGCT
Nsd3_CDS_4341.70	GCCAGAACAGACCAATGCTG
Nsd3_CDS_4341.71	AGAACAGACCAATGCTGGGG
Nsd3_CDS_4341.435	GGAGGCCACCTCCCCAGCAT
Nsd3_CDS_4341.72	ACAGACCAATGCTGGGGAGG
Nsd3_CDS_4341.434	GTCAGTACTTGATTGTGAGG
Nsd3_CDS_4341.433	AAGGTCAGTACTTGATTGTG
Nsd3_CDS_4341.73	AATCAAGTACTGACCTTCGA
Nsd3_CDS_4341.432	GCCTCTGGCTCTGCCTTCGA
Nsd3_CDS_4341.74	ACCTTCGAAGGCAGAGCCAG
Nsd3_CDS_4341.431	CCAAGCTAGTATGCCGCCTC
Nsd3_CDS_4341.76	CCAGAGGCGGCATACTAGCT
Nsd3_CDS_4341.77	GCGGCATACTAGCTTGGAAG
Nsd3_CDS_4341.430	CAGGCGATTTTAACAGGAGG
Nsd3_CDS_4341.429	TTCCAGCGATTTTAACAGG
Nsd3_CDS_4341.428	GTTTTCCAGGCGATTTTAAC
Nsd3_CDS_4341.78	CACCTCCTGTAAAAATCGCC
Nsd3_CDS_4341.427	CCTTGCGGCTGCTGTTTTCC
Nsd3_CDS_4341.79	CCTGGAACAGCAGCCGCA
Nsd3_CDS_4341.426	GGCTGGTAAGGACTTCCTTG
Nsd3_CDS_4341.425	CATTGTGATGGAGGCTGGTA
Nsd3_CDS_4341.424	TTGTGCATTGTGATGGAGGC
Nsd3_CDS_4341.423	CCCTTTGTGCATTGTGATGG
Nsd3_CDS_4341.422	GCTCCCTTTGTGCATTGTGA

Nsd3_CDS_4341.80	GCCTCCATCACAATGCACAA
Nsd3_CDS_4341.81	CCTCCATCACAATGCACAAA
Nsd3_CDS_4341.421	TATTACACTTCTGCAAATCT
Nsd3_CDS_4341.420	ACTTGTTC AATTTTCACAAC
Nsd3_CDS_4341.82	TTTGCTCTCCAGAATGCAAC
Nsd3_CDS_4341.83	CTCCAGAATGCAACAGGAGA
Nsd3_CDS_4341.85	TCAGTTTGT TTTATTCAACGA
Nsd3_CDS_4341.90	AAAACAGAAATAAGTGT CAG
Nsd3_CDS_4341.91	AAACAGAAATAAGTGT CAGG
Nsd3_CDS_4341.92	TAAGTGT CAGGGGGCAAGAC
Nsd3_CDS_4341.418	GGTTTTCACTTCTCTGACT
Nsd3_CDS_4341.93	AAGTCAGAGAAGTGAAAAGC
Nsd3_CDS_4341.417	GGAGATGACGCGCTCTGAGC
Nsd3_CDS_4341.94	GGCTCAGAGCGCGTCATCTC
Nsd3_CDS_4341.95	TCAGAGCGCGTCATCTCCGG
Nsd3_CDS_4341.96	TCATCTCCGGAGGCAACATC
Nsd3_CDS_4341.416	GCAGAACCAGATGTTGCCTC
Nsd3_CDS_4341.97	GAGGCAACATCTGGTTCTGC
Nsd3_CDS_4341.415	TCTGCTGCTTCTTCTACT
Nsd3_CDS_4341.414	CTCTGCTGCTTCTTCTAC
Nsd3_CDS_4341.98	AGCAGCAGAGAAGATCCATC
Nsd3_CDS_4341.413	TGACTCAGATCGAGTCCCTGA
Nsd3_CDS_4341.99	TGAGTCAGAGAAGTCCGCCG
Nsd3_CDS_4341.412	CTTCTTTGGCACAACCTCGG
Nsd3_CDS_4341.411	CTTCTTCTTTGGCACAACCT
Nsd3_CDS_4341.410	TCCTTTTTGATCTTCTTCTT
Nsd3_CDS_4341.100	GCCAAAGAAGAAGATCAAAA
Nsd3_CDS_4341.101	GAAGAAGATCAAAAAGGAGC
Nsd3_CDS_4341.409	CCGGTCTTCAGGGAGGCCTG
Nsd3_CDS_4341.408	CCCGGTCTTCAGGGAGGCCT
Nsd3_CDS_4341.407	ACCCGGTCTTCAGGGAGGCC
Nsd3_CDS_4341.103	CCCCAGGCCTCCCTGAAGAC
Nsd3_CDS_4341.104	CCCAGGCCTCCCTGAAGACC
Nsd3_CDS_4341.406	CTGTAACCCGGTCTTCAGGG
Nsd3_CDS_4341.405	TTTCTGTAACCCGGTCTTCA
Nsd3_CDS_4341.404	CTTCTGTAACCCGGTCTTC
Nsd3_CDS_4341.105	CTGAAGACCCGGTTACAGAA

D. Gene sets

Down_BRD4 knockdown	Down_NSD3 knockdown	LSC signature (Somerville)	Macrophage development (IPA)	SCHUHMACHER_ MYC_UP
NKG7	DIO2	CCT8	ACHE	ABCE1
B3GNT5	PHGDH	SLC16A1	APP	ACSL1
ZBTB16	ASNS	CCT7	BCL2	AHCY
MC5R	MPO	CALU	BMP2	AIMP2
IGFBP4	BZW2	SUCLG1	BMPR1A	AK3L1
PRTN3	MYC	PEBP1	BCR	AKAP1
GM1110	MT2	HMGB3	ABL1	ATP1B3
TSHR	HMGB3	USP14	CLEC11A	AUH
SLC16A1	PSAT1	IMP3	CALCA	BOP1
CPA3	SCD2	NDUFC1	CAST	CAD
SMYD2	TEX2	TIMM8A1	CASP8	CEBPZ
EXO1	BRI3BP	150003O22RIK	CEBPA	CTPS
DIO2	APEX1	CTPS	CEBPE	CTSC
NEK2	NPM3-PS1	NDUFA9	CD40	Cyp51
TK1	CTSG	ATP5B	CD47	DCUN1D4
RHOJ	MGAM	NDUFB2	CD81	DDX10
HELLS	MAGOH	PDE6D	CD9	DDX21
HIST1H1A	SLC7A5	MRPL51	CDC42	DHODH
CHEK1	NPM3	RRS1	CSF1	EBNA1BP2
HIST1H3G	CENPA	LAMP3	CSF1R	EXOSC7
DKC1	VAT1	KRTCAP2	CSF2	FABP5
MGL2	SHMT2	RRP15	CSF2RA	FASN
OOSP1	GM15645	FTSJ1	CSF2RB	FKBP4
2610318N02RIK	SRM	ARD1	CSF3	FXN
1700025G04RIK	FAM136A	ANGPTL4	C1QC	GART
NUF2	HTRA2	KDELR2	CUL4A	GCSH
PRSSL1	GAR1	CHCHD4	DMTF1	GPD1L
DTL	PUS7	SNRPA1	CDKN2D	GRSF1
PRPS1	ELANE	XRCC6	DLL1	HSPE1
PAPSS2	NIP7	CKS2	DUSP5	IARS
MCM6	KIF18B	CKS2	EGR1	KIAA0020
DCTD	MIF	LYAR	EEF1A2	KIAA0114
CDCA7	IMPDH2	SLC35A1	FASLG	LDHA
BZW2	2610528E23RIK	SFXN1	FOS	LRP8
BC005764	NCL	SFXN1	GATA2	MEST
STEAP3	GNL3	SLC25A37	GAB2	MRPL3
IMPDH2	SNHG12	PXMP2	GAB3	MTHFD1
MCPT8	GART	DDX19A	GFI1	NAMPT
EDNRA	E030024N20RIK	ILF2	HMGA1	NME1
AFAP1	TFPI	ILF2	INHA	NOLC1
MYC	WDR12	D6WSU176E	INHBA	PAICS
TMEM119	MTHFD2	MRPL39	ID2	PEBP1
GAS5	1110004E09RIK	PSME3	IKBKB	POLD2
PRIM1	TBCC	NSBP1	ITGAV	POLR2H
CTH	SPATA24	ORC2L	ITGB3	PPAT
KIF18A	SNHG3	BCAS2	IFNGR1	PRDX4
TEX2	METT10D	1110058L19RIK	IRF7	PRPS2

ELANE	PPM1F	D10ERTD322E	IRF8	PYCR1
MYBL2	TMEM97	MTF2	IFNA1	RABEPK
PBK	LOC624853	SERBP1	IFNA10	RANBP1
TIMM8A1	DKC1	CETN2	IFNA14	RPIA
SNORA21	SERPINE2	DUT	IFNA16	RRP1B
LIN9	METRNL	L7RN6	IFNA17	RRS1
PUS7	RPL34	MRPL35	IFNA2	SLC16A1
CKAP2	ATP5G1	EIF1AY	IFNA21	SLC20A1
TK1	ZFP706	2410022L05RIK	IFNA4	SLC39A14
SYCE2	MRPL22	2410022L05RIK	IFNA5	SLC39A6
TIPIN	MRPL15	LOC671878 /// SMS	IFNA6	SORD
ACY1	WDR61	MYB	IFNA7	SRM
FAR2	YARS2	TXNRD1	IFNA8	TARBP1
NETO2	TMEM48	IPP	IFNB1	TBL3
MTHFD1L	RCC1	FIGNL1	IFNE	TFRC
CDC20	SNHG1	ATAD3A	IFNG	TMEM97
1700106N22RIK	CIRH1A	PA2G4	IFNK	TRAP1
GSTM1	KIT	RPS27L	IFNW1	UCHL3
GPC1	TMEM93	MRPL45	IL1RN	UCK2
RETSAT	RSL1D1	PDCD2	IL10	VARS
D330028D13RIK	TRAP1	METAP2	IL15	VRK1
POLE2	FKBP4	COASY	IL3	ZNF239
KIT	MRPL50	FARSB	IL4	
ASPM	RAB33B	WDR36	IL6	
RAD51	AHCY	2810410M20RIK	KITLG	
CRYZ	SHMT1	ETFA	LIF	
CHST13	NANS	MKI67IP	LIFR	
CDCA7L	GM10653	PTTG1	MMP9	
NUP210	SSR1	1700020C11RIK	MDK	
NASP	FAM64A	RWDD4A	MLL	
MCM2	SLC7A1	GEMIN6	MLLT1	
SHMT1	ALDH18A1	1110004E09RIK	NKX2-3	
KIF20A	WDR43	RFC4	NFATC1	
MSH2	TIMM8A1	POLR2H	NFKBIA	
HIST2H2AB	PPAN	ATPBD1C	PAX5	
KIF2C	IPO7	D16ERTD472E	PPARG	
KIFAP3	MYBBP1A	SMYD2	PLCG2	
PRODH	DDX18	TASP1	PF4	
SMTN	H2AFX	TYMS /// TYMS-PS	PRDM1	
KIF14	2700007P21RIK	TNFSF5IP1	PIAS3	
ORC1L	CENPW	CDC16	RACGAP1	
CENPH	RPP30	GTF2I /// LOC669007	RGS10	
F630043A04RIK	GAS5	DLAT	RB1	
TFRC	1110038B12RIK	DLAT	RARA	
CENPP	0610007P14RIK	PRKRIR	SRF	
KIF20B	HSPE1	GTF2F2	STAT1	
SOCS2	RCC2	GSPT1	STAT6	
SPC25	EMG1	GALNT2	SPIB	
TSPAN2	WDR74	PTPRS	SPI1	
CCNB1	NUP62	HSDL2	SOCS1	
FANCD2	HSPD1	4933439F18RIK	SOCS3	

POLA1	GFI1	SUCLG2	TAL1	
FHDC1	EIF4E	SSBP3	THOC5	
PASK	1500012F01RIK	CDC73	TIMP1	
TRIP13	NOP10	COQ9	TRAF6	
UHRF1	MANF	TMEM180	TLR1	
C79407	NGFRAP1	ETFB	TLR2	
CDT1	CSTF1	DYNLRB1	TLR4	
TGM1	TMX4	EXOSC8	TLR5	
IL12A	POLR2H	CCDC6	TLR6	
CDC6	NAA10	EBNA1BP2	TGFB1	
MCM10	ENY2	PPAT	TNF	
RAD51AP1	SUCLG2	MRPL41	TNFSF10	
HIRIP3	PRTN3	1700029F09RIK	TNFSF11	
4930547N16RIK	HMG5	2310003L22RIK	TNFRSF11A	
AURKA	EIF1A	AASDHPPT	TNFRSF1A	
SLC28A2	FAM122B	XPOT	AKT1	
1700029F09RIK	IARS	2600001M11RIK	AKT2	
RFC4	HADH	MTF1	MAFB	
SRD5A1	VEGFA	4930579G24RIK	MYB	
CENPM	CLPP	UTP11L	VDR	
CBFA2T3	TRIP13	MTX2		
5730528L13RIK	WDR36	TMED5		
METTL1	PITRM1	D5WSU178E		
WEE1	PRPS1	IDH3A		
FAM64A	RUVBL2	DCUN1D5		
P2RY14	CEBPA	NUDT19		
GINS1	RPL22	CENPP		
HAUS4	FDX1L	4732479N06RIK		
CEP55	CHCHD4	NARS2		
RACGAP1	PPID	SEPHS1		
F730047E07RIK	UCK2	METAP2		
NUP43	RPL39	NUDT19		
KLRB1F	NSUN2	AGPAT5		
RAD54L	PHB	SERF1		
2610318N02RIK	UBE2C	PHKB		
TPX2	NPM1	1700065O13RIK		
RFC3	CCNB1	1110007M04RIK		
E330020D12RIK	ZFP692	TXNDC13		
IFRD2	TMED3	ST13		
CMTM3	PABPC4	METAP2		
CDCA8	BC085271	CLNS1A		
ALMS1	1500011K16RIK	RBM14		
POLR1B	SEC61A1	ENOPH1		
CDCA5	MSH2	MRPL44		
APEX1	RPF2	E2F6		
BARD1	IGFBP4	DKC1		
PPIL5	EXOSC3	AKR7A5		
CSR2	PARK7	OCRL		
CENPF	ATAD3A	PEBP1		
MCM8	TARS	1500011K16RIK		
SERPINE2	TDRKH	POLR3K		

MTBP	CEP55	TRIM45		
DUT	RRP9	PPP1R3E		
TBC1D30	PPIH	STRBP		
KIF17	RPL3	HDAC2		
CRIP1	NEDD4	TNFSF5IP1		
CLSPN	RPL30	DRG1		
ARHGAP10	PA2G4	EXOSC7		
WDR12	CYCS	MRPL18		
PLK1	PLK1	RAD1		
NOP58	FH1	ACP6		
UBASH3A	LYL1	NDUFB2		
DHFR	ORC5	NUDT5		
MCM7	NOP16	UBQLN4		
4930579G24RIK	FAM46A	E2F6		
PMF1	POP5	MRPS16		
UCK2	IDI1	TMEM186		
TTK	NOP2	EEF1E1		
SUV39H2	TIMM10	HDAC2		
MCM4	IDH3A	MTF2		
XRCC2	FBL	DTYMK		
TCFAP4	POLR2L	2310008M10RIK		
HMGB2	SNRPF	MYB		
GINS2	CDCA7	CBX5		
NPM3-PS1	1110059E24RIK	NOL5		
PLAC1L	PFKP	DTD1		
PTER	TRIM28	SIP1		
FANCB	NOP56	TTC4		
DOCK9	PPA1	MRPL50		
RPA2	GEMIN6	NUDT3		
MCM3	GRWD1	ZADH1		
PIK3IP1	EXOSC1	DLAT		
PABPC4	TADA1	CACYBP		
NSL1	1810029B16RIK	STRBP		
CABLES1	INSIG1	DGCR6		
FPGS	OAZ1	ILKAP		
2610528E23RIK	ACY1	2410018G20RIK		
WDHD1	CDK1	PCBD2		
SLC19A1	FASN	4632404H22RIK		
SMS	FAM65A	VKORC1		
BRCA2	DUT	CAD		
CST7	NDUFAB1	2810002O09RIK		
BUB1	ATG12	4930519L02RIK		
BRCA1	SC4MOL	UTP18		
SUCLG2	PTBP1	TRIM37		
NMRAL1	LARP4	CDK2AP1		
HIST1H2AB	LYAR	RBM14		
ECT2	2310008H09RIK	9230114K14RIK		
4930520O04RIK	RSL24D1	TMEM69		
WDR76	TXNDC5	RSBN1		
HIST1H2BB	HSPA9	WDR61		
FEN1	NDUFA11	ENY2		

LMNB1		HTRA2		
CKS1B		TIMM17B		
A630089N07RIK				
DNAHC8				
BRIP1				
HAUS5				
SPAG5				
UCK2				
TIMM8A1				
TMEM97				
CDC45				
LIG1				
KDELC2				
NCAPD2				
DLGAP5				
DIAP3				
CHAF1A				
PRC1				
PSAT1				
STMN1				
SPNS3				
5730590G19RIK				
PPAT				
CTPS				
TYMS				
KIF18B				
PKMYT1				
NPL				
EME1				
CENPN				
PALB2				
ERCC6L				
CDKN3				
KIF22				
MLF1IP				
RAB38				
TDRKH				
AHCY				
TMEM48				
GAR1				
EEF2K				
TACC3				
FAM54A				
SELM				
PLAC8				
AHCY				
BRD4				
FIGNL1				
TMEM97				
TROAP				
POLD2				

MGAT5				
SIPA1L1				
EEF2K				
MS4A3				
1110004E09RIK				
KIF15				
BC048355				
EXOSC2				
SHMT2				
NDC80				
BC030867				
PHGDH				
PECR				
DSN1				
GINS3				
AURKB				
WDR12				
3632451O06RIK				
ACSS1				
TRF				
TTC27				
HIST2H2BB				
RRM2				
TPMT				
KCNN4				
CDC25C				
POLE				
RPUSD2				
CDCA2				
CHDH				
NEIL3				
PRIM2				
PRMT7				
BARD1				
ACAT2				
E2F8				
SLC39A8				
GTSE1				
KIF11				
ZMYND19				
POLD1				
CIT				
PPIH				
HAUS5				
GNL3				
NAPEPLD				
BC020535				
NPM3				
PTPLA				
ESCO2				
DNAJC9				

HIST1H4B				
HIST1H1B				
CCDC15				
FKBP4				
EGLN3				
RRP15				
ACOT7				
USP6NL				
NAF1				
PDIA5				
DTYMK				
NUP107				
AMPD2				
CKAP2L				
CDK1				
CHTF18				
CBFA2T3				
POC1A				
RRM1				
CEP76				
GATM				
EXOSC8				
2410017P07RIK				
PRR11				
MCM5				
SMC2				
ZRANB3				
GSTO1				
CCBL2				
SH2D5				
GFI1				
GMPR				
ANLN				
ADCY3				
HSPB6				
RND1				
C1QBP				
TSR1				
CDC7				
TIMELESS				
SMS				
CDCA3				
ABCC2				
HSD11B1				
PHGDH				
PROS1				
MELK				
BCKDHB				
FANCA				
BIRC5				
CSRP1				

GM10052				
HIST1H2AO				
GM5643				
SRM				
HIST1H4C // HIST1H4C				
CLTB				
SNORD33				
RBL1				
ATP2B4				
RABL2A				
PPAN				
R3HCC1				
RAD51L1				
PREPL				
ISOC1				
UMPS				
MTHFD1				
IDI1				
CHAF1B				
GGA2				
RAD51C				
NCAPH				
LAP3				
ASNS				
SPC24				
PHF17				
RAMP1				
HMGB3				
6330545A04RIK				
ICAM2				
RUVBL1				
TMEM20				
HIST1H4F				
PTPRCAP				
6720463M24RIK				
CCNA2				
ZCCHC3				
PPIH				
NME4				
ATM				
SLC7A5				
CCNB2				
RBBP8				
TOPBP1				
MMP28				
RNF125				
GSTM3				
D930014E17RIK				
TTC39C				
ENDOD1				
NUP133				

NFKBIL2				
BC057079				
SLC7A1				
IQGAP3				
MREG				
AQP11				
NUP85				
NUP37				
GPT2				
DTD1				
POLA2				
KPNA2				
FANCF				
SCAMP5				
ADA				
MRPS28				
C230052I12RIK				
SNORA73B				
ORC6L				
IDI1				
MPHOSPH9				
SLAMF9				
STON2				
GCAT				
RTKN2				
ANAPC5				
PAQR4				
SUSD1				
CCNF				
NOP56				
TDP1				
TOP1MT				
SNRPA1				
LRRK1				
SNORA44				
E130306D19RIK				
PYCR1				
RHD				
ASS1				
INCENP				
CHEK2				
GALK1				
PKN3				
NUP35				
OSCP1				
CENPA				
PER3				
ALAD				
UTP20				
SIGLEC5				
KCNQ5				

BAMBI				
5930416I19RIK				
NUCKS1				
PSMC3IP				
KCNE3				
LMBR1				
RUVBL2				
ZC3HAV1L				
SLC29A1				
MTHFD2				
PPAPDC1B				
NET1				
AK3L1				
CAD				
GMNN				
GEMIN6				
BARD1				
SPATA24				
FOXM1				
CKS2				
PA2G4				
AKAP1				
PRMT3				
CHPT1				
SEMA6B				
QTRTD1				
FAM92A				
ZC4H2				
PPIL1				
RGNEF				
OAT				
ANKRD32				
SNORA73A				
CCNE1				
GM4968				
SNORA21				
NKRF				
LRDD				
NUDCD1				
1500012F01RIK				
FH1				
E130303B06RIK				
INTS7				
HDGF				
CBX5				